

**FROM MALT TO BRIGHT BEER AND BEYOND**  
PROTEOMIC STUDIES PERFORMED WITH HPLC AND  
UPLC CHROMATOGRAPHY FOLLOWED BY  
(NANO)ESI-QTOF-MS/MSMS IDENTIFICATION

by  
Fabienne Decker

THESIS SUBMITTED IN FULFILLMENT OF THE REQUIREMENTS FOR THE  
DEGREE OF DOCTOR RERUM NATURALIUM  
AT  
THE FACULTY OF TECHNOLOGY  
UNIVERSITY OF BIELEFELD, GERMANY

THIS DISSERTATION WAS CARRIED OUT AT  
BRAUEREI C. & A. VELTINS GmbH Co. KG  
AN DER STREUE  
59872 MESCHEDE-GREVENSTEIN

THESIS PRESENTED  
DECEMBER 2009

SUPERVISOR

PROF. ERWIN FLASCHEL, TECHNISCHE FAKULTÄT, UNIVERSITÄT BIELEFELD, GERMANY

SUPERVISORS AT BRAUEREI VELTINS

CIVIL ENGINEER STEFAN LOCH-AHRING, BRAUEREI VELTINS, MESCHEDE, GERMANY

JÜRGEN FARKE, BRAUEREI VELTINS, MESCHEDE, GERMANY

PROF. DR. KARL FRIEHS

---

GRADUATE DIRECTOR

PROF. DR. ERWIN FLASCHEL

---

FIRST REFEREE

PROF. DR. KARSTEN NIEHAUS

---

SECOND REFEREE

DR. RAIMUND HOFFFROGGE

---

OBSERVER

DATE OF EXAMINATION

---

DATE OF EXAMINATION AND DEFENCE

12.03.2010

„THE JOY OF SEEING AND UNDERSTANDING IS THE MOST PERFECT GIFT OF NATURE.  
THE IMPORTANT THING IS TO NOT STOP QUESTIONING.“

---

ALBERT EINSTEIN

THIS IS IN MEMORY OF MY DAD

## **Statement**

The experimental work and results of this thesis are based on research carried out at the laboratory (Instrumental Analytics, QA/QC) of Brauerei C. & A. Veltins GmbH Co. KG. Meschede (Germany). The external doctoral thesis was performed in cooperation with the Technische Fakultät, Universität Bielefeld (Germany).

To the best of my knowledge no part of this thesis has been submitted for any other degree or qualification. All results presented here are my own work unless referenced to the contrary in the text.



## Acknowledgement

I wish to thank the following persons for without whose help and expertise this thesis would not have been possible.

I would like to thank my research advisor, civil engineer Stefan Loch-Ahring, not only for the interesting topic and his support of my doctoral thesis but also for providing the possibility of working on it at the Veltins laboratory. Although being far away at Karlsruhe during the last year of my thesis you unfailingly had time, helpful suggestions and interest for my work.

A special thank you also goes to Walter Bauer, Jürgen Farke and the Veltins brewing company for their continued support of my thesis, especially in 2009.

Another very special thank you goes to my colleague Sascha Robbert for three years of discussion, technical support and great fun. Without your knowledge, suggestions and support I would not have never been able to complete this study.

I owe a further debt of gratitude to my colleagues, Claudia, Ricarda and Sandra for their friendly support. A warm smile can sometimes light up the dark.

I would like to thank Reinaldo Almeida (Advion) for his support in the final stages of this study and its advancement to new analytical levels.

A special thank you also goes to Prof. Erwin Flaschel for his regulatory support for this external doctoral thesis and attendance for reference. Without your own and Karsten Niehaus' support the shootings of the gushing phenomenon would not have been possible.

To Karsten Niehaus and Manfred Lissel, thank you very much for our discussions at Veltins and at Bielefeld University. Your valuable information always provided fresh food for thought.

To my partner, Wolli, a big thank you for all the calm and unflappable support over the whole three years.

# Content

<b>ABSTRACT</b>	<b>I</b>
<b>ZUSAMMENFASSUNG</b>	<b>II</b>
<b>ABBREVIATIONS</b>	<b>III</b>
<b>1 INTRODUCTION</b>	<b>1</b>
1.1 “Food for thought“	1
1.2 Proteins – a short refresher	2
1.3 From malt to beer and “beyond“	6
1.3.1 Barley ( <i>Hordeum vulgare</i> )	7
1.3.2 Malt production	8
1.3.3 The brewing process – wort production	9
1.3.4 The brewing process – boiling the wort and adding the hops	11
1.3.5 The brewing process – fermentation	12
1.3.6 The brewing process – filtration	13
1.3.7 Bright beer	15
1.3.8 “Going Beyond“ – colloidal stability and haze formation	17
1.4 Gushing	21
1.5 Barley protein species and classes	25
1.5.1 Barley and malt protein classification	25
1.5.2 nLTP1, nLTP2 and the class of ns-LTP’s	27
1.5.3 Proteins Z4 and Z7	30
1.5.4 Hordeins	31
1.5.5 Barwin	32
1.5.6 Inhibitor protein classes	33
1.5.7 Other protein classes	35
1.5.7 Proteins with “other functions“	36
1.6 Proteins from other origins	37
1.6.1 Hydrophobins – fungal proteins	37
1.6.2 Yeast proteins	38
1.6.3 Other proteins	38
<b>2 INSTRUMENTAL BACKGROUND</b>	<b>40</b>

## CONTENT

---

<b>2.1</b>	<b>“Ultra Performance Liquid Chromatography“ – Acquity UPLC™</b>	<b>40</b>
2.1.1	Peptide analysis using UPLC	41
2.1.2	Protein analysis with reversed phase chromatography (RPC)	42
<b>2.2</b>	<b>Mass spectrometer – Micromass QTOF micro™</b>	<b>44</b>
2.2.1	Ionization with an electrospray source	45
2.2.2	Ion separation with a quadrupole time of flight	49
2.2.3	MS-strategies	50
2.2.4	Tandem mass spectrometry – MS <sup>2</sup> -mode	50
2.2.5	Bottom up approach	52
2.2.6	Top down approach	53
2.2.7	Protein sequence analysis using MassLynx and PLGS software	53
<b>3</b>	<b><u>PROJECT OBJECTIVES</u></b>	<b>55</b>
<b>4</b>	<b><u>MATERIALS</u></b>	<b>56</b>
4.1	Chemicals	56
4.2	Buffers and eluents	58
4.3	Consumables	58
4.4	Instruments	59
4.5	Sample materials	61
<b>5</b>	<b><u>METHODOLOGY</u></b>	<b>63</b>
5.1	Sample types and treatment	63
5.2	Preliminary investigations using HPLC and HPLC-MS	63
5.2.1	Tryptic digestion for bottom up analysis	64
5.2.2	Bottom up approaches	65
5.2.3	Sample fractionation with the Dionex HPLC	65
5.2.4	HPLC-MS top down investigation	66
5.3	Protein quantification	67
5.3.1	Biorad Roti® Quant Universal assay and Nanoquant assay	67
5.3.2	2D-Quant assay	67
5.4	Investigations concerning haze	68
5.4.1	Haze preparation	68
5.4.2	Solubility tests	69

<b>5.4.3 Tryptic digestion of haze</b>	<b>69</b>
<b>5.4.4 Long-term storage of haze</b>	<b>70</b>
<b>5.4.5 Top down approaches</b>	<b>70</b>
<b>5.5 Gushing studies</b>	<b>71</b>
<b>5.5.1 Modified Carlsberg Test (MCT)</b>	<b>71</b>
<b>5.5.2 MCT with fractionated coarse groat</b>	<b>71</b>
<b>5.5.3 MCT with hop extract additives</b>	<b>72</b>
<b>5.5.4 MCT with enzyme additives</b>	<b>72</b>
<b>5.6 Protein precipitation</b>	<b>73</b>
<b>5.6.1 Early precipitation tests with fresh beer and haze</b>	<b>73</b>
<b>5.6.2 Phenolic extraction</b>	<b>74</b>
<b>5.6.3 Sample preparation for bottom up experiments after protein extraction</b>	<b>75</b>
<b>5.6.4 Sample preparation for top down experiments</b>	<b>75</b>
<b>5.7 UPLC-MS and UPLC-MS/MS studies</b>	<b>75</b>
<b>5.7.1 Bottom up approaches</b>	<b>75</b>
<b>5.7.2 Top down analysis of whole proteins</b>	<b>77</b>
<b>5.7.3 Top down and bottom up analysis in a single LCMS experiment</b>	<b>78</b>
<b><u>6 RESULTS AND DISCUSSION</u></b>	<b><u>80</u></b>
<b>6.1 Preliminary HPLC investigations</b>	<b>80</b>
<b>6.1.1 Non specific lipid transfer protein 1 (nLTP1)</b>	<b>80</b>
<b>6.1.2 Protein Z</b>	<b>83</b>
<b>6.1.3 Dionex HPLC beer sample fractionations</b>	<b>89</b>
<b>6.1.4 HPLC-MS analysis of brewing process samples</b>	<b>90</b>
<b>6.2 Protein quantification</b>	<b>93</b>
<b>6.3 Haze analysis</b>	<b>96</b>
<b>6.3.1 Fundamental observations concerning haze</b>	<b>96</b>
<b>6.3.2 Haze formation – a dynamic process</b>	<b>99</b>
<b>6.3.3 Solubility tests with lyophilised and freshly prepared haze</b>	<b>102</b>
<b>6.3.4 Freshly prepared haze and basic beer turbidity</b>	<b>104</b>
<b>6.3.5 Bottom up analysis of haze</b>	<b>109</b>
<b>6.3.6 Top down analysis of haze samples</b>	<b>111</b>
<b>6.3.7 Summary</b>	<b>113</b>
<b>6.4 Gushing</b>	<b>113</b>

## CONTENT

---

<b>6.4.1 The “Modified Carlsberg Test“ (MCT)</b>	<b>115</b>
<b>6.4.2 MCT investigations with hop additives</b>	<b>118</b>
<b>6.4.3 The impact of enzymes on the gushing tendencies of malt and barley</b>	<b>119</b>
<b>6.4.4 First UPLC-MS studies with MCT extract samples</b>	<b>121</b>
<b>6.4.5 Protein precipitation with MCT extracts</b>	<b>122</b>
<b>6.4.6 Bottom up investigations</b>	<b>124</b>
<b>6.4.7 Summary</b>	<b>135</b>
<b>6.5 From malt to beer and beyond</b>	<b>135</b>
<b>6.5.1 Top down approaches</b>	<b>135</b>
<b>6.5.2 Bottom up experiments</b>	<b>139</b>
<b>6.5.3 Top down and bottom up investigations in a single experiment</b>	<b>142</b>
<b>7 CONCLUSIONS</b>	<b>146</b>
<b>REFERENCES</b>	<b>148</b>
<b>APPENDICES</b>	<b>153</b>
<b>Appendix A, Summary of enzymatic MCT approaches</b>	<b>153</b>
<b>Appendix B, Peptide masses and sequences of MCT samples (B1 – B4)</b>	<b>155</b>
<b>Appendix C, Measurement of mass accuracy with protein standards</b>	<b>159</b>
<b>Appendix D, Precursor ion masses and charges of brewing samples (D1 – D7)</b>	<b>160</b>
<b>POSTER PUBLICATIONS</b>	<b>167</b>
<b>CURRICULUM VITAE</b>	<b>170</b>

## List of Figures

Figure 1	The basic structure of an $\alpha$ -amino acid in its unionized, amphoteric form. ....	2
Figure 2	Chemical formula of an L-proline (Pro/P). .....	4
Figure 3	The three structural shapes of horse heart myoglobin (>sp: P68082, pdb:1, WLA ), a protein standard used for mass spectrometry analyses of undigested proteins in this thesis. ....	4
Figure 4	Light microscopy pictures of a Celite stabiliser on the left and PVPP on the right. ....	14
Figure 5	Haze at the bottom of a bottle: a.) chill haze after about 4 weeks of storage at 0 °C and b.) permanent haze after longterm cold storage at 0 °C. ....	17
Figure 6	Model of haze formation. ....	19
Figure 7	Chemical structure of polyphenols. ....	20
Figure 8	Snapshot of a gushing beer. ....	22
Figure 9	Red and black grains observed with mould infection of malt material during gushing period 2008. ....	23
Figure 10	Infection modi/symptoms following Fusarium infection of cereals. ....	24
Figure 11	1- and 2D structural information on plant nLTPs. ....	28
Figure 12	3D structure of barley lipid transfer protein (NMR, 4 structures). ....	28
Figure 13	Waters Acquity UPLC <sup>TM</sup> . ....	40
Figure 14	Micromass QTOF micro <sup>TM</sup> ion optics and instrument overview. ....	44
Figure 15	Design of a normal electrospray (z-spray) source. ....	46
Figure 16	Serial instrument connections used for normal and nano-ESI infusion in this thesis. ....	47
Figure 17	The chip-based Nanomate robot system with ESI-chip. ....	47
Figure 18	LC coupling mode used with online LC/MS. ....	48
Figure 19	Peptide fragmentation nomenclature. ....	51
Figure 20	Top down versus bottom up approaches in proteomics. ....	52
Figure 21	Spectrum of the tryptic digested nLTP1 standard. ....	80
Figure 22	nLTP1 analysis by bottom up investigation and PLGS software identification. ....	81
Figure 23	Top down protein spectrum of a native, lyophilised nLTP1 standard. ....	82
Figure 24	Allocated ion series found with an nLTP1 protein standard. ....	82
Figure 25	MS survey scan of a tryptic digested protein Z SEC fraction. ....	84
Figure 26	Tuning effects observed with protein Z precursorion $m/z = 1345$ Da. ....	85
Figure 27	Amino acid sequence of protein Z4 (Swissprot entry: P06293). ....	86
Figure 28	Summary of sequence analogies determined for precursorions found in the terminal protein Z fragment during native protein analysis. ....	87
Figure 29	Changes in LC separation observed for the nLTP1 peak within the brewhouse cooking procedure. ....	90

## LIST OF FIGURES

---

Figure 30	<i>Extracted chromatograms and corresponding MS spectra of the m/z = 1384 Da precursor ion mass observed with nLTP1 rearrangement in the brewing process. ....</i>	91
Figure 31	<i>Isolable haze amounts found in brewing trial samples after long-term storage. ....</i>	97
Figure 32	<i>Haze isolated from brewing trial beer after long-term storage. ....</i>	98
Figure 33	<i>Haze development in the long-term storage (RT) of Pilsener beer samples. ....</i>	99
Figure 34	<i>Haze development observed in KZE treated and untreated Pilsener beer (0.5 L) stored at 0 °C and RT. ....</i>	100
Figure 35	<i>Solubility tests with haze materials. ....</i>	103
Figure 36	<i>Two different perspectives on freshly prepared haze (24 x 0.5 L beer bottles). ....</i>	105
Figure 37	<i>Microscopy observations of haze. ....</i>	105
Figure 38	<i>Basic beer turbidity isolated from young, even bottled Pilsener beer. ....</i>	106
Figure 39	<i>Development and changes in the outer appearance of basic beer turbidity during storage. ....</i>	107
Figure 40	<i>Incident light and light microscopy (20x) pictures of filter aids. ....</i>	107
Figure 41	<i>Filter aid components and typical basic beer haze structures found even in bottled and very young Pilsener beer samples. ....</i>	108
Figure 42	<i>LC-chromatograms of lyophilised and freshly prepared haze material analysed by top down approaches. ....</i>	112
Figure 43	<i>Snapshots of the multi-phase expansion of a gushing beer. ....</i>	114
Figure 44	<i>Variations within a single MCT batch of a gushing malt. ....</i>	116
Figure 45	<i>Three independent MCT approaches from one malt sample. ....</i>	117
Figure 46	<i>MCT approaches with hop extract additives. ....</i>	118
Figure 47	<i>Gushing behaviour of an enzymatically treated gushing malt sample. ....</i>	119
Figure 48	<i>Comparison of the gushing behaviour of enzymatically treated barley and malt samples. ....</i>	120
Figure 49	<i>MCT results observed for Corolase 7089 in different concentrations. ....</i>	121
Figure 50	<i>Native protein analysis (UPLC nanoESI-QTOF-MS) of a standard gushing and non-gushing malt extract sample. ....</i>	121
Figure 51	<i>UPLC-MS chromatogram of a standard gushing malt and a sample treated with Corolase 7089. ....</i>	122
Figure 52	<i>LC-MS peptide analysis of precipitated and tryptic digested protein pellets. ....</i>	123
Figure 53	<i>Native protein chromatogram of an untreated standard gushing malt and the “native“ (but denaturated) protein pattern after phenolic extraction. ....</i>	124
Figure 54	<i>55 minute detail of an 80 minute UPLC-MS TIC chromatogram. ....</i>	125
Figure 55	<i>UPLC-MS BPI chromatogram (5 – 70 mins) of a gushing Ireks malt and a non-gushing Durst malt. ....</i>	126
Figure 56	<i>The analytical path from a TIC chromatogram of a non-gushing Cargill malt sample to protein identification using the example of nLTP1. ....</i>	127

## LIST OF FIGURES

---

Figure 57	<i>Spectrum of a mixture of bovine trypsinogen (10 pM/μL, molecular mass = 23980.987 Da) and horse heart myoglobin (5 pM/μL, molecular mass = 16951.499 Da). .....</i>	136
Figure 58	<i>Top down UPLC nano-ESI-QTOF-MS BPI-chromatograms of brewing process samples. ....</i>	137
Figure 59	<i>Comparison of 45 minute details of the BPI-chromatograms for malt extract, beer, haze supernatant and haze dissolved in DMSO. ....</i>	137
Figure 60	<i>3D data maps of top down UPLC-MS experiments. ....</i>	138
Figure 61	<i>Schema of post column splitting and Nanomate settings for top down and bottom up tests combined in a single LC-MS run. ....</i>	143
Figure 62	<i>Overview of the analytical strategy in a combined bottom up and top down approach. ....</i>	144
Figure 63	<i>Mass measurement and charge state deconvolution in an online MCT top down test. ....</i>	145
Figure 64	<i>Extracted protein spectra of undigested protein fractions following offline application. ....</i>	145



## List of Tables

Table 1	<i>Proteinogenic amino acids, their abbreviations and side chain properties. ...</i>	3
Table 2	<i>Composition of barley grain.....</i>	7
Table 3	<i>Classification of barley protein fractions. ....</i>	7
Table 4	<i>Congress wort mashing program (laboratory scale).....</i>	10
Table 5	<i>Chemical attitudes of a standard bright beer. ....</i>	15
Table 6	<i>Additional proteins identified in malt extracts, beer and foam fractions. ....</i>	36
Table 7	<i>Chromatography separation principles. ....</i>	40
Table 8	<i>Overview of the database resources used and database entries relating to extracted species. ....</i>	54
Table 9	<i>Overview of brewing trial modifications 2006. ....</i>	61
Table 10	<i>Gradient timetable used for beer fractionation. ....</i>	66
Table 11	<i>Overview of enzyme additives. ....</i>	73
Table 12	<i>Development of gradient timetables for peptide separation. ....</i>	76
Table 13	<i>Development of gradient timetables for protein separation. ....</i>	77
Table 14	<i>Gradient timetable for bottom up experiments in combination with top down approaches. ....</i>	79
Table 15	<i>Protein quantification via Biorad RotiQuant Universal and Nanoquant assay. ....</i>	94
Table 16	<i>Results of protein quantification with 2D Quant assay (GE Healthcare). ....</i>	95
Table 17	<i>Changes in the amino acid concentration of KZE treated and untreated samples stored at 0 °C. ....</i>	101
Table 18	<i>Protein identification in haze following overnight digestion with trypsin. ....</i>	109
Table 19	<i>Masses and sequences identified for haze proteins in bottom up analysis. ...</i>	110
Table 20	<i>UPLC-MS conditions and general information about protein contents of analysed gushing and non-gushing malt extracts. ....</i>	126
Table 21	<i>Summary of identified barley (HORVU) proteins in bottom up experiments with malt extracts. ....</i>	129
Table 22	<i>Ancient protein species identified in bottom up experiments with malt extracts. ....</i>	130
Table 23	<i>Barley peptide masses and sequences identified in a non-gushing Cargill malt. ....</i>	131-132
Table 24	<i>Peptide masses and sequences of other origin identified in a non-gushing Cargill malt. ....</i>	133
Table 25	<i>Summary of protein hits identified in bottom up tests with brewing process samples. ....</i>	139
Table 26	<i>Ancient protein species identified in bottom up experiments of brewing process samples. ....</i>	140

## Abstract

Mass spectrometry based sequential protein identification in beer and brewing process related samples is rare in breweries. Routine investigations are instead based on simple and/or colorimetric standard protein quantification methods or a superficial quality evaluation of the malt raw material. The few protein studies that do provide precise protein identification data on molecular level usually encompass 2D gel electrophoretic separation and subsequent MALDI analysis.

This doctoral thesis is aimed at developing methods that rely on a combination of liquid chromatography and electrospray mass spectrometry (LC-ESI-QTOF-MS) while enabling the analysis of complex protein samples independently of a previous electrophoretic 2D gel separation. Instead a Waters HPLC system was tested and a UPLC system with greater separative power was applied. The analysis with both systems was optimized in a manner ensuring that the results delivered by subsequent (nano)ESI- and ESI-QTOF-MS and -MSMS analyses were as detailed as possible. The preliminary analyses with protein standards were mainly performed with the HPLC system while the UPLC was used for method development and optimization, enabling the advantages of this system to be fully exploited. Both bottom up and top down approaches were developed and applied to the in depth analysis of malt extracts (gushing and non-gushing samples), brewing processes samples, beer and haze samples, while paying respect in terms of adaptability to distinct, further research topics (e.g. foam stability). Besides describing the proteomes of individual samples as precisely as possible, the research was focused on the discovery of new proteins as yet unmentioned in connection with these samples.

In latter stages a combination of both bottom up and top down approaches within a single LC/MS experiment was developed and tested. Combining online LC/MS and offline (nano)ESI-MS analyses enabled the examination and simultaneous characterization of proteins including intact protein mass measurement, posttranslational modifications (brewing process modifications) and the corresponding peptide sequence. The introduction of online sample preconcentration on the column, post column splitting and parallel online fractionation successfully rendered previous 2D separation unnecessary, even with complex protein samples.

## Zusammenfassung

Sequenzielle Proteinidentifizierungen auf Basis massenspektrometrischer Untersuchungen aus Bier- und Brauprozessproben sind in Brauereien selten. Routineanalytiken basieren eher auf einfachen und/oder colorimetrischen Proteinquantifizierungsmethoden oder der oberflächlichen Beurteilung der Malzrohstoffqualität. Die wenigen Proteinstudien die genaue Angaben zu Proteinidentifizierungen auf molekularer Ebene machen, umfassen in der Regel 2D-gel-elektrophoretische Trennungen and anschließende MALDI-Analysen. Ziel dieser Doktorarbeit war die Entwicklung von Analysetechniken, die auf eine Kombination von Flüssigchromatografie und Elektrospray-Massenspektrometrie (LC-ESI-QTOF-MS) zurückgreifen und dabei unabhängig von einer vorweggeschalteten gelelektrophoretischen Trennung Analysen komplexer Proteinproben ermöglichen. Anstelle dieser wurde eine Waters HPLC-Anlage getestet und ein UPLC-System mit höherer Trennleistung genutzt. Die Analytik mit beiden Systemen wurde dahingehend optimiert, daß die anschließenden (nano)ESI- und ESI-QTOF-MS und -MSMS Analysen möglichst detaillierte Ergebnisse lieferten. Die einleitenden Analysen mit Proteinstandards wurden hauptsächlich auf der HPLC-Anlage betrieben, wohingegen zur Methodenentwicklung und -optimierung die UPLC genutzt wurde. Dabei konnten die Vorteile dieses Systems voll ausgenutzt werden. Sowohl "Top Down", wie auch "Bottom Up" Methoden wurden entwickelt, wobei auf eine mögliche Anpassung der Methoden an zukünftige Forschungsfragestellungen geachtet wurde. Während dieser Studie wurden Malzextrakte (gushend und nicht gushend), Brauprozessproben, Bier- und Trubproben untersucht. Protein Z and nLTP1 Proteinstandards wurden im Detail analysiert. Neben der möglichst genauen Darstellung des Proteoms der einzelnen Proben lag der Forschungsschwerpunkt auf der Entdeckung neuer, bisher noch nicht im Zusammenhang mit diesen Proben erwähnter Proteine. In der letzten Phase der Doktorarbeit wurde eine holistische Methode entwickelt, die sowohl "Top Down", als auch "Bottom Up" Analytik in einem einzelnen Experiment miteinander vereint. Durch die Kombination von "online" LC-MS und "offline" (nano)ESI-MS Analytik wurde die Möglichkeit geschaffen, Proteine auf Ebene der intakten Masse, posttranslationaler Modifikationen (Brauprozessmodifikationen) und der zugehöriger Peptidsequenz zu untersuchen und gleichzeitig zu identifizieren. Durch Einführung einer "online" Probenkonzentrierung auf der LC-Säule, Volumenstromtrennung hinter der Säule und paralleler Fraktionierung konnte die Notwendigkeit einer vorausgehenden 2D-Gel Trennung auch bei komplexen Proteinproben umgangen werden.

## Abbreviations, Symbols, Units

1D	One-dimensional
2D	Two-dimensional
3D	Three-dimensional
AA	Amino acid
ABA	Abscisic acid
ACS	American Chemical Society
BPI	Base peak ion
°C	Degree Celsius
Da	Dalton
DB	Database
DOC	Sodium desoxycholate
DON	Desoxynivanol
DTT	Dithiothreitol
ESI	Electrospray ionization
FWHM	Full width at half maximum size
h	Hour
HA	Haze-active
HPLC	High performance liquid chromatography
IUPAC	International Union of Biochemistry
kDa	Kilo-Dalton
KZE	Flash pasteurisation
LC	Liquid chromatography
LC-MS	Liquid chromatography mass spectrometry
LC-MS <sup>2</sup>	Liquid chromatography tandem mass spectrometry
LTP	Lipid transfer protein
M	mol/L
MCT	Modified Carlsberg test
mM	mmol/L
MM	Molecular mass
nm	Nanometer
nL	Nanoliter
nsLTP	non specific lipid transfer protein
RPC	Reversed phase chromatography
p.a.	Per analysis
PDA	Photo diode array
pH	„Pondus Hydrogenii“

## ABBREVIATIONS, SYMBOLS, UNITS

---

pI	Isoelectric point
PLGS	ProteinLynx Global Server
ppm	Parts per million
PTM	Posttranslational modification
PVPP	Polyvinylpolypyrrolidone
QTOF	Quadrupole time of flight
SDS	Sodiumdodecylsulfate
TCA	Trichloro acetic acid
TIC	Total current ion
TOF	Time of Flight
UPLC	Ultra performance liquid chromatography
UV	Ultraviolet
μm	Micrometer

# CHAPTER I

---

INTRODUCTION

### 1. Introduction

#### 1.1 „Food for thought“

Imagine a glass of bright beer in front of you. What are the associations this picture calls to your mind? Your answer could go something like this: a stable, lacy white and creamy beer foam head, a clear beer or, even a more figuratively, a dream. If you continue with this mental image the next step would be to take a sip or even a large draught. Your impressions would leave the realm of mere visual perception and reach a level associated with smell and taste. Your taste buds would first of all detect bitterness and various flavour components. But there are many other beer ingredients besides that which you are all used to but not able to distinguish or classify. Taking a closer look, ingredients like alcohol and water, sugars, vitamins, trace elements or mineral nutrients could be mentioned, but not that easily mastered mentally. Which is also the reason why you probably won't realize that:

**„Drinking beer equals protein consumption.“**

You might be wondering why we should attach any importance to this fact, as long as the taste and appearance of the beer are excellent? But there is still little knowledge of the foundations these attitudes are based on. How to do deal with a beer that fails to comply with the requirements of excellence? Answering this and other beer related questions of a biological nature always was and still is what motivates beer protein studies on a molecular level.

But why proteins, you may ask. To explain this we should first of all take a look at the raw materials. The malt sent on a journey through the brewing process could be described as a real protein bomb. What happens to the proteins in this process? Are they being modified when the wort is boiled? And which proteins will survive the brewing conditions and remain in the beer?

Proteins are one of the substance classes often referred to when speaking of beer quality and stability. Which is another good reason to take a closer look at them. Will it be possible to prove or also convulse theory?

There could be one last question you might ask: what about the other beer ingredients? This is indeed the key question to contemplate. Beer is a complex mixture. Interfering substances are one reason why proteomic studies are so difficult with beer. Analysing the majority of substances related to a problem would be hard or even impossible already, but it could also just be a single macromolecular class or even component that makes all the difference.

Proteins represent one class of biological macromolecules, and most the activities in living cells and organisms are performed by them (e.g. in the form of enzymes, cell signaling, ligand binding, structural components). That is the reason why they are being researched so intensively in the life sciences and not least of all in this thesis regarding malt, beer and colloidal haze.

„The most beautiful experience we can have is the mysterious.“<sup>1</sup>

(<sup>1</sup>Albert Einstein)

## 1.2 Proteins - a short refresher

Proteins and peptides are made from amino acids (AA). Linear chains of these structural units provide the so called primary structure of proteins and peptides. The huge variety of individual proteins is ensured by up to four levels of structure and the endless permutations and combinations of twenty-two proteinogenic amino acids. Two rather exotic amino acids (pyrrolysine and selenocysteine) can only be found in certain organisms but are like standard amino acids specified by the codons (three-nucleotide sets) of the genetic code.

$\alpha$ -amino acids with the amino group bearing carbon atoms next to the carbonyl group are the most common form found in nature. Except for glycine they all possess chiral  $\alpha$ -carbon atoms and can show both L- or D-configuration. The great majority found in proteins or peptides are L-amino acids. Variable side chains, amino and carbonyl groups are the common structural features linked to  $\alpha$ -carbon atoms (Figure 1).

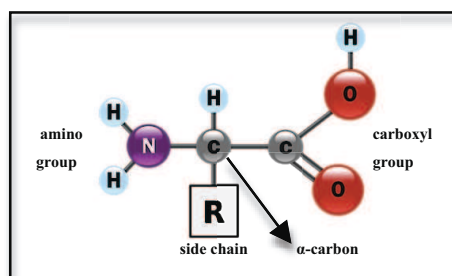


**Figure 1** The basic structure of an  $\alpha$ -amino acid in its unionized, amphoteric form [7].

The common hooks of amino groups (NH<sub>2</sub>) and carboxyl groups (COOH) are a precondition for peptidic bond formation (CO-NH) during translation. The step by step addition of amino acids (AA) results in short polymers in case of peptides or proteins when growing into polypeptides. The sum of chemical attitudes applied through the protein's constituent amino acids ultimately defines the protein molecule in both its structure and chemical reactivity.



## INTRODUCTION

Amino acids (Table 1) are classifiable by the chemical properties of their attaching side chains. Four groups can be distinguished:

- I.) amino acids with neutral side chain charge and hydrophobic (non-polar) polarity
- II.) amino acids with neutral and hydrophilic (polar) side chains
- III.) amino acids with acidic and hydrophilic (polar) side chains and
- IV.) amino acids with side chains showing basic and hydrophilic (non-polar) properties.

**Table 1 Proteinogenic amino acids, their abbreviations and side chain properties.** The three-letter code is universally accepted and used for protein and peptide sequence depiction, whereas one-letter notations are intended to facilitate the storage of sequence information and its comparisons using computers and databases.

Amino acid (AA)	3-letter code	1-letter code	Side chain	Side chain polarity and pH	Monoisotopic mass
L-Alanine	Ala	A	-CH <sub>3</sub>	hydrophobic, neutral	89.04761
L-Arginine	Arg	R	-(CH <sub>2</sub> ) <sub>3</sub> NH-C(NH)NH <sub>2</sub>	hydrophilic, basic	174.11161
L-Asparagine	Asn*	N	-CH <sub>2</sub> CONH <sub>2</sub>	hydrophilic, neutral	132.05343
L-Aspartic acid	Asp*	D	-CH <sub>2</sub> COOH	hydrophilic, acidic	133.03744
L-Cysteine	Cys	C	-CH <sub>2</sub> SH	hydrophilic, neutral	121.01969
L-Glutamic acid	Glu*	E	-CH <sub>2</sub> CH <sub>2</sub> COOH	hydrophilic, acidic	147.05309
L-Glutamine	Gln*	Q	-CH <sub>2</sub> CH <sub>2</sub> CONH <sub>2</sub>	hydrophilic, neutral	146.06908
L-Glycine	Gly	G	-H	hydrophobic, neutral	75.03196
L-Histidine	His	H	-CH <sub>2</sub> -C <sub>3</sub> H <sub>3</sub> N <sub>2</sub>	hydrophilic, basic	155.06941
L-Isoleucine	Ile	I	-CH(CH <sub>3</sub> )CH <sub>2</sub> CH <sub>3</sub>	hydrophobic, neutral	131.09456
L-Leucine	Leu	L	-CH <sub>2</sub> CH(CH <sub>3</sub> ) <sub>2</sub>	hydrophobic, neutral	131.09456
L-Lysine	Lys	K	-(CH <sub>2</sub> ) <sub>4</sub> NH <sub>2</sub>	hydrophilic, basic	146.10546
L-Methionine	Met	M	-CH <sub>2</sub> CH <sub>2</sub> SCH <sub>3</sub>	hydrophobic, neutral	149.05099
L-Phenylalanin	Phe	F	-CH <sub>2</sub> C <sub>6</sub> H <sub>5</sub>	hydrophobic, neutral	165.07891
L-Proline	Pro	P	-CH <sub>2</sub> CH <sub>2</sub> CH <sub>2</sub> -	hydrophobic, neutral	115.06326
Pyrrolysine	Pyl	O	-C <sub>12</sub> H <sub>19</sub> N <sub>2</sub> O <sub>2</sub>		297.34512
Selenocysteine	Sec	U	-CH <sub>2</sub> SeH	hydrophobic, neutral	168.05232
L-Serine	Ser	S	-CH <sub>2</sub> OH	hydrophilic, neutral	105.04253
L-Threonine	Thr	T	-CH(OH)CH <sub>3</sub>	hydrophilic, neutral	119.05818
L-Tryptophan	Trp	W	-CH <sub>2</sub> C <sub>8</sub> H <sub>6</sub> N	hydrophobic, neutral	204.08981
L-Tyrosine	Tyr	Y	-CH <sub>2</sub> -C <sub>6</sub> H <sub>4</sub> OH	hydrophilic, neutral	181.07383
L-Valine	Val	V	-CH(CH <sub>3</sub> ) <sub>2</sub>	hydrophobic, neutral	117.07891

\* If the amino acid type in the original protein can not be clearly identified as Asn or Asp, this ambiguity is indicated by Asx or B, whereas Glx or Z indicates Glu or Gln. The equivocality arises from the chemical hydrolysis of the peptide bonds which could also convert the Asn or Gln amide into the corresponding acid.

Proline is the only amino acid built by a secondary amine and is often chemically mentioned as an imino acid (Figure 2). It is an exception from the general amino acid formula owing to a side chain group linkage to the  $\alpha$ -carbon forming a heterocyclic structure which forces the peptide bond amide moiety into a fixed conformation. Its unusual structure is the reason why proline's  $\alpha$ -carbon is unable to donate a hydrogen bond for stabilizing an  $\alpha$ -helix or  $\beta$ -pleated sheet structure. Due to the lack of the hydrogen bonds proline can cause a slight bend in between  $\alpha$ -helices. As proline often occurs at final regions of  $\alpha$ -helices, turns and loops are common found structural shapes. Unlike other amino acids virtually provided in their *trans*-

isomeric form in polypeptides, proline can either exist in *trans*- or in *cis*-configuration. The *cis/trans*-isomerization can be a key influence on the folding of proteins.

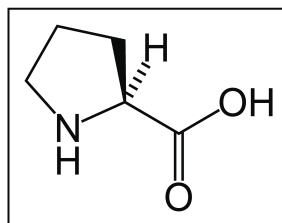


**Figure 2** Chemical formula of an L-proline (Pro/P) [21].

The primary protein structure is the linear amino acid sequence from the end where the amino group (N-terminus) is exposed till the end of the carboxy group (C-terminus). Yet this primary structure is still inadequate for explaining protein function and behaviour and are determined by the other levels of protein structures. The secondary structure refers to the manner in which a primary, linear polypeptide chain is folded owing to the formation of hydrogen-oxygen bonds between closely spaced amino acids of the same polypeptide chain. Two of these secondary structures are observable over certain regions of the protein. In the case of  $\alpha$ -helices hydrogen bonds are provided within the peptide chain, whereas  $\beta$ -strands are built from hydrogen bonds between two lengths of one polypeptide chain.

The biological properties of a protein are not determined by its primary or secondary structure, but by its three-dimensional shape (Figure 3). The unique molecular shape is dictated by the chemical attitudes of the amino acid sequence and the arrangement of the amino acid residues.

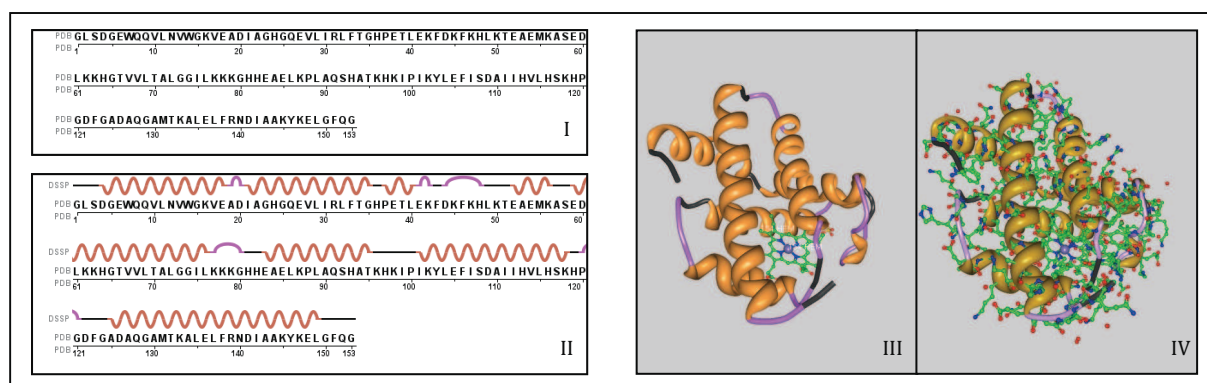


**Figure 3** The three structural shapes of horse heart myoglobin (>sp: P68082, pdb: 1WLA), a protein standard used for mass spectrometry analyses of undigested proteins in this thesis. Picture I shows the primary structure of the protein written in the one-letter code as used in the FASTA-format of the Swissprot database. The second picture also illustrates the secondary structure with helix-structures in brown, hydrogen bonded turns in lilac and the strands without secondary structure in black [23]. Pictures III and IV show two 3D models calculated by the RCSB – Protein Workshop Viewer [72].

Whole proteins or only regions of proteins may be hydrophobic, hydrophilic or amphiphilic because of hydrophilic side chains preferring surface location, while hydrophobic amino acids do not meet this precondition. Due to the make-up of their component amino acids proteins can be positively or negatively charged. Determined by the overall charge proteins can be characterized by distinct isoelectric points. In addition, protein residues can be chemically modified by posttranslational modifications. Beneath the peptide bond, electrostatic or hydrophobic interactions, hydrogen and disulfide bridges do have an influence on chemical and physical properties of proteins. Protein arrangement into stable, oligomeric complexes (quaternary structure) is the last biological process affecting the functional attitudes of a completed protein molecule. As a consequence protein function, stability and activity of proteins can be altered in many different ways and therefore the entity of protein structures and functions are almost unlimited.

A simple classification of proteins depends on a structural differentiation. Unconjugated proteins could be subdivided into globular and fibrously shaped structures. They can be distinguished from conjugated proteins with a non-protein moiety (prosthetic group), whereas the prosthetic groups could be defined via carbohydrates, lipids, metals, heme groups, phosphate residues or nucleic acids.

Depending on their actual state of function proteins can perform conformational changes. Physical and chemical attitudes can change owing to surrounding, external circumstances and influences. Protein charges are determined by the presence of free acidic and basic groups that are in turn influenced by the pH of a surrounding solvent. In case of acidic or basic properties hydration and solubility attitudes do strongly differ from one another. Especially the state of hydration depends on the net charge. A minimum degree of hydration and solubility could be observed with no net charge and therefore at the isoelectric point of the protein.

Solubility is the sum of amino acid composition, molecular shape and the physicochemical attitudes of the surrounding milieu (temperature, pH, polarity). Hydrophilic proteins tolerate aqueous layers and might be able to protect their hydrophobic counterparts by forming occlusion layers around them. The addition of salts or polar solvents could cause protein precipitation and is one attitude often used with purification, protein extraction and/or separation.

Denaturation is a characteristic feature potentially found amongst proteins. Exceptions do exist that are immune to chemical or heat treatment, but usually native structures (the 3D or quaternary one) are lost when a protein is exposed to heat, UV or X radiation, changes in the

pH or chemical detergents. Noncovalent bonds are degraded rearranging the protein into metastable forms. With the help of reducing agents even disulfide bridges can be broken down. Especially this kind of denaturation is often found to be reversible. Other treatments could be irreversible and result in completely disordered structures.

Due to their extraordinary importance during the malting and brewing process the protein family of enzymes will be described in short detail. Enzymes serve a wide variety of functions in all kind of living organism. Most enzymes show a homologue architecture consisting of a protein part, the apoenzyme, and a non-proteinogenous component (prosthetic group or coenzyme). A common definition often used for enzymes describes them as a protein catalyst that drives the degradation of organic macromolecules with very great specificity, but without being consumed itself.

Referring to the proteinogenic character enzymatic activity strongly depends on temperature. Maximum activity is achieved at optimal temperature. Enzymes do tolerate temperature differences within a typical temperature range, but most enzymes are no longer thermostable above 60 – 85 °C. Denaturation is a common consequence. Keeping in mind that the properties of the surrounding media (pH, acidity, ...) are of such great importance, enzymes are also sensitive to retardants. Heavy metal atoms or high alcohol concentrations could be inhibitory, even in combination with high temperatures.

### ***1.3 From malt to beer and beyond***

European bright beer (Pilsner) production traditionally relies on hulled, two-rowed barley (*Hordeum vulgare L.*). The literature often pays special attention to the following main stages of the beer production process: malting, mashing, fermentation and filtration. German breweries purchase their pre-malted barley with certain attitudes from malster's companies. Hence the actual brewing process ultimately starts with the mashing of the crushed malt. Once the starch is hydrolyzed into simpler soluble sugars the wort is separated. This wort, an aqueous mixture of soluble barley ingredients, is transferred to a kettle for the boil and addition of hops. The latter impart the characteristic bitterness and beer flavour. Yeast is pitched to induce the fermentation process after the wort has been cooled down. The simple, soluble and thus fermentable sugars created during the mashing procedure are metabolized and catabolized by the yeast and carbon dioxide and alcohol develop as well. After the fermentation process, cold storage, filtration procedures and bottling pave the way for marketing or shipping. Increasing demands are placed on product quality and shelf life,

accompanied by expanding market areas, output maximization and long distribution chains for export beers. That is also the point of analyses and academic investigations reaching beyond normal beer production. The extended time period from manufacture to consumption drives improvements in colloidal stability, raising an interest in the mechanisms of haze formation.

### 1.3.1 Barley (*Hordeum vulgare*)

The barley grain comprises a mixture of different chemical components in varying proportions. Beside the protein fraction, the substance classes listed in Table 2 could be used to characterize the grain. The protein content of barley ranges from 10 to 13 % dry weight [14, 41].

**Table 2 Composition of barley grain.**

Class	Barley components	Percentage of grain dry weight [%]
I	water	10 – 12*
II	polyphenols and bitter substances	0.1 – 0.3
III	small organic and anorganic compounds	2.4 – 3
IV	lipids	2.2 – 2.5
V	low molecular carbohydrates	1.4 – 2.6
VI	non-starch polysaccharides	10 – 13
VII	starch	60 – 65

\* [%] relating to the total moist mass of the barley and not the dried weight.

A closer look at the protein fraction requires a more precise specification either by the place of tissue origin and biological function or by the chemical attitude of solubility. Three groups can be distinguished:

- I.) Gluten, which is found in the aleurone layer serving an adhesive function,
- II.) Reserve proteins located in the outer part of endosperms (nutritional reservoir),
- III.) Histological or tissue proteins only found in the inner part of the endosperm.

Protein classification is also possible due to their solubility and extraction behaviour in a series of solvents (Table 3). These classical Osborne fractionation leads to four protein fractions which are extracted sequentially.

**Table 3 Classification of barley protein fractions.**

Protein fraction	Soluble in:	Tissue origin
Glutelins	alkaline/acidic solvent	protein reservoir of the outer endosperm
Prolamins	50 – 70 % (hot) alcohol solution	
Globulins	low concentration saline solution	tissue proteins of the starchy endosperm
Albumins	distilled water	

Albumins are extracted in water. The second fraction, the globulins, in dilute saline solutions like 0.5 M NaCl. In case of prolamin extraction alcohol/water mixtures can be used. Dependant on the kind of alcohol used, a more (50 – 60 % isopropanol) or less recent extraction (50 – 70 % ethanol) is achieved. The addition of reducing agents ( $\beta$ -mercapto-ethanol) supports solubilization of subunits which are stabilized by disulfide bonds. Otherwise these proteins might appear with the glutelin fraction that is only extracted after reduction of covalent disulfide bonds or denaturation. Extraction of the glutelin fraction is achieved by the use of acidic or alkaline solvents (e.g. 4 % sodium hydroxide) and can be even supported by chaotropic reagents like urea or SDS [41].

### 1.3.2 Malt production

Traditionally two-rowed barley (*Hordeum vulgare L.*) is used for the production of malt as a raw material for European bright beer. As part of the malting process the barley grain germination is induced under carefully controlled conditions. The nature of the malting process has an important bearing on the quality and beer brand as the malt contributes body, colour and beer flavour. The germination process harnesses amyolytic/hydrolytic enzymes, which are required to convert starch into soluble sugars. These sugars provide a nutritional reservoir for yeast fermentation later on in the brewing process.

During the steeping (hydration), the moisture content of barley grains increase under controlled conditions. A series of submersions and dry stands (air rest periods) raises up the water content from a starting value of 10 – 12 % to about 40 – 46 %. The germination setting in produces heat and carbon dioxide. Full hydration and first signs of tiny rootlets terminate this first part of the malting and lead to literal germination.

The endosperm of the grain consists of insoluble starch and offers the nutritional reservoir for germination. Two major reactions take place in seed growth and embryo development. Already existing, previously inactivated enzymes of the starchy endosperm ( $\beta$ -amylase and some carboxy-peptidases) and aleurone layer (endo- $\beta$ -1,3-glucanase, phytase, lipases and carboxy-peptidases) are activated and hormones like giberrellic acid (GA) are produced. The latter stimulate the production of further endosperm degrading enzymes in the aleurone layer ( $\alpha$ -amylase, limit dextrinase, glucanases, endo-peptidase, enzymes of the respiratory chain). These groups of hydrolytic enzymes either travel into the starchy reservoir, break down the starchy cell walls and change the starchs' attitudes from insoluble to soluble, or support tissue building (leaf and rootlets) in the embryo.

Germination is a critical step that needs to be carefully controlled. For economic reasons endosperm degradation should not exceed a minimum level (about 10 %) because enzymatic degradation will otherwise continue converting starch into sugars by total, the growth of the embryo will go on and brewing extract will be lost.

During kilning water is driven from the grain and the produced green malt is converted into friable dried malt. The heating operation blocks further endosperm modification, sugar conversion and prevents brewing extract. Hot air dries the grain to a residual moisture content of only 3 – 6 %. By varying the kilning temperatures and air flow different malt attitudes (colour and flavour) can be applied. After kilning the malt is preserved for storage. In an ideal case the enzymes will not resume their work until they are reactivated by renewed mashing in the brewery.

### **1.3.3 The brewing process – wort production**

Wort is an aqueous solution of soluble barley malt raw ingredients. Wort is produced in several stages like mashing, lautering and sparging.

The preparatory stage of the actual brewhouse mashing procedure starts with milling. Special attention is paid to keep flour production to a minimum, but at the same time ensure optimum kernel disruption and endosperm exposure, rendering these ingredients accessible for enzymatic activity. The beer used in this study was produced from raw materials that underwent a wet, squeeze-milling procedure. After the milling an infusion mashing system was applied to produce the wort.

Irrespective of the type of mashing procedure and system used, the main objectives remain the same. A number of mechanical, chemical and enzymatical actions take place to dissolve all soluble malt ingredients. Following the addition of water and heating, the starch grains swell up while gelatinisation sets in and enzymatic degradation is once more continued. The greatest attention can be placed on enzymatically driven reactions that render insoluble substances soluble and change the chemical structures of other malt constituents. The range of enzymes involved in the mashing procedure encompasses the amylase, endopeptidase and exopeptidase groups.

$\alpha$ - and  $\beta$ -amylase mainly convert the amylopectin and amylose of native starch into maltose and oligodextrins. The ongoing degradation of the latter also produces maltose and glucose units. In parallel, a proteolytic cleavage of proteins appearing as a mixture of nitrogenous components from a high molecular level down to individual amino acid elements, sets in.

## INTRODUCTION

---

Endo- and exopeptidases are the types of enzymes to be mentioned in connection with this process. But as a fact, the number of individual enzymes is enormous at specific amino acid cleavage sites. Endopeptidases dismantle genuine, macromolecular proteins (> 100 AA) down to the scale of polypeptides (10 – 100 AA) and oligopeptides (3 – 10 AA) and up to that of dipeptides.

A laboratory based, small-scale mashing procedure which is comparable to the large-scale brewing-house sequence is shown in Table 4 by way off an example. The laboratory congress wort procedure is used to determine the malt quality and is aimed at a much more effective, if possible nearly complete extraction of the barley components. The small-scale program includes all four resting periods and temperature changes, each of them influencing the enzyme activity and chemical reactions. The temperature and pH-changes during the mashing cause protein precipitation.

Once the starch conversion is completed, the temperature of the brewhouse mash is increased to the mashing out level (74 °C, with an additional rest), which ends with enzyme denaturation and the preparation of the mash for lauter transfer.

**Table 4 Congress wort mashing program (laboratory scale).**

Description	Temperature profile	Time [min]	Description
<b>Mash-in</b>	45 °C	0	preheated water
<b>Enzyme rest</b>	45 °C	60	degradation of cellulose by $\beta$ -glucanase, start of protein degradation by endoproteases
<b>Heating</b>	up to 70 °C in 25 mins	85	1 °C/min raise, prevents enzyme degradation protease activity until optimal temperature is passed start of $\alpha$ - and $\beta$ -amylase activity
<b>Rest</b>	70 °C	120	saccharification or $\beta$ -amylase stand start of enzyme-inactivation/denaturation, (preparation for mashing out)*
<b>Cooling</b>	to 20 °C	135	preparation for laboratory tests

\*final mashing stage in real brewhouse procedures: the temperature is raised again to 74 °C and another 10 minutes rest follows before the lauter tun transfer starts.

The mash is then transferred to a lauter tun to extract the wort. In a first step the first wort is separated by lautering, then the remaining wort is flushed from the spent grains in a second step (sparging). The separated and diluted wort is collected for boiling in the next stage. The remaining spent grains largely consist of husks, protein components, with little starch and few minerals. Owing to its still high nutritional value (energy content), the draff is often used as animal feed or for energy production.



### 1.3.4 The brewing process – boiling the wort and adding the hops

Following lauter transfer into the whirlpool, wort boiling is the next step in the brewing procedure. In addition, hops are added to the first wort during the boil. These activities mainly aimed at the following objectives:

1. The water loss in the boiling process allows the wort concentration to be adjusted. Excess water is lost through evaporation. A final adjustment is possible by water blending at the end of the boiling interval.
2. The heating procedure on the one hand inactivates the enzymes irreversibly and stabilizes the wort via sterilization on the other. Coagulable protein components could be removed as a kind of hot break. These reactions could all be subsumed under the generic term of wort stabilization. The destruction of the enzymes is aimed at preventing undesirable carbohydrate breakdown later on in the brewing process ( $\alpha$ - and  $\beta$ -amylase, as well as most of the enzymes that survived the mashing procedure are deactivated), while the colloidal stabilisation is a natural reaction to the high temperature and changes in the pH value, causing the precipitation of unstable proteins.
3. Hops are mainly added for flavour and an adequate extraction of the hops aroma components (bittering substances) are one of the main aims of the process. Other characteristic features of the hops are their usefulness for protein precipitation (coagulation) and the preservation of the product. Although the aroma development superficially depends on the hops dosage, there are also volatile flavours that derive from the barley and result from the malting procedure. The conventional pharmaceutical hops used in breweries come in form of hop pellets or extract hops. Combinations of both bitter and flavour hops dosages can be found in beer production. The overall composition of hop materials varies depending on the type, vintage, provenance, date of harvest, storage and conditioning method. The soft resin contains bitter acids (humulone and lupulone), which are thought to be the typical representatives of bitter substances. Two related series of hop acids do exist. Humulones with two dimethyl-allyl-lateral chains, so called  $\alpha$ -acids, can be differentiated from lupulones with three dimethyl-allyl-lateral chains called  $\beta$ -acids. Four additional analogues of the initial chemical shape have been characterised: co-, ad-, pre- and post-humulone or lupulone, respectively. Polyphenols and the essential oil fraction (more than 300 flavour components) are further important hop substance classes. The flavour associated with hops at first is the bitterness caused by iso- $\alpha$ -acids.

4. Hops and hot break removal is the last step of wort boiling. The type of hops used determines the manner of removal. In the case of pelletized hops the rotation principle of the whirlpool allows suspended particles to be separated. As the wort begins to rotate, solid particles travel into a trub cone in the center of the kettle while the whirling wort is transferred to tanks.

The boiling procedure can feature many modifications depending on the brewery, the type of beer produced and regional differences. The beer analysed in this thesis underwent a lauter transfer into a whirlpool with first dose of hop pellets ( $\alpha$ -acid bitter and  $\alpha$ -acid flavour hops) applied in parallel to the filling procedure. Internal boiler heating with vapour compression and calandria transfer for wort boiling were used. The second and third  $\alpha$ -acid flavour hops doses were added at the beginning and halfway through cooking process.

### **1.3.5 The brewing process – fermentation**

Anaerobic respiration in the form of alcoholic fermentation is a key process in any brewery. Yeasts ferment sugars to produce alcohol (ethanol), carbon dioxide and energy ( $\approx 97$  % heat development and  $\approx 3$  % ATP-storage). Fermentation depends on many parameters including the type and viability of the yeast itself, the composition of the wort, the quantity and composition of the yeast nutrients and the processing parameters (providing an enormous range of time, temperature, volume and pressure combinations).

The type of brewers' yeast depends on each brewery, as they often use their own yeast strains. Certain biochemical and physical attitudes match the desired fermentation pattern. The strains must be clean and sanitary to keep bacteria or wild yeasts from adulterating the wort. The yeast is cultivated in yeast propagating vessels. Irrespective of the yeast type all yeast strains feature a large compendium of enzymes including all six groups of IUPAC nomenclature. These enzymes play a part in the nutrient uptake, synthetic reactions, growth, metabolism and cell reproduction. Wort fermentation strongly depends on the pitching rate and condition of the yeast, i. e. its age or the number of the used yeast cycles and hence yeast vitality (age of the yeast, cell autolysis).

The composition of the wort is the second key parameter determining the degree of fermentation. The pH-value, redox potential, type and number of nutrients, temperature and degree of aeration will be pre-determined by the wort. For yeast nutrition carbohydrates are the first to name. The carbohydrates glucose, fructose, sucrose, maltose and maltotriose are fermentable by brewers' yeast, whereas dextrans (low and high molecular ones),  $\alpha$ - and  $\beta$ -

glucans are largely unfermentable. The nitrogen content is a second key concern for yeast and of great importance to yeast reproduction. Starting with the assimilation of small peptides at the beginning of the fermentation process, the main nitrogen source for yeast protein generation during fermentation is provided by amino acids. Proline is the only amino acid in wort that is not consumed by yeast owing to a lack of permeability and transport into the cell [20]. Adequate aeration affects the fatty acid metabolism. A small amount of unsaturated lipids is required to prevent yeast autolysis. In addition, the aeration is of great importance at the beginning of the fermentation process because the oxygen will be almost completely consumed by dissimilation during yeast growth and reproduction. Vitamins acting as growth regulators and minerals are the last groups of components needed for proper yeast growth. This large number of different substances is found in wort in adequate trace amounts.

Fermentation by-products are a natural concomitant of anaerobic respiration. Higher alcohols, ester, aldehydes and vicinal diketones are metabolic products affecting the flavour and taste of the beer. A large amount of tanning agents and polyphenols is lost in fermentation because of changing pH-values and subsequent precipitation, which is another aspect influencing the aroma and taste.

The fermentation process of the beer used in this study starts with the transfer of the hopped wort from the whirlpool into open starting vessels. The wort is pitched with yeast and is subjected to a procedure called „Drauflassverfahren“. Following the removal of the cold break the actual primary fermentation, a pressure fermentation process, starts. Before the filtration the green beer passes through a two-stage cellar process. A two-tank procedure is applied for ongoing fermentation and maturation on one hand and cold storage on the other.

### **1.3.6 The brewing process – filtration**

Although a secondary fermentation results in a kind of natural purification, its degree is inappropriate for bright beers and marketing demands. Clarification can be accomplished by a combination of several filtration steps and flash pasteurisation, as was the case with our beer.

The stabilisation process can be subdivided into four steps:

1. pre-clarification by a separator (physical separation taking advantage of centrifugal force and sedimentation)
2. filtration via a kieselguhr cartridge filter (in combination with a PVPP stabilisation filter)
3. flash pasteurisation (KZE)
4. and sheet filtration as a conclusion.

Filtration is the process step required to lend the beer clarity, one of the quality aspects demanded for distribution and sales. The filtration process is aimed at removal of yeast cells, coagulated proteins, protein-tannin-complexes (colloids), hop resins, barley gums and even beer-spoiling microorganism.

Pre-clarification helps improve the life cycle of kieselguhr filter systems, especially with very hazy beers. The primary filter cartridge material is kieselguhr (silica), which could also be described as skeletal remainders forming a diatomaceous earth naturally deposited on ocean floors (Figure 4). In literature this kind of primary filter aid is often said to remove proteins, especially haze-active proteins with high levels of proline, glutamine (> 30 %) and polypeptides [10, 11, 13]. The adsorptive effect depends on the number, size, size distribution and type of functional groups exposed on the silica surface [19]. In theory the combination with a PVPP stabilisation filter unit should lead to the best known removal of colloidal protein-polyphenol-complexes achievable so far [10, 11, 13, 19].

In flash pasteurisation the beer is heated to a maximum temperature of 72 °C. In-house experiments have shown that heat treatment leads to a more stable product during cold storage with greatly reduced haze production. KZE is one of the options for directly influencing a product's shelf life, which might be explainable by  $\beta$ -glucosidase denaturation [40].

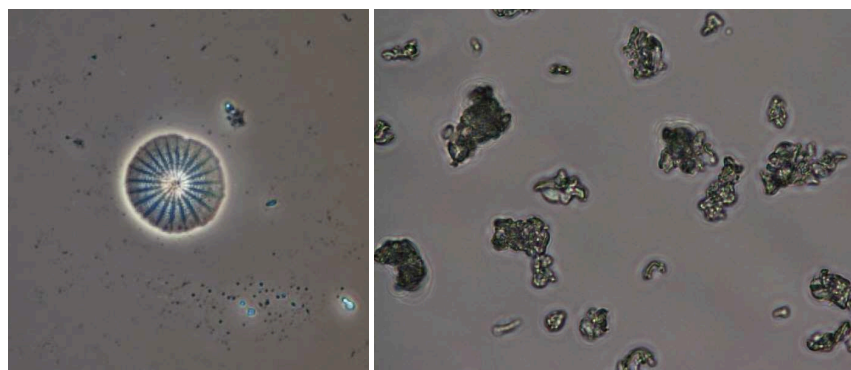


**Figure 4** Light microscopy pictures of a Celite stabiliser on the left and PVPP on the right. Both stabilisers were observed in water suspension and enlarged 20-fold.

The secondary filtration step involves sheet filtration and concludes the stabilisation procedure. The clarification level depends on the stability of the pressure profile and the preceding filtration steps.

The finished beer is now ready for filling, a first or in some cases second pasteurisation, depending on the brewing process, followed by its distribution, sale and ultimately consumption.

### 1.3.7 Bright beer

As already mentioned above, the foam head and clarity are two of the first characteristics by which consumers, but also manufacturers, assess beer quality. Standard laboratory analyses are meanwhile performed for quality assurance. The density, pH-value, extract, bitter units, alcohol content, colour, foam Nibem, carbon dioxide and oxygen content, free amino nitrogen, total and soluble nitrogen, but also higher alcohols, vicinal diketones, esters, amino acids or aldehydes can be routinely determined. Microbiological standard tests also exist. The following table (Table 5) summarizes some typical "Pilsener" beer values, analysed with standard laboratory tests.

**Table 5 Chemical attitudes of a standard bright beer.**

Test	Value	Unit
Density [20°C]	1.00776	[g/ccm]
Extract	11.29	[%]
pH	4.43	[pH]
Foam Nibem	95/191/277	[10 s <sup>-1</sup> ] / [20 s <sup>-1</sup> ] / [30 s <sup>-1</sup> ]
Colour	6.7	[EBC]
Alcohol	4.92	[Vol. %]
CO <sub>2</sub>	5.18	[g/L]
Total O <sub>2</sub>	0.05	[mg/L]

Taking a closer look at the protein content, not many tests are applied for either deriving the protein volume indirectly (total nitrogen, free amino nitrogen analysis, Kjeldahl-method, coagulable nitrogen, turbidity measurement following addition of tannic acid for artificial haze development) or direct measurement using colorimetric protein assays (spectrophotometric methods). The information available in literature puts the average beer protein content in the range of 380 mg/L, estimated by Bradford-Assay, to 500 mg/L, the exact method not being mentioned, while general nutritional values are ranked around 3 – 5 g/L [35, 27].

The information available on a molecular level is scant, with only occasional structural identifications of beer proteins. These protein species are often referred to in beer foam theory to explain foam quality, stability and adhesion and are therefore called foam-positive proteins. They are thought to be equally implicated in the production and stabilisation of foam. Foam develops in four phases with fluid transitions (a mechanism that will also be important for the gushing phenomenon to be discussed later):

1. bubble formation with nucleation sites (any kind of source, but as small as possible to provide a homogeneous distribution)
2. creaming (rising of the bubbles)

3. disproportion (fusion of bubbles)

4. drainage (liquids start to drain)

The sources of nucleation “germs” differ and include polypeptides, dragged air, metal ions, iso- $\alpha$ -acids, melanoidins and carbohydrates [12, 41].

Protein Z4, protein Z7 and nLTP1 (non-specific lipid transfer protein 1) are the proteinaceous key contributors to consider, when speaking of foam-promoting proteins. The common explanation found in literature refers to their ability to interact with hop acids, resulting in a stable foam [10, 11]. Protein Z4, Z7 and nLTP1 are members of the hordein storage protein family. Structural and chemical modifications brought about in the brewing process by the unfolding of the structure, lipid adduction, acylation and glycation are thought to increase their amphiphilicity, leading to foam-promoting forms [28, 32, 34, 35, 37].

A number of foam studies is based on protein separation via 1D- or 2D gel electrophoresis. They were able to show that the majority of proteins can be displayed with three fractions: the first at 7 – 15 kDa, a second distinct fraction around 40 kDa and the largest above 90 kDa [28, 31, 34]. Leiper *et al.* found glycosylated proteins in beer foam, including nLTP1 and protein Z. They were glycosylated with varying amounts of hexoses and pentoses. Their findings only indicated the directly involvement of nLTP1 in foam stability, whereas protein Z (in its pure form) appeared to serve no direct function. The results for nLTP1 find support in the mass spectrometrical analyses and results of Perrocheau *et al.* and Jegou *et al.* [37, 53, 54].

Hao *et al.* compared the protein content of foam and beer on one hand and made a further distinction between the 7 – 17 kDa and 40 kDa band on the other. The combination of protein separation with SDS-gel electrophoresis and structural protein identification via mass spectrometry revealed a much larger amount of beer and foam related proteins. About 30 proteins were identified, 15 of which were found both in beer and foam. These proteins included the classical protein Z and nLTP1, but were mostly water-soluble (with the exception of two hordeins) [34]. The approach used in Hao’s study applies a classic proteomic strategy and is hence one of only a few methods (see also Perrocheau *et al.* [55]) that would be comparable to the approach pursued in this thesis, thus enabling direct comparisons of the protein results for beer. Although foam or foam stability are not the subject of this thesis, the main proteins to be mentioned in this context are nonetheless important, as they will be reappear in other beer related phenomena (haze development, gushing). It is impossible to strictly separate the functions related to these proteins by only taking them into account for one quality aspect. The quality of the foam and the maintenance of foam proteins will for example always have to be taken into consideration, even when

trying to eliminate proteins in the brewing process in order to reduce haze formation. Both aspects have a great economic impact because of the constliness of the breweries' stabilisation and filtration efforts in this respect. The real paradox or contentious issue regarding the filtration procedure will hence remain the prickly question of either supporting the foam quality or preventing haze formation.

### 1.3.8 “Going beyond” – colloidal stability and haze formation

The formation of haze is a serious quality problem for bright beers and particularly evident in their bottled form (Figure 5). In storage, products that were originally clear right after the packaging can develop chill-haze, which may result in permanent turbidity. Colloidal stability is of great importance here as it determines the shelf life of the product. Consumers moreover judge the quality of their beer from its immaculate visual appearance, which needs to be maintained right up to the expiration date. Haze formation is an interesting topic and the subject of academic research, even for long distribution chains of export beers that tend to be consumed near the end of their shelf life and are increasing their market share with very high cost pressures.

The discussion revolves around three main types of haze nowadays, biological contamination having fallen by the wayside in recent years. Pseudo-haze, an invisible form, may consist of very small particles, which are attributed to carbohydrates, oxalate, residual starch or proteins from damaged yeast, dead bacteria from the malt or  $\beta$ -glucan from inadequately modified malt. With 90° angle light, measurements show high light scatter (Figure 5).



**Figure 5** Haze at the bottom of a bottle: a.) chill haze after about 4 weeks of storage at 0 °C (left) and b.) permanent haze after longterm cold storage at 0 °C (right). Chill haze is a reversible type of haze that dissolves again after warming to room temperature. The particles range from 0.1 to 1  $\mu\text{m}$  in size and their control is important as they are regarded as inducers of permanent haze. The enormous amorphous haze here is a characteristic feature of the beer used for this thesis. In the literature particle sizes range from 1 to 10  $\mu\text{m}$  [9].

Similar sources are mentioned in connection with visible hazes, but normally both chill and permanent hazes are said to depend on protein-polyphenol interactions [8, 9, 29]. Chill haze, the unstable form, is thought to result from the hydrophobic bonding of polyphenols with low molecular mass and proteins. Permanent haze (evident even at 20 °C) is instead said to be formed by interactions between polymerized polyphenols and proteins, while the polyphenol polymerization is thought to be promoted by oxidative reactions, acid catalysis, enzymatical reactions, oxygen during wort boiling (in combination with Maillard-reactions), or by metal ion induced oxygen radicals (hydroxyl radicals, developing from Haber-Weiss and Fenton reactions) [1 – 3, 9, 19, 30]. The most commonly stated opinion therefore holds a protein polyphenol interaction responsible for haze formation. The efforts of the brewing industry are aimed at minimizing one or both of these components by filtration through PVPP (polyvinyl-pyrrolidone) and diatomite (Celite). In theory, the latter selectively removes proteins which may include haze-active (HA) proteins, whereas PVPP is used to remove HA polyphenols. The main disadvantage of using those stabilisers (mainly PVPP) is their high costs connected.

So both in terms of quality improvement and cost reduction, detailed knowledge of the haze formation process may be helpful in optimising the stabilisation treatment.

Regularly cited haze model developed in recent years focus on reactions taking place between HA polyphenols and HA proteins (or their fragments). High levels of proline are mentioned as characteristic of HA proteins [8, 10, 11, 27]. The special pyrrolidine ring structure causing unfolded molecular protein regions may also facilitate the entry of polyphenols into the protein backbone. HA polyphenols are thought to interact with binding sites of the HA proteins to form intermolecular bridges via:

- a. hydrogen bonding, between the oxygen atoms of peptide bonds and hydroxyl groups of polyphenols
- b. hydrophobic interaction, between hydrophobic amino acids and the ring structure of the polyphenol groups or
- c. ionic bonds between positively charged protein groups ( $\epsilon$ -NH<sub>2</sub> groups of lysine) and negatively charged polyphenol groups [8, 13, 16, 17].

In this regard the haze models of Haslam, O'Rourke, Siebert, Beart, Gracey and Kaneda propose the most popular mechanism [see 13, 16 – 18, 25, 41, 42].

The protein-polyphenol composition of beer has been reviewed extensively and conclusions often refer to this mechanism owing to the ability of HA components to form hazes with each other in model reactions. As a result these interactions have been assumed to be responsible



for haze reactions in beverage containers, too [13, 16 – 18, 30, 43, 44]. But as a matter of fact, the exact mechanisms and involved components are unknown to this day. Polyphenol polymerization may not be the only way to achieve a permanent haze. The initial haze nucleus (germ) is thought to be the key factor. Compounds involved in haze formation might only accumulate on haze germ surfaces in disperse systems like beer, without actually playing an active part in it (means being haze-active). Thus the formation could be a physico-chemical interaction, a result of particle concentration, agglomeration (following DLVO-theory's) and Brown's molecular movement. A haze formation scheme is given below without referring to a concrete mechanism.

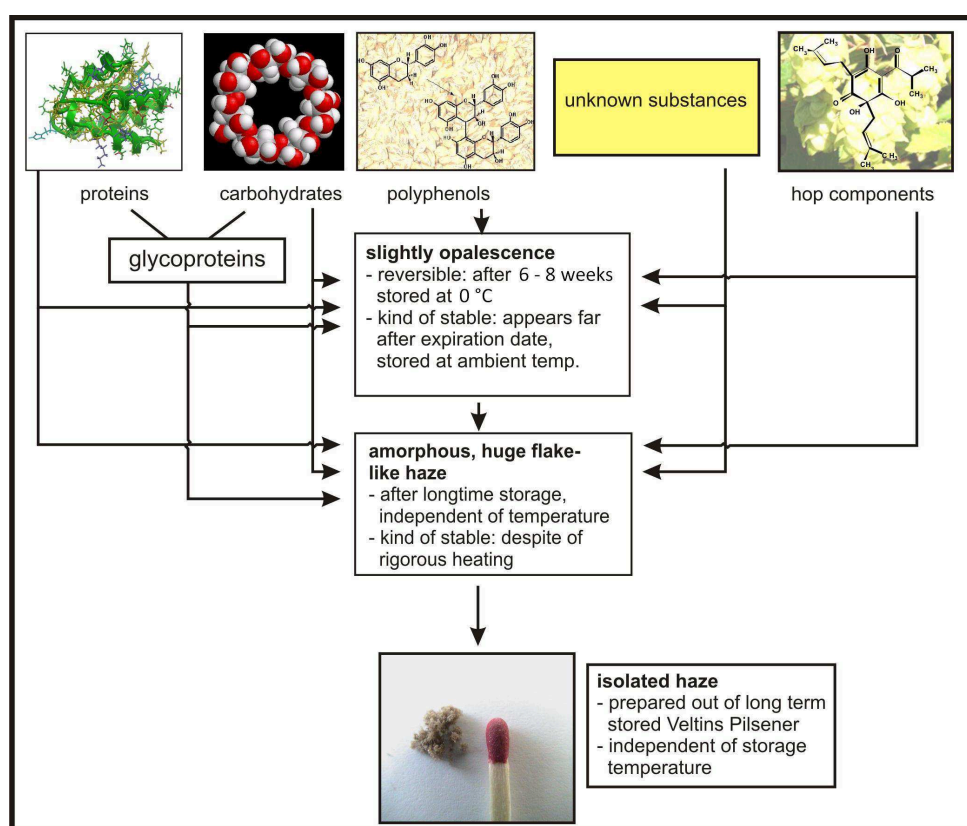
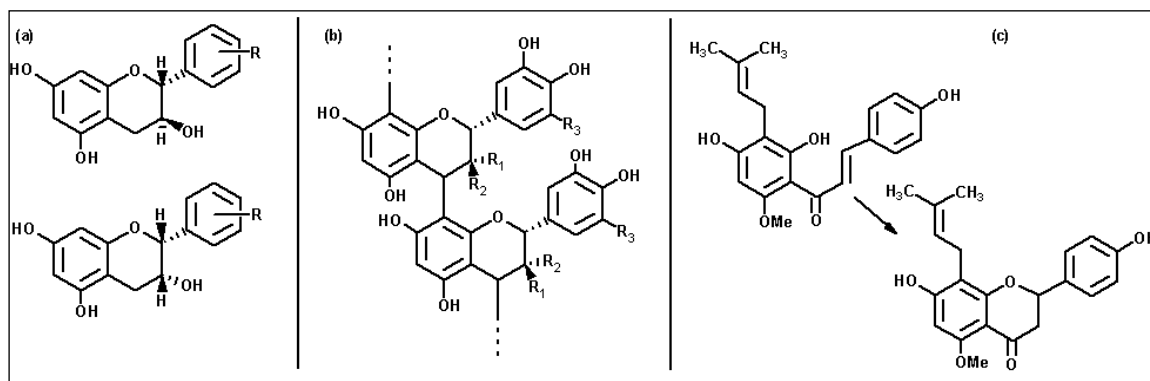


Figure 6 Modell of haze formation [40].

Taking a closer look at the phenolic components first, sources are found in both malt and hops. The substance class of polyphenols has a really high diversity. Regarding beer and haze certain flavanoids such as flavan-3-ols catechine, epicatechine, galocatechine and epi-galocatechine, phenol carboxylic acids like gallic acid and vanillic acid, as well as prenylflavanoids like xanthohumol and isoxanthohumol are mentioned [30, 46 – 51]. Polymeric polyphenols (proanthocyanidins) usually occur as dimers, trimers and polymers of the flavan-3-ols or flavanols [45]. The most popular representatives in beer are the dimers

procyanidin B<sub>3</sub> and prodelphinidine B<sub>3</sub> [45, 50, 51]. Proanthocyanidins are considered to be the most important agents for haze formation (Figure 7) [8, 9, 41, 44].



**Figure 7 Chemical structure of polyphenols.** a) the Flavan-3-ols: (+)-(gallo)catechine (the upper structure) and (-)-epi(gallo)catechine, b) procyanidine with R<sub>3</sub> = H; catechin (R<sub>1</sub> = H, R<sub>2</sub> = OH) and epicatechin (R<sub>1</sub> = OH, R<sub>2</sub> = H); prodelphinidine with R<sub>3</sub> = OH: gallocatechin (R<sub>1</sub> = H, R<sub>2</sub> = OH), epigallocatechin (R<sub>1</sub> = OH, R<sub>2</sub> = H), c) prenylflavanoids: xanthohumol and isoxanthohumol.

In-house analyses of chill haze and permanent haze neither found any signs of malt-derived monomeric polyphenols (epicatechine, catechine) nor their polymeric structures (procyanidin, prodelphinidin etc.). The results instead indicated the involvement of hop components such as the prenylflavanoids xanthohumol and isoxanthohumol, as well as  $\alpha$ - and  $\beta$ -acids [40].

The discussion of haze proteins is also highly controversial, starting with the question of whether foam-active and haze-active proteins can be clearly distinguished and ending with protein analyses/identifications often do not using chill or permanent storage haze, but hazes of the filtration process.

During the malting and brewing process the original barley proteins are thought to be chemically modified and to be subjected to proteolysis, resulting in mixtures of modified and unmodified polypeptides (high to low molecular masses), oligopeptides, and amino acids. Regarding the literature Maillard reactions do occur during malting and wort boil, but also continue even when stored in low temperature [37]. Reducing sugars and amino compounds, such as amino acids or proteins, are thought to participate in these non-enzymatic browning reactions comprising highly complex pathways that are not yet fully understood. As a result glycosylation of proteins from reactions with terminal  $\alpha$ -NH<sub>2</sub> groups and/or  $\epsilon$ -NH<sub>2</sub> groups of side chain lysine's may be possible [1 – 3].

The barley albumin proteins Z and nLTP1 were the first beer proteins to be characterized and have been related to haze formation and foam stability in equal measure [8, 34]. Besides the proteins Z and nLTP1, a variety of hordeins, the predominant barley storage protein family with high levels of proline and glutamine, were said to be involved in haze formation [8, 10,

27]. The barley trypsin inhibitor CMe precursor (IAAE, chloroform/methanol (CM) soluble) was identified in eluates of silica filter aids. Beer of a CMe band lacking barley cultivar showed less haze. Therefore this protein was grouped with the haze-active proteins [11].

Various tests were performed with silica eluted protein and beer proteins after (immuno) precipitation. These protein fractions were further separated by gel electrophoresis. A small number of proteins could be allocated to typical, well-known molecular mass fractions (ca. 10 – 15 kDa, around 40 kDa, and 90 – 1000 kDa), but clearer identification proved impossible given the lack of more varied barley protein standards or structural protein identification via mass spectrometry. Two important glycoproteins measuring 16.5 and 30.7 kDa were found by Leiper *et al.*, but could not be attributed to specific proteins [27]. Omura *et al.* applied affinity blotting and identified mannoproteins derived from yeast cell walls to be amongst the constituents of beer haze particles [52].

A combination of 2D gel electrophoretic separation and mass spectrometric analyses was used by Iimure and collageous [56]. They investigated the protein content of isolated beer haze and proteins adsorbed by silica gel (an approach usually referred to remove haze-active proteins). Their results include a protein classification to haze-active, moderately haze-active and haze-inactive proteins. Haze activity was found for BDAI (barley dimeric alpha-amylase inhibitor), CMb (component of the tetrameric alpha-amylase inhibitor) and the aforementioned CMe. Protein Z4, protein Z7 and nLTP1 were identified as moderately haze active. In addition the proline content of beer proteins, beer haze proteins and silica-eluted proteins was estimated. While high proline contents could be supported in silica eluted proteins, it was the other way round with haze proteins. Values of haze samples varied in a wide range giving both the highest and lowest proline levels in the study.

#### **1.4 Gushing**

Gushing is commonly defined as a spontaneous, heavy overflow of the beverage right after the bottle is opened despite it having been stored at appropriately cool temperatures and in absence of any kind of agitation. Overfoaming can occur at exactly the moment the bottle is opened or immediately afterwards (Figure 8). The phenomenon has been known for long time and is not exclusive to beer. In commercial terms it represents an additional quality issue.

Two gushing types can be distinguished:

1. Primary gushing, a type of malt related gushing
  - caused by fungal contamination, fungus-derived metabolites and gushing factors.

2. Secondary gushing, a non-malt related type. A rather technical/mechanical effect, which could be caused by processing-related factors such as:

- calcium oxalate formation
- damaged or rough bottle surfaces, damaged crown caps
- over-carbonation
- foreign particles (packaging materials, tenside residues or filter breakthrough)
- excessive haze
- metal ions
- narrow bottle neck designs, acting as a speeding orifice
- shaking and/or differences in temperature

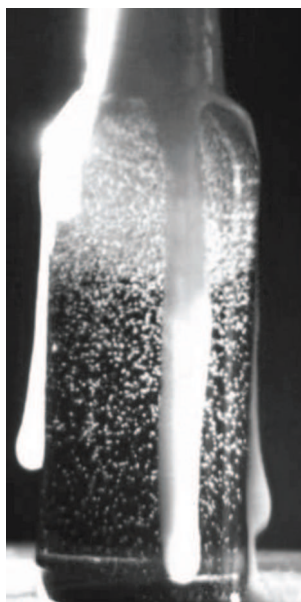


**Figure 8** Snapshot of a gushing beer.

Technological parameters are well-known and adjustable in the brewing process, hence providing an opportunity for counterreaction and prevention during beer production. But the gushing germs discussed in the context of primary gushing, in contrast, still harbour scope for research. At the moment no secure prediction method exists for the gushing tendency of malts. The quality of the malt is assessed by “Modified Carlsberg-Tests” in standard testing, but there is no possibility of tracing or directly affecting parameters which promote gushing.

One known fact about gushing is that the tendency to overfoam is stronger after rainy summers. This phenomenon was also observable in the dramatically boosted gushing tendency of brewing malts in central European countries such as Germany in 2008. This had been preceded by a year with unusual climate. While April 2007 had still been nearly dry and very warm, May and the summer months brought more rainfalls and lower temperatures than

the respective averages. The harvested barley and subsequent malts therefore showed a number of conspicuous problems and variations in quality. The following tendencies were noticeable in respect of the quality of the malt:

- more red and/or black grains (Figure 9)
- higher protein content
- lower sorting grade with smaller diameter and more strip waste
- lower extract yield
- slightly more soluble nitrogen
- higher percentage of partly glassy kernels
- higher percentage in end fermentation
- slightly more of  $\beta$ -glucan
- higher mycotoxin contents (desoxynivalol) but no distinct relationship traceable in comparison to standard Carlsberg-Tests (the standard test for gushing prediction).



**Figure 9** Red and black grains observed with mould infection of malt raw material during gushing period 2008.

In principle fluctuations in analytical malt values are owed to microbial diseases and infections (moulds, yeast and bacteria) of weathered barley plants and grains.

1. In the cultivation period the degradation caused by field fungi (*Fusaria*, *Stemphylium*, *Alternaria* or *Cladosporium*) could affect each stage of plant development (Figure 10).
2. In storage the same role could be played by storage fungi like *Aspergillus* or *Penicillium*.
3. Malting stimulates the growth of both field and storage fungi a quickly expanding population of malting fungi (*Mucor*, *Rhizopus*, ...).

The selected microbial species only show a small section of the highly diverse barley mycoflora (more than 150 species of filamentous fungi and yeasts have been found to act as surface contaminants or internal invaders [57]). Mycotoxin production as a gushing indicator

is a hot topic as far as microbial producers are concerned. Although intense attention had been focused on the mycotoxin Desoxynivalol (DON) in the past, no distinct DON correlation was observable in the high-gushing period 2008 (neither with the standard gushing test nor single microbial producers). With about 400 mycotoxin types known today they can of course not be entirely excluded, especially given their characteristic traits such as survival on cereal grains and high stability.

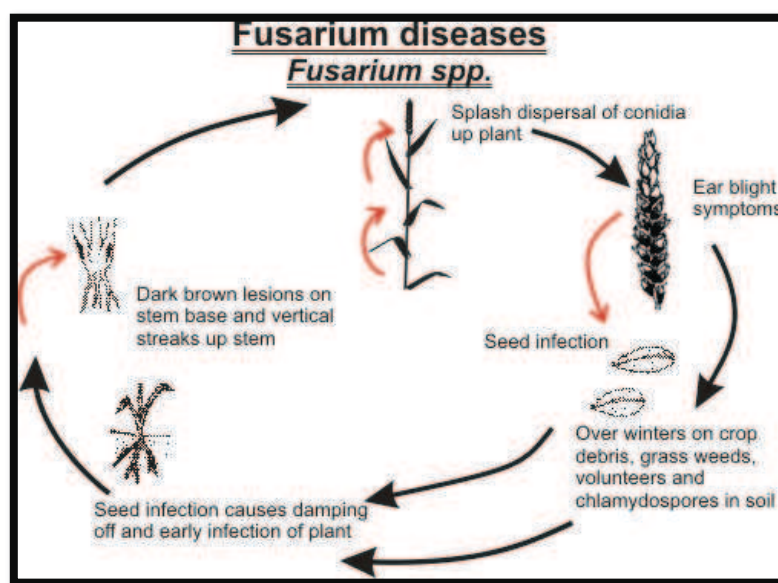


**Figure 10 Infection modi/symptoms following *Fusarium* infection of cereals [24].** Each plant development stage could be affected. Primary seedling sources are contaminated crops and spores or chlamydospores found in soil. Basic stem base infectants are conidiospores from harvest residues. Ear infections can result from two different mechanisms: a.) air transport by wind transport from residues and b.) incremental splash dispersal of conidia by rain drops from the ground across the stem and leaves (might not leave any further decay symptoms on these plant parts).

In recent years the research has been focused on *Fusarium* fungi in the barley ecosystem. They are distributed worldwide and known as harbingers of "Fusarium Head Blight" (FHB), significant enzyme production and quality issues (qualitative/quantitative changes in grain components, production of toxic metabolites and factors that promote gushing, less germination). Together with a small number of the aforementioned species, metabolites of these microbes of proteinaceous, glycopeptide or peptide character are summarized under the term gushing factor. Properties of proteins include hydrophobicity, common cysteine residues (pattern), production and secretion by fungi. The very first gushing factor was mentioned by Amaha in the 1970's and was classified as a "Nigrospora Gushing Factor" (NGF). The following attributes were assigned to the hydrophobic polypeptide: a molecular mass of 16.5 kDa, isoelectric point of 4.0, water-solubility, heat stability, surface activity and protease resistance. Later on it was estimated that this protein might be a dimeric hydrophobin [67].

Hydrophobins, a class of small proteins expressed by fungi, were not identified until the 1990's. Their molecular masses range from 7 – 20 kDa ( $100 \pm 25$  AA) [67 – 70]. Again hydrophobicity, surface activity caused by self-assembly into amphiphilic films between phases (interphases) and fungal secretion are determining characteristics. The strong surface activity resembles an interwoven rodlet structure [4, 5, 33]. By virtue of their rough surface rodlet layers may serve as gushing germs for CO<sub>2</sub> bubbles or may stabilise gas bubbles in the fluid. In this context carbon dioxide is not the primary gushing factor, as the presence of condensation nuclei seems to be essential once more. Nucleation seems to occur by micellation of surface-active substances and CO<sub>2</sub> is the forcing agent by then. As long as the exact mechanism is unknown gushing could be simply described as an imbalance of the factors promoting and preventing it.

Fungal infections were referred to as being stress inducers for increased synthesis of nLTPs in grains. The brewing process offers possibilities to further modify (by glycation for example) these proteinaceous gushing factors later on. Weideneder *et al.*, as well as a Japanese research group isolated several kinds of secondary gushing factor whose attitudes were assigned to the family of non-specific lipid transfer proteins (nLTP) [5]. While the factors isolated by the latter research group originated from wort, Weideneder isolated fractions of gushing inducing substances from wheat and then transferred the results to beer. Due to the N-terminal signal peptide and localization in extracellular layers/cell walls, protein secretion was assumed to be a response to fungal infection and/or abiotic environmental stress. Two possible mechanism are:

- a.) up-regulation of nLTP1 genes in the barley embryo as a result of infection stress or
- b.) release of cell wall bound nLTPs because of microbial metabolic activities [5].

Hipelli *et al.* also predicted nLTP enrichment following *Fusarium* decay and gave a hint to the development of highly surface-active peptides from protease degradation of nLTP, glycosylated nLTP and other protein species. Rising concentrations of peptide condensation nuclei seemed to be the drivers of unhindered CO<sub>2</sub> bubble release.

### ***1.5 Barley protein species and classes***

#### **1.5.1 Barley and malt protein classification**

In barley seeds approximately half of the total protein content is provided in the form of storage proteins, synthesized or released during seed development and broken down during germination to support early seedling growth [14, 58]. In dry weight the storage proteins



content is about 10 – 12 %. The simplest barley protein classification is the differentiation between functional and storage proteins. While functional proteins have a specific function in seed development or germination, storage proteins provide a carbon, nitrogen and sulfur reservoir. A more exact and commonly used definition was applied by Osborne. Barley proteins are divisible into four classes by their chemico-physical attitudes [14, 15]:

1. albumin: the water-soluble protein fraction
2. globulin: soluble in saline solutions
3. prolamin: the so called hordein, soluble in aqueous alcohol
4. glutelin: main fraction of the barley prolamine, soluble with acidic or alkaline solutions.

Classical albumin storage proteins with typical sedimentation coefficients of 2 Svedberg units (S) have not been characterized from monocots and the poaceae family (barley, wheat, rice), but from seeds of many dicot plants. A wider comparison demonstrates that 2 S albumins belong to the larger group of the prolamin protein superfamily. These proteins have a characteristic pattern of cysteine residues and comprise  $\alpha$ -helices arranged in a right-handed superhelix. Beneath the 2 S albumins the superfamily also includes non-specific lipid transfer proteins (nLTPs) from various tissues and several proteins present in cereal endosperms (trypsin inhibitors,  $\alpha$ -amylase inhibitors, grain softness proteins or puroindolines).

Globulines are widely distributed in seeds of mono- and dicotyledone species. Two types of storage proteins could be distinguished: 11 – 12 S and 7 – 8 S. Protein structures often base on subunit assemblies (trimers or hexamers). Globulin subunits typically have molecular masses of 40 – 60 kDa, whereas mature proteins could show high molecular masses up to 450 kDa. In barley species 7 S storage proteins can be found at the embryo/aleurone layer.

Prolamins are not wide distributed, but mainly present at cereal and grass species. These protein class has a huge importance in food processing and nutrition. Prolamins show extensive variations in structure and properties and are classically subdivided in two groups: monomeric prolamine and polymeric glutenin subunits. Molecular masses usually range in between 40 – 105 kDa. Both protein groups can be further subdivided on the basis of their electrophoretic mobility at low pH.  $\alpha$ -,  $\beta$ -,  $\gamma$ - and  $\omega$ -gliadins can be distinguished, whereas  $\gamma$ -gliadins are sulphur-rich and  $\omega$ -gliadins sulphur-poor. Basing on their molecular masses high and low molecular mass subunits of glutenins are widely spread [14].

Malt differs from barley by virtue of three technical features. One is a kind of induced, artificial stress owing to drying and hydration steps. Another one is the provision of hydrolytic enzymes synthesized during germination and the last one is the friability of the



internal grain structure caused by the breakdown of cell walls and proteins. For brewing purposes the attention is normally focused on the water-soluble protein fraction. The classical terminus of the water-soluble protein fraction has been further classified by Østergaard [36] and comprises:

1. housekeeping enzymes
2. chaperones
3. defense proteins and enzyme inhibitors
4. desiccation stress proteins
5. oxidative stress proteins and
6. proteins with other functions.

Housekeeping enzymes have been characterized to perform essential metabolic functions in all living beings. Some reports also indicate that housekeeping enzymes act as virulence factors for a great variety of pathogens, especially field fungi and bacteria. After secretion and reassociation on the surface of the pathogen they might directly interact with the host to trigger signal transduction and support colonisation, persistence and invasion [86].

Common chaperones are heat shock proteins and are expressed in response to temperature or other cellular stress. They were identified in *Saccharomyces cerevisiae* expressed under conditions of high temperature stress.

Østergaard suggested that most proteinaceous inhibitors were probably involved in the seed's defense against pathogens and not in the inhibition of endogenous enzymes. For this reason inhibitors and defense proteins were placed in the same group.

Desiccation stress proteins could be both induced by the removal of water (direct desiccation damage) or by a metabolically derived damage. Oxidative stress proteins are thought to originate because of an increased production of reactive oxygen species or free radicals [14].

### **1.5.2 nLTP1, nLTP2 and the class of ns-LTP's**

Lipid transfer proteins (LTPs) have been isolated and described as proteins that transfer lipids between membranes in "in vitro" assays. Plant LTPs show a broad specificity and thus are prefixed with "ns" (non-specific). Non-specific lipid-transfer proteins (ns-LTPs or also nLTP's) are capable of binding lipid compounds in the tissues of higher plants and fungi. They are coded by nLTP genes, showing high sequence homology within and between phylogenetic trees (monocots and dicots in the case of barley, maize, spinach or castor bean for example) [38, 61].

Barley nLTPs are basic proteins stabilized by four intramolecular disulfide bonds (Figure 11). Within the proteins a large hydrophobic cavity shaped like a tunnel structure forms a lipid binding site. They might be involved in the formation of hydrophobic cutin or suberin layers protecting the grain from fungal attack or water diffusion.

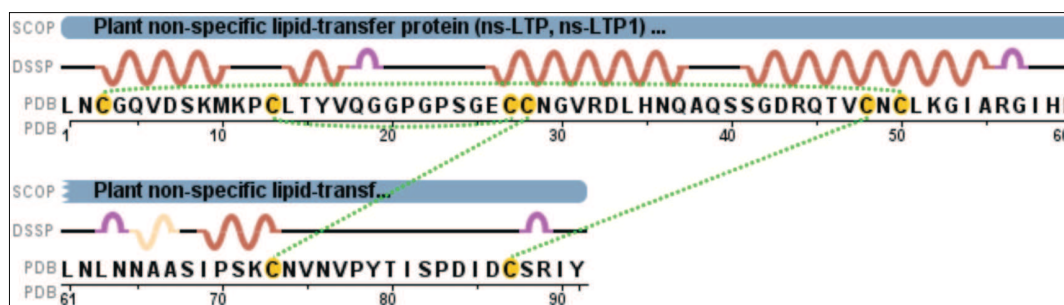


**Figure 11** 1- and 2D structural information on plant nLTPs. Conserved cysteine residues are accompanied by yellow dots and resulting disulfide bridges are shown in green interperuncations (the figure was derived from Protein Data Base (PDB) entry 1LIP).

Two major lipid binding protein classes have so far been identified: nLTPs, including nLTP1 ( $\approx 9$  kDa) and nLTP2 ( $\approx 7$  kDa), and the group of indolines. The latter are of minor importance for this thesis and will therefore not be described in greater detail [34].

After processing native barley nLTP1 comprises 91 AA with a molecular mass of 9694 Da. The structure includes 4  $\alpha$ -helixes, a C-terminal arm, the prementioned 4 disulfide bonds and a hydrophobic cavity (Figure 12).

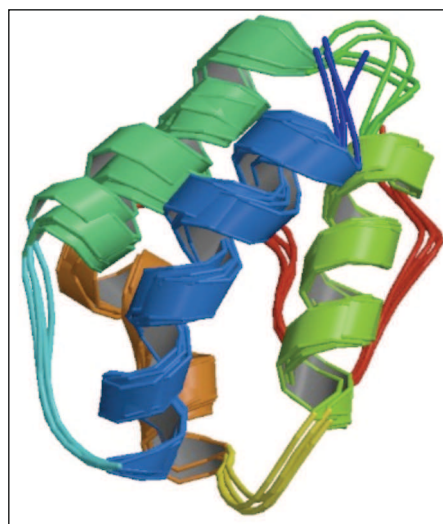


**Figure 12** 3D structure of the barley lipid transfer protein (NMR, 4 Structures). The processed protein comprises AA positions 27 – 117. (3D structure calculated from PDB (LIP1) for Swissprot entry P07597\_NLTP1).

In addition, a cysteine residue pattern (8 conserved Cys residues) matching a genuine plant nLTP signature and a possible acyl group binding site have been identified. The former provides the pre-requisites for typical disulfide bond formation.

Participation in the defence of plants against microbial pathogens and in the formation of hydrophobic cutins layers is also attributed to nLTP1. It might support phospholipid and galactolipid transport across membranes, but the exact *in vivo* function is still unknown [37, 38, 61].

nLTP1 originates from the barley aleurone of developing and germinating seeds and is classified as an abundant soluble protein (albumin) [59]. It is recognized as heat-stable, resistant to extreme pH values and only slightly affected by proteases. nLTP1 belongs to a superfamily of so-called bifunctional  $\alpha$ -amylase inhibitors. Due to posttranslational modifications (lipid-like linkages) the barley nLTP1 isomers (nLTP1b, nLTP1c) mentioned in literature vary. The native barley seed forms only show poor foaming properties and are subjected to further modifications during the malting and brewing process, creating surface active beer nLTP1 with good foaming potential. Modifications might include hydrolysis, disulfide bond reduction combined with unfolding (increase of amphiphilicity), glycosylation via Maillard-reactions, and acylation [8, 37, 38, 53, 54, 60, 61].

As mentioned more explicitly in the gushing introduction, nLTP1 was also connected to this phenomenon. The observation of up-regulated nLTP genes in barley in response to infection with microbial pathogens is the main fact supporting this hypothesis [5, 6, 62].

nLTP2 is also found in the aleurone of seeds. Development starts during grain filling and release begins with grain compartmentalization and starch hydrolysis. It is involved in the transport of rigid suberin monomers and mentioned as a potential phospholipid transfer protein in general. The original 102 AA of barley nLTP2 are processed further into a mature form. After processing the proteins consists of 67 AA with a molecular mass of 6988 Da. Again four disulfide bonds are characteristic. It was successfully identified in barley, malt and beer 2D gels [55], but the additional information available is scant because analyses were often performed with wheat or rice homologues. Glycation in the kilning step of malting and during the brewing process might be possible. In addition, a cross-linkage with nLTP1 via disulfide bridges is under discussion. No real proof has been provided yet because the conformational state could not be shown in case of SDS/DTT disulfide-bridge reduction in structural analyses [54].

### 1.5.3 Proteins Z4 and Z7

Protein Z (antigen 1), the major endosperm albumin, is the second protein class mentioned for its foam-positive or foam stability enhancing character [11, 56]. Regarding the tolerance for high temperatures, extreme pH-values and proteolysis it is also said to survive the malting and brewing process relatively intact. Protein Z is a member of the small family of serine proteinase inhibitors, the barley serpin family. This fact includes an important phenomenon to be mentioned here because barley and wheat protein Z species are the only such species found in plants to show a relationship to the serpin superfamily.

Glycosylation of protein Z by both pentoses and hexoses might create glycoproteins during the malting and brewing processes. The relevance to haze formation and foam development or stabilization is a less discussed topic, which is why the information to be found in literature is scant. Opinions greatly diverge: in single cases glycosylated protein Z is generally excluded from being involved in haze and foam mechanism [28], but most research groups do not even distinguish between unglycosylated and glycosylated protein Z species.

Speaking of a "Protein Z" collectively is misleading because two protein forms, protein Z4 and Z7, can be distinguished. They are expressed by two separate but highly related, small gene families. Protein Z4 (antigen 1a) is encoded on chromosome 4, whereas protein Z7 (antigen 1b) is encoded by two genes of chromosome 7 [10, 11, 63]. Comparison of the linear amino acid sequence shows a homology of 72 %.

In barley and malt, protein Z4 is the dominant form providing about 80 % of all protein Z found, and it was also the first beer protein to be characterized. In the literature protein Z4 is seen as contributing to both foam stability and haze formation [10, 34]. As a major component of the endosperm albumin it is released from the starchy endosperm, where it exists in free and bound form [38]. An inhibitory function during grain filling or germination might be possible, but the exact biochemical function of the serpin remains unclear, as no target protease has been identified in plants.

The primary structure is built from 399 AA, resulting in a molecular mass of 43276 kDa. A reactive center loop (RCL) is the characteristic feature found with all protein Z types. The RCL can be detected at the carboxy terminus of the protein and includes the amino acid positions from 343 to 367. Conformational changes in this part of the molecule create heat- and protease-stable molecules, as a minimum. The RCL extends from the body of the protein and directs the binding process to the target protease. The protease cleaves the serpin at the reactive site within the RCL, establishing a covalent linkage between the carboxyl group of

the serpin reactive site and the serine hydroxyl of the protease. The resulting inactive serpin-protease complex is highly stable. At Swissprot these informations are not provided by experimental findings but were instead estimated by parallels to protein Z homologues.

The 2D gelelectrophoresis findings indicated several protein Z4 species with acidic pI differences. Protein Z migration in gels were related to Maillard reactions and partial sugar modifications during the malting and brewing process. Positive protein Z allocations to 7 – 17 kDa regions are explicable by protein Z fragments (MM: 4033 Da) deriving from the upper region of or around the RCL [34, 64].

The amino acid variations in the RCL sequence deliver the explanation for protein Z4 and Z7 showing different inhibitory properties and cleavage susceptibilities. Protein Z7 consists of 397 AA and has a molecular mass of  $\approx 42690$  Da after having been processed into a mature form. This type of protein Z is expressed in the endosperm at intermediate level. It inhibits chymotrypsin in vitro, whereas the underlying RCL mechanism is the same as in protein Z4.

A third protein Z related gene has been described in barley, coding for a so called protein ZX. This protein consists of 398 AA and has a molecular mass of 42975 Da. The characteristical features are identical to proteins Z4 and Z7, but its in vitro function includes chymotrypsin, cathepsin G and trypsin inhibition. The BSZx protein shows an 80 % sequence homology to protein Z4. There is no information to be found in the literature to indicate that protein Zx has an impact on the brewing process.

#### **1.5.4 Hordeins**

The hordein class, as the seed's main storage protein fraction, can make up as much as half of the total protein content of mature grains. Hordeins could be summarized by the terminus of the gliadin/glutenin protein family. The hordein values found in literature greatly vary, but appear to correlate with the nitrogen fertilization of barley plants. Prolamin and glutelin fractions can be further subdivided into B-, C-, D- and  $\gamma$ -hordeins, depending on their electrophoretic mobility at low pH levels [14]. Globular 3D structures are often observed in hordeins. Their prolamin and glutamin content is high and they show poor water-solubility in general. Prolamin and glutelin fractions can be separated in 50 – 90 % alcohols owing to the difference in their solubility [65]. In literature special attention is focused on barley hordein as a source of haze-active proteins [11, 13, 28].

B-hordeins represent the major fraction within the barley grain (approximately 80 % of the total hordein content). Their proteins species are rich in sulfur, with only a low lysine content,

provided in the form of polymers stabilized by interchain disulfide bridges, and unsusceptible to Maillard reactions. B3-hordein and a D-hordein precursor were identified in beer foam [34]. B-, D- and also  $\gamma$ -hordeins were identified in barley and malt 2D gels [37].

The B3-hordein (HOR 3) is a sulfur-rich seed storage protein fragment with a molecular mass of 30195 kDa. Only scant information is available, but in view of the sequence similarities it belongs to the gliadin/glutenin family.

The D-hordein precursor is identical to the Swissprot entry for D-hordein. With 679 AA after processing into the mature protein form and a molecular mass of 72113 Da, it belongs to the group of larger proteins that could be assigned to high molecular foaming fractions after 2D gel separation. A search of the protein databases turns up around 14 different D-hordein types. Conserved domains and sequence similarities could lead to multiple positive identifications for one peptide. The three other D-hordein species of importance for this study can be characterized by the following attributes: D-hordein (Q02056) comprises of 441 AA, resulting in a molecular mass of 45994 Da and a pI of 8.32, D-hordein (Q84LE9) features 757 AA, leading to a molecular mass of 80409 Da and a pI of 8.01, and the last D-hordein species (Q40045) has a molecular mass of 50786 Da (454 AA) and a pI of 7.6. A positive identification of hordein fragments may be attributable to posttranslational modifications and/or proteolytic processing during the malting and brewing process.

The  $\gamma$ -hordein 3 (HOG3), at least features a characteristic structure consisting of an N-terminal half with repeating units of proline-glutamine blocks and a C-terminal half where the repeats are dispersed and less conserved. It also belongs to the gliadin/glutenin superfamily and appears to perform proline targeting and the transport to the vacuoles of developing barley endosperm. Similarly to the B3-hordeins it is a rather small protein with a molecular mass of 33188 Da made up of 289 AA.

### **1.5.5 Barwin**

Barwin is a 125 AA-residue protein found in barley seeds and malt extract, but also in beer and foam [34, 37, 66]. In respect of the close similarity of its AA sequence with wound-induced proteins it can be classed as a defense protein and more precisely, with the pathogenesis related protein family. By virtue of its binding capacities it appears to be involved in the biological catabolic processes of cell wall macromolecules and chitin. In cases of bacterial or fungal decay it might be also involved in the defense mechanisms (like a kind of plant lectin). The protein is not processed any further during maturation and its molecular

mass has been estimated at 13737 Da. The amino acid composition produces a theoretical pI of 7.76. Two posttranslational modifications can be found with Barwin: 3 disulfide bonds and a pyrrolidone carboxylic acid.

### 1.5.6 Inhibitor protein classes

A large number of seed proteins have been identified which inhibit the catalytic activity of one or more animal proteases. Based on their AA sequences the inhibitors can be classified into structurally and evolutionarily related protein families. The inhibitor protein family can be subdivided into seven subfamilies:

- 1.) the protease inhibitor family L6 = cereal trypsin/ $\alpha$ -amylase inhibitor family
- 2.) the protease inhibitor family = potato type/serine protease inhibitor family
- 3.) the protease inhibitor family L3 = leguminous Kunitz type inhibitor family
- 4.) the serpin family (also see protein Z)
- 5.) the thiol protease inhibitor class
- 6.) the serine type endopeptidase inhibitor protein subfamily and
- 7.) the thaumatin family (for example THHR and THHS).

Multiple serine protease inhibitors provided by the same homology family could be present in a grain. In addition, multiplicity may be owing to posttranslational processing of initial inhibitor gene products during seed maturation, germination or growth.

The largest number of barley inhibitor proteins is provided by the trypsin/ $\alpha$ -amylase inhibitor family. Owing to the extractability of these proteins in organic mixtures of chloroform and methanol, they are also called chloroform/methanol (CM) soluble proteins. Their inhibitory action is directed against insect or other pathogenic enzymes, but not against barley enzymes. Some inhibitor proteins are known to either inhibit bovine trypsin or  $\alpha$ -amylase activity from barley attacking insects, but none of the inhibitors are able to hinder both substrates. Barley  $\alpha$ -amylase, which will be de novo synthesized in seed germination, is not attacked by the  $\alpha$ -amylase/trypsin inhibitors. The main function seems to reside in protecting the starchy endosperm from insects or pathogenous invaders.

The inhibitors are cysteine rich molecules with 4 – 5 disulfide bonds that are essential for their inhibitory function. Most members of this group show similar molecular masses and similar isoelectric points, as well as similar posttranslational modifications. Multiple positive identifications with one peptide peak or spot (2D gels mentioned in literature) might be explicable by these features but also by a possible quaternary structure of these inhibitors.

They could be stitched together to form a heterotetramer of one CMa, one CMb and two CMd subunits (protein chains). Depending on the reducing preparation or separation procedures, the heterotetramer could be destroyed, resulting in monomeric chains that are no longer clearly distinguishable.

While barley and malt extracts show a huge variety of  $\alpha$ -amylase/trypsin inhibitors, only a few hits were found in beer or foam. Perrocheau *et al.* tried to find an explanation for their fade in the beer. Despite many lysine residues, a lack of glycosylation might be a possible answer if residues are located in protected regions within the 3D protein structure. An unfolding of the protein structure and lack of glycolysation might counteract protein solubility [37].

With malt extracts the  $\alpha$ -amylase/trypsin inhibitors CMb (IAAB), CMa (IAAA) and CMd (IAAD) are mentioned, as well as the trypsin inhibitors Cmc (IAAC), CMe (IAAE) and pUP13, pUP38, and the  $\alpha$ -amylase inhibitors BMAI-1 (IAA1) and BDAI-1 (IAA2) [34, 55]. The different nomenclatures refer to the inhibitory activity of the proteins, but also excludes more than one substrate. In beer and foam fractions the number falls to 6 protein candidates, while four species derive from the group of the  $\alpha$ -amylase/trypsin inhibitors. It might be interesting to note that this protein group was also the only other one identified in haze beneath nLTP1 and protein Z [56]. These results are in big contrast to the explanation provided by Perrocheau *et al.*, as they could indicate the survival of these protein species in the brewing process.

Three proteins (ICIC, ICIA and ICIB) can be allocated to the protease (potato type I serine-protease) inhibitor superfamily and are also referred to as subtilisin/chymotrypsin inhibitors. They inhibit both subtilisin and chymotrypsin and therefore show a type of bifunctionality. The molecular masses of these three proteins range from 8.2 – 9 kDa and their pI's from 5.4 – 6.3. They might be involved in wound defense responses. Only ICIA is mentioned in literature and has been identified from barley 2D gels and beer foam [55, 56].

The L3 subfamily contains a single IAAS protein, which is also called  $\alpha$ -amylase/subtilisin inhibitor BASI. This protein independently inhibits subtilisin and  $\alpha$ -amylase. After PTM the mature protein consists of 181 AA, has a molecular mass of 19.9 kDa and a pI of 6.58. This protein has not been identified in malt or beer before.

The thiol protease inhibitor subfamily includes cystatin Hv-CPI 8 and 5, CYSP1 and CYSP2. These substances stop, prevent or reduce the activity of cysteine-type endopeptidases. No further information is available about CPI 8 and CPI 5 proteins except their respective molecular masses of 12.8 kDa (122 AA) and 15.9 kDa (151 AA) and their pI's of 9.8 and 8.45. Both proteins have not been mentioned in malt or beer analyses before.



CYSP1 and 2 could be synthesized by the aleurone cells following stimulation by gibberillic acid. They have also not been identified before. Both proteins have a rather acidic pI of 4.77 and 4.96 and molecular masses of around 25 kDa after maturation.

The serine type endopeptidase inhibitor protein subfamily comprises 5 barley proteins, but an enormous number of related proteins could be found in wheat, too. They stop, prevent or reduce the activity of serine-type endopeptidases, enzymes that catalyse the hydrolysis of non-terminal peptide bonds. Only Cmd3 has been mentioned by Perrocheau *et al.* in their 2D gel malt research.

### **1.5.7 Other protein classes**

To explain the results of this study three additional protein classes will be introduced: the pathogenesis related protein family, the plant thionin family and the small hydrophilic plant seed protein family (also called late embryogenesis abundant type family).

The pathogenesis related protein class includes a large number of protein species, whereas the proteins can in turn be subdivided into two subfamilies: the CRISP subfamily with PR12, PR13 and PR1 and the actual pathogenesis related protein class (e.g. Barperm1, PR5 or PR4). What all these protein species have in common is their involvement in the plant's defensive reactions to pathogens like bacteria and fungi. Their molecular masses and pIs strongly differ from one to the other and no common regularity is observable.

The plant thionin family comprises a small number of proteins which are abundant in the barley endosperm. The precise functions are unknown but a cytotoxicity to animal cells had been observed. Thionins are amphipathic proteins which inhibit the growth of bacteria and fungi. Therefore they were thought to be involved in plant defence as a kind of resistance factors against pathogens. The proteins are built up from a homodimer subunit structure which contains a thionin domain and an acidic protein part. Despite of highly divergent AA sequences they are folded in a structurally similar way.

The small hydrophilic plant seed protein family is made up of five late embryogenesis abundant proteins. These are commonly found proteins that are abundant in higher plant seed embryos, especially before the embryo's terminal desiccation (osmotic stress). They could also be induced by abscisic acid (ABA) or salt stress. For this reason they are thought to be involved in desiccation tolerance by acting as osmoprotective proteins or desiccation damage repair proteins.

### 1.5.8 Proteins with "other functions"

Only one of the eleven additional proteins mentioned for malt extracts, beer or foam by other research groups could be found in the work for this thesis. The 10 other proteins will not be described in greater detail [34, 37], as they could not be proven here. For sake of completeness they are included in Table 6.

The eleventh protein, which was identified in beer, is a ubiquitin/ribosomal protein S27a.2 (UBIQ). With a molecular mass of 17671 Da it can be explained as a dimer of the 40 S ribosomal protein S27a with 3 AA removed after the last repeat. The 40 S ribosomal protein monomer should be mentioned directly alongside ubiquitin because it is synthesized as a C-terminal extension protein (CEP) of ubiquitin.

**Table 6 Additional proteins identified in malt extracts, beer and foam fractions [34, 37].**

Protein description	Molecular mass [Da]	Source
Carbonic anhydrase, chloroplast precursor	35075	foam
Hypothetical protein	20553	foam
Calreticulin	47038	foam
Endoplasmin homolog precursor	92917	foam
RNA-dependant RNA polymerase P1-P2 fusion protein	98742	beer
Photosystem II P680 chlorophyll IIA apoprotein	56150	beer
Glutamyl-tRNA synthetase	61863	beer, foam
BTI-CMe 2.1	13710	malt extract, beer
Probable trypsin inhibitor CMe 2.2	16172	beer
Embryo globulin	72253	beer

Ubiquitin normally appears as a polyubiquitin precursor with tandem head to tail repeats. In the mature protein one to three additional AA residues can be removed after the last repeat. A single ubiquitin contains 76 AA and has a molecular mass of 8525 Da. An ubiquitin extension protein is synthesized as a single copy of ubiquitin fused to a ribosomal protein (here: S27a). In the following translation the extension proteins could be cleaved from ubiquitin. Ubiquitin is a protein modifier that can covalently attach to target lysines. If attachment to proteins is performed by an Lys<sub>(48)</sub>-linked ubiquitin polymer, it could lead to protein degradation via the proteasome. The attachment of an ubiquitin monomer or an alternatively linked polymer meanwhile fails to show this effect and also might also be required for biological function in cases of stress response, for example.

Several additional proteins identified in this study could also not be allocated to distinct protein families. They are therefore summarized under the generic term of "proteins with other function" (classification by Østergaard). Protein species to be mentioned in this context

include a putative synaptobrevin VAMP, a grain softness protein, and a glyceraldehyde 3 phosphate dehydrogenase.

A small number of newly identified proteins is still missing from this summary because they could neither be traced to distinct protein families nor subsumed under the umbrella term of "proteins with other functions". They shall be introduced in the discussion of the results and will be grouped to the classification by Østergaard, if possible.

## ***1.6 Proteins from other origins***

### **1.6.1 Hydrophobins – fungal proteins**

Hydrophobins are small secreted fungal proteins with a molecular mass of 7 – 20 kDa. They are highly surface-active and hence able to assemble themselves into amphiphilic films on hydrophobic or hydrophilic surfaces/interfaces. The resulting films are insoluble and highly stable owing to their rodlet ultrastructure, resembling on an interwoven mosaic layer.

Hydrophobins have been found to be ubiquitous in filamentous fungi, in aerial structures of mushroom caps, spore surfaces and aerial hyphae. Their functions are related to sporulation, fruit body development (spore dispersal), infection structure formation and secretion into the growth environment, but they also play a protective role against desiccation and wetting. They are involved in fungal adherence to surfaces, where they act as interfaces between fungal cell walls and air or solid interfaces. In this respect they might play a key role in the fungi's interaction with other organisms such as plants [5, 6, 67, 68]. Hydrophobins can be produced by all mycelial fungi regardless of whether they are gushing inducers or not. The gushing capacity of hydrophobins from varying fungi could hence broadly vary.

All hydrophobins show a common pattern: eight cysteines provide a basis for the formation of 4 disulfide bonds. In addition, a typical hydrophobin related amino acid pattern has been observed (X<sub>2-85</sub>-C-X<sub>5-10</sub>-C-C-X<sub>11-39</sub>-C-X<sub>8-23</sub>-C-X<sub>5-9</sub>-C-C-X<sub>6-18</sub>-C-X<sub>2-13</sub>). The lack of aromatic amino acids is as typical as a proportion of 30 – 50 % hydrophobic amino acids [67].

Hydrophobins are said to be gushing inducers. The strong surface activity and rough surface of the rodlet layers may be a prerequisite for carbon dioxide bubbles to attach, turning them into gushing germs.

Fusaria were found to produce hydrophobins in the growing period in the field but also later on, during the malting process [71]. The hydrophobin levels of malt could be related to the gushing volume of beer [67, 69, 71]. Hydrophobin release during the malting is affected by

losses in the brewing process (spent grains, hot trub, perhaps yeast proteases). Despite these losses significant amounts were still found in finished beer afterwards.

Hydrophobins are represented by two classes: class I and class II hydrophobins (e.g. HFB I and HFB II from *Trichoderma reesei* [70]). Class II hydrophobins form less stable interfaces than class I hydrophobins, enabling rearrangement and reaggregation following disruptions. Assemblages formed by hydrophobins generally require relatively harsh conditions to break down (TFA for class I and 60 % ethanol for class II hydrophobins). Class I layers tend to show a rodlet-type appearance, whereas class II layers build needle-like structures. *Fusarium culmorum* hydrophobin 3 (FcHyd3) is a member of the class I hydrophobins while FcHyd5 belongs II. FcHyd5 has been found to cause gushing, while the class I hydrophobin FcHyd3 lacked this effect [68]. The gushing trigger effect is supported by results yielded with hydrophobins isolated from different gushing active fungi (*Fusarium*, *Trichoderma* and *Nigrospora*), which induced gushing in beer after the addition of concentrations as low as 0.003 up to 0.1 ppm [67].

### 1.6.2 Yeast proteins

Yeast provides the vast majority of enzymes and proteins supporting catabolic and anabolic mechanisms in cell growth and propagation. During fermentation and ongoing cellar storage active protein release (stress reactions or ageing in pitching cycles) is as possible as an inactive release owed to cell autolysis. Yeast proteins can hence be expected in beer samples. Nevertheless only few proteins were referred for evidence in beer or haze. Enolase 2 and triosephosphate isomerase (several roles in metabolic pathways) have been mentioned for beer [55], while thioredoxin 2 has been referred to as moderately haze-active in both beer and haze [56].

### 1.6.3 Other proteins

With respect to its low protein content, hops could also be a possible protein source [9, 41]. The literature has so far failed to show any indication of hop-deriving proteins, but being one of the raw materials used for beer production it should not be entirely excluded.

The same applies to beer-spoiling microorganism (*Pediococcus*, *Lactococcus*, *Lactobacillus*, *Micrococcus*, *Pectinatus*, ...). Although the microbiological contamination of beer is of minor importance today it can not be entirely excluded, either. Dead bacteria from the malt or their

metabolites (*Fusaria*, *Aspergillus*, *Stemphylium*, *Penicillium*, *Nigrospora*, ...) might be another source. Especially microorganism are a source of proteins owing to their potentials for active protein release or disruption after cell death. Haze formation is the primary topic when speaking of bacteria or foreign yeast decay [8, 9].

A final fact to be mentioned here is the taxonomic relationship between barley and other economically useful plants or such as wheat, maize, rice or soybeans. This could be a reason for ancient protein identifications in cases of high percentage sequence homologies and/or lacking information for special barley protein.

## **CHAPTER II**

---

### **INSTRUMENTAL BACKGROUND**

## 2 Instrumental Background

### 2.1 “Ultra Performance Liquid Chromatography” – Acquity UPLC™

Liquid chromatography can be useful for proteomic studies as a complementary approach to established standard gel-based workflows. LC-based approaches are able to deliver supplementary information and might help to overcome some of the existing limitations of 2D electrophoresis. A common feature of both methods is that they can only be used for actual protein identification and/or characterization in combination with mass spectrometry.

The differences of specific molecule properties provide a basis for separation in protein and peptide chromatography. Reversed-phase chromatography exploits hydrophobic attitudes for separation, whilst charge-based separations are performed via ion exchange chromatography (Table 7).

**Table 7** Chromatography separation principles [73].

Molecule property	Separation technique
Surface net charge	Ion exchange chromatography or chromatofocussing
Size (MM)	Gel filtration
Hydrophobicity	Reversed-phase chromatography or Hydrophobic interaction chromatography
Ligand specificity	Affinity chromatography

A Waters Acquity UPLC™ system (Figure 13) was used for this study. The core system includes a photodiode array detector (PDA), allowing detection of substances at wavelengths from 190 to 600 nm. The main advantages in comparison to traditional HPLC-systems result from the application of sub-2 µm-hybride particles (1.7 µm) instead of 5 µm particles.

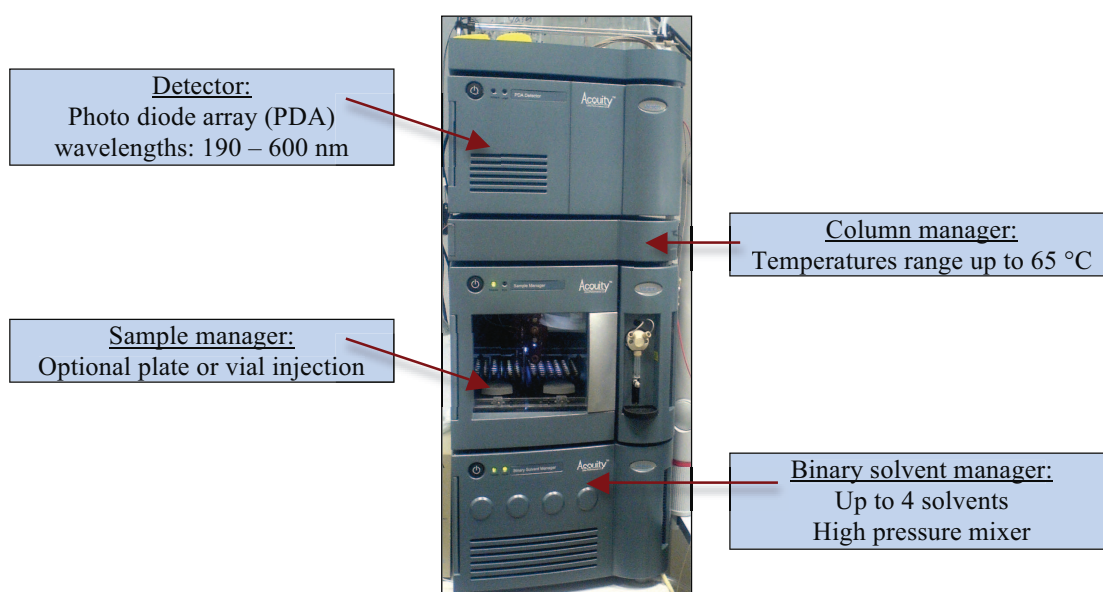


**Figure 13** Water Acquity UPLC™. Standard core system with photodiode array detector system.

The resolution, separation speed (reduced run times) and efficiency are clearly enhanced, as the van Deemter correlation shows a very broad minimum (optimum correlation between resolution and flow rate) for 1.7  $\mu\text{m}$  particles. Separations can hence be performed more quickly without losses of resolution. The smaller particle sizes simultaneously call for higher back pressures and need of high flow rates. The system's limits are reached with a maximum back pressure of 15000 psi. The UPLC system can be directly interfaced with the mass spectrometer via the detector unit.

### 2.1.1 Peptide analysis with UPLC

Reversed-phase chromatography (RPC) is a typical LC separation technique applied in the study of peptides. Common RPC columns often feature silica-based packaging with covalently bound hydrophobic groups (alkyl chains).  $\text{C}_{18}$ - (n-octadecyl-),  $\text{C}_4$ - (n-butyl-) or phenyl groups are typical moieties imparting the specificity to the column. The underlying mechanism is an adsorption process (hydrophobic interaction) involving the designed ligands and solute. Peptides with a certain degree of hydrophobicity are separable with good resolution and recovery, whilst attention must be paid to the length of the alkyl chain substituents: the longer the alkyl chains are, the better will more hydrophilic samples be retained.

The column lengths and packing particle sizes selected, are also of great importance for optimal RPC effectiveness. The required optimum pore size is highly dependent on the polypeptide weight. Pore sizes of around 100Å are normally adequate for peptides. The choice of column length is more closely related to sample complexity than to peptide weight. In tryptic digests longer column can be advantageous, but usually common column lengths range between 50 and 100 mm.

Initial RP-LC binding conditions are primarily aqueous, allowing the solute molecule to bind to the immobilized hydrophobic ligand. This interaction can be explained by the so called adsorption model, where solute and mobile phases compete for binding sites in the stationary phase. Desorption of the bound solute follows from the decrease of polarity. This is the result of increasing levels of organic modifiers. Shallow organic gradients resolve bound peptides, with each peptide having a specific critical point of narrow organic solvent concentration. After desorption a new interaction with the stationary phase is negligible and due to a complete and sudden release sharp peaks are produced with peptides.



Common mobile phase systems often consist of an aqueous solution and an organic modifier. Acetonitril is a typical organic solvent by virtue of its high volatility and UV transparency. Small percentages of an ion-pairing reagent (TFA) or other acid could be used as additives to maintain low pH-values and minimize the ionic interaction between the solute and stationary phase. If mass spectrometry detection is to follow the application of formic or acetic acid helps to shore up sensitivity [73, 74]. Another advantage of the aqueous starting gradient is the high mass capacity achievable with RPC columns. As long as the strength of organic solvent is low enough, large sample volumes can be accomodated and concentrated on the head of the column.

The columns used in this study for peptide separation all featured C<sub>18</sub> modifications. Two different types of columns were selected:

- 1.) UPLC BEH C<sub>18</sub>; 2.1 x 50 mm, 1.7 μm, 130 Å.

The packaging consists of a Bridged Ethyl Hybrid. This material tolerates changes in a wide pH-range (1 – 12) and is designed for both high efficiency and sensitivity purposes with combined LC-MS approaches [75].

- 2.) UPLC BEH SHIELD RP C<sub>18</sub>; 2.1 x 50 mm, 1.7 μm, 135 Å.

In comparison to the BEH C<sub>18</sub>-column the Shield-column has an additional modification in the particle chemistry: a polar group, a carbamat-group is bridged to the BEH particle. This also enhances the retention of phenolic compounds. The pH range sensitivity is identical to that of standard BEH-columns [75].

Both columns are endcapped and column bleeding is reduced to zero, which is critically important in a combined LC-MS approach.

### 2.1.2 Protein analysis with reversed phase chromatography (RPC)

In the presence of non-polar solvents proteins could cease their activity and undergo conformational changes. As these effects are mainly to be expected at higher volume percentages of organic solvents during gradient elution, RPC approaches were for a long time not eschewed in protein studies. The development of specific column ligands and adaption of the LC separation equipment overrides these assumptions today. As long as a number of facts are paid attention to protein analysis can be performed via RPC approaches without irreversible bioactivity losses.

The choice of column packing is once more the first fact to think about. Silica-based columns are also commonly used with proteomic RPC approaches, but might not be the best choice with

aqueous buffers at alkaline pH-values. Protein retention in silica-based RPC columns normally correlates well with a rising degree of hydrophobicity. Hydrophobic samples show a better interaction with short alkyl chain phases, while hydrophilic samples are better suited to C<sub>12</sub>- or C<sub>18</sub>-columns. To avoid a significant loss of bioactivity a C<sub>4</sub>- or C<sub>5</sub>-column might be a better initial choice with unknown protein samples. Optimum pore sizes depend on the weight of the protein and might call for very large dimensions, but one of the average pore size used for protein separation is 300 Å. The column length needs to be carefully selected to minimize denaturation and should be as short as possible. Longer columns boost endurance in a possibly harsh organic environment, which might affect less stable sample compounds. In addition, the resolution is significantly affected by long columns. The typical column length should not exceed 50 to 100 mm in analytical approaches.

For polypeptide separation only gradients make sense. Shallow gradients are selected to effectively separate similar proteins. The choice of organic solvent can be adapted to either the chemical properties of the solute and/or in order to avoid backpressure limitations, which increasingly surface with large proteins and viscous mixtures. Acetonitril is once more the most widely used organic solvent, but where bioactivity is concerned this solvent is not the best choice. Isopropanol or methanol are more suitable for the elution of bioactive molecules. If bioactivity is of minor importance and the primary structure of the analyt remains unaffected, acetonitril will be solvent of choice to minimize backpressure limitations even in an UPLC system. Only a single column type was selected for proteomic studies in this thesis, as literature provides no information on native or intact protein analyses of malt, brewing process or beer samples. The analytical approach used here is not directly comparable to other research groups as their analyses normally start with gel electrophoresis, and not LC-separation, before the MS-analysis. The column was carefully selected, more for maintaining good separation and sensitivity features than the bioactivity.

The UPLC BEH 300 C<sub>4</sub>-column used features the typical 1.7 µm UPLC particles and 300 Å pore sizes. Other column dimensions (lengths: 2.1 x 50 and 2.1 x 150 mm) were also tested. The column type is particularly designed to provide excellent peak shapes, high efficiency and recovery for proteinogenic macromolecules, which are too large or hydrophobic for separation in columns with smaller pores or longer chain bonded phases. Stability is provided across a broad range of both temperature and pH values [75].

## 2.2 Mass spectrometer – Micromass QTOF micro™

The QTOF micro (YA-series, first generation) is a hybrid quadrupole time of flight mass spectrometer with an electrospray ionization source (ESI). The system comprises the quadrupole mass analyser and an orthogonal acceleration time of flight (TOF) mass spectrometer (Figure 14). To protect the main analyser from contaminants, the high, performance research grade quadrupole mass analyser is incorporated via a prefilter assembly. A hexapole collision cell between the mass analysers can be used to induce MSMS fragmentation and for structural identification. Ions emerging from the second mass analyser are detected by a microchannel plate detector. The MassLynx software controls the QTOF micro runs and is used for data acquisition and data processing [76].

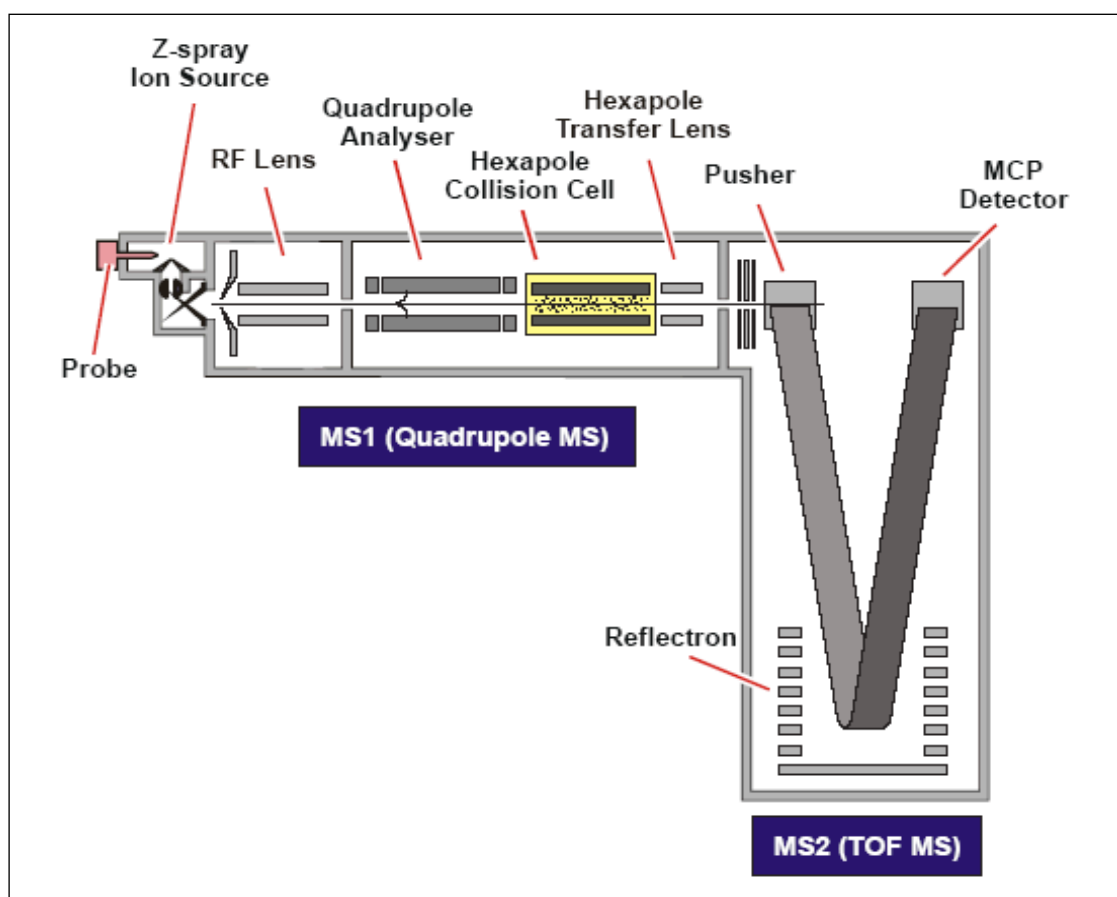


Figure 14 Micromass QTOF micro™ ion optics and instrument overview [76].

The ions are generated in a Z-spray source and then transferred to the first quadrupole analyser (MS1) via an independently pumped RF lens (the Radio Frequency hexapole). Upon leaving the quadrupole analyser, the ions flight is conducted into the orthogonal time of flight analyser, the TOF MS (MS2). The ion beam is focused into the pusher by a series of acceleration, focusing, steering and tube lenses. A section of the ion beam is pulsed towards

the reflectron, which redirects the ions to the detector. On their way from the pusher to the detector the ions are separated into mass to charge ratios ( $m/z$ ) according to their flight times. Every 33 microseconds a full spectrum is recorded by the detector. In the case of a one spectrum per second acquisition rate, each spectrum is the sum of about 30000 individual detector spectra. The maximum resolution given for this instrument series is 5000. But in optimal external and internal conditions, the resolution can also pass this 5000 mark (absolute maximum 5500).

### 2.2.1 Ionization with an electrospray-source

Ionization takes place at atmospheric pressure (API) conditions in the QToF micro. Using the Z-spray allows for two different ionization techniques:

- 1.) Atmospheric Pressure Chemical Ionisation (APCI), which was not used in this study and
- 2.) Electrospray Ionisation (ESI).

The ESI technique can be applied to polar compounds ( $< 200$  Da) as well as large biomolecules such as proteins (up to 100 kDa). Both positive  $(M+H)^+$  and negative  $(M-H)^-$  quasi-molecular ions can be produced via ESI, but for the peptide and protein studies in this thesis only the positive ion mode was used. The mobile phase of the LC column or infusion pump can be ionized as a consequence of applying a strong positive charge to the eluent emerging from the nebuliser. A mist of positively charged droplets (aerosol) emerges from the nebuliser. The aerosol shows a typical Taylor cone owed to the repulsive coulombic forces between equally charged ions. On their way from the nebuliser to the inlet of the MS, the charged droplets shrink in size as the solvent evaporates (desolvation heater), while the droplet charge remains constant. In terms of a sufficient charge density (Rayleigh limit: charge repulsion overrides the surface tension) smaller droplets are created by droplet fission. The process continues until nanometer-sized droplets are produced and nearly solventless sample ions are ejected from the droplet surface into the gas phase by ion evaporation .

It is a characteristic trait of ESI spectra that ions occur as singly or also multiply charged species because the charges can be distributed across all the potential charge sites of the analyte. Low mass molecular compounds generally form singly charged ions by gaining a proton, while high molecular mass polymers (peptides) and biomolecules (proteins) form multiply charged ions. Fragmentation effects are of little significance with ESI, despite in source fragmentation via “Collision Induced Dissociation“ (CID).

In peptide analysis the charge states of multiply charged ions is easily determined as they normally stay within the bounds of MS resolution capacities. The mass differences between the peak and isotope peaks can be used to determine the charge state of n-charged ions.

1.) single charged ions ( $n = 1$ ):  $m/z = (M+H)/1$ ;  $1/n \text{ Da} = 1/1 \text{ Da}$  peak differences

2.) double charged ions ( $n = 2$ ):  $m/z = (M+H)/2$ ;  $1/n \text{ Da} = 0.5 \text{ Da}$  peak differences

3.) n charged ions :  $m/z = (M+H)/n$ ;  $1/n \text{ Da}$  distribution.

Once the charge state of a peptide is known its exact mass is determined. Proteins of high molecular mass can however only be analysed, if multiple charged ions have been formed. This effect extends the mass range of the mass spectrometer, which typically ranges between  $m/z$  limits of 2000 and 4000. Large macromolecules can be determined according to their  $m/z$  ratios by virtue of characteristic charge state distributions and because their observable mass range is effectively reduced. Each multiple charged ion is assignable to a charge stage within a series of charge states (the number of charge stages could run very high). The series can be used for molecular mass determination of a proteins that would in single charged state far exceed the MS resolution.

Depending on the chromatographic interface the ESI spray is suitable for capillary LC flows (flow rate compatibility up to 1 mL/min) on the one side (Figure 15) and for nano-LC flows on the other one (Figure 16).

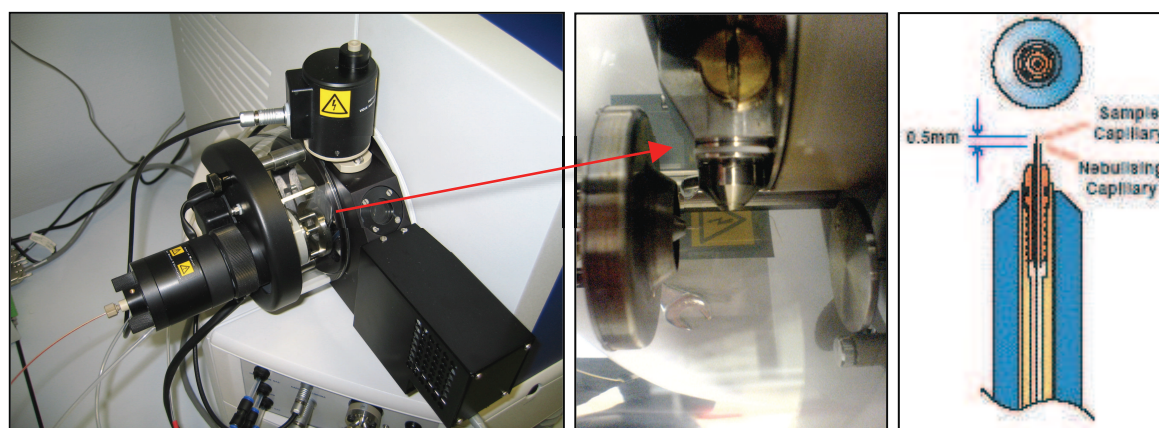


**Figure 15** Design of a normal electrospray (z-spray) source. The left picture shows the source, which serves as an interface between LC and MS. The centre picture shows an enlarged view of the section located between the source capillary and sample cone aperture, which directs the ions into the ion block. The right-hand picture is a diagram of the electrospray tip, whose position has a strong bearing on the intensity and stability of the ion beam.

In this thesis the nano-LC infusion was realised with a fully automatized, chip based ESI-system. The Advion Nanomate<sup>TM</sup> HD robot-system combines the strengths of LC, fraction

collection and chip-based infusion within a single integrated system and can be directly interfaced between LC and MS.

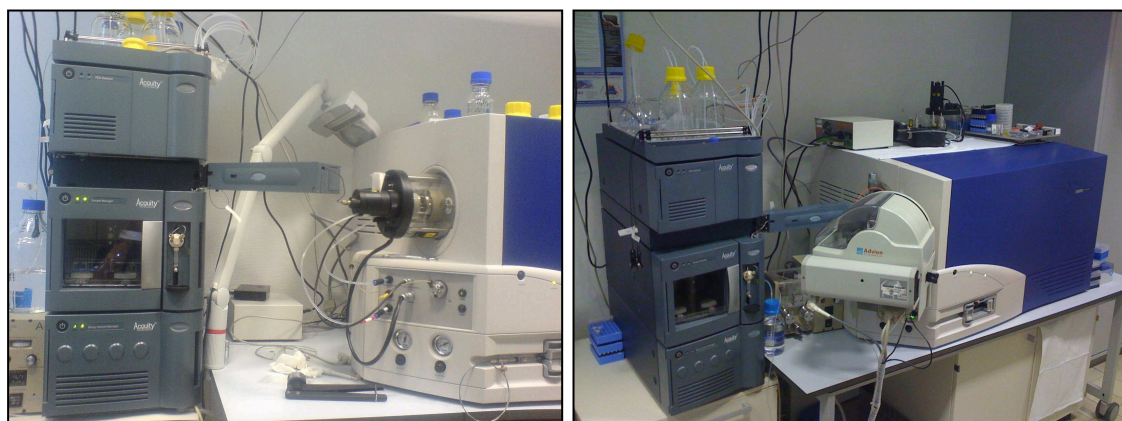


**Figure 16** Serial instrument connections used for normal and nano-ESI infusion in this thesis. The left-hand picture shows the normal ESI-spray assembly, while the right-hand picture shows the nano-ESI-spray instrument units interfaced by the Nanomate system.

The robot operates in two different modes. During chip-based infusion, the samples are applied by either conductive tips or a coupler. While the coupler is used for online LC/MS separations (LC chip coupling mode), tip based infusion will be relied upon for the injection of single samples or reinjection of fractionated samples (infusion mode) from sample well plates. In the case of online LC, the effluent is splitted after the column (post column splitting) and only a small portion is directed to the microfluidic ESI chip (Figure 17), whilst the other portion goes to waste.

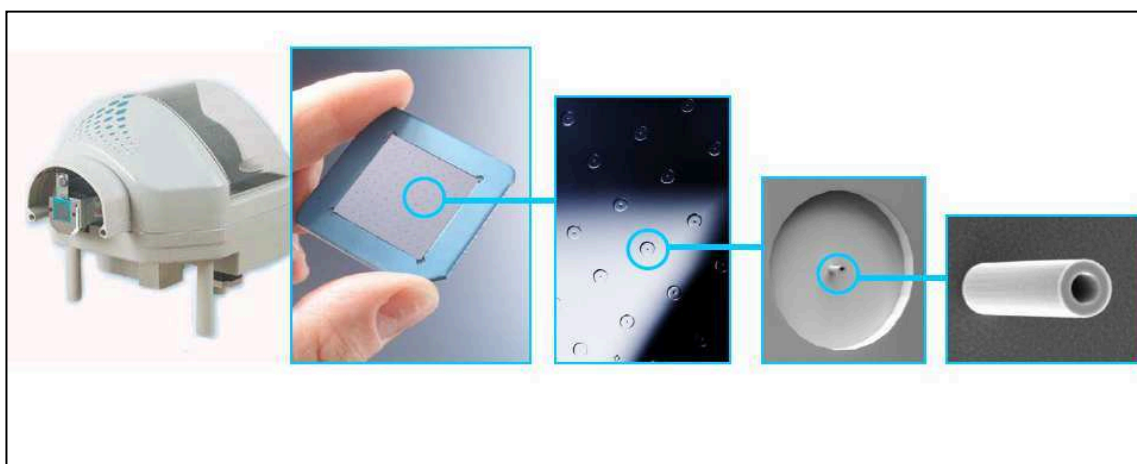


**Figure 17** The chip-based Nanomate robot system with the ESI-chip. The chip's construction is shown in detail. In infusion mode high voltage is applied to a pipette tip, which is directly in front of the micro-chip and a single nozzle. The nano-electrospray is introduced into the MS source via a single nozzle [78].



The ESI chip comprises an array of 400 nano-electrospray nozzles of roughly 0.5  $\mu\text{m}$  in diameter. The design of the nozzles allows for a stable and efficient spray. As the resulting field strength is unique, only very low amounts of spraying solution are required and sample carryover is eliminated. Thus the technique yields reproducible, sensitive and less discriminated information.

The second mode is the LC/MS fraction collection mode. In online LC/MS the solvent is directed to the MS source by the coupler. The LC effluent is split on the post column side, with part of the solvent directed to the ESI-spray interface, while the remainder is collected in multi-well plates. The collection is usually time based and the Nanomate system allows 96 or 384 well plates to be used. Each collected fraction therefore reflects a small time segment of the online chromatogram. The main advantage lies in the fact that these fractions are available for future analysis, including the reinjection of fractions of interest or their in-depth analysis via MS/MS. Especially with very complex samples, the fractionation offers an opportunity for longer analysis periods without requiring LC reinjection and more of the initial sample material.

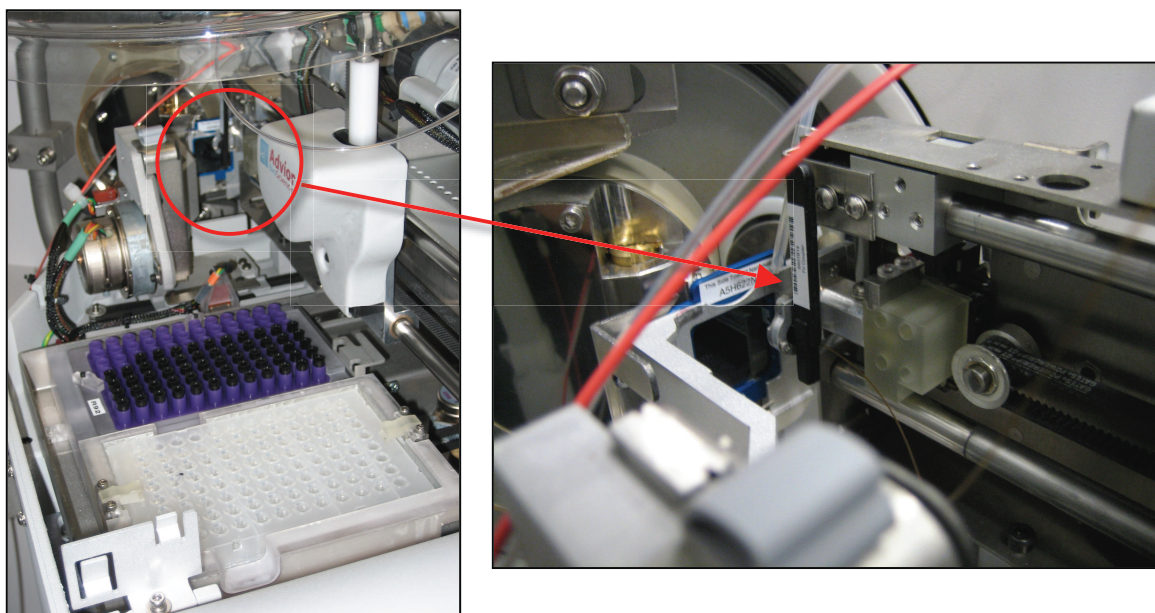


**Figure 18** LC coupling mode used with online LC/MS. The left picture shows the interior construction of the Nanomate robot system with the 96 well plate and infusion tip frame at the front. As only the coupling mode is selected, the robot arm is in parking position above the frames and the coupler is directed towards the ESI chip. In coupling mode with parallel fraction collection the robot would be placed directly above the well plate. The second picture shows an enlarged view of the coupling region and the black coupler attached to the ESI chip.

### 2.2.2 Ion separation with a quadrupole time of flight

The quadrupole mass analyser assembly comprises four (= quad) parallel rods (= poles). These rods are placed at equal distance from a central axis and a fluctuating electric field is applied between these rods via radio frequencies (static and alternating electric potentials between opposite rod pairs). As charged ions are injected from the source along the central axis (resultant electric field is zero at the axis), only ions whose selected mass matches the magnitudes and frequencies of the electric field in the assembly can reach the ion detector. Ions whose masses are either too small or too large will strike the rods on their way through the quad assembly and be lost. The ions are hence selectable by varying frequency and potentials of the electric field. If the electric fields fluctuate in a constant manner, the masses of all the ions formed in the source can be scanned sequentially from high to low mass and low to high mass in order to create a mass spectrum. In a normal MS or full scan mode, mass ranges are scanned from a selected start mass to a selected end mass within a defined scan time.

In contrast to the quadrupole mass analyser unit, the RF hexapole only serves the function of ion guidance and not mass selection. Through a focussing effect ions are directed into a beam. The same effect can be assumed for the hexapole transfer lens. The collision cell is also a RF-only quadrupole. Fragmentation is performed by collision induced dissociation (CID), where the molecular ions fragmentate in an argon gas phase.

Once extracted and transferred into the drift tube (TOF analyser), the ions are accelerated. A pulsed voltage is applied to ensure that all the ions leave the source at the same time. Following an initial acceleration phase, the ions reach a velocity that is inversely proportional to their masses. The same relation applies to the time is taken the ions to travel through the analyser traverse. Each  $m/z$  value hence features a characteristic time of flight from pusher to detector. With single charged ions the lighter species arrive at the detector first, followed by successively heavier ones. With multiply charged ions the TOF is proportional to the ion root mass, a correlation that can be exploited to calculate the mass of unknown proteins.

The theoretical upper  $m/z$  limit examinable via TOF-MS is about 350 kDa, which makes it very useful for analysing substances of high molecular mass such as proteins. The problem with TOF separation is the spread of velocities for identical  $m/z$  ions, resulting in lower resolutions. For this reason a reflectron is applied to synchronize the arrival of those ions, but with very high masses a lower resolution has to be accepted. With a resolution above 5000 FWHM (full width, half height), the accuracy of the system's mass measurements is above 5



ppm. Dead time corrections (intensity dependent mass assignment) are compensated with the support of the MS software and can in case of mass drift after instrument tuning and calibration be diminished by applying internal standards or lock masses. The QTOF micro provides two distinct lock mass infusion methods. In normal ESI a special automated dual lockmass source enables automated, exact mass measurement from a second sprayer, eliminating the need for T-plumbing and potential ionisation interferences between analyte and standard. In nano ESI-MS the lock mass has to be spiked into the LC effluent by tee-ing the connection between LC and Nanomate.

For final signal detection the ion current is amplified by a cascading effect of multichannel plates (MCPs) and converted to a voltage pulse detected by a TDC (time to digital converter).

### **2.2.3 MS – Strategies**

The state of the sample entering the MS decides on the MS-strategy. If proteinogenic samples are digested, the peptide mixture can be either analysed by peptide mass fingerprinting (PMF) in single MS mode, or by sequence analysis in tandem mass spectrometry (bottom up approach). PMF after tryptic digestion and whole protein analysis (top down approach) can both be performed in MS mode. The mass charge ratios of the analyte are measured for the masses to be calculated. As peptide mass fingerprinting is usually performed by MALDI-TOF analysis it will not be discussed in the context of this thesis.

Tandem mass spectrometry (MS/MS) can be used to elucidate peptide sequence information, whereas the fragmentation mechanism enables protein sequence analyses and characterizations of great specificity.

### **2.2.4 Tandem mass spectrometry – MS<sup>2</sup> – Mode**

Tandem mass spectrometry (MS/MS) exploits a fragmentation mechanism resulting from collision induced dissociation. Molecular ions collide with neutral gas phase molecules (argon) within a RF hexapole collision cell. As a consequence of the collision, the kinetic energy of the analyte molecule is transformed into internal energy. Bond breakages can be observed and fragmentation into smaller fragment ions occurs. A hybrid instrument like the QTOF micro allows for various MS/MS strategies including product ion scans, precursor ion scans or neutral loss scans, all of which are possible.

In product ion scans the first quadrupole analyser is used to select a precursor ion. This ion is then allowed to enter the collision cell where it undergoes CID fragmentation. A number of fragments, the product ions, are subsequently transferred to the TOF analyser. Fragmentation occurs at low-energy CID levels in the hybrid instrument. This fragmentation mechanism (Figure 19) usually results in the production of two complementary product ion series (b- and y-ions). As each peptidic bond of the peptide backbone could become disrupted, the fragment ion series form ladders that are indicative of the primary peptide sequence.

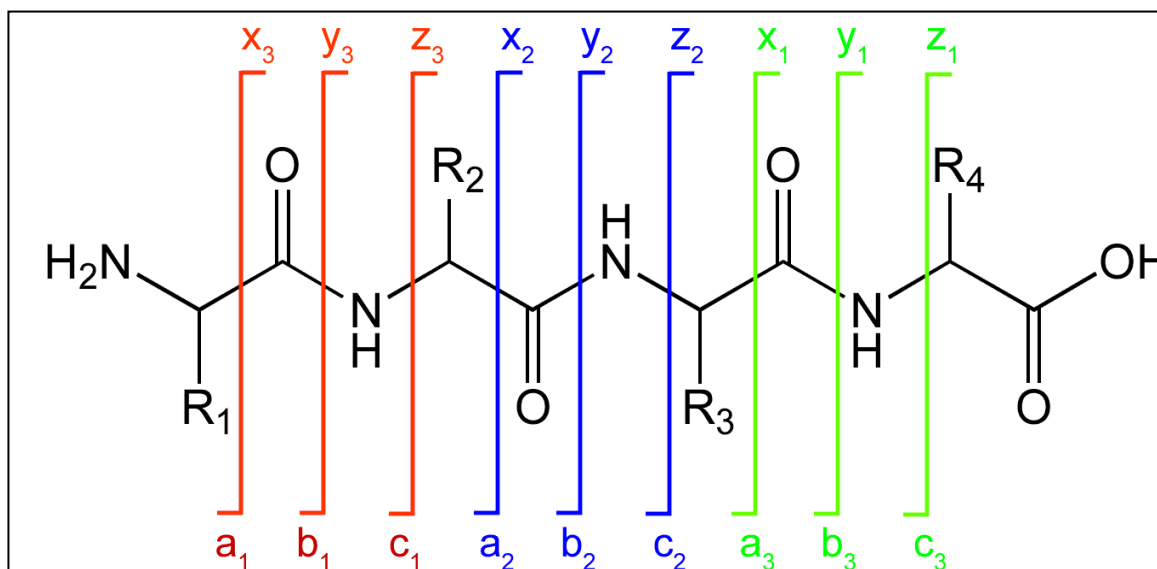


**Figure 19 Peptide fragmentation nomenclature [79].** The b-ion series contains ions with N-terminal charges, means the N-terminal amino acid and extensions from it, while b-ion series include the C-terminus of the peptide and ongoing extensions from this residue.

The b-ions represent the total mass of the amino acids, whereas the y-ions show the total residue mass plus 19 Da. In addition, a-ions are often paired with the b-ion series, showing a 28 Da mass shift owing to the C=O group difference. With a-, b- and y-ion series, peaks could be observed with mass shifts of -17 Da due to the loss of ammonia or -18 Da in case of water. The other ion series (c-, x- and z-series), as well as internal fragments, tend to appear with high energy CID approaches. The fragmentation pattern of a peptide in a MS<sup>2</sup> product ion spectrum is therefore indicative.

The QToF micro uses data directed analysis (DDA) for precursor ion discovery. The software tool enables the instrument to perform DDA, switch from MS to MS/MS mode and then return to MS mode in compliance with data-dependent criteria. This feature provides a possibility of sample measurement even with online LC-MS/MS, including precursor selection in real time. The system continuously records MS survey spectra throughout a chromatographic run and dynamically detects candidates for full product ion analysis. Whilst

components of adequate ion count rates eluting, the  $m/z$  value is determined and the QTOF switches to transmit the discovered precursor  $m/z$  only. This is followed by the run of a collision energy profile fitting to the targeted precursor  $m/z$ , and simultaneously MS/MS spectra are recorded. Up to eight precursor ions can be determined in parallel. Afterwards the system returns to MS survey, in order to trace the next component.

Samples could nonetheless be analysed by classical procedures involving sample analysis in a MS mode, precursor ions identification and a re-run of the sample material in MS/MS mode, in order to acquire MS/MS data from each of the precursor ions.

### 2.2.5 Bottom Up approach

In bottom up approaches complex protein mixtures or purified proteins are digested by proteases and the resultant peptides are analysed via MS for native protein identification. Especially complex protein mixtures can be digested to peptide level and then separated by online chromatography coupled with ESI-MS. Digests can contain a large variety of peptides. The original protein is identified by comparing the peptide mass spectra with theoretical peptide masses calculated from proteomic databases. Bottom up approaches are the methods most commonly used for protein identification and characterization, but have some limitations in terms of complete sequence coverage, with only single fractions of the total peptide population of a given protein being identified and hence only single sections of the protein sequence being obtained. This renders the identification of posttranslational modifications difficult. Usually trypsin is the enzyme of choice in bottom up approaches as it allocates the basic residues of arginine and lysine to the C-terminus of a peptide. This is beneficial for fragmentation and sensitivity with CID tandem mass spectrometry, but unspecific protein sequence cleavages and self-digestion are possible.

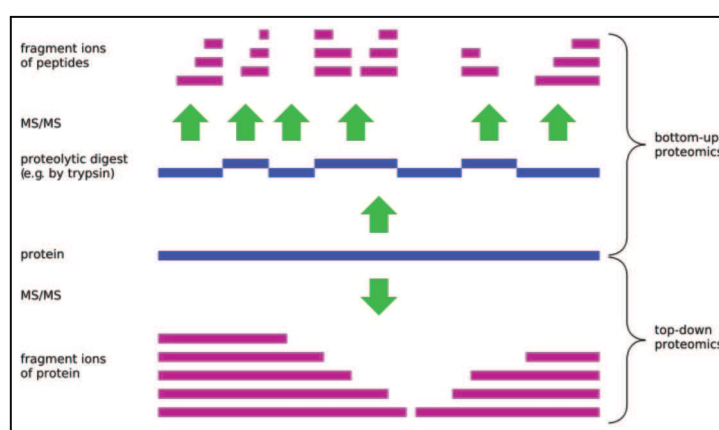


Figure 20 Top down versus bottom up approaches in proteomics [80].

### 2.2.6 Top Down approach

Intact protein ions or large protein fragments are subjected to gas-phase MS fragmentation. The determination of product ion masses from multiply charged product ions is possible, but this analytical method could lead to ambiguities as the charge state of the product ions can differ from that of the charged protein precursor ion.

Two major advantages of this MS strategy lie in the availability of complete protein sequences and the ability to locate and/or characterize post translational modifications without a time consuming digestion procedure. The top down approach is subjected to several limitations. The spectra of multiply charged proteins are highly complex and limit approaches to isolated or only simple protein mixtures.

Usually ESI-QTOF-MS is not the appropriate instrumentation for these approaches, because CID is not the favoured technique with top down proteomics and the resolution is limited, rendering online separations nearly impossible. But with the QTOF micro, stationary experiments are possible even including LC pre-fractionation with the help of the Nanomate robot system.

### 2.2.7 Protein sequence analysis with MassLynx and PLGS software

The MassLynx software controls both the UPLC and the MS instrument and can support any other interaction between Waters devices. The core of the MassLynx software is provided by a sample list, a key feature for initiating any activities related to several samples. The software is able to control each part of the MS system, from the solvent manager via the sample to the detectors or the lock spray source.

ProteinLynx™ Global Server (PLGS) is an IT platform providing a range of tools for protein identification, characterization and quantification by exploiting the specificity of exact mass data. This includes data processing, database searches, *de novo* sequencing and BLAST homology searching. The database management allows the integration of individually created databases as well as automatic web uploads. With this thesis the Swissprot/Trembl database (UniprotKB release) in *fasta*-format was used. This first download in 2006 (March 21<sup>st</sup>) contained all entries available at that point in time. The entire database was then downloaded again in 2009 (July 7<sup>th</sup>). In addition, species-dependent entries were extracted and attached to the PLGS software (Table 8). Species were selected with regard to the brewing raw materials,

## INSTRUMENTAL BACKGROUND

phylogenetic relationship and probable involvement in the respective quality issues. This helped to significantly shorten the PLGS evaluation times.

**Table 8 Overview of the database resources used and database entries relating to extracted species.** The UniprotKB includes Swissprot and TrEMBL releases that were regularly updated.

Database	No. of the release	Date	Species	Number of entries
UniProtKB	49.3, Swissprot	06.03.2006	All	212.425
	32.3, TrEMBL			2.666.963
UniProtKB 15.5	57.5 Swissprot 40.5 TrEMBL	07.07.2009	All	470.369 8.594.382

Database	Species	Database entry	Number of entries	Comment
UniProtKB, release 15.5 (July 7, 2009)	barley	barley	5.041	2.106 common protein entries with both names
		<i>Hordeum Vulgare</i>	2.106	
	wheat	wheat	36.723	5.834 common protein entries with both names
		<i>Triticum Aestivum</i>	6.782	
	yeast	<i>Saccharomyces</i>	40.226	no further distinction into subspecies
	hops	<i>Humulus</i>	194	175 for European hop
	stemphylium	<i>Stemphylium</i>	431	microorganism with possible gushing potential
	penicillium	<i>Penicillium</i>	37.488	
	fusaria	<i>Fusarium</i>	4.614	
	aspergillus	<i>Aspergillus</i>	102.216	
	nigrospora	<i>Nigrospora</i>	1	
	pediococcus	<i>Pediococcus</i>	2.324	possible beer spoiling microorganism
	lactobacillus	<i>Lactobacillus</i>	92.561	
pectinatus	<i>Pectinatus</i>	22		
megasphaera	<i>Megasphaera</i>	19		

## **CHAPTER III**

---

### **PROJECT OBJECTIVES**

### 3 Project objectives

Structural protein identifications of beer and brewing related samples are few and far between. The analyses performed in breweries are instead based on simple, standard protein quantification methods or superficial quality assessments on the malt side. The few proteomic studies including distinct identifications on a molecular level to have been performed with this sample material so far usually involved gel electrophoresis and additional MALDI-analysis. This project is aimed at the development of alternative structural protein identification approaches that do not depend on gel electrophoretic separation. The strengths of UPLC separation should be applied instead and optimized before any (nano)ESI- and ESI-QTOF-MS and -MSMS analysis. An existing protein extraction method (phenolic protein extraction [81]) had to be adapted to the complex and highly sugar-rich sample material and then optimized. Purified and pre-concentrated samples were analysed for peptides after tryptic digestion, as well as for “native“ (whole) and denatured proteins. The analyses were mainly based on bottom up approaches, in order to obtain structural information on the general protein content and composition. On the other hand the instrumental resources were to be tested and used to their full advantage in method development. Especially this part of the project was to be performed in a manner ensuring adequate adaptability to other, distinct research topics (e.g. foam stability, haze development). The instrumental part should include both bottom up and top down techniques.

The composition of beer proteins, the protein content of brewing process samples and the quality aspect of storage haze formation were of great interest right from the start of the project. One of the main focus areas was identification and tracing of single, even well-known proteins like nLTP1, protein Z and some others very recently identified by in house tests. Early analyses were performed via HPLC-MS. Given the increased gushing tendency in 2007/2008, the research focused on this quality problem for about a year, because the initial results yielded by the way of standard gushing tests (Modified Carlsberg-Test) had revealed a need for in-depth proteomic investigations. At the time the methods were entirely adapted to UPLC separation. Towards the first methods developed for “native“ (whole) protein as well as peptide studies with this research topic, further method development was proceeded for highly complex but also low concentrated samples. Both bottom up and top down approaches were applied to further analyse the malt, brewing process, beer and haze samples. In the final stages the combination of both bottom up and top down protein approaches in a single LC/MS experiment was tested with the aforementioned sample material [82].

## **CHAPTER IV**

---

**MATERIALS**



## 4 Materials

In the absence of other information all the materials and chemicals were purchased from the following producers: Merck (Darmstadt, D), Roth (Karlsruhe, D), Sigma Aldrich (Steinheim, D) and Steiner (Siegen, D). All chemicals were of reagent grade (p.a. „pro analysis“) as a minimum. MS solvents were even of extra pure MS grade (hypergrade) until spring 2009. But with the acetonitrile crisis of 2009 the grade had to be switched to HPLC grade. The further manufacturers of chemicals and materials relied upon included: AB Enzymes (Darmstadt, D), Bio-Rad Laboratories (Munich, D), Brennereibedarf Franz Eckert (Tholey, D), Eppendorf (Hamburg, D), GE Healthcare (Munich, D), Hopsteiner (Mainburg, D), Mallinckrodt Baker (Deventer, NL), Phenomenex (Aschaffenburg, D), Promega (Madison, USA), SunChrom (Friedrichsdorf, D) and Waters (Milford, USA).

### 4.1 Chemicals

#### Enzymes:

Alkozym S 500  
 $\alpha$ -Chymotrypsin (*Bovine pancreas*)  
 Corolase<sup>®</sup> 7089, LAP, L10, PP, TS  
 Dexlo<sup>®</sup> CL  
 Gammaprotease RFG 660L  
 Papain suspension (*Papaya latex*)  
 Pepsin (*Porcine gastric mucosa*)  
 Proteinase K  
 Rohalase<sup>®</sup> Barley L, SEP  
 Rohament<sup>®</sup> CL  
 Thermolysin (*Bac. thermoproteolyticus rokko*)  
 Trypsin (sequencing grade modified)  
 Trypsin buffer

#### Manufacturer:

Brennereibedarf Franz Eckert  
 Sigma Aldrich  
 AB Enzymes  
 Brennereibedarf Franz Eckert  
 AB Enzymes  
 Sigma Aldrich  
 Sigma Aldrich  
 Sigma Aldrich  
 AB Enzymes  
 AB Enzymes  
 Sigma Aldrich  
 Promega  
 Promega

#### Fluids:

Acetic acid, 100 % waterfree, p.A	Merck
Acetone	Merck
Acetonitrile (ACN), hypergrade LCMS	Merck
Acetonitrile, HPLC-grade	Steiner
Ammonia, 32 %	Merck
$\beta$ -Mercapto-ethanol	Roth
Benzol	Merck
Butanol	Merck
Chloroform	Merck
Diethyl ether	Merck
N, N-Dimethylformamide (DMF), > 99.8 %	Fluka
Dimethyl sulfoxide (DMSO)	Sigma Aldrich
Ethyl acetate	Merck
Ethyl alcohol (EtOH), 96 %, gradient grade	Merck

## MATERIALS

---

Ethylenediaminetetraacetic acid (EDTA)	Sigma Aldrich
Ethyl hexanoate	Merck
Formic acid (FA), 98 – 100 % purity	Merck
Heptane, Hexane	Merck
Hydrochloric acid (Titrisol®)	Merck
Isoamyl alcohol	Merck
Methyl alcohol (MeOH)	Baker and Merck
n-Propanol, octanol	Merck
Pentane	Merck
Phosphoric acid	Merck
Pure water, 18.2 mΩ, < 0.5 TOC	Millipore (Synthesis A10 system)
Sodium azide	Merck
Sodium deoxycholate (DOC)	Merck
Sodium hydroxide	Merck
Trichloroacetic acid (TCA)	Merck
Trifluoroacetic acid	Merck
Tris(Hydroxymethyl)aminomethane	Merck
Undecane	Merck
 <u>Gas:</u>	
Argon 5.0	Linde gas
Nitrogen	Peak Scientific, N <sub>2</sub> generator
 <u>Hops extracts:</u>	
Hop Extract G, 30 % and 20 %	Hopsteiner
Iso-Extract, 30 %	Hopsteiner
 <u>MS-standards:</u>	
Bovine serum albumin (BSA)	Sigma Aldrich
Cytochrome C	Sigma Aldrich
[Glu <sup>1</sup> ]-Fibrinopeptide B (Human, synthetic)	Sigma Aldrich
Lectine	Sigma Aldrich
Leucin encephaline, synthetic, 97 %	Sigma Aldrich
Myoglobin (Horse heart)	Sigma Aldrich
nLTP1 lyophilisate (February 2006)	TU Berlin
Bovine trypsinogen	Sigma Aldrich
 <u>Solids:</u>	
Ammonium carbonate	Merck
Ammonium hydrogen carbonate	Roth
D-(-) Fructose	Merck
D-(+) Glucose, anhydrous	Merck
Dithiothreit (DTT)	Roth
D-(+) Maltose monohydrate	Merck
Guanidinium hydrochloride (Gua-HCl)	Roth
Iodacetamide	Sigma Aldrich
Maltotriose	Merck
Phenol	Roth
RapiGest™SF*	Waters
Sodiumdodecyl sulfate	Roth
Urea	Roth

Test-Kits:

2-D Quant Kit, protein quantification	GE Healthcare
Biorad Roti <sup>®</sup> Quant Universal Assay	Roth
EZ:faast GC/MS, amino acid-kit	Phenomenex

**4.2 Buffers and eluents**

All buffers and solvents were prepared using de-ionised Millipore water. Buffers were autoclaved and stored at room temperature. LC-solvents were degassed by ultrasonification (10 minutes as a minimum). In the absence of contrary information the UPLC solvents were prepared over a time range of 2 – 5 days and 0.1 % formic acid was usually added.

Buffer:

Ammonium carbonate buffer	50 mM (pH 8.5)
Ammonium hydrogen carbonate buffer	50 mM (pH 7.8)
PBS buffer	1 x (pH 7.4)
Tris-HCl buffers	50 mM (pH 2 – 10)

UPLC solvents:

Eluent A	De-ionised water + 0.1 % FA
Eluent B	Acetonitril + 0.1 % FA
Weak wash (adapted to each starting gradient)	5 % ACN + 0.1 % FA
Strong wash	90 % ACN + 0.1 % FA

**4.3 Consumables**

Agitation spatula (enzymes skewers, PV)	Steiner
Biosphere Filter Tips, 10 µL, PCR-clean	Eppendorf
Crimp caps, steel, 11 mm	WICOM
Crimp vials, clear and brown glass, 2 mL	WICOM
epT.I.P.S Standard, 2 – 200 µL	Eppendorf
epT.I.P.S Standard, 50 – 1000 µL	Eppendorf
Falcon tubes, 15 and 50 mL	Steiner
Folded Filter, 595 ½, 125 mm	Whatman
Folded Filter 150 and 320 mm	Macchery & Nagel
Light cyclers capillaries	Roche
Micropipette, stainless steel	Steiner
NuTip <sup>™</sup> , C <sub>18</sub> silica material, 10 – 200 µL	SunChrom
Pasteur pipette, glass, disposable, 150 mm	Hirschmann Laborgeräte
Petri dishes (145 mm/20 mm)	Greiner Bio-One
Pipette tips, 0.5 – 5 mL	Brand
Protein LoBind tubes, 1.5 mL	Eppendorf
Protein LoBind microplates, 384/V-PP clear	Eppendorf
Reaction tubes, standard, 1.5 and 2 mL	Eppendorf
Twin.tec PCR plates, 96 and 384/V-PP	Eppendorf
Vessels, standard and semi-micro	Ratiolab
Vial, 2 mL (clear and brown glass)	WICOM

Vial inserts, glass, 100 µL

Phenomenex

#### 4.4 Instruments

##### Analytical balance:

MX5 analytical balance

Mettler Toledo (Columbus, USA)

PG 6002 S analytical balance

Mettler Toledo (Columbus, USA)

XS 205 analytical balance

Mettler Toledo (Columbus, USA)

##### Cabinet dryer:

TV 30 b

Memmert (Schwabach, D)

UL 30

Memmert (Schwabach, D)

##### Centrifuge:

Benchtop centrifuge, 3k 15

Sigma (Steinheim, D)

Benchtop centrifuge, Universal 320 R

Hettich (Tuttlingen, D)

+ angle rotors: 6, 12 and 30 places

Centrifuge beaker, 1 L, polycarbonate

Nalgene (Tuntenhausen, D)

LC carousel centrifuge

Roche (Penzberg, D)

Minifuge, 1 – 2 mL

neo Lab (Heidelberg, D)

Multifuge 3 S-R

Kendro (Langensellbold, D)

Multifuge 4KR

Kendro (Langensellbold, D)

Multifuge 4 KR, 4500g

Heraeus (Hanau, D)

Rotator LD 79

Labinco (Giessen, D)

##### Congress wort:

Congress wort cooker

Bender & Hobein (Bruchsal, D)

##### GC-MS:

Agilent 689 N Network GC system

Agilent Technologies (Böblingen, D)

Agilent 5975 (Insert XL Mass Selective Detector)

Agilent Technologies (Böblingen, D)

MPS2 Twister

Gerstel (Mühlheim a. d. Ruhr, D)

##### Gushing-Test-equipment:

DLFU laboratory disk mill

Bühler Miag (Braunschweig, D)

Hand corker

AAP+CRO Anlagenbau

Heat-plate, type: PZ44, 450 °C

HGL (Laborbedarf)

Rotor mixer, Gastronom GT 95

Steiner (Siegen, D)

Sieves, > 200 µm, 200 – 800 µm, 800µm – 2 mm

Steiner (Siegen, D)

Shaker BTM, SM 30 Control

Bühler GmbH (Hechingen, D)

Shaker, Laboshake

Gerhardt (Königswinter, D)

##### Freezers and fridges:

-80 °C freezer

GFL (Großburgwedel, D)

-20 °C freezer

Bosch (Gerlingen-Schillerhöhe, D)

0 °C refrigerator

Medizin/Labortechnik F. Gossner KG

##### Glass equipment:

Beakers, various, 50 – 1000 mL

Steiner (Siegen, D)

Funnels, 50 – 250 mm

Steiner (Siegen, D)

## MATERIALS

---

Measuring glasses, 10 – 500 mL	Brand (Wertheim, D)
Pipettes, various, 1 – 100 mL	Brand (Wertheim, D)
Volumetric flasks, various, 5 – 500 mL	Steiner (Siegen, D)
<u>HPLC and UPLC-columns:</u>	
Jupiter C <sub>18</sub> , 5 $\mu$ m, 300 Å, 150 x 2 mm	Phenomenex
Synergy 4 $\mu$ m MAX RP C <sub>12</sub> , 80 Å, 100 x 4.6 mm	Phenomenex
X-Bridge™ BEH300 C <sub>18</sub> , 5 $\mu$ m, 150 x 4.6 mm	Waters
UPLC BEH300 C <sub>4</sub> , 1.7 $\mu$ m, 2.1 x 150 mm	Waters
UPLC BEH300 C <sub>4</sub> , 1.7 $\mu$ m, 2.1 x 50 mm	Waters
UPLC BEH C <sub>18</sub> , 1.7 $\mu$ m, 130 Å, 2.1 x 50 mm	Waters
UPLC BEH SHIELD RP C <sub>18</sub> , 1.7 $\mu$ m, 2.1 x 50 mm	Waters
<u>LC-Instrumentation:</u>	
Acquity® UPLC	Waters (Eschborn, D)
Chromeleon, Summit software	Dionex (Germering, D)
Dionex ICDX 500	Dionex (Germering, D)
Empower, HPLC software	Waters (Eschborn, D)
External pump, model 510, 0.5 – 5 mL	Waters (Eschborn, D)
Fraction collector FC III	Waters (Eschborn, D)
Summit HPLC (Gina 50, P580, ED 40 ECD)	Dionex (Germering, D)
MassLynx, UPLC software	Waters (Eschborn, D)
UPLC PDA detector	Waters (Eschborn, D)
Waters HPLC 2695 separation module	Waters (Eschborn, D)
Waters HPLC 2996 photodiode array detector	Waters (Eschborn, D)
Waters HPLC 2475 multi $\lambda$ fluorescence detector	Waters (Eschborn, D)
<u>Lyophilisation:</u>	
Control unit LD1-1M	Christ (Osterode, D)
Vaccum Lyophilisation Alpha 2-4	Christ (Osterode, D)
<u>MS-Instrumentation:</u>	
MassLynx software	Waters (Eschborn, D)
QTOF micro™	Micromass (Manchester, UK)
Triversa nano Mate™ HD	Advion (Manchester, UK)
<u>Nitrogen determination:</u>	
Automated Segmented Flow Analyser 3 vario MAX CN	Seal Analytical (Norderstedt, D) Elemental (Hanau, D)
<u>Pipettes:</u>	
Reference®, variable 0.5 – 10, 10 – 100, 100 – 1000 $\mu$ L	Eppendorf (Hamburg, D)
Reference®, fix, 200, 1000 $\mu$ L	Eppendorf (Hamburg, D)
Multipette, 12 channels 30 – 300 $\mu$ L	Eppendorf (Hamburg, D)
Pipettus Akku	Hirschmann Geräte (Eberstadt, D)
Transferpette, 1 – 10, 10 – 100, 0.5 – 5 mL	Brand (Wertheim, D)
<u>Photometer:</u>	
DR 5000 photometer	Hach-Lange (Berlin, D)

## MATERIALS

---

### Ultrasonification:

Sonorex Super Bandelin (Mörfelden-Walldorf, D)  
 Sonorex Super RK 255 H Bandelin (Mörfelden-Walldorf, D)

### **4.5 Sample materials**

#### Beer:

Beer standard without KZE 20090210064  
 Beer standard with KZE 20090220062  
 Coagulable nitrogen of Veltins Pils monthly beer standards  
 IEX/SEC fractions of Veltins Pils, lyophilisate TU Berlin  
 Ultrafiltrat (5000 Da) Veltins Pils, lyophilisate Technikum Uni Bielefeld

#### Brew 604 (2007)

Lautering  
 Pumping  
 Start of cooking  
 Cooking finished  
 Pitching wort

#### Brewing process samples:

Cold wort, production scale 20090220103  
 Congress wort, Palatia malt, gushing malt 20085130100  
 Congress wort, Bamberger malt, non-gushing malt 20085130101  
 First wort, production scale 12.01.2009

#### Brewing trial 2006:

**Table 9 Overview of brewing trial modifications 2006.**

trial 2006 sample ID	V1 20062420130	V2 20062420057	V3 20062410156	V4 20062350037	V5 20062410085	V6 20062410030	V7 20062330163	V8 20062340081
description	standard		test stabilisation		test stabilisation		test stabilisation	
	KZE		KZE		KZE		KZE	
hop type	pellet		pellet		pellet		CO <sub>2</sub> -extract	
stabilisation	stabilisation procedure							
hydrogel [g/hL]	60		30		30		30	
PVPP [g/hL]	15		5		5		5	

#### Haze:

Beer standard 02/00 20000620132  
 Beer standard 11/01 20014520052  
 Beer standard 09/02 20023710087  
 Beer standard 02/03 20031020108  
 Beer standard 09/03 20033610071  
 Beer standard 05/04 20041810084  
 Beer standard 09/05 20053510063  
 Beer standard 02/06 20060710063

## MATERIALS

---

Beer standard 05/07	20071720086
Beer standard 01/08	20080220086
Beer standard 04/08	20081510086

### Malt and MCT-samples:

Barley, unmodified	Prestige (May 2008)
Bamberger, non-gushing malt	20085130101
Cargill, non-gushing malt	20081030051
Durst, 100 % brew, non-gushing malt	20081920059
Ireks, 100 % brew, gushing malt	20081420137
Malteurop, gushing malt	20081040063
Palatia, gushing malt	20085130100
Sebastien, gushing malt	average sample

# CHAPTER V

---

## METHODOLOGY



## **5 Methodology**

### **5.1 *Sample types and treatment***

#### **A. Beer**

Both Pilsener beer standards (taken daily or monthly) and Pilsener beer samples (haze samples) stored for longer periods were used for this study. Beer standards (KZE/non-KZE) were furthermore placed in stock and repeatedly examined.

Only 0.5 L packages were selected as far as possible. For further testing the beer volume was always degassed for at least 10 minutes and immediately prepared to minimize oxidative damage. For protein precipitation the beer samples were lyophilised. To do this, 100 mL volumes of degassed beer were placed in petri dishes (width: 145 mm) and frozen at -80 °C for at least 6 h. Following a 24 h lyophilisation period the powder was transferred to 50 mL Falcon-tubes and stored at -20 °C. The weight of each sample was determined both before and after lyophilisation.

#### **B. Brewing process samples**

First wort was allowed to cool down and was centrifuged at 4500 rpm for 1h. Cold wort was also subjected to centrifugation. The fluid supernatants were used for further analysis on the one hand and lyophilised for protein precipitation on the other.

Fermenting room samples were clarified by filtration (folded wort filters). These samples were analysed directly and not subjected to any further treatment.

#### **C. Congress wort samples**

50 g fine malt grist and 450 mL preheated water (45 °C) were mixed. The congress wort was prepared in line with the standard lab-scale mashing procedure (Table 4). The supernatants were lyophilised and stored at -20 °C.

#### **D. Malt extracts**

Malt extracts were prepared via the “Modified Carlsberg Test“ procedure (MCT), a preparation method that will be described in greater detail in section 5.5.1. For protein precipitation and determination the extracts were again lyophilised and stored at -20 °C.

### **5.2 *Preliminary investigations with HPLC and HPLC-MS***

The first HPLC approaches were performed with untreated, degassed beer samples (0.33 L and 0.5 L daily Pilsener standards) on the one hand and IEX and SEC pretreated Berliner and

Veltins Pilsener beer samples (TU Berlin) on the other one. The latter were fractionated, dialysed and lyophilised, though was a nLTP1 (02/2006) standard from the TU Berlin, too.

Pilsener beer  $\xrightarrow{D, L^*}$  IEX  $\xrightarrow{D, L^*}$  SEC (into 14 fractions)  $\xrightarrow{D, L^*}$  1D SDS gelelectrophoresis  
 (\*D = dialysis, L = lyophilisation)

Both bottom up approaches with Nanomate infusion or external syringe LC-MS application and first “native“ protein HPLC-MS runs were tested.

### 5.2.1 Tryptic digestion for bottom up analysis

Beer samples were subjected to tryptic digestion directly, whereas 10  $\mu$ l trypsin stock solution (0.1 mg/mL) were added per 100  $\mu$ L beer sample volume. After overnight digestion and acidification they were analysed by nano ESI-MSMS (DDA experiments).

Respectively 0.5 – 1 mg of the lyophilised sample material were dissolved in 100  $\mu$ L *RapiGest*<sup>TM</sup> SF-solution (0.1 % in 50 mM NH<sub>4</sub>HCO<sub>3</sub> buffer). Common procedures for protein dissociation are based on denaturing agents such as urea, guanidine or SDS. These reagents can inhibit enzyme activity, suppress MS signals, or interfere with them. Using *RapiGest*<sup>TM</sup> SF instead enabled denaturation without enzyme inhibition. MS signal interference was also of minor importance as the surfactant breaks down after sample acidification. This step was always performed with the samples of this study, in order to stop enzyme reactions and to enhance the intensity of the MS signal.

#### A. Reduction and alkylation (optional for protein identification)

- 1.) Addition of 1 M DTT (in 50 mM NH<sub>4</sub>HCO<sub>3</sub>) up to a final sample concentration of 5 mM and incubation for 60 mins at 30 °C.
- 2.) Tubes were allowed to cool down to RT and than a freshly prepared 55 mM iodacetamide solution (in 50 mM NH<sub>4</sub>HCO<sub>3</sub>) was added up to a final concentration of 15 mM. Incubation took place in the dark for 30 mins at RT.

#### B. Digestion

- 1.) The trypsin solution was either freshly prepared or taken from stock (-80 °C storage) and allowed to rest (30 mins at 37 °C) for activation.
- 2.) Addition of trypsin: 10  $\mu$ L to each tube.
- 3.) Incubation at 37 °C overnight for at least 12 h.
- 4.) TFA or FA addition up to a final concentration of 0.5 % or pH-value of 2.

For the IEX and SEC beer fractions that were strongly contaminated with salt an additional ZipTip cleanup procedure was required.

### **C. C<sub>18</sub> ZipTip cleanup**

- 1.) Conditioning of the NuTip C<sub>18</sub> material. 20 µL 90 % MeOH were aspirated and dispensed with 0.1 % FA. Two repeats followed.
- 2.) 5 equilibration cycles with 20 µL 0.1 % FA followed.
- 3.) The samples were loaded to the tip by slow aspiration and dispensation, with no air passing through the sorbent bed. The procedure was repeated 20 times.
- 4.) Washing step (5 times): 20 µL 0.1 % FA were aspirated and discarded.
- 5.) Elution with 20 µL 50 % MeOH

The entire procedure was repeated 3 times. For sample concentration the last eluting step was omitted in the second and third repetition. The first eluate was used for direct elution into the well plate. After this procedure the samples were ready for Nanomate analysis.

### **5.2.2 Bottom up approaches**

The selected nano ESI and standard ESI source conditions broadly varied depending on the quality of the sample material and had to be individually adapted according to their behaviour in the pre- and survey scans.

In comparison to standard ESI infusion, the Nanomate infusion is rather gentle. The voltages applied to the electrospray nozzles ranged from 1.5 to 1.75 kV and the source temperature was limited to 120 °C, with the desolvation temperature kept at ambient temperature. Just for reference: standard ESI conditions normally approach a desolvation temperatures of 200 °C, source temperatures of 120 °C and a desolvation gas flow of 550 L. Irrespective of the sample infusion type (Nanomate or standard ESI via external syringe), DDA experiments were performed with up to eight MSMS channels. [Glu<sup>1</sup>]-fibrinopeptide was used for MS tuning and calibration. Therefore the survey scans covered a mass range of 200 – 2000 Da. The MSMS mass ranged between 70 and 1500 Da.

### **5.2.3 Sample fractionation with the Dionex HPLC**

Standard Pilsener beer samples were fractionated with the help of a Dionex HPLC system to concentrate the protein and separate it into single fractions (creating the project's own nLTP1 and protein Z standards). In a twenty-one minute HPLC run the flow was directed to an

external fraction collector. The effluent was distributed to glass test-tubes within a 20 second time window. A series of up to 30 homologue sample injections could be collected by the tubes via this procedure.

A Jupiter C<sub>18</sub>-column (5  $\mu$ , 300 Å, 150 x 2 mm) was selected for separation purposes under the following HPLC conditions: eluent A = H<sub>2</sub>O + 1 % CH<sub>3</sub>COOH, eluent B = MeOH + 1 % CH<sub>3</sub>COOH, flow rate 0.5 mL/min, sample injection volume = 150  $\mu$ L and column temperature 40 °C. The elution was monitored with a PDA detector in scan mode from 210 to 600 nm. The gradient timetable (Table 10) was developed with regard to adequate separation but also time parameters, as the samples were serially injected and the test-tube volumes limited.

**Table 10 Gradient timetable used for beer fractionation.**

time	A [%]	B [%]	flow	curve
0.00	97.0	3.0	0.500	linear (1)
1.50	97.0	3.0	0.500	linear (6)
5.00	50.0	50.0	0.500	linear (6)
12.00	1.0	99.0	0.500	linear (6)
17.00	0.0	100.00	0.520	linear (6)
18.00	0.0	100.00	0.520	linear (6)
18.50	97.0	3.0	0.500	linear (6)
21.00	97.0	3.0	0.500	linear (6)

The fractions were injected into the MS via the Nanomate and analysed for whole proteins.

#### 5.2.4 HPLC-MS top down investigations

Untreated brewing process and beer samples, as well as the standards and beer fractions (TU Berlin) were analysed for whole proteins. The HPLC was serially connected to the QToF micro via the standard ESI source (desolvation temperature 150 °C, source temperature 100 °C, desolvation gas 550 L). MS tuning and calibration were performed with a mixture of two protein standards over a mass range of 600 – 3500 Da: myoglobin (5 pM/ $\mu$ L) and bovine trypsinogen (10 pM/ $\mu$ L) in 50 % ACN + 0.2 % FA.

A Synergy MAX RP C<sub>4</sub> column was selected for whole protein analysis. Eluent A featured 0.1 % FA/H<sub>2</sub>O and eluent B MeOH with 0.1 % FA. 100  $\mu$ L sample volume were injected and separated in a 21 minute HPLC run (conditions identical to Table 10). The column temperature was also 40 °C. Again the PDA was in scan mode, but this time from 190 to 600 nm.

### **5.3 Protein quantification**

#### **5.3.1 Biorad Roti<sup>®</sup> Quant Universal assay and Nanoquant assay**

Roti Quant Universal protein determination is achieved via an enhanced Biuret reaction. The determination procedure used in this study complied with the instruction manual for vessel approaches. BSA calibrations were performed with both freshly prepared BSA/water and BSA/5 % EtOH standards. The concentrations ranged from 0 to 2000 µg/mL. The photometer determination wavelength was 503 nm. 100 µL sample volumes were used and beer samples needed to be diluted (1:20). Depending on their concentration the dilution factor for the malt extracts could even be as high as 500 or 1000.

The sugar cross-reactivity of the assay was tested by virtue of the known sugar content of beer. For this reason sugar solutions of glucose, fructose, maltose and maltotriose were prepared. The sugars were added to the BSA standard in realistic concentrations for Pilsener beer samples (maltose = 50 mg/L, glucose = 37.5 mg/L, maltotriose = 125 mg/L and fructose = 175 mg/L). In addition, increasing concentrations of the sugar solutions were individually determined: maltose 0.1 – 1000 mg/L, fructose 0.065 – 650 mg/L, maltotriose 0.065 – 650 mg/L and glucose 0.02 – 200 mg/L.

Samples were analysed by Roti Nanoquant, a procedure also based on a modified Bradford test. 15 mg of sample lyophilisate were dissolved in 2 mL water, followed by a preparation in line with the test instructions. Both the sugar and polyphenol crossreactivity was tested.

#### **5.3.2. 2D-Quant Assay**

The BSA standard curve calibration was prepared as prescribed by the instruction manual, but the 2D-Quant standard protein quantification procedure was slightly modified for beer and MCT extract samples. The sample volumes usually assayed amounted to 30 µL. Three duplicates were prepared throughout. Up to the centrifugation the procedure complied with the 2D-Quant manual. Owing to the very speedy resolution of the protein pellets after centrifugation the procedure had to be prolonged and performed incrementally.

The tubes were initially centrifuged at 15000 rpm for 10 min before 800 µL of the supernatant was removed. This was followed by a second centrifugation at 15000 rpm for 10 mins. 150-180 µL of the remaining 200 µL supernatant volume was then removed, followed by a final centrifugation (identical conditions as before). The remaining fluid was removed with a micro pipette until nearly dryness. Following the preparation of the protein pellets the procedure

once more complied with the instructions in the manual. The incubation time of the working colour reagent was 20 minutes throughout and the adsorbance was measured at 480 nm. Microvessels were used for the final preparation and colorimetric determination. Again the assay was tested for sugar crossreactivity with the same parameters as in the Roti Quant assay.

#### **5.4 Investigation concerning haze**

The term haze is applied to reversible chill haze (0 °C storage haze) and permanent storage haze (RT storage), but also to the basic turbidity found even in bottled beer.

##### **5.4.1 Haze preparation**

###### **A. Stored beer samples**

In the case of chill haze all the preparation and purification steps had to be accelerated and the centrifugation had to be performed at 4 °C, in order to minimize the loss of reversible material. Immediately after opening the stored beer bottles the liquid beer volume was largely removed with the help of a water jet pump. The haze sediments were then concentrated by centrifugation. Usually several bottles of one beer batch were mixed in 1 L beakers, in order to yield a visible haze portion at the end. After the degassing of the samples the initial centrifugation process was applied at 4500 rpm for 1 h. The supernatant was disposed of and the haze material dissolved and purified in 10 mL pure water. Following its transfer to 50 mL Falcon tubes, the second centrifugation could be performed at 6000 rpm for 30 mins. Again the supernatant was removed, followed by 3 additional washes. The wash volume was lowered to 5 mL and another centrifugation was performed at 6000 rpm for about 30 mins. Following a final cleaning procedure the haze material was either stored at -80 °C (native, untreated form) or lyophilised and then stored at room temperature (the powdery form was very stable and showed no hygroscopic attitude).

The lyophilised material was used for protein quantification in the Vario Max N and protein precipitation tests. Both bottom up and top down analyses were applied to lyophilised haze, while the native material was only subjected to top down runs.

###### **B. Basic beer turbidity**

500 mL of bottled beer or samples taken after the filtration procedure were decanted into 1 L centrifugation beakers in their entirety. The material was briefly degassed and spun at 4500

rpm for one hour. Immediately with centrifugation stop beakers were removed and in case of solid particle swirls in the middle of the fluid this part was isolated and transferred into 50 mL Falcon tubes using a 5 mL pipette. The remaining supernatant was disposed of as quickly as possible, as this kind of turbidity easily dissolves and could only be concentrated with difficulties. The invisible sediment was removed from the beaker bottom and wall with 10 mL pure water. The washing solution was combined with the particle isolates. After a 1h centrifugation at 6000 rpm a very low amount of sediment would usually be visible. Several washing steps followed, gradually decreasing the volumes of washing solution along with the size of the sediment tubes. In a final step the sediment was decanted into 100  $\mu$ L glass tube inserts or even smaller PCR capillaries. The haze material was lyophilised for weight measurement, while the microscopical analyses were performed with native and lyophilised haze.

#### **5.4.2 Solubility tests**

Both the lyophilised and native haze material were subjected to an extensive series of solubility tests. The chemical solvents included water, RapiGest<sup>TM</sup>SF (0.1 %), urea (1, 3, 5, 7, 9 M), guanidinium HCl (0.5, 1, 2, 3 M), dimethyl sulfoxide, dimethylformamide (100 %), methanol (ammonia, pH 10), n-hexane, n-octane, methanol, ethanol, acetone, acetonitrile, TFA or FA, phenol,  $\beta$ -mercaptoethanol, mixtures combining urea with 3 M Gua-HCl, urea with DTT, as well as 3 M Gua-HCl, DTT and non-ionic, cationic, anionic and amphotensides. The solubilization process was either supported by ultrasonification or mechanical micro-pistill treatment. In case of the latter procedure ca. 5 mg haze were exposed to 500  $\mu$ L solvent. A first mixture was achieved by pipette movement only, followed by a number of squeezing and centrifugation operations. After each centrifugation the supernatant was removed and new solvent was added to the haze remainder (if provided).

#### **5.4.3 Tryptic digestion of haze**

##### **A. Procedure I**

Native haze (from at least 5 bottles (0.5 L)) was diluted with 100  $\mu$ L  $\text{NH}_4\text{HCO}_3$  buffer (50 mM) and 100  $\mu$ L RapiGest-solution (0.1 %). After ultrasonification the digestion procedure complied with section 5.2.1. Denaturation and alkylation were included, but the ZipTip procedure was omitted.

**B. Procedure II**

Native or lyophilized haze was denatured by applying 6 M Gua-HCl with 3 mM DTT in 50 mM TRIS-HCl (pH 8). The denaturation mixture's final volume did not exceed 200  $\mu$ L. Incubation took place for 1 h at 60 °C. Alkylation was interposed where desired, otherwise the GuaHCL concentration was diluted to > 1 M (1:6 with 50 mM  $\text{NH}_4\text{HCO}_3$ ). To minimize the dilution of components of interest, the starting volume should not be excessive (100 – 200  $\mu$ L) after the denaturants are added. Dilution was required for tryptic digestion at adequate cleavage conditions. Once digested, the haze samples were ready for Nanomate infusion and top down experimentation following overnight digestion and sample acidification. In some cases cloudy hazes had to be isolated after the digestion. The supernatants were transferred after centrifugation and used directly in the DDA experiments.

**5.4.4 Long-term storage of beer samples**

Beer sample standards were stored over long periods of time in order to analyse the dynamics of haze development. Two beers, one of which had undergone KZE-treatment, while the other one was unpasteurized, were stored at 0 °C as well as room temperature. The haze was then prepared, lyophilized and weighed at intervals of 2 – 4 weeks. Samples were taken over a period of approximately 8 months. Longer observation periods (up to eight years) could only be facilitated via beer originating from various batches. This material was provided from in house stocks.

Any beer supernatant yielded in the preparation of the haze was stored at -20 °C. These samples were used for GC-MS amino acid analysis. The samples were prepared using the EZ:faast amino acid test kit. 14 species of amino acids were traced, including alanine, glycine, valine, leucine, isoleucine, threonine, proline, asparagine, aspartic acid, phenylalanine, ornithine, lysine, tyrosine and tryptophan.

**5.4.5 Top down approaches**

Both lyophilized and native haze were analysed for whole proteins. Small amounts of the material were treated with DMSO and subjected to UPLC-MS detection after ultrasonification. In a 60 minute LC run the samples were separated via an Acquity UPLC BEH 300 C<sub>4</sub> column (2.1 x 150 mm). Eluent A comprised H<sub>2</sub>O and 0.1 % FA, eluent B acetonitrile and 0.1 % FA. At a flow rate of 0.3 mL/min the gradient increased from 5 % to 80 % for eluent A over 50 minutes.



## 5.5 *Gushing studies*

### 5.5.1 Modified Carlsberg Test (MCT)

#### 1.) Extraction of gushing components:

100 g coarse groat and 400 mL water were mixed at top speed for exactly one minute. The suspension was then centrifuged at 4500 rpm for 10 mins. 300 mL of the supernatant were transferred to an 800 mL beaker and the volume heated and reduced to a final volume of 180 – 190 mL over about 20 minutes. The boiled extract was then clarified via filtration and immediately cooled down to RT in a water bath. 5 mL sodium azide stock solution (13.6 g/L) were added to the malt extract and the volume was replenished to a final volume of 200 mL.

#### 2.) Substitution of Bonaqua by malt extract:

0.33 L-bottles of Bonaqua water with a standardised CO<sub>2</sub> content were opened and the liquid level adjusted with the help of a water jet pump, in order to substitute 50 mL of Bonaqua by 50 mL of thoroughly mixed malt extract. Each malt extract was distributed to 3 Bonaqua bottles. Once the oxygen in their headspaces had been replaced by agitation and foaming, the bottles were immediately recapped, followed by a 3 day period of agitation.

#### 3.) Prediction of gushing potentials:

After 72 h of shaking (RT, 70 directional changes a minute) the bottles were allowed to rest for 10 minutes. Right before opening the bottles were turned upside down 3 times for 10 seconds each before resting for an additional 30 seconds. The overflow volume lost, was estimated by weighing and the malt's gushing tendency predicted by applying the following classification:

0 – 5 g weight loss	no gushing potential
5 – 50 g weight loss	possible gushing potential
> 50 g weight reduction	gushing potential.

### 5.5.2 MCT with fractionated coarse groat

The coarse malt groat was first fractionated by sieving. Yielding 4 fractions: the flour fraction with particle sizes under 200 µm, two groat fractions (particle sizes 200 – 800 µm and 800 µm – 2 mm), and the husk fraction with particle sizes over 2 mm. The fractions were used in place of the malt groat and underwent the entire MCT procedure.

### **5.5.3 MCT with hop extract additives**

The hop extracts (hop extract G and iso-extract) were added to the MCT extracts before the refilling and transfer to Bonaqua-bottles. On a brewery scale the hop extracts can be added at the end of fermentation, in case of hop extract G; at the bottling or storage tank and before filtration, but not with finished beer in case of the iso-extract.

The hop extract stock solutions were adapted to MCT scale and selected with regard to the manufacturer's description for large-scale brewing (strong gushing 1 g/hL hop extract G and extremely strong gushing 3 g/hL hop extract G). As the information available on iso-extracts turned out to be scant, they were treated in the same manner as hop extract G.

Two different approaches were tested. In the first the hop dosages were calculated for the 200 mL malt extract volume and in the second for the Bonaqua-bottle volumes, taking into account the dilution resulting from 50 mL extract being transferred to the bottle.

After the transfer to the Bonaqua water bottles the MCT complied with the standard MCT procedure (Section 5.5.1).

### **5.5.4 MCT with enzyme additives**

A great variety of enzyme additives was tested for possible anti-gushing effects. Table 11 summarizes the dosage parameters selected on the basis of enzyme data sheets, the enzyme activity, and optimal temperature.

In the first test series the enzymes were added as soon as the malt extract reached the optimal temperature. The samples were then placed in a shaker and lightly agitated for a period of 3 h, over which they were allowed to cool down. From then on the preparation complied with the standard MCT procedure.

In the second test series the enzymes were added to the MCT extracts after cooling and before bottling. The standard MCT procedure was followed.

Corolase 7089, TS and thermolysine were subjected to an additional test. Again the enzymes were added to the MCT extracts at the optimal temperature, but then the extracts were placed on magnetic heating plates and their temperatures kept at the enzyme's optimal level for three hours, while the fluid was lightly agitated. The subsequent MCT procedure complied with the description in Section 5.5.1.

**Table 11 Overview of enzyme additives**

enzyme	optimal temperature	optimal pH-value	recommended dosage (protein content)	test dosage
<b>Corolase 7089</b>	50 – 55 °C	7 – 7.5	0.01 – 0.5 %	0.01 %
<b>Corolase TS</b>	70 – 75 °C	7 – 7.5	0.01 – 0.5 %	0.01 %
<b>Corolase L10</b>	60 °C	6 – 7	1 – 3 mL/hL beer	0.01 % of protein content
<b>Corolase LAP</b>	60 – 65 °C	6 – 9	0.02 – 0.5 %	0.02 %
<b>Gammaprotease RFG 660L</b>	55 – 60 °C	9 – 10	0.05 – 0.5 %	0.05 %
<b>Corolase PP</b>	40 – 45 °C	7 – 9	0.01 – 0.5 %	0.01 %
<b>Rohalase Barley L</b>	55 – 65 °C	5 – 6	0.1 – 0.3 mL/hL beer	0.01 % of protein content
<b>Rohalase SEP</b>	50 °C	5	undefined	0.01 % of protein content
<b>Rohament CL</b>	60 °C	4 – 5	0.5 – 1 mL/hL wort	5 µL
<b>α-chymotrypsin</b>	25 °C	7.8	undefined	8 U
<b>Heparinase I</b>	25 °C	8.5	undefined	8 U
<b>Papain</b>	25 °C	6 – 7	undefined	8 U
<b>Thermolysine</b>	70 °C	8	undefined	8 U
<b>Alkozym S 500</b>	55 – 60 °C	4.2 – 5	0.5 L/t cereal starch	50 µL
<b>Dexlo CL</b>	up to 80 °C	6	0.2 L/t cereal starch	20 µL
<b>Lyticase</b>	25 °C	7.5	undefined	8 U

## 5.6 Protein precipitation

### 5.6.1 Early precipitation tests with fresh beer and haze

A large number of classical protein precipitation approaches were tested with fluid beer samples, dialysed beer (MWCO: 1000 Da and 15000 Da) and lyophilized haze (reswelled and dissolved in DMSO). The methods shall be mentioned for completeness' sake but not described in detail, not being applicable to the sample materials. The following methods were tested:

- 1.) TCA-DOC precipitation (2 % sodium deoxycholate, 100 % TFA)
- 2.) TCA precipitation (100 % TCA)
- 3.) Acetone precipitation (cold acetone (-20 °C))
- 4.) Ethyl alcohol precipitation (cold 100 % and 90 % ethyl alcohol)
- 5.) TCA-DOC/acetone precipitation (2 % DOC, 100 % TCA, acetone (-20 °C))
- 6.) Acidulated acetone/methyl alcohol precipitation (1mM HCl + acetone (-20 °C), methyl alcohol (-20 °C))
- 7.) TCA/ethyl alcohol precipitation (20 % TCA and ethyl alcohol (-20 °C))
- 8.) Phenol/chloroform/isoamylalcohol extraction (25:24:1, buffered or acidulated phenol).

### 5.6.2 Phenolic extraction

Only lyophilised samples were used for this precipitation procedure. The original instructions developed by Niehaus *et al* [81] were adapted for this analysis. The initial sample weights were adapted to the different sample types.

- 1.) MCT extracts (0.5 g), congress wort (1.0 g), cold wort (1.5 g), unhopped first wort (2.0 g), beer (0.75 g) or beer supernatants of haze samples (0.75 g) were dissolved in 25 mL deionized, autoclaved water. Following the addition of 200  $\mu$ L freshly prepared 1 M DTT and 2 mL 1 M Tris-HCl (pH 7), the solved samples were agitated in a rotator (30 min, 18 rpm, at RT).
- 2.) 6 mL of phenol solution (1 kg phenol/110 mL water) were added and the samples mixed under the same conditions again. Following centrifugation (6000 rpm, 30 mins, 4 °C) and the separation of a phenolic and aqueous phase, the lower phenolic phase and the cloudy interphase immediately above it were transferred to new 15 mL Falcon tubes. This transfer was effected with glass pipettes instead of plastic tools in order to minimize the loss of protein material.
- 3.) Another 200  $\mu$ L 1 M DTT and 300  $\mu$ L 8 M ammonia acetate were added to the protein phases. A final rotator agitation (same conditions as before) followed. Overnight precipitation was started with the addition of 25 mL cold methyl alcohol (-20 °C), with the samples stored at 4 °C.
- 4.) The precipitated proteins were separated by centrifugation (6000 rpm, 30 mins, 4 °C) on the second day. The supernatants were discarded.
- 5.) 2 washing steps followed. The pellets were dissolved in 5 mL of 70 % ethyl alcohol (-20 °C). Supernatants were removed after an incubation period of one hour at 4 °C and centrifugation (6000 rpm, 15 mins, 4 °C).
- 6.) The final washing was performed with 5 mL of acetone cooled to -20 °C. This was followed by a ten minute refrigerated incubation period and a final centrifugation. The supernatants were discarded and the fluids remaining removed with pipettes.
- 7.) The protein pellets were dried under a stream of nitrogen. The degree of dryness could be assessed by the increasing transparency of the pellet.
- 8.) For ongoing bottom up and top down analysis the pellets were resolved under denaturing conditions. Depending on their size, the pellets were covered by 50 – 100  $\mu$ L 3 M GuaHCl with 15 mM DTT. Usually overnight incubation was applied for reswelling and resolving.

### **5.6.3 Sample preparation for bottom up experiments after protein extraction**

For the bottom up approaches the prepared protein samples had to be diluted. Autoclaved 50 mM  $\text{NH}_4\text{HCO}_3$  buffer (pH 7.8) was used throughout. The samples were diluted to a factor of three as a minimum. Any cloudiness to appear was eliminated by centrifugation (12000 rpm, 15 mins). The supernatants were then transferred into fresh tubes and subjected to tryptic digestion, with the alkylation step omitted. The trypsin concentration was adapted to the sample protein concentrations (determined by 2D-Quant). A 1:100 trypsin protein ratio was selected. Following overnight digestion the samples were acidified with 2  $\mu\text{L}$  FA and subjected to UPLC-ESI/MS, UPLC-nanoESI/MS and nanoESI/MS analyses. DDA experiments were performed for structural protein identification.

### **5.6.4 Sample preparation for top down experiments**

The precipitated protein samples were diluted in the manner described in Section 5.6.3. Following centrifugation, aliquots were used for UPLC/MS, UPLC-nanoESI/MS and nanoESI/MS- experiments, while the rest was stored at  $-80\text{ }^\circ\text{C}$  for additional bottom up analyses.

## **5.7 UPLC-MS and UPLC-MS/MS studies**

### **5.7.1 Bottom up approaches**

Owing to their high protein content, the bottom up method was developed using MCT extract samples (following phenolic protein extraction). The digested samples were analysed in various respects. Both UPLC-ESI/MS and UPLC-nanoESI/MS applications were tested. As the Nanomate system provided the additional feature of online LC sample fractionation, the latter approach became the standard method. An UPLC BEH  $\text{C}_{18}$  1.7  $\mu\text{m}$  2.1 x 50 mm column was selected for peptide separation and analysis. MS tuning and calibration was performed with Glu-Fib, usually in a mass range of 300 – 2.000 Da for survey scan mode and 70/100 – 1.600 Da for the MSMS experiments. For higher resolution a double tuning could be performed with LeuEnk before the Glu-Fib tuning. The column was heated to  $50\text{ }^\circ\text{C}$ . Eluent A was again aqueous (+ 0.1 % FA) and eluent B adapted to possible higher UPLC backpressures, i. e. ACN with 0.1 % FA. The weak wash was adjusted to the gradient starting conditions. Peptide analysis was developed via a number of overlapping procedures:

- 1.) To gain a general overview, a first survey chromatogram of the peptide LC run was produced with the Nanomate in LC-chip coupling mode (scan-mode),

- 2.) The same LC gradient could be used for online DDA, online fractionation in scan mode or a combination of peptide fractionation and DDA experiment (again with the Nanomate in LC-coupling mode),
- 3.) In contrast to the online approaches, DDA experiments with reinjected peptide fractions provided an opportunity for long, very stable acquisition periods and additional protein data (Nanomate in infusion mode).

For accurate mass determination a lock mass had to be applied to the LC effluent. As the nano-ESI source did not allow for parallel lock mass application, a branch pipe tee was inserted into the UPLC-Nanomate connection and a GluFib lockmass solution (0.5  $\mu\text{g}$  in 50 % ACN with 1 % FA) spiked with the help of an external pump. The flow rate of the external pump was adjusted to 0.1 – 0.2 mL/min and thus 50 – 100 counts per lockmass scan. The MS acquisition only switched to the lockmass channel every 30 – 60 seconds.

The method development started with 30 minute LC runs, which were prolonged to 60 mins in first instance. In a second step the gradients were elongated to 80 mins and the flow was doubled to fully utilise UPLC and UPLC column capacities (Table 12). The samples were injected three times (7.5  $\mu\text{L}$  in partial loop mode) before the initial separation run. Using this technique of online column sample preconcentration should favour the detection of low abundant peaks.

**Table 12 Development of gradient timetables for peptide separation.**

<b>30 mins UPLC run</b>				<b>60 mins UPLC run</b>				<b>80 mins UPLC run</b>			
<b>Time</b>	<b>A [%]</b>	<b>B [%]</b>	<b>Flow</b>	<b>Time</b>	<b>A [%]</b>	<b>B [%]</b>	<b>Flow</b>	<b>Time</b>	<b>A [%]</b>	<b>B [%]</b>	<b>Flow</b>
0	95	5	0.1	0	90	10	0.1	0	95	5	0.2
1	95	5	0.1	1	90	10	0.1	3	95	5	0.2
20	65	35	0.1	43	70	30	0.1	65	70	30	0.2
25	20	80	0.1	55	20	80	0.1	70	20	80	0.2
27	20	80	0.1	58	20	80	0.1	74	20	80	0.2
27.5	95	5	0.1	59	95	5	0.1	75	95	5	0.2
30	95	5	0.1	60	95	5	0.1	80	95	5	0.2

The first peptide fractionations were conducted to 96 well plates. Enhanced separation capacities, peak sharpening and peak resolution required smaller time fraction windows. 384 well plates were chosen and the number of collected fractions first raised from 96 to 180 and than to a maximum of ca. 380 wells. The first 3 wells of the sequence were always abolished because of the 3-fold sample injections.

Up to 8 MSMS channels could be used for DDA experiments. The charge state profiles always included the 1 – 4 fold positive charge state. Each charge state was directed to a preassigned charge state collection with defined MSMS fragmentation energies.

In case of online DDA measurement, the MSMS experiments were controlled by the levels peptide ion count rates had to reach. Stationary DDA experiments following reinfusion of peptide fractions were cycle time based. The cycle time windows were increased in parallel to ever more accurate peptide fractions. At last 30 mins DDA experiments only had 15 precursor ions selected, which means MSMS times of up to 20 minutes. This choice of parameters should enhance the identification rate for very low abundant peptide fragments.

### 5.7.2 Top down analysis of whole proteins

UPLC-ESI/MS and UPLC-nanoESI/MS applications were tested. Working with the standard ESI-source involved adjusting the cone gas pressure and desolvation temperature to 650 L/h and 300 °C because of the higher LC flow (0.3 – 0.4 mL/min). The softer ionization used with the UPLC-nanoESI approach turned out to be the preferred method for several reasons. Just a small amount of the analyte was needed, providing the opportunity for online fractionation and additional structural identification after proteolytic digestion (bottom up approaches).

A mixture of myoglobin and trypsinogen (myoglobin = 5 pM/μL, bovine trypsinogen = 10 pM/μL in 50 % ACN + 1 % FA) was used for MS tuning and calibration over a wide mass range of 300 – 3000 Da. An UPLC BEH 300 C<sub>4</sub> column was selected for whole protein analysis. The dimensions of the first column (2.1 x 150 mm) were reduced to 2.1 x 50 mm in the later tests. As the chemical attitudes of the sample proteins were unknown, the peptide column (UPLC BEH C<sub>18</sub>) was also tested for their abilities in protein chromatography.

Early tests started with short, 30 minute UPLC runs with the gradient compositions changed regularly. To enhance peak separation, the separation times were soon prolonged to 60 mins and to 75 mins in the last instance. The gradients developed as shown in Table 13. The higher flow rate of 0.4 mL/min resulted in nearly base peak separated, sharp peaks, even for very complex sample mixtures.

**Table 13 Development of gradient timetables for protein separation.**

<b>First 60 mins UPLC run</b>				<b>60 mins UPLC run</b>				<b>80 mins UPLC run</b>			
<b>Time</b>	<b>A [%]</b>	<b>B [%]</b>	<b>Flow</b>	<b>Time</b>	<b>A [%]</b>	<b>B [%]</b>	<b>Flow</b>	<b>Time</b>	<b>A [%]</b>	<b>B [%]</b>	<b>Flow</b>
0	95	5	0.3	0	97	3	0.4	0	98	2	0.4
2	95	5	0.3	2	97	3	0.4	2	98	2	0.4
40	65	35	0.3	50	65	35	0.4	50	70	30	0.4
48	20	80	0.3	55	10	90	0.4	60	10	90	0.4
56	20	80	0.3	56	10	90	0.4	70	10	90	0.4
57	95	5	0.3	57	97	3	0.4	71	98	2	0.4
60	95	5	0.3	60	97	3	0.4	75	98	2	0.4

The eluents used were: Eluent A = H<sub>2</sub>O + 0.1 % FA, eluent B = ACN + 0.1 % FA, strong wash = 90 % ACN + 0.1 % FA, while the weak wash was always adapted to the starting conditions of the LC gradient. The beneficial attitudes of an ACN solvent in the UPLC separation of macromolecules could be verified during the acetonitril crisis 2009, when methyl alcohol was tested as an alternative organic solvent.

A 5 µL sample injection volume for partial loop injection was not exceeded. Multiple sample loading was tested once more. 3 sample loadings became the standard, but up to 7 loadings are possible with this method. The linear conditions of the 2 minute LC loading matched the starting conditions of the protein chromatography.

As described in the previous chapter, a lock mass could be applied by external spiking in the case of nano ESI infusion. Native protein analysis followed a similar strategy as the bottom up approaches. To gain a general overview, the protein chromatography was monitored in full scan mode first. In a second, identical experiment the LC run could be conducted to well plates for protein fractionation. The first tests relied on plates with 96 wells, which were later replaced by 384 well plates. In the end special Protein LoBind plates (384 deepwell) were introduced in order to allow for protein anchorage problems with standard plastic materials.

The protein fractions could be used for different approaches afterwards. On the one hand fractions could be reinfused for bottom up experiments providing an opportunity for analysing the PTMs. On the other hand the contents of the wells (both in fluid form or after lyophilisation) could be used for tryptic digestion and sequential protein identification.

### **5.7.3 Top down and bottom up analysis in a single LC experiment**

The combination of bottom up and top down analysis was achieved by fusing online LC-MS and nano ESI infusion. Intact mass measurement and primary sequence determination was performed via online UPLC-MS(MS) with simultaneous fraction collection. For top down efforts after the UPLC-MS run, the previously collected fractions were observed by automated nano ESI infusion. As only small amounts of analyte were needed for the nano ESI reinfusion, proteolytic digestion could be performed with the remaining sample mass. This was followed by bottom up experiments.

The samples (beer, MCT-extracts, brewing process samples) were lyophilised and proteins precipitated with phenol (see. 5.6.2). The dissolved proteins were analysed by online-RP-UPLC using the UPLC BEH 300 C<sub>4</sub> (2.1 x 50 mm, 1.7 µm). Proteins were separated in a 80 minute run (Table 14) at a flow rate of only 400 µL/min.



The eluent compositions and other system parameters were identical to those described in Section 5.7.2. The UPLC involved the Triversa Nanomate system in LC/Fraction collection mode. The flow rate was split by the Nanomate to 300 nL/min and directed to the QTOF for intact protein analysis in full scan mode (400 – 2000 Da).

**Table 14 Gradient timetable for bottom up experiments in combination with top down approaches.**

<b>80 mins UPLC run</b>			
<b>Time</b>	<b>A [%]</b>	<b>B [%]</b>	<b>Flow</b>
0	98	2	0.4
3	98	2	0.4
56	70	30	0.4
70	20	80	0.4
74	20	80	0.4
75	98	2	0.4
80	98	2	0.4

Top down observations were achieved by automated nanoESI reinfusion of 5  $\mu$ L of the analyte volume. Remaining fractions were lyophilised, digested and dried or directly digested in a second test. The peptides were resolved and analysed in infusion mode at 200 nL/min. DDA tests were carried out for 4 precursor ions.

# CHAPTER VI

---

## RESULTS AND DISCUSSIONS

## 6 Results and discussions

### 6.1 Preliminary HPLC investigations

#### 6.1.1 Non specific lipid transfer protein 1 (nLTP1)

Earlier, native, lyophilised nLTP1 standard material at TU Berlin had been prepared from commercial available Berliner Pilsener beer. The nLTP1 identified with the help of an immunoblot at the TU Berlin was confirmed by the bottom up investigations of this thesis. The general, underlying identification procedure will be explained for nLTP1 and in an exemplary fashion for the other sequential protein identification approaches of this study.

Tryptic digested and desalted nLTP1 standards were subjected to nano ESI infusion and DDA experiments. 4 to 8 MSMS channels were used for precursor ion fragmentation by charge state selection. As a result of the adequate enzymatic cleavage, the survey scan showed several doubly, ternary and quaternary charged peptide precursor ions (Figure 21).

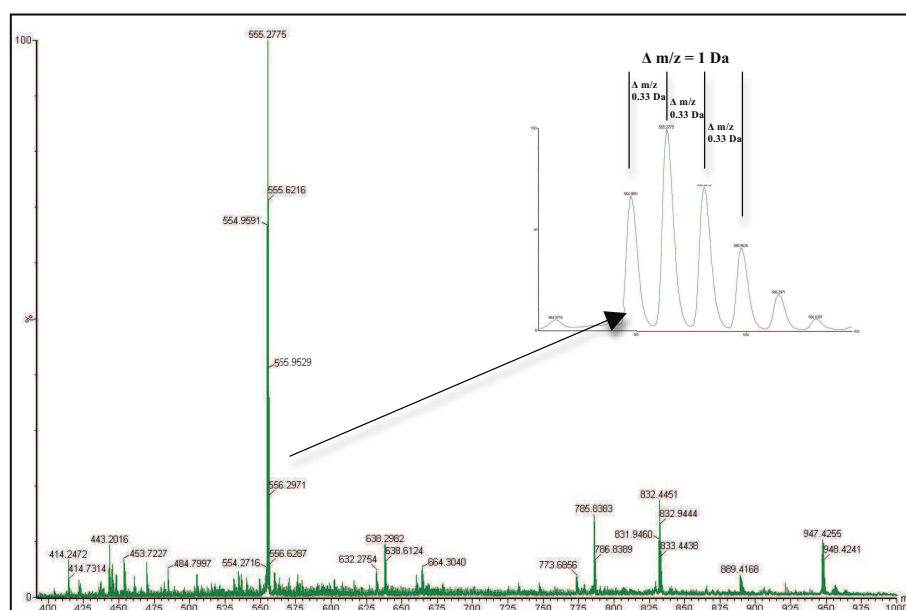


**Figure 21 Spectrum of the tryptic digested nLTP1 standard.** The mass range was expanded to 400 to 1000 Da and shows typical charged nLTP1 peptide ions. The triple charged precursor ion at  $m/z = 555.2775$  Da is highlighted at the upper right and the charge state is explained by the mass differences annotated between the peptide peaks.

A standard charge state profile was selected for precursor ion fragmentation. The emerging spectra were used for protein identification with the PLGS software (Figure 22). The nLTP1 standard was validated by several digests. Different precursor ions found in the cleavage mixture were fragmented and could be assigned to two peptide fragments subsequently. The typical peptide precursor ion masses were  $m/z = 832$  Da (2+) and 554 Da (3+) for the 1662 Da peptide or  $m/z = 664$  Da (2+) and 443 Da (3+) for the 1326 Da peptide. The peptide

## RESULTS AND DISCUSSION

sequences identified from the whole protein sequence always remained the same with the standard material, in spite of ten potential trypsin cleavage sites in the protein sequence. The position of the peptide fragments within the 3D protein structure could be localized at the outer protein surface. This location may facilitate the accessibility to proteolysis and therefore disposal of typical peptides.

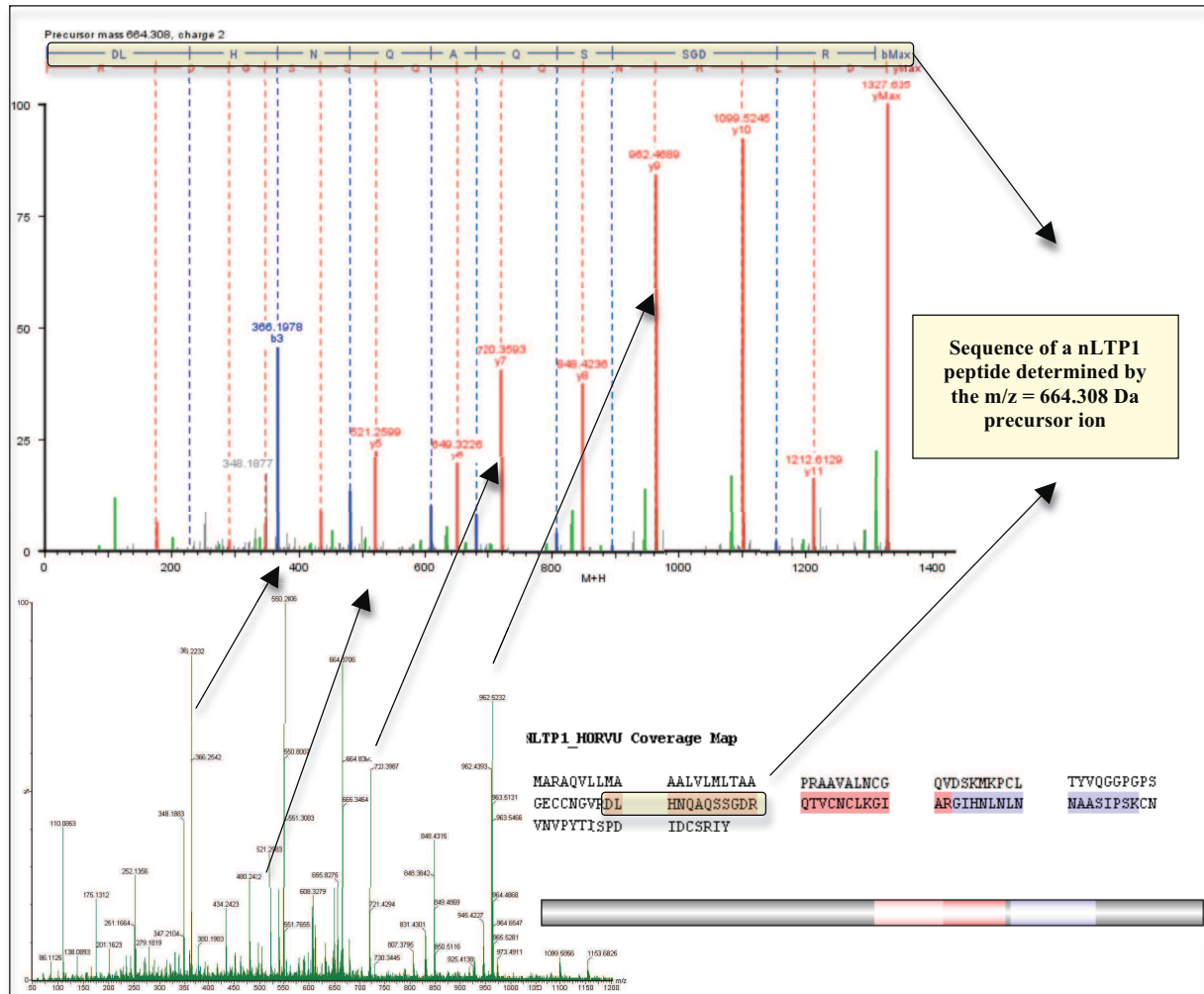


**Figure 22 nLTP1 analysis by bottom up investigation and PLGS software identification.** The MSMS-spectrum at the bottom belongs to the doubly charged precursor mass 664.308 Da. The upper spectrum was already processed by the PLGS software and the y- and b-ion series were determined. The amino acid sequence of the identified peptide is shown above the spectrum. This peptide sequence was used for a Swissprot database search and matched part of the nLTP1 protein sequence.

Top down ESI-MS tests revealed a typical protein character for the nLTP1 standard. nLTP1 spectra showed multiply charged ions deriving from the full-length protein by virtue of charge distribution over the analyte's potential charge sites (Figure 23).

The protein standard showed more than one typical nLTP1 ion series. Up to nine ion series could be determined amongst the the charge state distributions. Mass calculations revealed a striking coherence between the ion series, resulting in  $162 \pm 2$  Da mass differences for the

## RESULTS AND DISCUSSION

calculated protein molecules (Figure 24). The 162 Da pattern hinted at the involvement of dehydrosugars, with an interest being focused on hexose units of glucose or fructose.

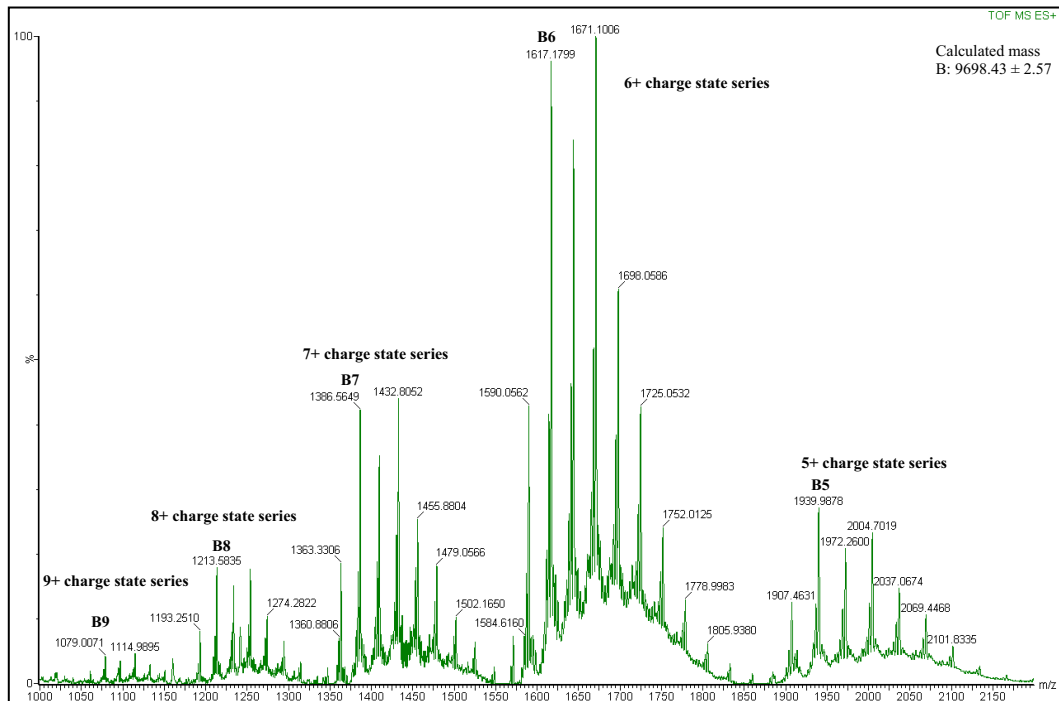


**Figure 23 Top down protein spectrum of a native, lyophilised nLTP1 standard.** The spectra contain several charge state series with charge state distributions from 5+ to 9+. The B-ion series of the unmodified nLTP1 is highlighted and the calculated mass (MassLynx) is shown.

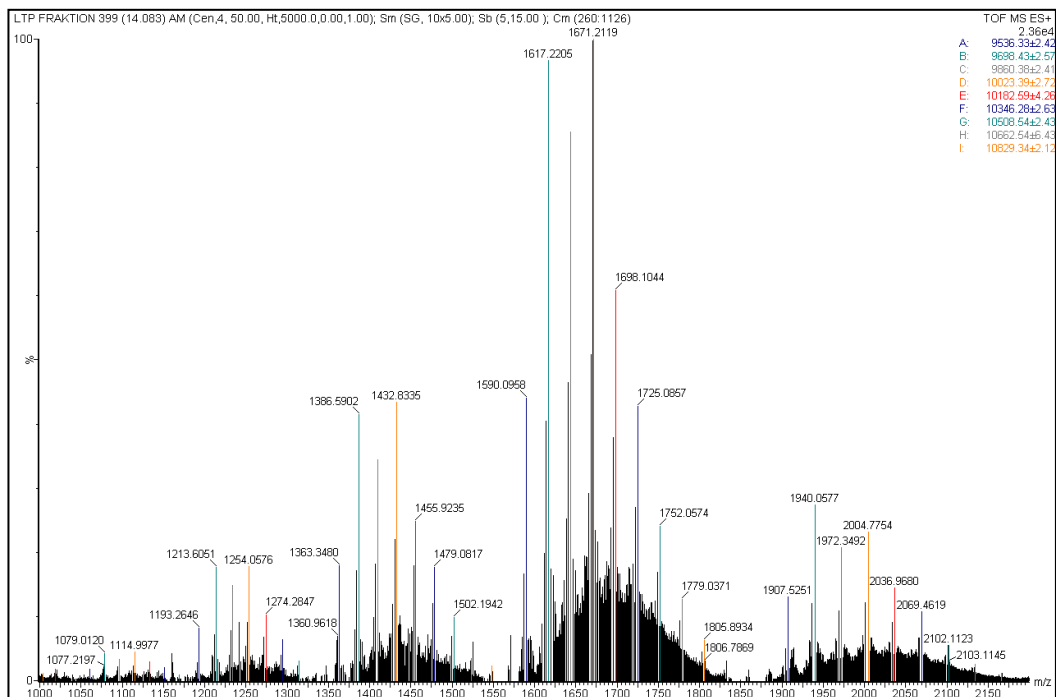


**Figure 24 Allocated ion series found in an nLTP1 protein standard.** Charge state distributions comprise 5+ to 9+ ions. The calculated masses of the ion series show variations of  $162 \pm 2$  Da. The B-ions series belongs to the nLTP1 species (9694 Da) to be found on Swissprot (P07597).

No further distinction between the sugar candidates was possible owing to their protein attachment on the one hand and their identical masses on the other. The 162 Da pattern allowed for various interpretations. A native nLTP1 protein species could have been side chain modified across a range extending from one sugar up to growing numbers of single dehydrosugar units in parallel resulting in different source protein molecules with increasing masses. Another explanation could be provided by one or even more polysaccharide side chain modifications, where differing masses would be explicable by the fragmentation and loss of single and multiple dehydrosugar units in the sample pretreatment and/or ESI-ionization. Neither or both explanations may apply. Perhaps different nLTP1 species are developed through out the brewing process owing to glycation and Maillard reactions. From an analytical point of view no further distinction of the chemical modification mechanism or a direct allocation to nLTP1 glycation in the brewing process was possible. Another peculiarity emerged with the a-ion series of the nLTP1 standard. The calculated protein was smaller (-162 Da) than the mass of the natural nLTP1 molecule which could be found at Swissprot. This fact indicated a priori sugar modification of the protein annotated at Swissprot.

HPLC runs of the native nLTP1 standard also failed to provide any proof of different modified nLTP1 species, as only one broad peak was observable for the extracted nLTP1 masses. Their existence can however not be entirely precluded owing to the peak width of up to 2 minutes. Peak tailing and a peak shoulder were characteristic. The peak shoulder and the whole peak slightly shifted and changed shape in the extracted chromatograms of the different nLTP-ion series. The instrument resources and method parameters did not allow for maximal and hence adequate resolution at this point of the study.

Based on the experience with the nLTP1 standard the protein could be identified in fluidic, degassed beer samples and in other SEC fractions by both bottom up and top down analysis. The peptide species determined were identical to the peptides identified in the standard.

### **6.1.2 Protein Z**

The protein Z standard material included SEC fractions of different beer batches (Berliner and Veltins Pilsener). The expected masses were calculated by SDS-PAGE at TU Berlin and the fractions showed a gel spot at approximately 40 kDa and an additional spot at 3.5 – 4 kDa. Bottom up analysis did not directly lead to the identification of protein Z after a database search, even though the spectra showed adequate numbers of charged (2 – 4-fold) peptide ions. The main precursor ions were 1345, 1179, 1009 and 965 Da (Figure 25). In MSMS

fragmentation the precursor ions proved highly stable even when high fragmentation energies were directly applied and suited to these ion masses.

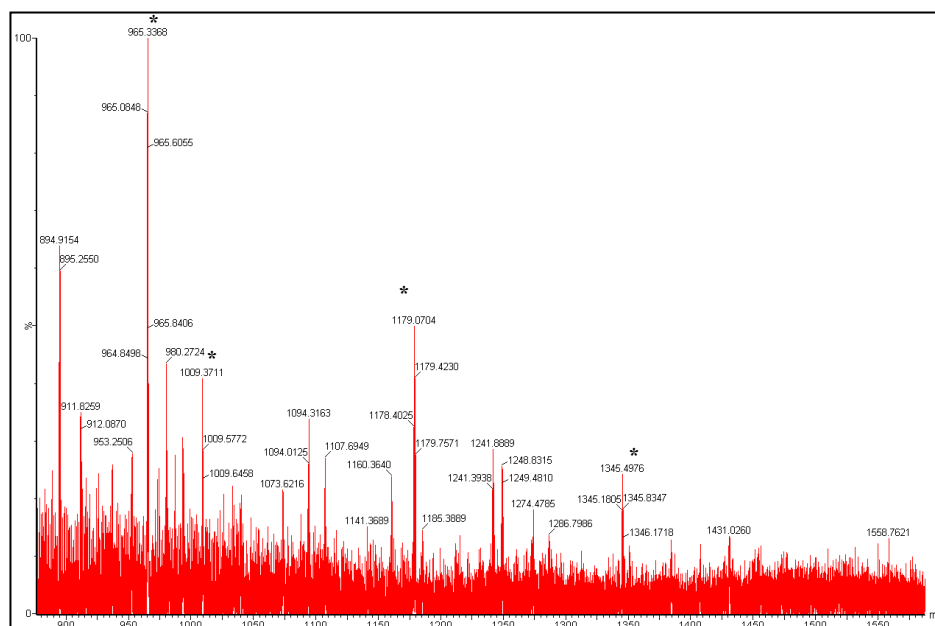


**Figure 25** MS survey scan of a tryptic digested protein Z SEC fraction. The mass range between 850 and 1600 Da was enlarged for clarity. The mass range of the experiment was 100 – 2000 Da, but the ions at the lower mass range were hardly recognizable owing to strong background noise. Typical precursor ions are marked with an asterisk.

A positive protein Z identification was ultimately possible via precursor ions detected at the low mass range, but allowed no further distinction between proteins Z4 and Z7. As the peptide determined originated from a homologue protein region, strong sequence similarities led to unrepeatable database matches for both species.

Top down investigation with protein Z fractions also showed typical characteristics. As expected, RP-HPLC separations resulted in a later elution of the high molecular mass protein peak in comparison to the smaller nLTP1 protein. The protein peaks were broad (width:  $\approx$  1 min) again but this time only featured slight tailings. While the LC separation complied with the expected rules, MS full scans did not reveal a typical protein spectrum. No multiply charged ion series were observable with protein Z. The native protein Z spectrum instead had the same appearance as the spectra of digested samples.

Despite the top down approach, different MS tunings were tested with the sample material, including a peptide tuning (300 – 2000 Da) with high resolution at the lower mass range and a protein tuning (1000 – 3000 Da) appropriate for proteins with a higher molecular mass. In the first case myoglobin was used as a single calibration standard after GluFib tuning for high resolution, while a mixture of bovine trypsinogen and myoglobine was used for the high molecular mass protein approach. Both spectra showed the typical abundant precursor ions

mentioned above but a zoom in revealed an interesting fact concerning the peak resolution. In the peptide tuning the 1345 Da precursor-ion's charge state could be determined as ternary, whereas the inadequate resolution in the tuning and calibration of native protein did not allow such an exact distinction (Figure 26).

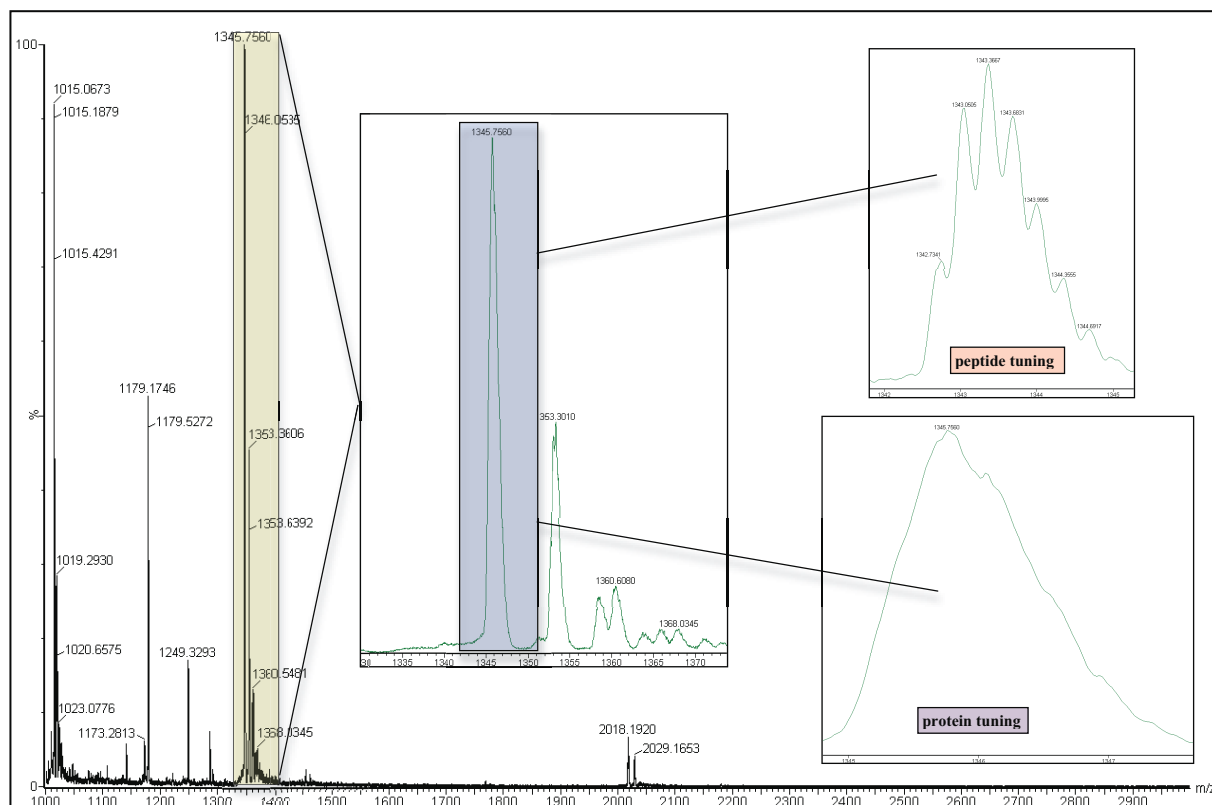


**Figure 26** Tuning effects observed with protein Z precursor ion  $m/z = 1345$  Da. Peptide tuning revealed the triple charge state of the precursor ion, while the inadequate resolution of the protein tuning did not enable charge state recognition.

The rather peptidic character could also be observed with other presursorions mentioned above, but none of them exceeded a quaternary charge state. Mass calculation with the MassLynx software resulted in a:

- 1.) 4032.2 Da peptide in case of the triple charged 1345 Da ion and the attendant quaternary charged 1009 Da ion,
- 2.) 3856.4 Da peptide with the 965 Da (4+) and 1286 Da (3+) ion,
- 3.) 3743.3 Da peptide fragment for ion signals of 937 Da (4+) and 1249 Da (3+) and
- 4.) a 3533.3 Da peptide mass in case of 1179 Da (3+) and 883 Da (4+).

Based on the results of the SDS-PAGE (an additional 3.5 – 4 kDa spot in the protein Z lane), the whole amino acid sequence of protein Z was manually analysed and masses were determined (BioLynx, Protein/Peptide Chain Editor) to reveal matching peptide candidates. A comparison of the peptide masses calculated from the “native“ protein spectra and by the



software resulted in a hit comprising the last 37 amino acids (position 363 → 399) of the protein sequence (Figure 27). The mass of this peptide (4032.45 Da) was nearly identical to the mass calculated from the 1345 Da and 1009 Da ions, only showing a small mass difference of  $\Delta m/z = 0.25$  Da.

>P06293|PRTZ\_HORVU Protein Z - *Hordeum vulgare* (Barley).  
 MATTLATDVRLSIAHQTRFALRLRSAISSNPERAAGNVAFSPLSLHVALSLITAGAAA  
 TRDQLVAILGDGGAGDAKELNALAEQVVQFVLANESSTGGPRIAFANGIFVDASLSL  
 KPSFEELAVCQYKAKTQSVDFQHKTLEAVGQVNSWVEQVTTGLIKQILPPGSVDNTT  
 KLILGNALYFKGAWDQKFDESNTKCDSFHLLDGSSIQTQFMSSTKKQYISSDNLKV  
 KLPYAKGHDKRQFSMYILLPGAQDGLWSLAKRLSTEPEFIENHIPPQTVEVGRFQLPK  
 FKISYQFEASSLLRALGLQLPFSEEADLSEMVDSSQGLEISHVFHKSFVEVNEE**GTEAG**  
**AATVAMGVAMSMPLKVDLVDFVANHPFLFLIREDIAGVVVFVGHVTNPLISA**

**Figure 27** Amino acid sequence of protein Z4 (Swissprot entry: P06293). The sequence shown in red is the calculated peptide fragment matching the peptide calculated for 1009 Da (4+) and 1345 Da (3+). The sequence highlighted in yellow matches the reactive center loop (RCL) sequence.

Two different peptide sources were to be considered. Either the native protein Z (43.3 kDa) could have been the source, or the smaller protein Z fragment (3.5 – 4 kDa) found by SDS-PAGE. At this stage of the research the exact origin could not be pinpointed, but the position of the peptide fragment at the end of the protein sequence was noticeable, as was the close vicinity to the reactive center loop (RCL) also encompassing an overlapping region of 5 amino acids. That a RCL extension of the protein body was observed with the protein class of serpins and conformational lability and RCL rearrangement was mentioned for the serpin-like PAI-1 protein [34, 64, 83] might provide an explanation for the development of this peptide fragment. Protease cleavage at the RCL might result in a highly stable inactive serpin-protease complex ( $\approx 40$  kDa) on the one hand and a cleavage product (the terminal peptide fragment) on the other. In the case of a native protein Z source this mechanism would be realistic as the remaining stable protease protein core was unrecognizable in MS detection due to neutral ion loss.

RCL conformation could also allow for another interpretation: chemical fragmentation could be facilitated in the preliminary protein Z preparation by enhanced terminal sequence accessibility. Both scenarios deliver explanations for the two protein Z spots found in single gel lanes. A final explanation is based on the similar presumption of a protein backbone breakage. Perhaps an enhanced accessibility of the terminal sequence section promoted

insource fragmentation of the entire protein Z molecule, resulting in the same two fragments. The real mechanism could not be revealed but the possibilities mentioned should be kept in mind in the case of indistinct gel spots and/or equivocal LCMS recovery [34, 64].

Other precursor ion masses could also be allocated to sequence details of the terminal peptide. Assuming an in source fragmentation mechanism, the C-terminal amino acids of the resulting internal fragments would no longer include the hydroxyl-group after ionization. The loss (17 Da mass difference) had to be accounted for by software calculation (Figure 28).

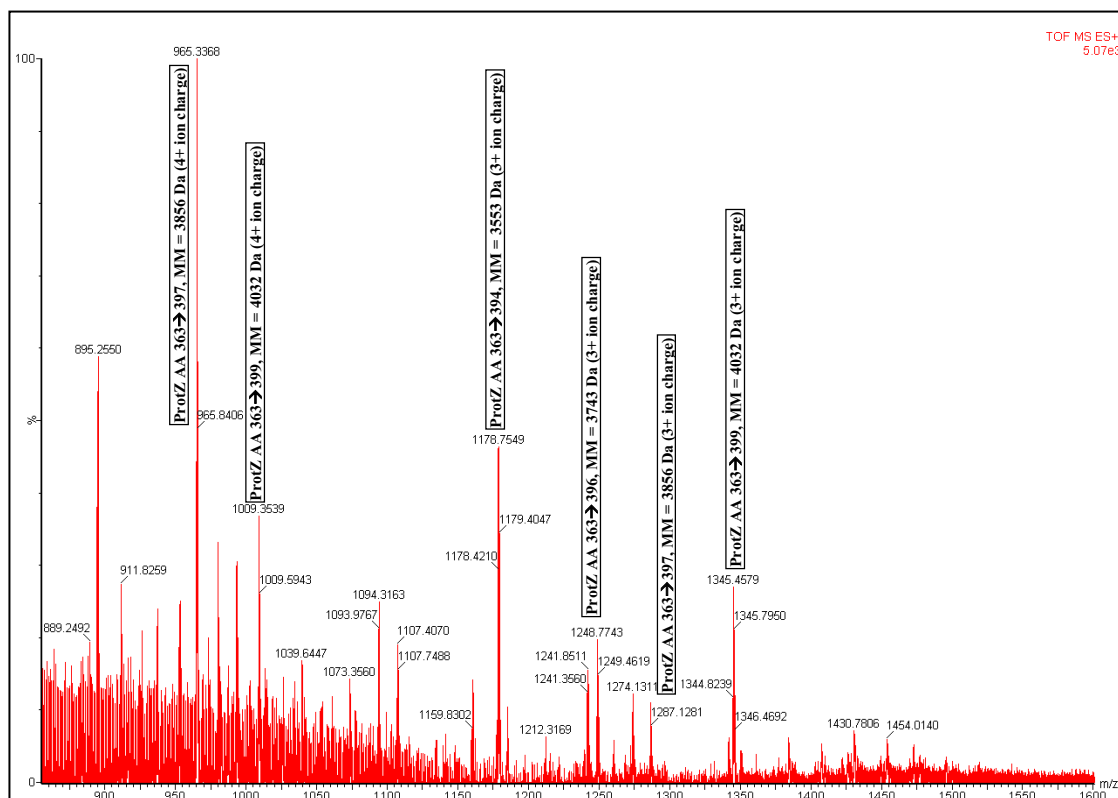


**Figure 28 Summary of sequence analogies determined for precursor ions found in the terminal protein Z fragment during native protein analysis.**

Thus the precursor ion masses 965 Da (4+) and 1286 Da (3+) were matched to the sequence, which included AA positions 363 – 397.

#### 1.)-VDLVDFVANHPFLFLIREDIAGVVVFVGHVTNPLI + internal fragment (OH)-SA

Peptide mass calculations based on the spectrum yielded 3856.4 Da, while software calculations predicted 3857.1 Da. A mass deviation of  $\Delta m/z = 0.7$  Da was accepted for this and all the following comparisons.

Amino acid positions 363 – 396 matched the predicted masses of the precursor ions 937 Da (4+) and 1249 Da (3+). While software calculation resulted in a 3744 Da mass, 3743.3 Da was calculated from the spectrum.

## 2.)-VDLVDFVANHPFLFLIREDIAGVVVFVGHVTNPL + internal fragment (OH)-ISA

A final clear allocation was successful in the case of 88 3Da (4+) and 1179 Da (3+). The sequence prediction had included the AA positions 363 – 394. Software calculation determined a peptide mass of 3533.9 Da and the mass predicted by the spectrum was 3533.3 Da.

## 3.)-VDLVDFVANHPFLFLIREDIAGVVVFVGHVTN + internal fragment (OH)-PLISA

No precursor ions could be found for the peptide fragments including the AA positions 363 – 395 and 363 – 393. Due to ion count rates near the background noise two additional fragments were only to be found with some difficulties. They brought positive matches for AA 363 – 392 and 363 – 391.

Native protein HPLC analysis performed with beer samples, fractionated beer and samples of the brewing process showed the same characteristic protein Z peak at the rear of the chromatogram. The spectra only contained the typical precursor masses mentioned above, but never displayed multiple charged ion signals characteristic with proteins. These observations again provided no opportunity for an exact determination or allocation to the small protein Z fragment or an entire protein Z molecule. A possible protein Z fragment could even emerge from the malt grain developed owing to unfavourable brewhouse conditions or an enzymatic cleavage reaction in the brewing process.

Bottom up analysis matched protein Z4 in the case of beer and Koag samples. In almost every case the precursor ion hits and predicted peptide masses differed from the ions described in detail above. The majority of peptide hits resulted from doubly charged ion species and could be allocated to the interior, centre part of the protein sequence. Only once was a peptide deriving from the 1345 Da precursor ion identified with coagulable nitrogen (Koag), although a theoretical trypsin cleavage site (lysine) was to be found downstream at sequence position 362. A valid explanation is difficult. A high stability of this part within the entire protein might be possible on the one hand, but maybe absolutely entire protein Z molecules only exist in small numbers (no RCL modification). The probability of both a cleavage at this lysine residue and of a positive identification owed to matching fragmentation energies could be lowered to a minimum. On the other hand the terminal fragment could have been released just before tryptic digestion. If this fragment would really undergo insource fragmentation, identical native protein and peptide spectra would be realistic. Any further fragmentation and identification in bottom up approaches could be complicated by the stability of the precursor

ions. Internal fragmentation would not leave the peptide level and therefore not reach the level of amino acid ladder determination.

### **6.1.3 Dionex HPLC beer sample fractionation**

Fractionation tests with beer samples were successful. nLTP1 and protein Z were narrowed down to several fractions depending on their large peak widths. In a 21 minutes chromatogram nLTP1 was found at fractions 24 to 27 (time scale: 8 to  $\approx$  9.7 mins), while protein Z elution appeared at  $\approx$  13 minutes (fractions 40 – 42). The focus was identifying the native proteins and further concentrate the sample material by solvent evaporation. The latter process was time consuming because of the large fraction volumes after a series of 20 – 30 LC runs. The first tests were stopped as the possibility of denaturing proteins with the heat applied for evaporation could not be excluded and an evaporation by gas overflow exceeded the time resources, especially in case of rather aqueous fractions. Lyophilisation was also tested, but the results indicated protein losses owed to attachment to the petri dishes. Additional problems occurred with the re-elution and resulting sample dilution, as the desired solvent volume and therefore dilution factor were too high. If the solvent volumes were too small foaming effects could hardly be avoided. Besides that the instrumentation provided an opportunity for preconcentrating single beer proteins into fractions, but would have to be optimized for future usage. A semi-preparative column could be taken into account, opening the way for higher injection volumes and final protein concentrations in the fractions.

Native protein MS investigations did not reveal any new facts about the wanted protein standards. nLTP1 showed the known protein spectra as described in detail above. The identification difficulties with protein Z also persisted and the spectra of the fractions were consistent with the spectra realised for the protein Z standard. The other fractions of the LC run were also analysed for native proteins, but failed to reveal any new expertises. By contrast a high carbohydrate content was to be found in the beer samples. The carbohydrates eluted early in the LC separation (fractions 5 – 7; minute 1 – 2 of the run) and could be successfully separated from the proteinaceous content. After lyophilisation the powdery content of these fractions was large in comparison to protein fractions. Two different sugar series could be detected by MS investigations. 162 Da mass differences were a characteristic feature found with the sugar series. Fractions 5/6 contained one of the sugar series and the ions showed a high fragmentation potential. The series started with ion masses of 649 Da and could be back-calculated to zero Da. The second series (fraction 7) was shifted in mass and reached up to

705 Da. Neither a distinct sugar identification (hexose origin) nor an explanation for the 56 Da mass difference (perhaps a loss of (2 CO) from the sugar residue) between the two sugar series proved possible. The sugar series nonetheless deserve attention because they also appeared in untreated beer samples and exert a highly interfering influence (high ion count rates) in the upper mass range.

#### 6.1.4 HPLC-MS analysis of brewing process samples

Samples from the entire brewing process were analysed for nLTP1 in the spring of 2007. Top down analysis was based on 21 minute LC runs with the HPLC in online chip-coupling mode. MS tuning and calibration over a mass range of 600 – 3500 Da were performed with bovine trypsinogen and myoglobin. Mass calculation of the standard proteins yielded a  $\Delta m/z = 0.2$  Da mass difference for 16951.449 Da the accurate mass of myoglobin and  $\Delta m/z = 0.07$  Da in respect of the 23980.987 Da trypsinogen.

Six samples of the brewing process shall be analysed in greater detail here (Figures 29 and 30). Results were observable in two independent brews and each sample was tested at least twice. nLTP1 monitoring was performed for the lautering (brewhouse), pumping (brewhouse → whirlpool), cooking start and stop (whirlpool), pitching of the wort (before yeast dosage) and for fermentation tank samples.

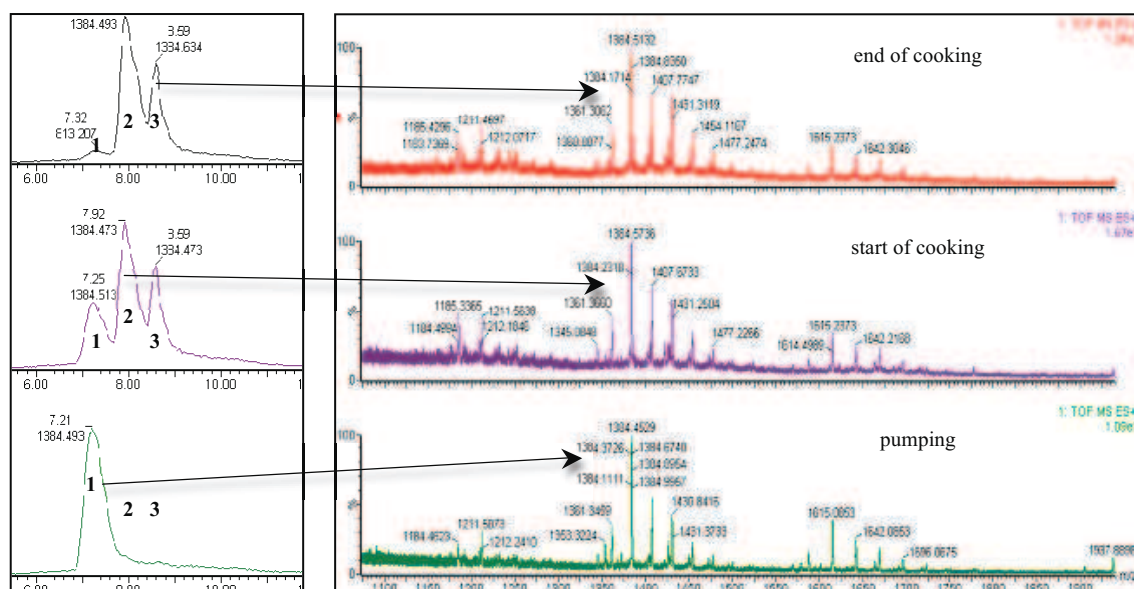


**Figure 29** Changes in LC separation observed for the nLTP1 peak within the brewhouse cooking procedure. Extracted chromatograms based on the  $m/z = 1384$  Da precursor ion mass.



## RESULTS AND DISCUSSION

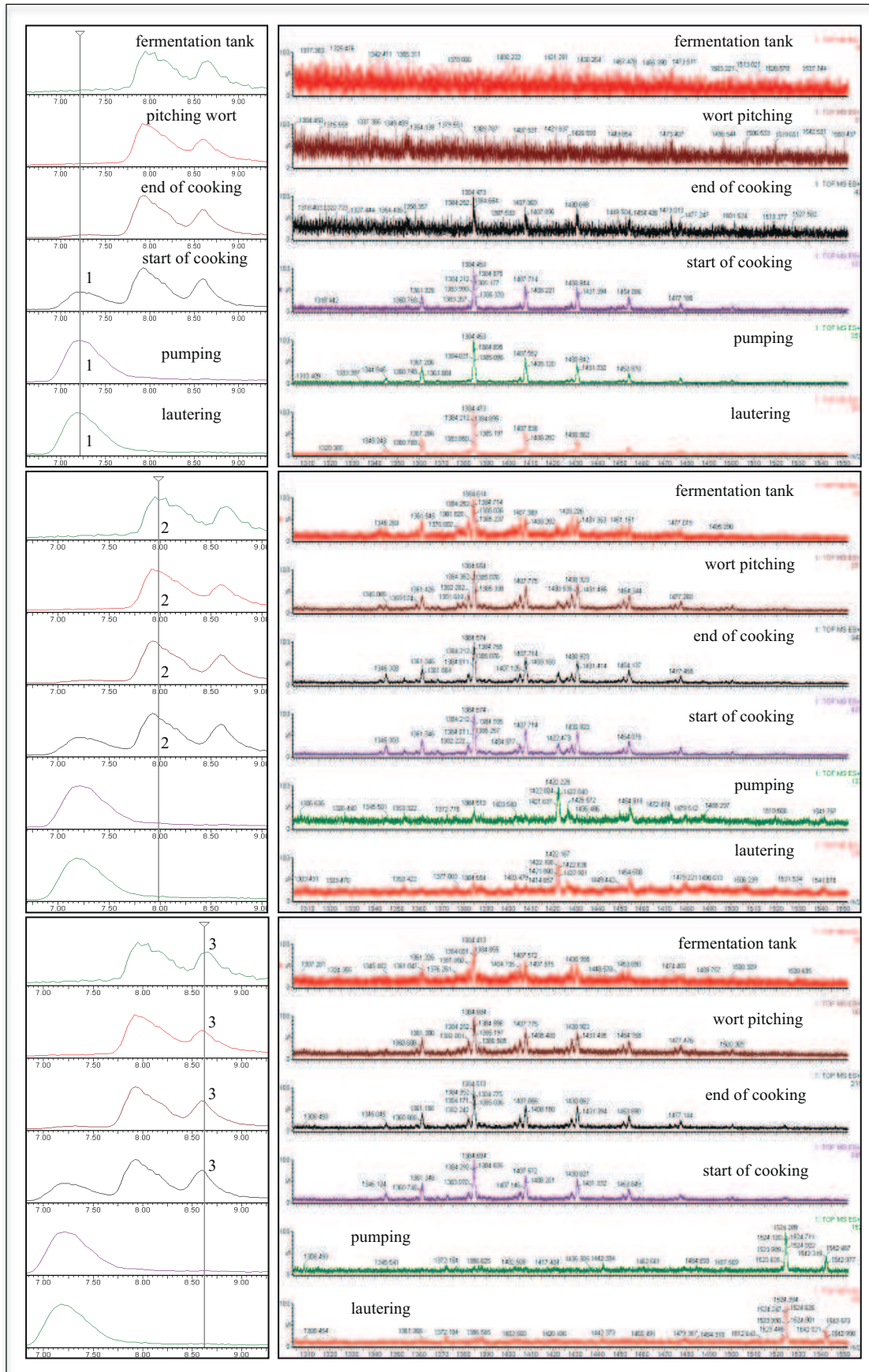


**Figure 30** Extracted chromatograms and corresponding MS-spectra of the  $m/z = 1384$  Da precursor ion mass observed with nLTP1 rearrangement in the brewing process.

Tracing of the main precursor ion masses like  $\approx 1384$  Da indicated protein changes during the cooking process. Chromatograms extracted from lautering and pumping samples only showed one malt derived nLTP1 peak. The chromatographic behaviour matched the nLTP standard, but the peak width was sharper (1 min). The most abundant ion peak always appeared at  $m/z = 1384$  Da. Starting from 9520 Da, only the known nLTP masses based on 162 Da mass differences could be calculated. The mass errors calculated for the brewing samples were greater than those derived from the standard and therefore led to mass differences ranging from 8 – 13 Da. As possible sugar modifications appeared with this first, malt derived peak, the probability of previous modifications during the malting process were probable.

Once heated at the start of the cooking procedure, the original chromatography peak changed shape and split up into two additional peaks. The precursor mass followed this time shift and could be allocated to these two peaks. The traceable nLTP ion series remained the same, whereas the ion count rates of peak 2 were higher than those of peak 3. At the end of the cooking process the nLTP1 peak showed no further changes in chromatographic behaviour. The main precursor mass of 1384 Da could still be allocated to the two, latter peaks, whereas the first, original malt peak nearly vanished. While the peak ion series and the main precursor ion mass remained stable in spite of their time shifts in the LC run and slight differences in the ion count rates, some other concise ions increased with the newly developing peaks. No direct connection to the nLTP species could be established. Water adduct peaks (2 – 3) appeared in the nLTP1 spectra of the pitching wort and fermentation tank. Lipid-like mass shifts of 294 and 312 Da, which were mentioned in literature, could also not be found.

Despite the changes in chromatographic separation, no additional charge state of the ion series or mass change of the nLTP appeared. Considerations to be taken into account with regarding these findings include an internal rearrangement of the protein molecule, or modifications of the protein backbone lacking further mass changes, with the literature tending to the first assumption [5, 28, 34]. A modified 3D shape after unfolding during the wort boiling in reducing conditions provided by the wort extract or protein hydrolysis might be explanations for altered separation attitudes. The lack of additional sugar related ion series precluded estimations as to whether sugar modifications during the cooking procedure are a realistic assumption or not.

## **6.2 Protein quantification**

The beer protein measurements performed in breweries classically involve Kjeldahl or Dumas methods, direct spectrophotometric analysis, Biuret methods, dye binding methods, or turbidity analysis.

In this thesis the Kjeldahl method was only used for the protein quantification of Pilsener beer samples. The protein amounts were around 3.8 g/L, but because the entire nitrogen content of each sample (protein and non-protein nitrogen) is measured, the method yields excessive protein contents. Depending on the different amino acid sequences of the proteins various correction factors should ideally be applied, which is critical fact for samples of unknown protein contents. There is a realistic probability of the protein amounts calculated by this being too high.

Similar problems appear if the nitrogen is determined by the Dumas method. In this thesis an automatised Macro N analyser was used for determining of beer and haze samples. Lyophilised beer and haze were used for the analysis. The beer sample results (0.441 g/L, approx. 1 % [w/w]) appeared to be realistic, but the concentrations determined in the haze were extremely high. The protein ratio was 57 % [w/w] and could not be backed by any other result of this thesis. As both methods are also sensitive to small peptides and amino acids, possible explanations included amino acid determination and mass calculation errors resulting from this species.

The free amino nitrogen was determined with Continuous Flow and a ninhydrin based method. Five representative amino acid standards (proline, alanin, histidine, asparagine and arginine) were used for method evaluation. But due to the chemical structure of the amino acids (1 or 2 primary nitrogen(s) or combinations of primary and secondary nitrogens), the mass errors realised with standard concentrations of 200 mg/L were so high (27 – 93 %) that the method was of little use for the desired tests.

Spectrophotometric methods are often susceptible to the interference of prominent beer substances, or the chemical mechanism only matches a minority of the wider class of target analytes. Similar problems surfaced with the Biorad Roti Quant Universal and Nanoquant assay performed for this thesis. In both cases BSA calibration was successful and the linear curves only showed minimum standard errors. While the Universal assay delivered exceptionally high protein amounts, the Nanoquant assay tended in the opposite direction. The amounts realised for Pilsener beer were surprisingly low (Table 15).

**Table 15 Protein quantification via Biorad Roti<sup>®</sup> Quant Universal and Nanoquant assay.**



## RESULTS AND DISCUSSION

---

<b>Protein assay</b>	<b>Roti Quant Universal</b>	<b>Nanoquant</b>
<b>R<sup>2</sup> (BSA calibration)</b>	0.999	0.994

<b>Sample</b>	<b>Protein [g/L]</b>	<b>Protein [g/L]</b>
<b>Veltins Pilsener</b>	33 – 42	0.1 – 0.15
<b>Ancient Pilsener</b>	31 – 54	/
<b>MCT extracts</b>	600 – 1230	0.009 – 0.01
<b>Congress wort</b>	/	0.064 – 0.1

The protein concentrations measured in the beer and especially the MCT extract samples threw doubts on the results with the Roti Quant Universal. Twelve ancient Pilsener beer samples were analysed and showed a positive correlation between the protein values and their total sugar concentrations as determined by IC analysis. Therefore the assay was first tested for interferences and crossreactions with beer sugars and found to be impeded by the sugar concentrations found in beer. Increasing concentrations of the sugars were then also tested. Maltose, maltotriose and glucose showed increasing interference, but the greatest falsification resulted from fructose, where rising concentrations disproportionately boosted the protein test results.

A lectin solution and a mixture of proline, catechin, lectin and myoglobin were also tested. Proline is the most abundant amino acid in beer. Catechin was selected to represent the group of polyphenols and the proteins myoglobine and lectin were used to simulate the possible influence of another, more complex protein, and to insert a known concentration of a protein standard. The Universal assay was negatively influenced by both solutions and the protein concentrations were very high.

The need for the same tests was highlighted in the Nanoquant assay, as well. The low protein concentrations of MCT extracts and congress wort samples (results not shown here) did not meet the expectations. In comparison to the beer protein concentrations found in literature, the test amounts were over 3 times lower. Sugar crossreactivity could not be observed in the Roti Nanoquant assay. Again the lectin solution and mixture described above were tested. The test results were indifferent. The amounts quantified in the lectin solution were nearly double the actual protein concentration. The natural colour of the protein standard solution may cause light absorbing interferences. By contrast, the results for the mixture were 6 up to 8 times too low. The test seemed to suffer from suppression effects by polyphenol or amino acid components. Tests were not upgraded to distinguish between both substance classes.

Because of the indifferent results the protein quantifications were now assigned to the 2D-Quant assay. This protein assay showed no interaction with sugars or the other test substances. BSA calibration proved easily possible with aqueous and 5 % ethanolic BSA

## RESULTS AND DISCUSSION

solution ( $R^2 \geq 0.993$ ). The 2D-Quant assay was used for determining the protein content of a wide range of samples including MCT extracts of malt and barley, congress wort, brewing process samples, Veltins Pilsener and ancient Pilsener beer, foam fraction, resolved haze and haze supernatants. The results are shown in Table 16. Owing to the small number of interfering substances tested the results were not expected to be absolutely precise. Mass errors may be caused by other interfering beer components or also the underlying chemical quantification mechanism. A lack of reported results did not allow the results of this thesis to be supported, despite the fact that beer samples are mentioned with a protein content of 0.5 g/L in the literature.

**Table 16 Results of protein quantification with 2D-Quant assay (GE Healthcare).**

Sample type	Protein concentration [g/L]	Protein amount % [w/w]
<b>Barley MCT extracts</b> (lyophilisate)	/	5.4
<b>100 % gushing malt extract</b> (lyophilisate)	0.923 g/L extract	2.1
<b>MCT extracts of various malts</b> (lyophilisate)	0.97 – 1.3 g/L extract	1.93 – 2.55
<b>MCT extracts of various malts</b> (fresh, fluidic sample)	0.97 – 1.335 g/L extract	/
<b>Phenolic extraction of MCT extracts</b> (extraction of lyophilisate)	0.64 – 0.88 g/L extract	1.21 – 1.75
<b>Cold water extracts of malt</b> (Fresh, fluidic volume)	2 – 2.5 g/L extract	/
<b>First wort</b> (fresh, fluidic volume)	1.83 g/L wort	/
<b>Congress wort</b> (fresh, fluidic volume)	1 – 1.13 g/L wort	/
<b>Cold wort</b> (fresh, fluidic volume)	0,85 – 0.9 g/L wort	/
<b>Veltins Pilsener</b> (fresh, fluidic volume)	0.42 – 0.53 g/L beer	/
<b>Ancient Pilsener</b> (fresh, fluidic volume)	0.45 – 0.75 g/L beer	/
<b>Concentrated foam fractions</b> (fresh, fluidic volume)	0.7 – 1.14 g/L absolute*	/
<b>Haze sample supernatants</b> (fresh, fluidic volume)	0.4 – 0.5 g/L supernatant	/

\* Reverse calculation of a distinct beer volume was not possible due to the foam preparation procedure.

Protein quantification of haze material was not possible, as the recommended solvents (concentrations of the solvents) did not suit the tolerance levels mentioned for the test procedure. In most cases the haze formation is attributed to the development of protein-polyphenol complexes. Supernatants of increasingly older haze samples were hence analysed for a possible loss of proteins from the fluidic volume. The detected protein amounts did not indicate an appreciable decrease, but rather seemed to be stable, with fluctuations within a

small range. These variations did not show a downward drift and could also be explained by the methodological mass errors observed with other sample types.

In contrast to the first wort (sampling point: after lautering), the MCT extract, congress wort and cold wort samples showed similar protein amounts. Decreasing concentrations in the brewing process can be explained by protein precipitation in the additional boiling procedure. This is a common feature of all these samples, with only the boiling times differing amongst them. Variations in protein amounts (especially with MCT extracts) were measured because of different malt varieties were used for this study. While the test results of lyophilised and fresh, fluidic MCT extracts matched, calculations of samples after phenolic extraction showed minimized trace amounts. An incomplete precipitation of the entire protein content might be just as possible a cause of the corruption of the results because of interfering, denaturing solvents, which were needed for resolving the protein pellet after the precipitation procedure. In finished beer, the protein content was once again reduced by a factor of two. Pilsener beer varieties strongly varied, but the majority ranged at approximately 0.6 g/L. A second loss of proteins might be attributable to yeast growth, enzymatic degradation, ongoing precipitation during storage/maturation, as well as the filtration procedure.

### **6.3 Haze analysis**

#### **6.3.1 Fundamental observations concerning haze**

The results of the brewing trial 2006 predicated some interesting facts about haze. Haze development and haze attitudes were found to depend on the hop raw material and the stabilisation treatment (PVPP, hydrogel, KZE) [40]. The results indicated a positive effect in the case of KZE treatment, gave no indication of barley derived polyphenols, but of hop components like xanthohumole, isoxanthohumole,  $\alpha$ - and  $\beta$ -acids, and indicated the best visual chill haze stability for KZE treated beer produced with hop extracts despite of the diminished stabilisation. In general the visual appearance of the haze was highly indifferent to the trial modifications and included slight to severe opalescence as well as flaky sediments after the first storage period. This general tendency could also be confirmed throughout long-term storage.

Depending on the tests of the brewing trial the haze amounts isolable from 500 mL beer volumes strongly deviated after 2 ½ years of storage (Figure 31). With one exception the samples stored at RT showed greater amounts of haze than the samples stored at lower temperatures. Temperatures around 0 °C appeared to diminish haze development. As the

exact underlying mechanisms are so far unknown a chemical process is as likely as a simple physical explanation. Diminished Brown's molecular movement and a reduction in the kinetic energy level of the haze molecules might decelerate haze development. Given its low temperature distribution, a physicochemical mechanism like the Stern layer model might also be answerable, or perhaps a combination of both mechanism and additional parameters (particle concentration).

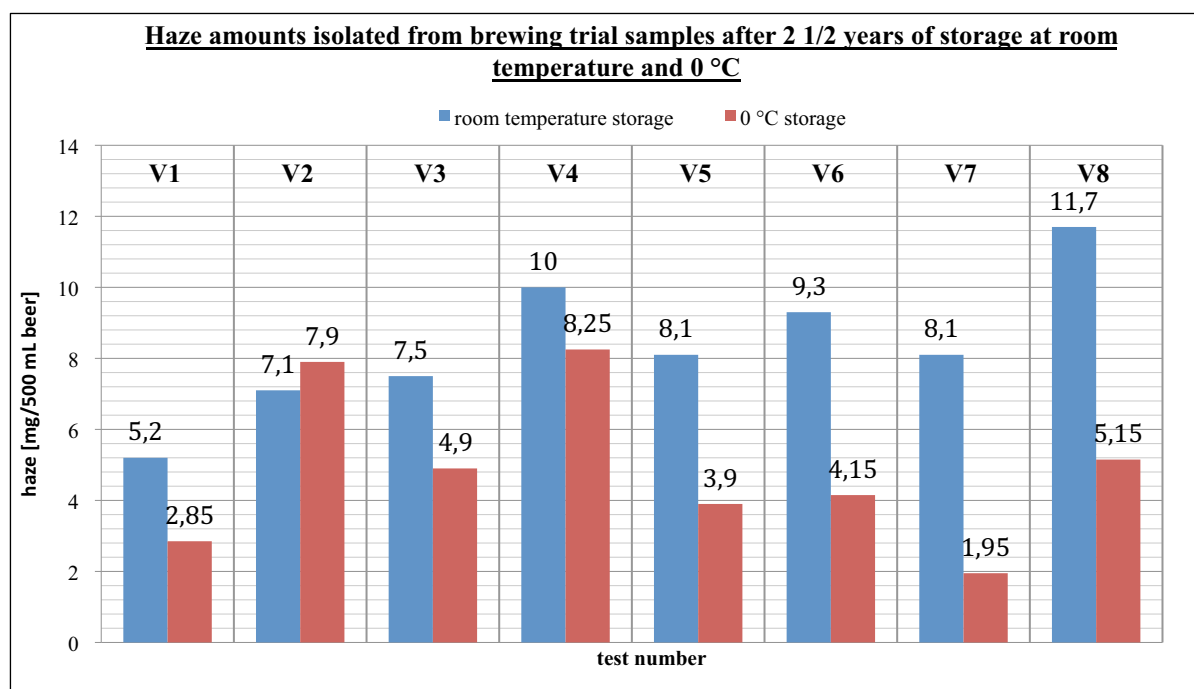


**Figure 31 Isolable haze amounts found in brewing trial samples after long-term storage.**

Regardless of the storage temperature, haze stability was always better after KZE treatment (V1, V3, V5 and V7). In this regard a second observation was possible concerning the haze in samples stored over longer periods of time. Once the haze had been isolated on a larger scale (1 – 3 beer crates), the colour differences found in the isolated haze material appeared to depend on the KZE treatment. The haze of KZE-treated beer haze was always light brown after lyophilisation, while samples that had not been KZE treated showed a dark brown haze (Figure 32).

Even at the beginning of the storage period repeated analysis of beer sugar contents indicated a possible denaturation of yeast  $\beta$ -glucosidase during the additional KZE heating procedure. As the KZE treatment might impact a number of other yeast deriving enzymes or metabolites, a diminished sugar degradation or cleavage of other substances is possible. A lack of degradation products may stop the natural browning reaction (perhaps a type of Maillard

reaction) and/or haze development due to a loss or only decrease of possible activator substances.



**Figure 32 Haze isolated from brewing trial beer after long-term storage (2 ½ years).**

Haze development tended to aggravate after the filter aids were reduced (V1 vs. V3 and V2 vs. V4) with both storage temperatures. Tests with an additional change of the hop material only counterbalanced the effect in case of cold storage (0 °C). Samples stored at room temperature showed increased haze stability only for hop pellets dosage and in the absence of KZE treatment (V6). In all other cases the absolute haze amounts indicated contradictory findings.

If the stabilization effects were only to be assessed by absolute haze volumes, brewing modifications in V7 would be best for long-term cold storage, while the standard stabilisation via KZE applied in V1 would be best for storage at room temperature. Both tests have the KZE treatment in common, but the different storage conditions already raise the question which effect is to be aimed for. In view of the consumer’s impressions, a number of additional factors need to be taken into consideration:

- 1.) young beer samples quickly develop chill haze in cold storage
- 2.) the consumer might detect chill haze if storing the beer in a refrigerator
- 3.) owing to varying haze shapes and contingents in the bottle, absolute haze amounts will not match the consumer’s visual impressions
- 4.) long-term storage is unlikely with consumers
- 5.) reversible chill haze and first RT haze might develop into a permanent haze.

From this perspective the brewing industry should rather focus its research on chill haze. Owing to their low concentrations in chill haze, hop substances are only a minor component, but the results of the brewing trial, visual bottle assessments and the absolute haze amounts after long-term storage indicated a positive effect for hop extract applied in combination with

KZE treatment (V7). The reduction in filter aids, especially costly PVPP, furthermore facilitate cost savings.

**6.3.2 Haze formation – a dynamic process**

Haze development is a dynamic, ongoing process, not a temporary event. Steadily increasing haze volumes observable in the long-term storage of Pilsener beer are shown in Figure 33. The observations refer to Pilsener beer samples stored at room temperature for periods ranging from 3 to 104 months (8 years and 8 months). The first sampling date was selected with respect to clear, visible haze developing in storage at room temperature. Because of the long storage periods the samples included various batches of beer that had not been produced under identical brewing conditions. Different production parameters may result in additional mass errors.

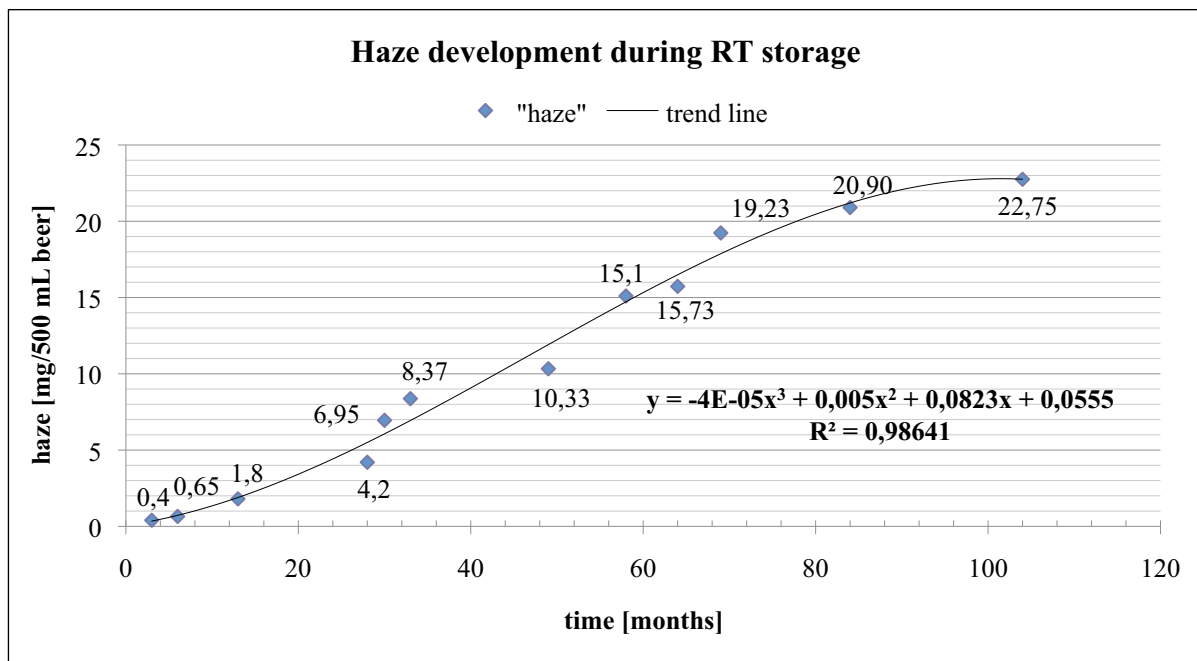


**Figure 33 Haze development in the long-term storage (RT) of Pilsener beer samples.**

The general trend of haze formation could be shown by a third order polynomial trend line, where the coefficient of determination reached its maximum value. The development seems to follow a start up phase with only slightly increasing haze amounts. From about 30 months the data follow a nearly linear trend until the storage period reaches 90 months, when haze development stagnates. From this point onwards the haze volumes of even older beer samples always range in between 22 and 23 mg/500 mL. The development appeared to come to an end that might be explicable by a complete uptake of haze constituents from the fluidic phase.

## RESULTS AND DISCUSSION

This idea was the motivating force for subjecting the fluidic supernatant of ageing haze samples to protein quantification tests. Proteins and polyphenols are the main haze catalysts described in literature. The occurrence of barley derived haze polyphenols could not be supported by the brewing trial and hop derived polyphenols were only found to be minor components. These results might suggest an extraordinary role for the proteins. With the haze volumes found in this study, a distinct diminishment of the protein concentration was hence expected. But the results of 2D-Quant protein quantification did not meet these expectations. Protein concentrations were almost identical to those of fresh beer and failed to show a clear reduction. Deviations within the test series may be attributable to the standard error of the test. The only factor that might skew the test results was the natural beer colour, which turned darker during storage.

Two beer samples (KZE and non-KZE treated) were stored for ca. 200 days at different temperatures (0 °C and RT) in order to verify and improve the results (Figure 34). Samples were taken regularly, the haze was isolated and the supernatants were directed to protein quantification. Amino acid tests were furthermore carried out to trace changes on the level of basic protein modules.

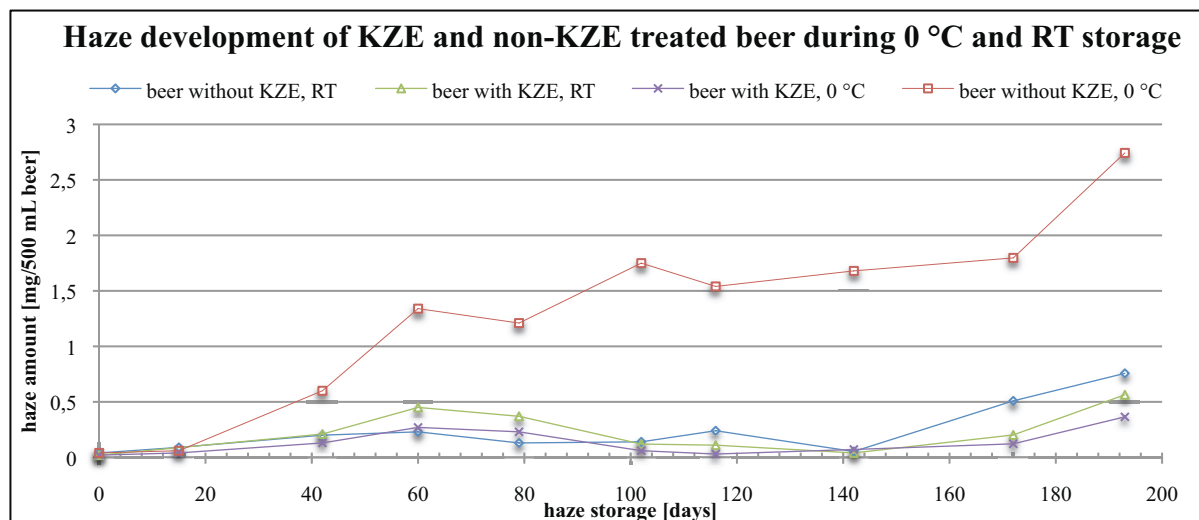


Figure 34 Haze development observed in KZE treated and untreated Pilsener beer (0.5 L) stored at 0 °C and RT.

The haze formation in untreated beer samples stored at 0 °C supports the findings of the 2006 brewing trial. The lack of KZE treatment and storage at low temperatures promoted a disproportional increase of the chill haze. The significant impact of the KZE treatment is clearly shown by the comparisons with KZE treated beer stored at 0 °C. After 15 days the haze volumes start to develop differently. After ca. 100 days the haze volumes of untreated

## RESULTS AND DISCUSSION

samples stored at 0 °C are roughly 5 times larger than those found in KZE treated samples. This factor was almost observable until the very last date of sampling. After about six months of storage the KZE effect can also be seen in samples stored at room temperature.

2D-Quant protein quantification of haze supernatants once more failed to show decreasing protein contents. The studied time period is rather short in comparison to the long-term storage samples and included the initial haze formation phase. Changes at this haze formation stage may not be significant.

Amino acid determination found proline to be the most abundant amino acid in beer and haze supernatants. Proline is the only amino acid not to be metabolised by yeast, which might explain the high values. Initial concentrations in KZE treated beer (8300 µmol) were strongly enhanced in comparison to untreated samples (5400 µmol), but estimates are difficult as the amino acid determinations from the brewing trial did not support the results of this study.

Over the 200 days of storage the initial concentrations fell to final proline levels of 4000µmol (corresponding to 230 mg/500 mL beer) if stored at 0 °C as well as RT. The second highest AA concentration was found for alanine, which remained stable in both beer types. All the other results are summarized in Table 17. The results of 0 °C stored beer samples are displayed due to the short storage time and the expected bigger changes during preferential conditions for chill haze formation.

**Table 17 Changes in the amino acid concentration of KZE treated and untreated samples stored at 0 °C.**

amino acid	KZE beer: concentration [µmol]	non-KZE beer: concentration [µmol]	KZE beer: final AA concentration	non-KZE beer: final AA concentration	comment
<b>proline</b>	8300	5400	4000	4000	most abundant AA; decrease in storage
<b>alanine</b>	1500	1400	1500	1400	stable in storage
<b>glycine</b>	480	450	480	450	stable in storage
<b>valine</b>	700	600	700	600	stable in storage
<b>phenylalanine</b>	420	225	360	190	decrease in storage
<b>leucine</b>	340	260	340	260	stable in storage
<b>isoleucine</b>	130	130	130	130	stable in storage
<b>aspartic acid</b>	20	50	50	80	slight increase in storage
<b>lysine</b>	30	30	60	60	doubling in storage
<b>tyrosine</b>	170	270	340	320	increase in storage
<b>tryptophane</b>	40	90	140	150	increase in storage

The results of the amino acid determination render predictions concerning their involvement in haze formation difficult. Distinct decreases in the supernatant were only observable for



proline and phenylalanine. In view of the haze protein amounts determined via Dumas Macro N analysis, both these amino acids might act as additional nitrogen sources adulterating the quantification results. The concentrations of all the other amino acids remained stable in storage or even increased, perhaps owing to a degradation mechanism, and did not appear to play any part in haze formation.

### **6.3.3 Solubility tests with lyophilised and freshly prepared haze**

Chill haze and permanent, irreversible storage haze should be completely dissolved, if possible in preparation for LC-MS protein investigations. The either powdery haze lyophilisate or wet, freshly prepared material was to be subjected to an extensive series of solubility tests, creating a need to find solvent(s) that are LC-MS compatible on the one hand and would not result in a complete denaturation or destruction of the target analyte on the other.

Various alkenes (pentane, hexane, heptane, nonane, undecane) failed to dissolve all the aforementioned haze types, as was the case with pure water, buffered water (ammonium carbonate, pH 3), acetone, acetonitrile, buffered acetonitrile (ammonium carbonate, pH 3), the ethyl esters (ethyl acetate, ethyl hexanoate), diethyl ether or alcohols (EtOH, MeOH).

Increasing solubility of chill haze was observable in dimethyl formamide (80 %), methyl alcohol with ammonia (pH 10) and dimethyl formamide (100 %), respectively. While methyl alcohol with ammonia supported HPLC analysis, the last solvent was more suitable for ionization in the Nanomate system. For a long time the best dissolution of lyophilised chill and permanent haze was observable in dimethyl sulfoxide, which was therefore initialised in HPLC and used for ongoing MS analyses. Although DMSO caused interferences and greatly intensified background noise (suppression of the analyte ion signal) in direct MS infusion mode, this effect did not exert such a strong influence on the LC-MS investigations. In RP chromatography the small DMSO molecules eluted early, immediately after the injection peak. Increasing levels of MS source contamination only emerged in the larger sample series. Dimethyl sulfoxide has a high polarity index. The results of the solubility test suggested that chill haze constituents are highly hydrophobic. This assessment could be supported by in house investigations, where hop polyphenols (xanthohumole, isoxanthohumole) and hop  $\alpha$ - and  $\beta$ -acids (colupulone, cohumulone, adlupulone, colupulone, lupulone and humulone) were successfully identified as haze derived substances [40], but the haze preparation methods developed for polyphenol analysis and brewing trial samples, did not suit protein analysis.

For this reason the solubility tests were extended and to also include freshly prepared haze material that had not been lyophilised.

The solvents aforementioned showed the same results for fresh haze. In addition TFA, FA, ammonia, phenol, urea (1, 3, 5, 7, 9 M), guanidinium hydrochloride (0.5, 1, 2, 3, 6 M) and  $\beta$ -mercaptoethanole were also tested, for example in combinations including urea or Gua-HCl and 15 mM DTT, 15 mM SDS, DTT and iodacetamide (55 mM), or comprising SDS and iodacetamide. To promote dissolution, the process samples were mechanically mixed and squeezed with the help of a micropistill. A multistage preparation procedure was introduced. A comparison of the findings with lyophilized and fresh haze indicated general dissociation tendencies. Complete dissolution of lyophilised haze was easily possible with strong acids and ammonia, but these chemicals did not suit the available instruments. With other solvents the complete dissolution of the haze lyophilisate remained difficult and depended on the haze batches. The best results were achievable with 9 M urea or 6 M Gua-HCl in combination with SDS and iodacetamide. After 3 to 5 solution stages the remaining haze pellet had a diffuse, soaked appearance of the brown colour typical for haze (Figure 35). Fresh haze could be completely dissolved in a greater range of mixtures comprising highly concentrated chemical denaturants (5, 7 and 9 M urea, 6 M Gua-HCl) and the various additives mentioned above. In nearly all cases the remaining pellet was very small and of a whitish colour. The shapes of the remaining pellets varied and also depended on the haze batches. These residues were of great interest as their visual, external appearance resembled the shapes of filter aids, making them likely candidates as possible activators (nucleation germ) in haze formation.

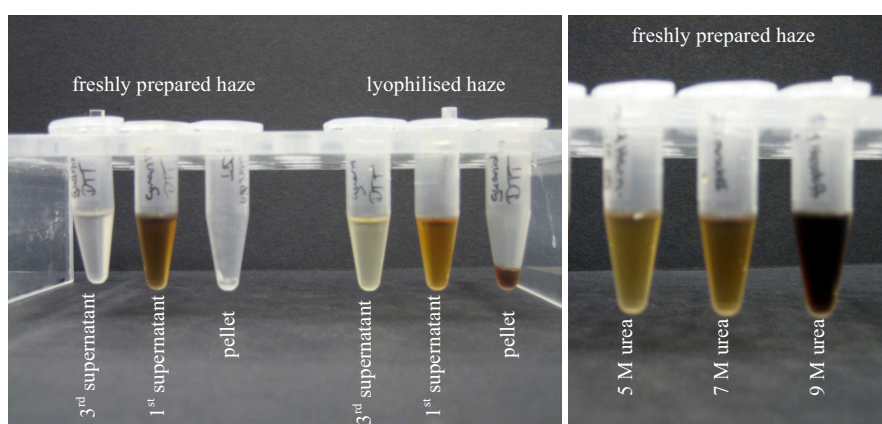


**Figure 35 Solubility tests with haze materials.** Left: the haze was thrice treated with 6 M Gua-HCl and 15 mM DTT. The remaining pellet, the first and the last supernatant are shown. Right: first supernatant upon dissolving of fresh haze in different urea concentrations (+15 mM DTT).

The initial results of the lyophilisation tests indicated a negative effect of the lyophilisation procedure and therefore a need to use freshly prepared haze for ongoing protein analysis. The

removal of water molecules in lyophilisation appeared to increase the coherence of the haze substances/particles. An enhanced physical attachment of the haze particles might explain this, but could not be proven. Both haze types could be adequately dissolved in chemicals normally used for protein denaturation (urea, Gua-HCl SDS), disulfide bond reduction ( $\beta$ -mercaptoethanole, DTT) and/or the irreversible alkylation of SH groups (iodoacetamide), but not before their different chemical properties were combined. These chemical attitudes could indicate the possible involvement of disulfide bond linkages and hydrophobic interactions in haze formation. But the results only indicated protein involvement and failed to provide clear proof, as the chemicals might also strongly influence other substance classes. A striking effect furthermore set in when the haze solvents were further diluted. Their degree of solubility was unstable. The haze sedimentation reappearing immediately after dilution with water or buffers might be explicable by shifts in the concentration or balance of chemical dynamics. Similar effects occurred with some haze solvents after 1 or 2 weeks of storage (no regularity observed). A diffuse, rather slimy haze cloud appeared at the bottom of the glass vials, also in centrifuged samples. This reversibility entailed a number of further problems with the applied instruments. On the one hand the highly concentrated solvents were not directly usable for MS infusion owing to strong chemical interferences and on the other a tryptic digestion for bottom up approaches was impossible because the digestion was limited by protease tolerances, even with the identified solvents. Similar problems emerged in protein quantification (2D-Quant) and protein precipitation.

Using RapiGest<sup>SF</sup> (0.1 %) meant that instrumental problems could be bypassed for tryptic digestion and peptide analysis, but not for native LC-MS protein analysis. By parallel solubility limitations of fresh haze were overruled, whereas lyophilised haze showed the same indifferent solubility behaviour as described above. The RapiGest reagent was originally developed to support the in solution digestion of proteins, but as a protein solubilizer and mild denaturant it was found to provide an adequate haze solvent. RapiGest would furthermore not modify peptides or suppress endoprotease activity. Following sample acidification and centrifugation, the samples could be subjected to MS-analysis as the reagent breaks down in the low pH values resulting from sample acidification.

#### **6.3.4 Freshly prepared haze and basic beer turbidity**

After changing the centrifuge and therefore rotor type, the isolation of storage haze revealed a detail already observable for freshly prepared haze in the solubility tests. While the old

centrifuge with swinging bucket rotor was designed for differential centrifugation, the new device featured a fixed angle rotor designed for rate zonal separation. Separations at early times yielded in a completely brown pellet, but a biphasic haze pellet appeared when the haze was prepared on a larger scale later. These pellets had a white fraction that usually settled at the bottom, with another brown fraction above it (Figure 36). The isolated pellets featured various external shapes, depending on the age of the sample and amount of haze. The samples from long-term storage yielded marbled, as well as completely brown pellets with samples that were up to two years old featuring an additional white phase. This white phase was of great interest because it was overbalanced in preparations of younger haze samples and thought to be a possible catalyst for haze formation. Attempts at separating both fractions were not successful after lyophilisation. The lyophilisation procedure resulted in a homogenous mixture and a very stable, non hygroscopic, brown haze powder.



**Figure 36** Two different perspectives on freshly prepared haze (24 x 0.5 L Pilsener beer bottles). The larger brown pellet was prepared from a 6 years old beer standard, whereas the white pellets were found in two year old beer.

A manual separation of freshly prepared fractions followed by microscope analysis was also problematic owing to the extreme difficulty of separating without blending. All the microscope images showed a similar, indifferent composition. Soil like networks with rough surfaces were commonly found haze formations. As in-solution drift set in, very small, cubic and indifferently shaped particles were released from the compact haze structures (Figure 37).

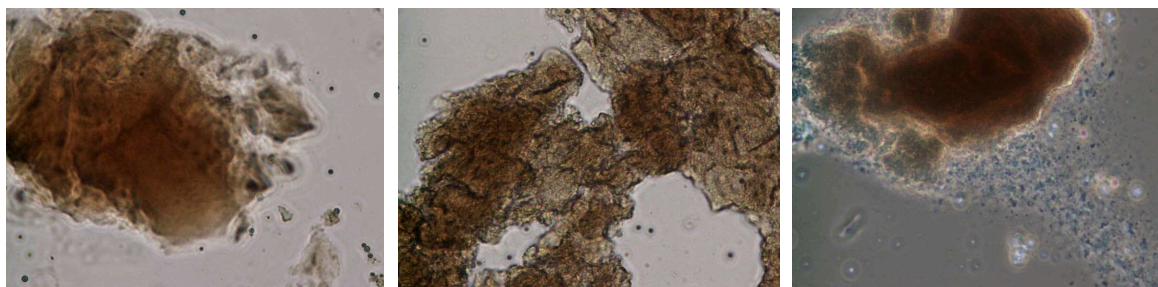


**Figure 37** Microscopy observations of haze. Left: a typical soil like haze particle found in lyophilised and fresh haze (20x ocular). Centre: the rough haze surface in magnification (40x). Right: particle drift from a solid haze soil after dissolution set in (20x).

In normal circumstances dead yeast cells, beer spoiling organisms or calcium oxalate crystals were not observable with storage haze, their microscopical appearance being highly characteristic and well-known. While it was impossible to allocate haze particles to a concrete source of origin, their specific structures could be described. Larger fibrillar or indifferently shaped particles proved as characteristic as the appearance of other, very small spherical structures. The latter were thought to be able to embed themselves into the craters of already existing particles with rough surfaces. The larger fibrillar or indifferently shaped structures might act as haze nucleation germs for one another. Both assessments tend to assume a rather physical attachment process rather than a chemical condensation mechanism.

Advances in the preparation of the haze provided further facts throwing doubt on the classical, chemical condensation mechanism. The successful isolation of the basic beer turbidity to be found in all beers immediately after bottling revealed the haze attitudes already described above. It was possible to isolate a very small, slightly varied haze portion (100 – 200 µg/500 mL beer volume) from standard Pilsener beer and a large variety of ancient Pilsener beers. All haze pellets without exception comprised a white fraction (slightly varying colour shades), often revealing a crystalline, refractive appearance under the incident light microscope (Figure 38).

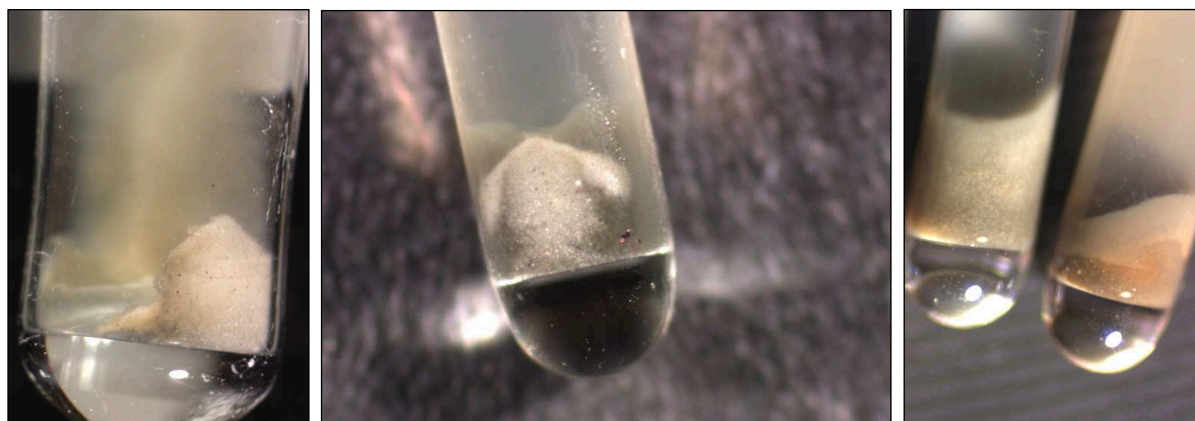


**Figure 38 Basic beer turbidity isolated from young, even bottled Pilsener beer.** Following short term storage the haze changes its outer appearance to a light brown colour (right).

The brightly coloured fraction underwent a permanent change during storage, resulting in a rapid increase of the visible haze volume in the PCR capillaries within a relatively short time. The purely white, crystalline character was only observable for a short period immediately after the bottling. After only a few days of storage the typical brown haze appearance became evident (Figure 39).



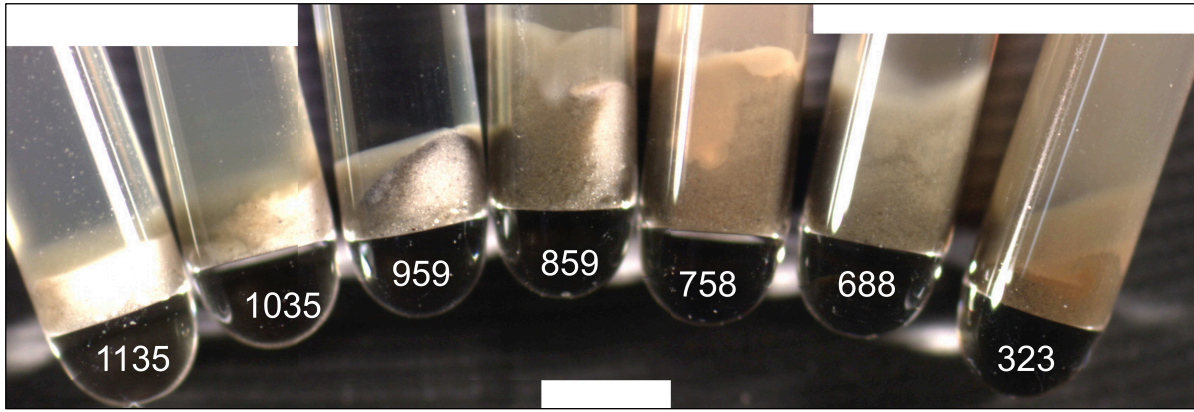


**Figure 39 Development and changes in the outer appearance of basic beer turbidity during storage.** The left capillary displays the youngest sample: lower figures correspond to longer storage times.

The specific outer appearance of the basic haze pellet resembled various filter aids in colour and shape (Figure 40). The filter aids were hence prepared in the same manner as real beer samples and investigated using incident light microscopy and ongoing microscopy analyses.

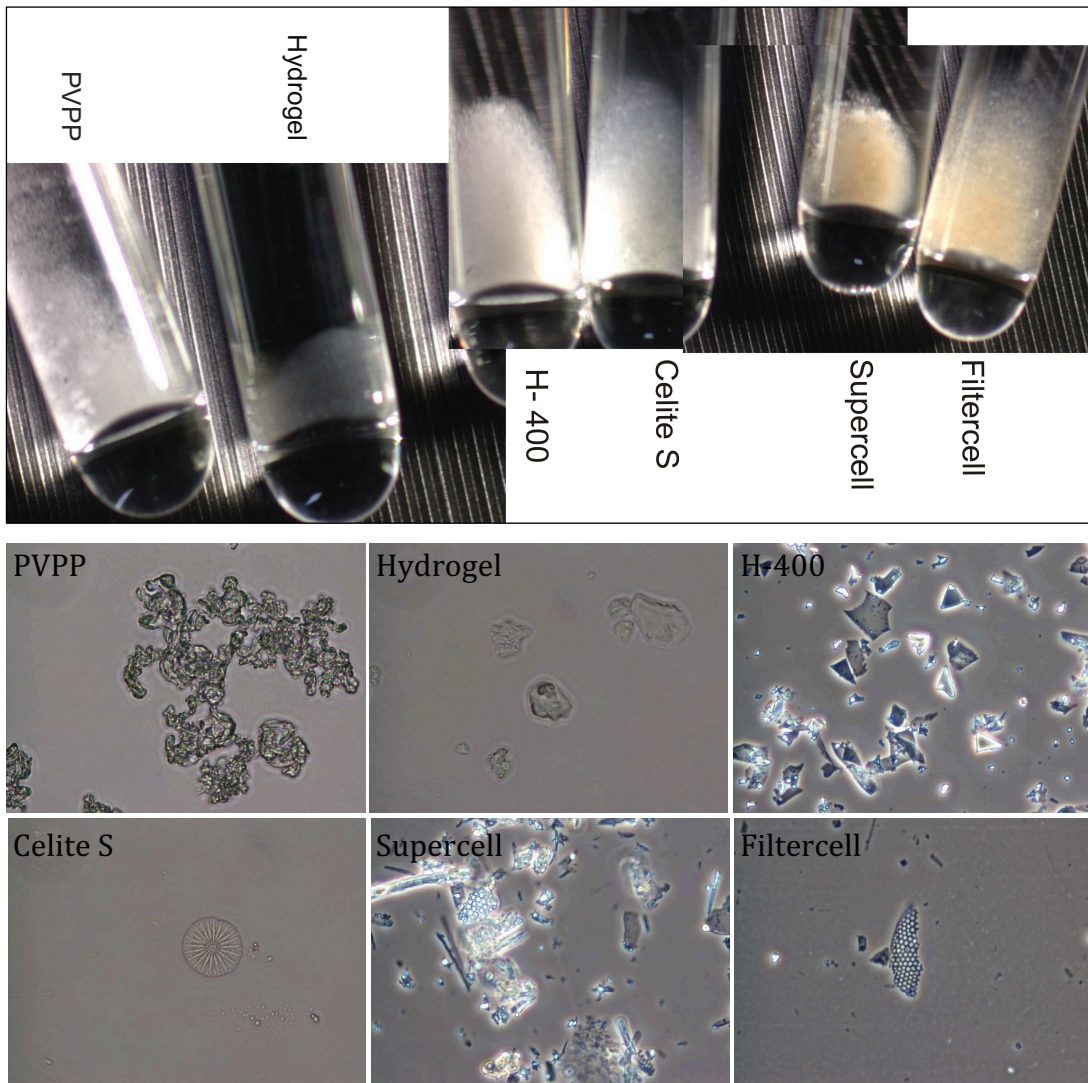


**Figure 40 Incident light and light microscopy (20x) pictures of filter aids.**

Light microscope images revealed typical, characteristic structures for filter aids. Supercell and Filtercell showed comb like structures in varying fragments and sizes. Diatomite structures or their fragments proved typical for Celite S, while H-400 mainly consisted of sharp edged, shallow fragments. Hydrogel and especially PVPP showed a soil like shape with rough surfaces and featured extensive network accumulations. The latter were reminiscent of structures observed even in long-term storage haze, but for now microscope analysis of basic haze isolates supported the a priori assumption of filter aid components serving as possible haze activators. Light microscope images showed structures that could be directly allocated to Celite, Filtercell or Supercell fragments as well as other filter aids (depending on the exact filter aid mixture used for the brewing procedure in the respective brewery) (Figure 41).

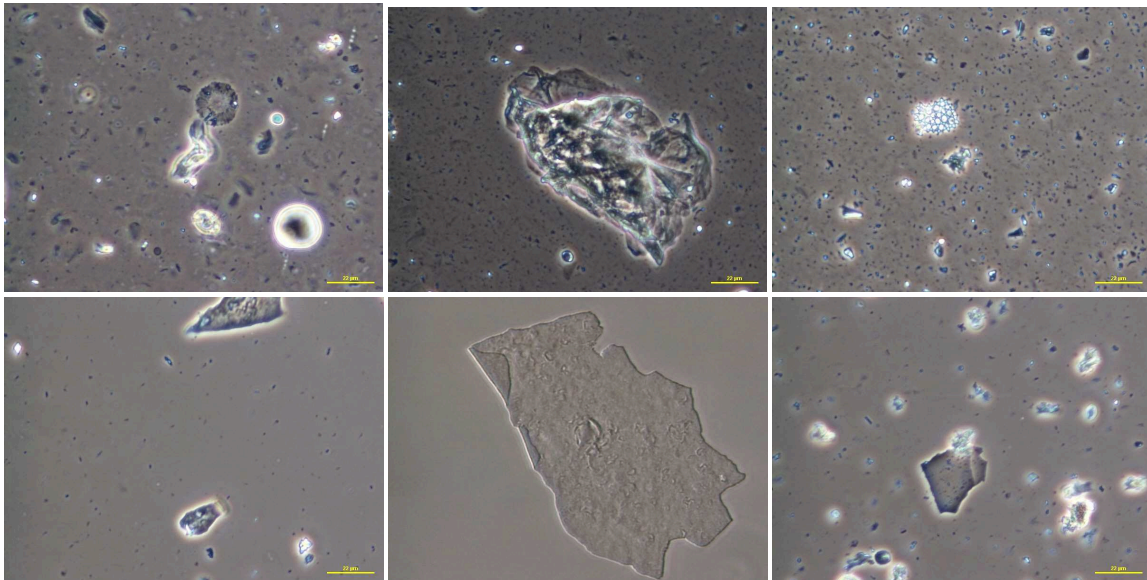


**Figure 41** Filter aid components and typical basic haze structures found even in bottled and very young Pilsener beer samples.

A striking fact was the height of the identified components, which was many times larger than the exclusion sizes of the filters, but this parameter also depended on the different filter systems used at the breweries. The appearance of large filter aid components, as well as larger fibrills or other haze structures, could be explicable by the application of so called slippage filter systems, filter breakthroughs and line shocks. The results indicated a basic filter aid adulteration as well as an addition of turbidity components that could not be retarded by the filtration line. The rough surfaces of these particles were thought to act as haze nucleation germs and the explanatory emphasis was shifted to virginal physical attachment instead of a chemical condensation mechanism.

### 6.3.5 Bottom up analysis of haze

Thirteen barley proteins could be identified as possible haze constituents by bottom up approaches so far. One third of the protein hits could be supported by more than one peptide fragment, while the others could only be identified by a single peptide hit after fragmentation of one peptide ion. These hits included prominent, heat-stable protein species such as protein Z4, protein Zx, non-specific lipid transfer protein 1 (nLTP1) and several  $\alpha$ -amylase/trypsin inhibitors. These protein hits also correspond to results reported by Iimure *et al.* [56].

Table 18 summarizes the proteins identified in haze after tryptic digestion. Owing to the similarity of their amino acid sequence three D-hordein species were identified for one and the same peptide fragment. A further distinction was impossible in this study as was only one peptide fragment had been identified for these protein species.

**Table 18 Protein identifications in haze following overnight digestion with trypsin.**

Full protein name ID's	Accession No.	MM [Da]	No. of ion hits (No. of peptide fragments)	Peptide [m/z]
SPZ4_HORVU Protein Z4	P06293	43276	5 (5)	707.47 (2+); 750.51 (2+); 685.48 (2+); 394.74 (2+); 577.82 (2+)
BSZx_HORVU Protein Zx	Q40066	42974	1 (1)	435.78 (2+)
IAAB_HORVU Alpha-amylase/trypsin inhibitor CMb	P32936	16526	1 (1)	593.29 (2+)
IAAA_HORVU Alpha-amylase/trypsin inhibitor CMa	P28041	15499	1 (1)	534.81 (2+)
IAAE_HORVU Trypsin inhibitor CMe	P01086	16135	2 (2)	772.84 (2+); 807.81 (2+)
BARW_HORVU Barwin	P28814	13737	1 (1)	650.34 (2+)
NLTP1_HORVU Non-specific lipid transfer protein 1	P07597	12301	5 (3)	664.33 (2+) , 443.23 (3+); 832.09 (2+), 554.99 (3+); 1005.51 (2+)
IAA2_HORVU Alpha-amylase inhibitor BDAI-1	P13691	16429	5 (4)	414.16 (2+); 552.65 (3+), 828.47 (2+); 970.94 (2+); 1116.67 (2+)
Q84LE9_HORVU D-hordein	Q84LE9	80410	1 (1)	668.88 (2+)
Q40054_HORVU D-hordein	Q40054	75108	1 (1)	668.88 (2+)
Q40045_HORVU D-hordein	Q40045	50786	1 (1)	668.78 (2+)
TCPB_YEAST T-complex protein 1 subunit	P39076	57203	1 (1)	572.84 (2+)

Except for the D-hordein species and a SR541 signal recognition particle (P 49968, attitudes unknown) all the proteins identified here were water-soluble. Without exception these water-



## RESULTS AND DISCUSSION

soluble proteins could be allocated to the defense protein plus enzyme inhibitor class (classification by Østergaard).

Nearly all protein hits were provided with a 100 % probability by the ProteinLynx Global software (PLGS) and positively identified several times over. The only exceptions were found with P11643 IAAD and the P49968 SR541 signal recognition particle. In both these cases the probabilities were around 0 %. A positive consideration of these two protein species was therefore impossible and the results are only included here for completeness.

In addition, a small number of yeast derived and two wheat proteins were identified. Owing to single positive hits and low probabilities (< 50 %) only one of the yeast candidates remained. A T-complex protein 1 subunit beta of *Saccharomyces cerevisiae* was identified multiple times with a 4.6 to 80 % probability. A closer look at the peptide sequences reveals that the number of ions observable in haze samples was only very small (Table 19). These results were independent of the sample preparation (lyophilised or fresh; solvent type) and the fragments were identified by repeated hits.

**Table 19 Masses and sequences identified for haze proteins in bottom up analysis**

Full protein name	Detected sequence	Position	Ion charge	[M+H] <sup>+</sup> average
SPZ4_HORVU Protein Z4	K-ISYQFEASSLLR	291-302	2	1414.6
	K-QILPPGSVDNTTK	161-173	2	1370.54
	K-QTVEVGR	277-283	2	788.87
	K-QYISSSDNLK	219-228	2	1155.24
	R-DQLVAILGDDGAGDAK	61-76	2	1499.76
BSZx_HORVU Protein Zx	R-SLPVEPVK	357-364	2	868.51
IAAB_HORVU Alpha-amylase/trypsin inhibitor CMb	C-RIETPGPPYLAK	55-65	2	1186.82
IAAA_HORVU Alpha-amylase/trypsin inhibitor CMa	R-SHPDWSVLK	97-106	2	1069.54
IAAE_HORVU Trypsin inhibitor CMe	R-TYVVSQIC*HQGPR	45-57	2	1544.76
	R-C*C*DELSAIPAYC*R	67-79	2	1614.67
BARW_HORVU Barwin	L-RVTNPATGAQITAR	69-81	2	1301.46
NLTP1_HORVU Non-specific lipid-transfer protein 1	R-GIHNLNLNNAASIPSK	83-98	2 and 3	1663.87
	R-DLHNQAQSSGDR	59-70	2 and 3	1328.34
	K-C*NVNVPYITSPDIDC*SR	99-115	2	2011.23
IAA2_HORVU Alpha-amylase inhibitor BDAI-1	R-VPEDVLR	64-70	2	827.95
	K-LEC*VGNRVPEDVLR	57-70	2 and 3	1656.89
	R-DC*C*QEVANISNEWC*R	71-85	2	1942.1
	K-LLVAGVPALC*NVPIPNAAAG TR	120-141	2	2233.63
Q84LE9_HORVU D-hordein	R-QYEQQTEVPSK	97-107	2	1336.63
Q40054_HORVU D-hordein	R-QYEQQTEVPSK	97-107	2	1336.63
Q40045_HORVU D-hordein	R-QYEQQTEVPSK	97-107	2	1336.63
TCPB_YEAST T-complex protein 1 subunit	R-LASAAALDALTK	126-137	2	1144.65

\* Carboxyamidomethyl-cysteine modification due to the sample preparation procedure

In the case of protein Z4, no known peptide of the RCL or rear fragment region could be observed. The peptide fragments derived from the main sequence of the larger front region or

entire protein Z molecule. Five of the 34 possible trypsin cleavage fragments were found in case of protein Z. The identified protein fragments covered 14.5 % of the entire AA sequence. Although the sequence coverages were high for nLTP1 (49.45 %) and IAA2 (41.8 %), the recovery of protein cleavage fragments was low, as was the case with the other identified proteins.

A large percentage of doubly charged peptide ions overbalanced the three triple charged ions. No other peptide ions were found in haze throughout the entire study. These results are significant as latter findings will show much more extensive variations of peptide ion species and charges for beer or brewing process samples, despite of the same sample preparation and treatment.

### **6.3.6 Top down analysis of haze samples**

Top down investigation supported the results of the solubility test series. Lyophilisation had a critical impact on the ongoing haze analysis. RapiGest could not be used for LC-MS investigations because the column's compatibility could not be fully guaranteed by the manufacturer. Comparative LC-MS analyses of lyophilized and fresh haze material found remarkable differences in the peak separation and ion count rates. Freshly prepared haze material (dissolved in DMSO) revealed a larger number of peaks in LC separation, while peaks were down to a minimum with very low ion count rates in lyophilized haze (Figure 42). As the haze samples were analysed for whole proteins, the peaks were expected to discover typical protein ion spectra with multiply charged ions. The findings of this thesis did not support these assumptions as the LC chromatograms and attendant spectra failed to indicate any proteins. Neither the nLTP1 typical protein spectra were found nor any other kind of proteinogenic spectrum. Instead the already known, corresponding protein Z ions (1345 Da, 1009 Da etc.) could be recognized. In addition, only doubly, ternary and quaternary as well as their corresponding single charged ion species could be observed. Without exception the mass calculations turned up molecular masses of 2 – 4 kDa. The weight indicated a rather peptidic character for the detected top down species. It may be possible that only the peptides are involved in haze formation, and no whole proteins. Their small height might allow for attachment to or within rough particle surfaces (simple chromatographic principle).

Owing to the soft ionization during Nanomate infusion, protein bond breakages were thought to be unlikely, especially as different ionization techniques were tested. If peptides derived from backbone breakages of weak protein bonds, this effect should also be observable for the

same identified protein species in a top down analysis of other sample materials (especially beer). This could not be confirmed. A basic peptide content might also feign a haze protein content in bottom up approaches. Tryptic digestion of proteins might either be impossible (no additional cleavage sites in the small AA sequences) or unnecessary if only peptides were released into the haze solution

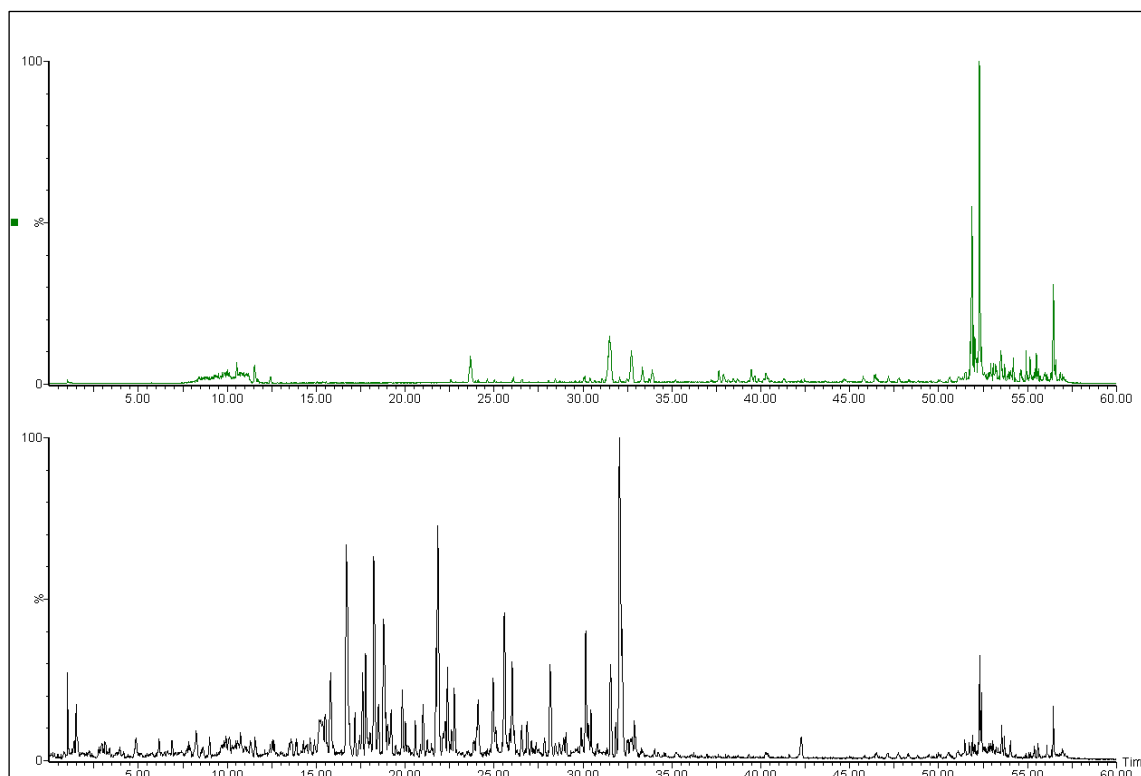


**Figure 42** LC chromatograms of lyophilized (top picture) and freshly prepared haze material (bottom) analysed by top down approaches. In both cases the haze was dissolved in DMSO. Peptides mainly eluted at minutes 15 and 35 in the 60 minute chromatography.

If there are only the peptides involved in haze formation, the 2D-Quant protein quantification results observed in haze supernatants might also be realistic. Peptides might not be detected by the quantification mechanism, especially if they are only minor components.

Haze solutions were not subjected to direct peptide analysis without further digestion. This test should be performed in further research projects in order to confirm the theory of haze being based on peptides. The origin of the haze peptide species could only be estimated: protein degradation or cleavage may take place in the brewing process or effected by yeast enzymes.

### **6.3.7 Summary**

If all the results of the haze study are taken into consideration they fail to support the classical protein polyphenol haze model. Neither barley polyphenols nor whole proteins were identified. By contrast, hop derived components and peptides were successfully identified in haze, while both substance classes were previously thought to be minor components. Studies performed in the brewing trial and for this thesis also revealed a number of unknown, but characteristic haze ion signals (ion series with constant mass differences, possible sugar signals, etc.), which could not be allocated to a source of origin. These results shall not be described in greater detail here, but deserve a mention as some of these unknown components appeared to be highly abundant in LC-MS analysis.

The need for further investigation, especially of chill haze, has been explained before and the observations of basic beer turbidity delivered a number of facts that contradict classical haze concepts. The findings of this study appear to confirm a physical attachment process in haze formation, but a chemical mechanism could also not be ruled out entirely.

The following statement sums up the results of this study: If the shelf life and quality of stored beer is to be enhanced, the influx of basic beer turbidity should be kept to an utmost minimum.

### **6.4 Gushing**

The bottled beer of most German breweries showed stronger gushing tendencies in 2008. An unusual weather phenomenon (rainy summer following a very dry spring) had affected the growth and harvest of the barley in the previous year of 2007. The gushing agents were therefore attributable to “weathered” barley and a type of primary gushing caused by the fungal/microbiological decay of the resulting malt.

Gushing is the spontaneous and violent degassing of carbonated bottled beer in the absence of shaking. Tests carried out in cooperation with Bielefeld University tracked and recorded this gushing phenomenon using a high resolution digital video camera. Single frames (Figure 43) from the short films revealed a multi-phase expansion. Immediately after opening the beer bottle (Frame 1), very small bubbles start to nucleate explosively from the entire supersaturated, fluidic beer volume (Frames 2 – 4). This first observation was remarkable because it provided the first ever indication that the nucleation germs for gushing are

distributed throughout the entire beer volume and not related to the bottle walls (scratches) or induced at the glass bottom (sedimented particles).



**Figure 43** Snapshots of the multi-phase expansion of a gushing beer. The single frames were taken from short videos recorded by a high resolution camera of Bielefeld University.

At the onset of the second phase more bubbles appear and previously formed microbubbles start to expand by carbon dioxide uptake (Frames 4 – 7). This process is thought to be supported by surfactants (foam stabilising, foam active substances) able to enter the bubble walls, stabilising the bubbles. As the bubbles grow and start rising to the surface, these substances are thought to align themselves with their hydrophobic backbones towards the gas inside and their hydrophilic components towards the outside forming stabilizing membranes [36, 84]. The bubbling continues to expand until the lifting force is reached and the bubbles start to rise to the surface (Frames 7 – 9). The bubble frontier meanwhile moves from the bottom of the bottle to the top (Frames 9 – 18). This strong migration movement leads to the so called gushing effect (starting in Frame 14) with spontaneous overflow as the migrating bubbles drag the beer fluid along. Despite the gushing effect, a last phase is reached in the bottle, which shows an ongoing development of large bubbles across the whole volume. This last observation is another interesting fact to mention because gushing samples with moderate gushing behaviour also showed this unusual bubble size development. When a bottle of non-gushing beer is opened, single, small sized bubbles usually immediately emerge from scattered points of the volume (normally generated at the bottle wall or bottom). These bubbles are tiny and will not expand significantly until they start to rise to the surface.

A second observation with gushing beer concerned the foam stabilities, which were enhanced even if the developing foam did not show the typical tees with finest creaminess.

Taking both observations into account, the gushing bubbles seem to be stabilized by other means than normal beer bubbles are. It is possible that the stabilizing bubble layer has a different composition.

### **6.4.1 The “Modified Carlsberg Test” (MCT)**

The original Carlsberg-Test procedure (MEBAK, Vol. III, chapter 9.2, 1996) was modified in 2007 and introduced in the breweries on a large scale to assess the quality of the malt and predict gushing tendencies. Malt quality assurance via MCT was based on the assumption that gushing components were water soluble, still active and soluble after boiling in the brewing procedures, and active in the pH value and other conditions given in beer. Gushing predictions concerned the loss of overflow volume after opening Bonaqua water bottles spiked with malt extracts. The exact gushing agents were unknown then and still are today. A large variety of MCT strategies were tested to create unique and comparable gushing results, as well as find possible gushing inhibitors. The MCT results were compared with dialy

routine analyses such as the assessment of malt supplies for black or red grains, semi glassy kernels, grain sizes or impurities. Special tests such as mycotoxin and pesticide quantification, long-term storage of freshly bottled beer (RT, 30 °C and 0 °C) followed by a visual assessment of the samples after opening them in the regular manner and tests with pure malt brews or for other technological parameters (secondary gushing parameters) were also performed. No direct correlations were to be found between the MCT results and other possible gushing parameters like mycotoxin contents or the number of red/black grains. As the results of the routine and special analyses had also lacked significance, the efforts of this thesis were directed at MCT additives and the discovery of gushing inhibitors.

A prerequisite for such an approach was the discovery of a 100 % gushing positive malt with stable, comparable MCT results. The latter fact was hard to realize as the first results with brewing malts were found to be highly indifferent. While non gushing malts (V = 0 – 5 g loss) unflinchingly showed the same results with minimal deviation and intended to be non gushing malts, the findings in gushing malts (probable/actual gushing) greatly differed from one MCT batch to another (Figure 44).

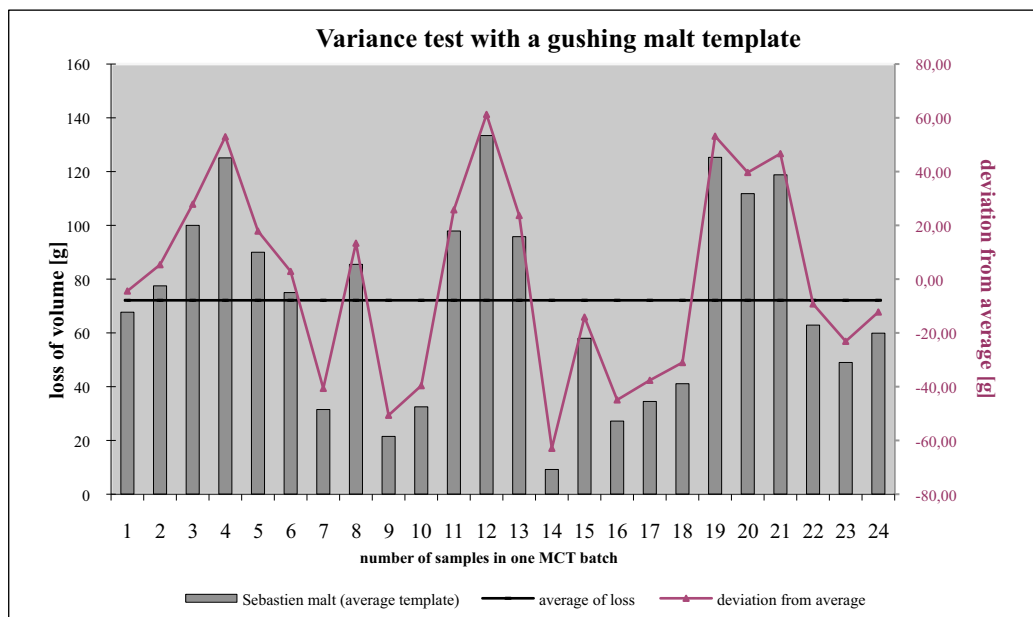


**Figure 44 Variations within a single MCT batch of a gushing malt.**

Variance tests with multiple preparations of a single malt type in a single MCT batch were indifferent, as were repetitions with a single malt sample and different MCT batches or preparations by different users carried out in intervals of a few days. Malts featuring a full gushing tendency in the first instance showed a probable or non gushing tendency in the next test, with the whole situation reversed again in the third. No regularity could be derived from



the observations. Even an analysis of causes related to the user or preparation procedure and their subsequent adjustment for maximum compliance could not eliminate this problem. Efforts to homogenize the malt samples before and after milling or to mix the finished MCT extracts before transferring them to the Bonaqua bottles had no effect on the variations (Figure 45).

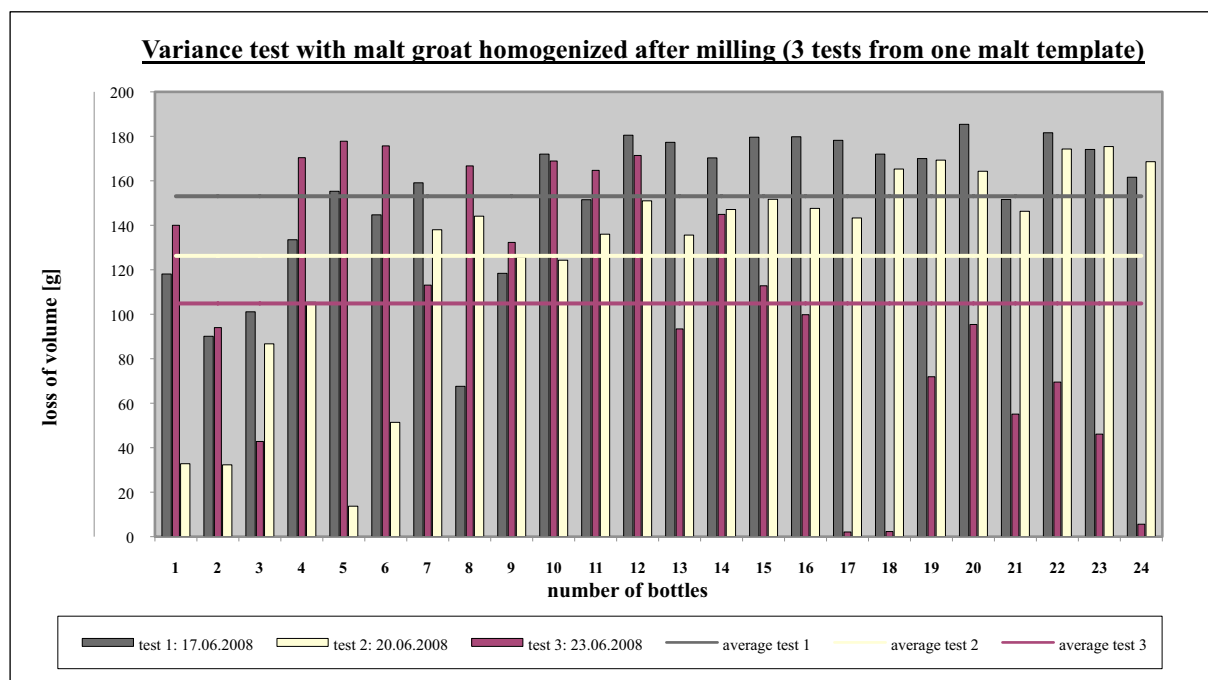


**Figure 45** Three independent MCT approaches from one malt sample. The basic malt sample was homogenized after milling and MCT batches were prepared at intervals of 3 days.

Coarse groat was fractionized by size because the heterogenous distribution of husks, coarse groat, fine groat and flour into individual MCT appendages was also thought to be a possible cause of variance, especially in cases of microbiological decay and/or metabolites being attached to individual grain compartments. The results of the MCT test series performed with groat fractions showed the same indifferences and there was no indication that gushing was favoured by individual groat compartments.

In most cases the main problem with the MCT procedure appeared to be an uneven distribution of the agents promoting gushing. The heterogeneity of the malt extract was thought to be responsible for this as streaking effects were again observable in thoroughly mixed extracts. A 100 % gushing malt was ultimately found despite the intransparent MCT results and used for the following inhibition test series. Regardless of the variances also found with the gushing volumes of this standard reference, the results were only taken into consideration and analysed in depth if the inhibition effects reached a maximum, resulting in zero gushing after sample treatment.



### 6.4.2 MCT investigations with hop additives

The research concerning the gushing behaviour being focused on malt derived gushing factors, little attention had been paid to the influence of hops in recent years. Not much information is available on this topic, but older reports and a small number of actual publications mention anti gushing properties of hop additives owed to the suppressive effects of their resinous and oily constituents [33]. Four commercially available anti gushing hop extracts were subjected to MCT tests (see Figure 46 for an excerpt of the findings).

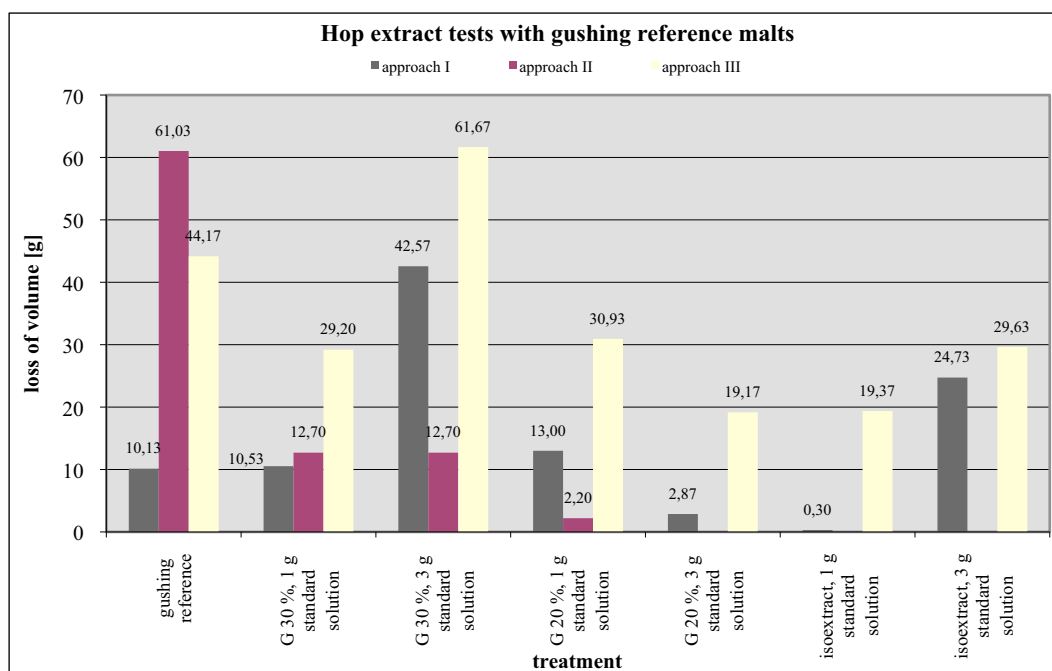


**Figure 46 MCT approaches with hop extract additives.** The approaches were repeated with the same standard gushing reference malt. The dosage of the hop additives was adapted to weak (1 g standard solution) and strong gushing (3 g standard solution). The second approach was not performed with the isoextract.

Both products were CO<sub>2</sub> extracts. The hop extract G solution comprised  $\alpha$ - and  $\beta$ -acids, iso- $\alpha$ -acids and hop oils, whereas the isomerized extract only contained iso- $\alpha$ -acids. Neither the hop extract G (30 % and 20 %) additive nor the isomerized hop extract (30 % and 20 % isoextract) completely inhibited gushing. Repeats of the MCT approaches again showed very indifferent results.

None of the various MCT approaches revealed a clear inhibition (gushing volume = 0 g) tendency after dosing with hop extract. Separate experiments indicate the results reported in literature, but these could not be confirmed by multiple repetition. As the aforementioned premise was not met and the results deviated unregularly, the findings of this thesis confirm that hop extracts did not have a suppressive effect on the gushing behaviour.

### 6.4.3 The impact of enzymes on the gushing tendencies of malt and barley

As already mentioned, the discussions on gushing often refer to proteinogenic gushing activators or stabilizing agents. It was known from literature and manufacturer informations that the dosage of commercially available enzymes (proteases) was found to affect the gushing behaviour and in some cases even inhibited it. The key problem was that the associated cleavage mechanism of these enzymes was undefined and unspecific. The investigations therefore aimed at finding proteases with specific cleavage mechanisms and to narrow down the number of possible protein substrates on the one hand and to enable comparative LC-MS studies on the other.

The additives were tested with malt extracts as well as a barley extract. Eighteen individual enzymes and two mixtures were tested. The selected enzymes included specific, unspecific and glyco enzymes. Their dosage was adapted to the protein content of the extracts according to 2D-Quant protein quantification. If manufacturer information was available, the minimum enzyme concentrations were used. Additional information about the enzymes, their cleavage mechanism, the dosage and test modifications is summarized in Appendix A. The enzymes were subjected to MCT extractions in order to denaturate the protein content. The results were compared to the same gushing reference that had been used in the hop extract studies.

Irrespective of the test modifications, four enzymes (Corolase 7089, Corolase TS, Corolase PP and thermolysine) and one mixture (Corolase 7089 + Corolase LAP) always showed a total inhibition of gushing in comparison to the standard gushing malt sample (Figure 47).

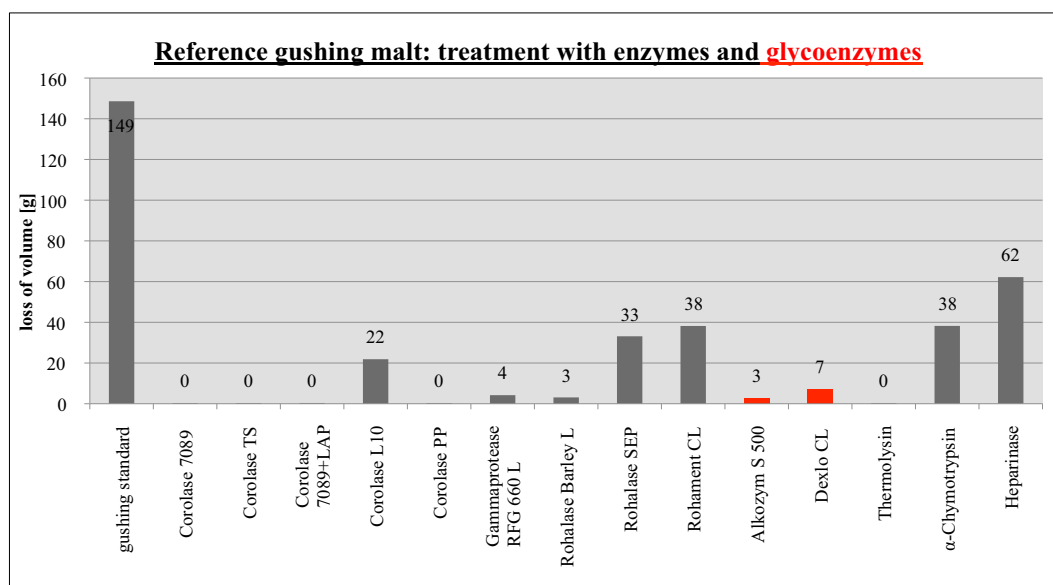


Figure 47 Gushing behaviour of an enzymatically treated gushing malt sample.

The cleavage mechanism of the identified inhibitor enzymes again remained unspecific, while predominant cleavage of hydrophobic amino acids and side chains was a common feature. Complete inhibition of the gushing indeed supported the assumption that proteins might be involved in the gushing phenomenon. Unfortunately the results did not allow the promoters to be narrowed down to individual gushing proteins or protein classes.

The very same enzyme tests did not result in a total inhibition in the case of barley extracts (Figure 48). Although the general gushing tendency of the barley reference resulted in similar overflow volumina as the malt extracts, the barley proteins appeared to be hydrolysed to a lesser extent. Inhibitor enzymes identified in malt extracts only reduced the obvious gushing behaviour of the barley samples to a probable gushing tendency.

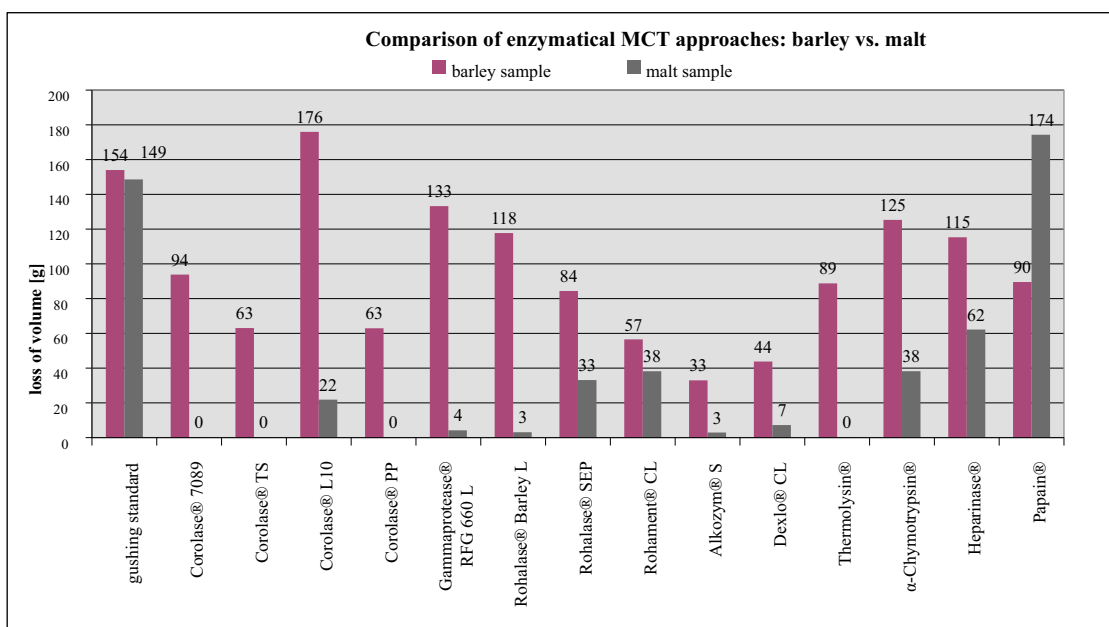


Figure 48 Comparison of the gushing behaviour of enzymatically treated barley and malt samples.

A lower enzyme susceptibility might be explained by a greater stability owed to the absence of additional conformational, chemical or enzymatical changes that the grain would undergo in the malting procedure. Modifications occurring in the malting process appeared to promote further enzymatic degradation in the enzymatical MCT approaches.

For the UPLC-MS studies in hand Corolase 7089 was selected and the lack of cleavage specificity accepted. The results for the enzyme showed maximum reproducibility and minimum deviation. In addition, Corolase 7089 exerted its inhibitory effect even after short exposure times and in even lower enzyme concentrations (Figure 49).

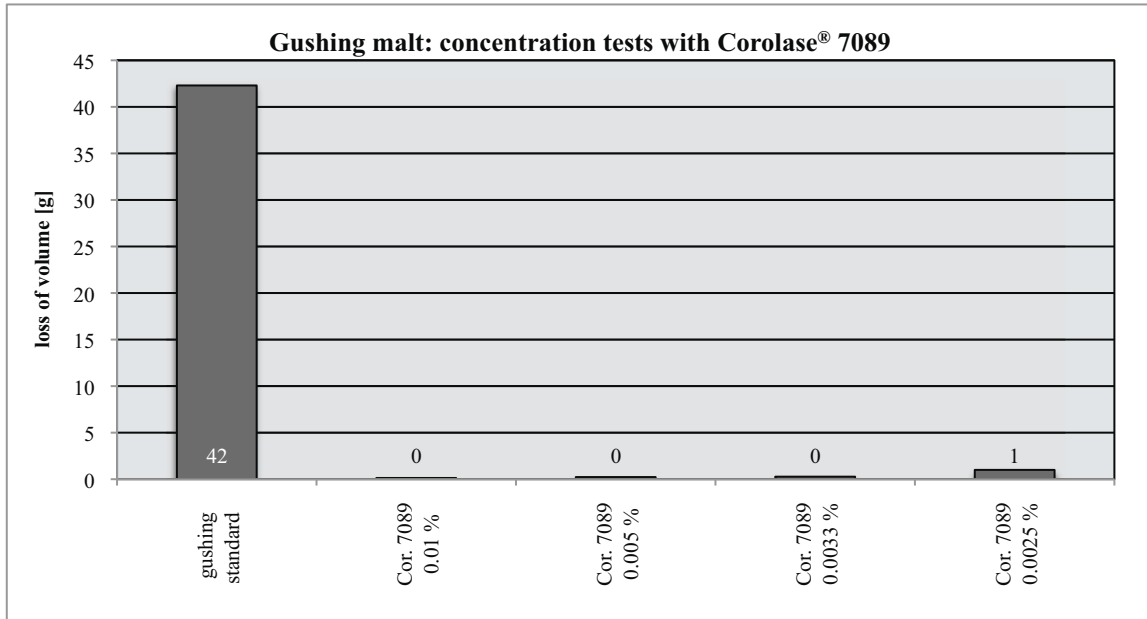


Figure 49 MCT results observed for Corolase 7089 in different concentrations.

Halving the concentration (0.005 %) or reducing it by a factor three or four (0.0033 and 0.0025 %) showed the same inhibitory effects as the minimum enzyme concentrations (0.01 %) recommended by the manufacturer.

#### 6.4.4 First UPLC-MS studies with MCT extract samples

UPLC-ESI/MS chromatograms of undigested standard gushing and non-gushing malt extracts showed strong correlations on a native protein level (Figure 50), but the number of observable protein peaks remained small.

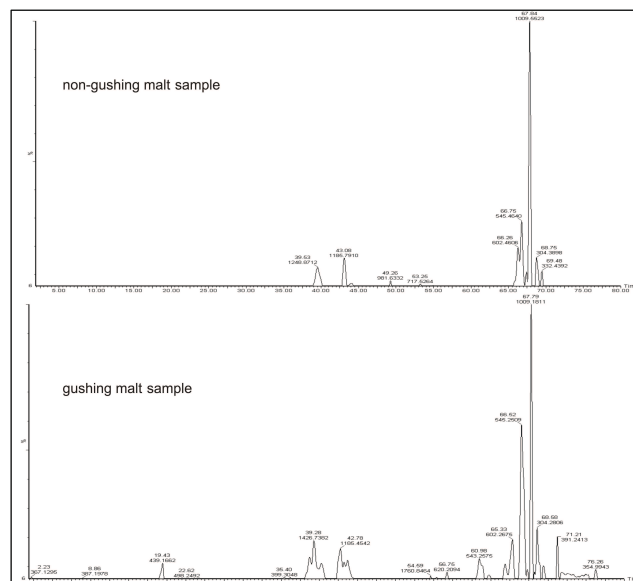
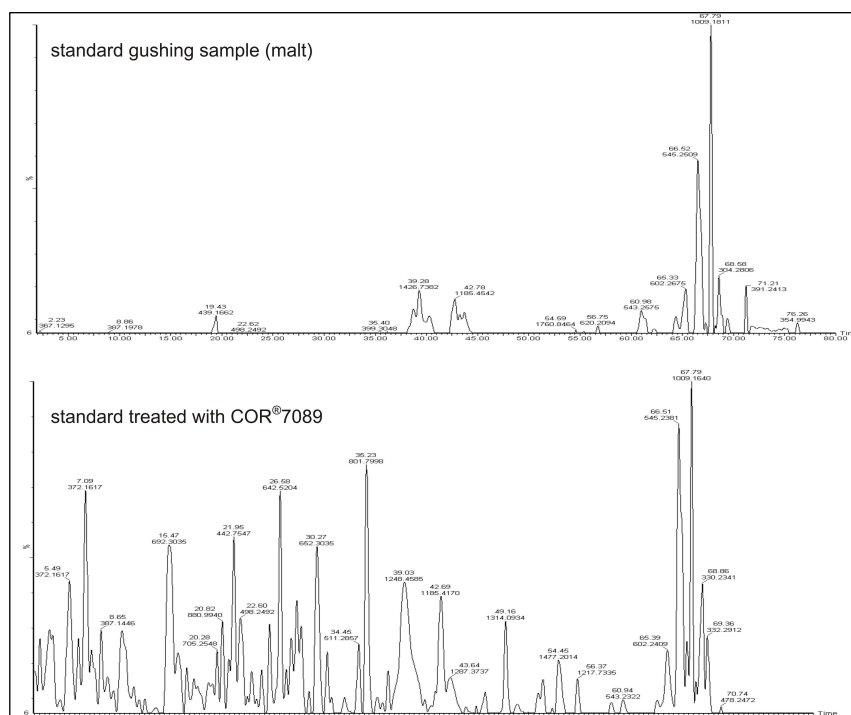


Figure 50 Native protein analysis (UPLC nanoESI-QTOF-MS) of a standard gushing and a non gushing malt extract sample.

The small number of isolatable proteins as well as their low ion count rates did not allow any further differentiation or definitive comparison of the protein contents or compositions.

Similar problems beset the analysis of enzymatically treated gushing malt samples (Figure 51). A direct comparison of the standard gushing malt and identical samples treated with Corolase 7089 showed the expected increase of peptide specific peaks, but as the ion counts were low again, the peptides could not be identified and allocated to native protein species.



**Figure 51 UPLC-MS chromatogram of a standard gushing malt and a sample treated with Corolase 7089.** Enzyme treatment resulted in a typical boost of peptide specific peaks, whereas the enormous later peaks of the original sample were still retained. Spectra of these later peaks indicated large, multiply charged species that appeared to be unaffected by the enzyme treatment and could not be separated during the LC-MS run.

#### 6.4.5 Protein precipitation with MCT extracts

The aforementioned UPLC-MS investigations were hampered by the low protein concentrations and ion abundancies of the analysed MCT extracts (beer and other brewing process samples), insufficient for adequate protein identification by top down and/or bottom up approaches. Preliminary tests with SPE preparation, small scale ultrafiltration and dialysis, as well as several precipitation procedures did not have the desired effect of preconcentrating or precipitating the proteins and were often strongly influenced by other beer substance classes (especially sugars). The twofold need to boost protein concentrations and eliminate interfering substances was a limiting parameter that could be solved by phenolic protein

extraction. The precipitation procedure used was developed and provided by the research group led by Karsten Niehaus (Faculty of Biology, University Bielefeld) and adapted to the needs of this study. Method adjustment was performed with MCT extracts because the protein content was expected to be higher and more significant than in beer samples. In addition, the exact protein content of gushing positive MCT extracts were of great interest as the aforementioned results indicated a possible involvement of this substance class.

The phenolic phase was initially subjected to LC-MS analysis. Then the phenolic phase with the interphase above it were tested regarding their protein content. Combinations of both fractions were found to provide a greater variety of proteins in the LC-MS tests and were therefore always used for the structural identification in hand.

In a second test, the trial concentration and pH parameters of the Tris-HCl-buffer were changed. 0.5, 1, 1.5 and 2 M concentrations were tested first. Comparisons were based on the LC-MS ion count rates of tryptic digested protein pellets. The highest count rates were achieved with 1 M Tris-HCl buffer (Figure 52).

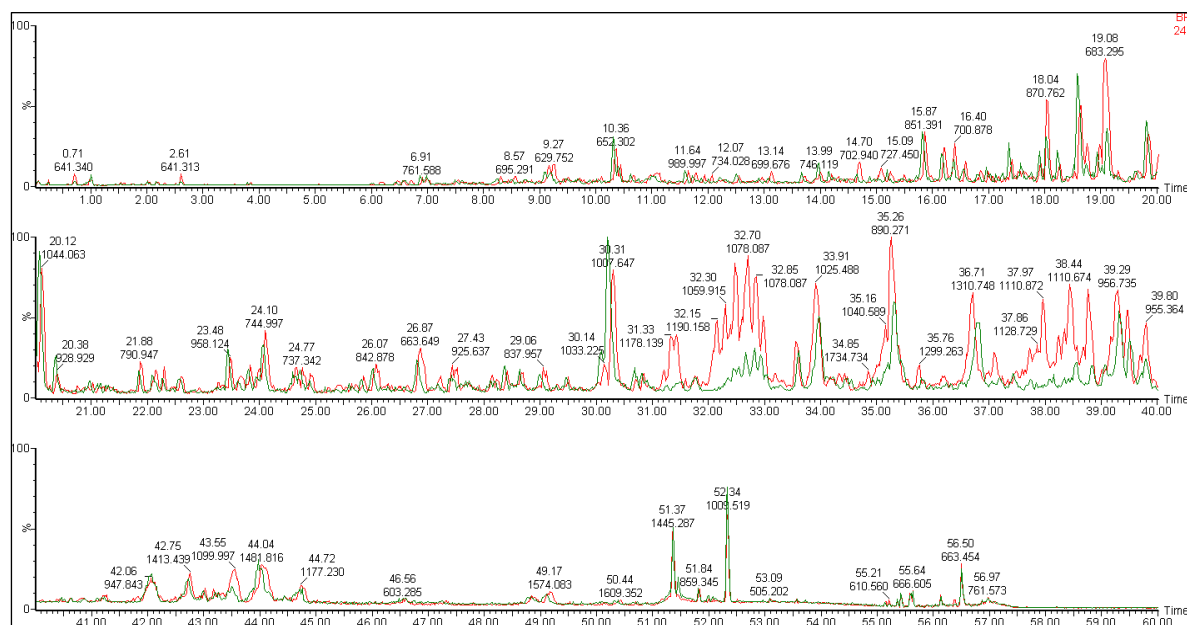


**Figure 52** LC-MS peptide analysis of precipitated and tryptic digested protein pellets. Protein precipitation was performed with different Tris-HCl buffers. The red chromatogram with the higher ion count rates shows peptides derived from proteins precipitated with 1 M Tris-HCl (pH 7). The green curve shows protein precipitation with 2 M Tris-HCl (pH 7).

Further pH modifications were therefore only tested with 1M Tris-HCl buffers. Overlays of these chromatograms indicated that a neutral pH of 7 or 8 resulted in the best ion yield and the highest number of peptide specific peaks.

A last critical preparation step was the resolution of the protein pellet. Recommended buffers matched an ongoing gel electrophoretic separation but not the LC-MS instrumentation. To

obtain good resolution effects, a minimum of 3 M Gua-HCl and 15 mM DTT were necessary for overnight resolution. Mechanical treatment in support of the solution process was impossible as the proteins showed strong foaming tendencies. Once developed this protein foam was so stable that it would not degenerate again.

All the modifications mentioned above boosted the sensitivity of native protein analysis and the number of separated protein peaks in UPLC-MS scan mode (Figure 53). Ion count rates of peptide species also rose to a high signal to noise ratio when enzymatical treatment had been applied to the gushing samples.

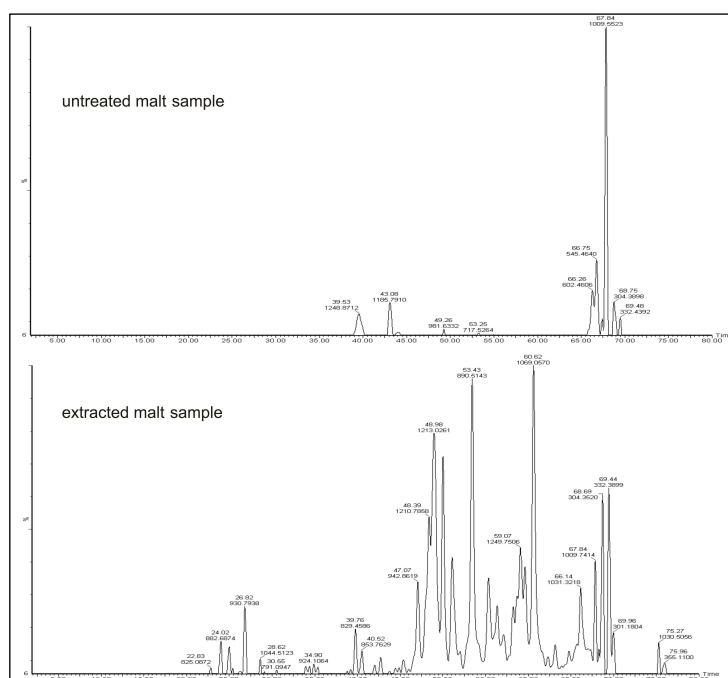


**Figure 53 Native protein chromatogram of an untreated standard gushing malt (top) and the "native" (but denaturated) protein pattern after phenolic extraction.**

Before the tryptic digestion the samples had to be diluted (1:3) to enzyme compatible concentration ranges. As the diluted samples developed turbidity, additional centrifugation operations were introduced before the UPLC injection.

The successful establishment of the protein precipitation procedure provided a basis for the bottom up experiments in hand and a structural protein identification for malt extracts.

#### 6.4.6 Bottom up investigations

Precipitated and tryptic digested gushing and non-gushing MCT extracts were separated in 60/80 minute UPLC runs after 3-fold sample loading (online column preconcentration) in an UPLC BEH-C<sub>18</sub> column. The additional sample loadings strongly enhanced the peptide ion

count rates. In nanoESI-MS analysis the scan mode resulted in an efficient ionization with a stable and constant ESI spray. The greatest advancement of the new method was owed to the parallel fraction collection realisable via the Nanomate robot system. The LC run was split and directed to 384 well plates, while twenty second fractions were collected in the MS scan mode and precursor ion discovery. Single fractions of abundant precursor ions were reinfused for DDA experiments and MSMS investigations (Figure 54). The DDA experiments in hand obtained a complete set of fragment ions with a high signal to noise ratio.

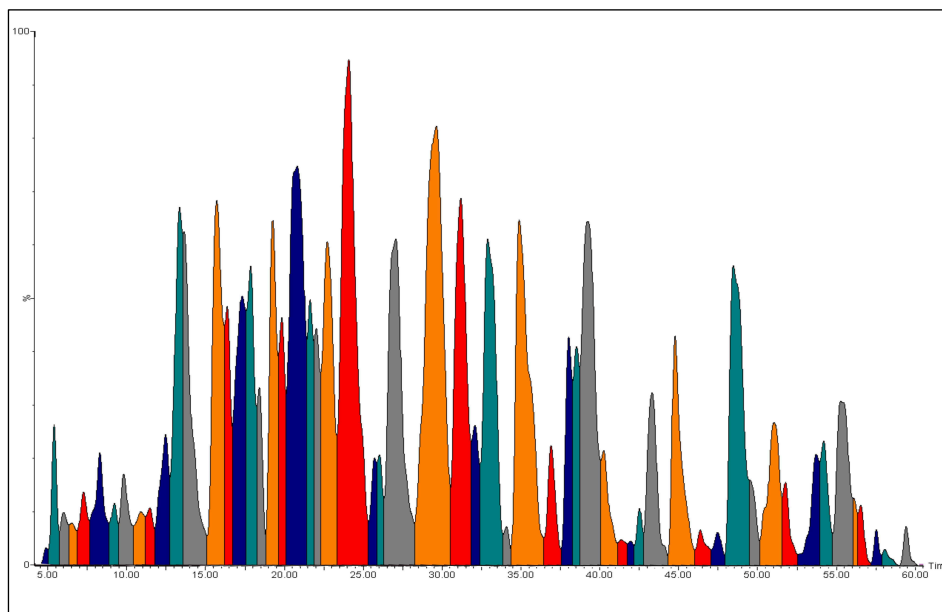


**Figure 54** 55 minute detail of an 80 minute UPLC-MS TIC chromatogram (scan mode). The main peptide peaks of the tryptic digested non gushing malt extract are shown in colour and equal the most abundant peptide precursor ion masses. 59 minutes of the LC run were split into equal well plate volumes (time window: 20 seconds) resulting in 180 fractions per sample. The first 5 and last 16 minutes of the LC run did not feature any rising peptide peaks and were not collected.

A broad range of malt extract samples was analysed for this study. Three examples and their results will be highlighted in greater detail. A brief summary of the test conditions and pertinent sample information is shown in Table 20.

A direct comparison of the gushing negative Durst malt and the gushing positive Ireks malt revealed a strong visual correlation of their UPLC-MS chromatograms with identical peptide peak shapes and numbers (Figure 55). The ion count rates also corresponded.

The limited time during the elution enabled the detection of a peptide precursor ion but rendered a direct, online DDA identification difficult (but not impossible), mainly because of inadequate peak width, low confidence and instrumental MS limitations. Therefore the peptides were usually targeted in the offline analyses of the previous collected fractions.



## RESULTS AND DISCUSSION

**Table 20 UPLC-MS conditions and general information about protein contents of analysed gushing and non-gushing malt extracts.**

Additional information	Cargill malt	100 % Durst malt	100 % Ireks malt
Gushing behaviour	non gushing	non gushing	gushing
LC run [mins]	60 and 80	80	80
No. of collected wells	180	380	380
No. of fractions reinjected	80	95	95
Duration of DDA experiments	20	30	30
No. of DDA channels	8	5	5
No. of analysed precursor ions	24 per DDA	15 per DDA	15 per DDA
Theoretical no. of possible precursor ion analyses	1920	1425	1425
Weight of the protein pellet [g/0.5 g lyophilisate]	0.0130	0.0132	0.0135
Protein content [%] ([w/w] lyophilisate)	2.6	2.64	2.7
2D-Quant protein amounts [g]	0.0088	0.0084	0.00875
2D-Quant protein contents [%] ([w/w] pellet and [w/w] lyophilisate)	67.69 1.76	63.64 1.68	64.81 1.75
No. of identified proteins (barley + ancient origin)	<b>62 + 7</b>	<b>43 + 15</b>	<b>38 + 8</b>

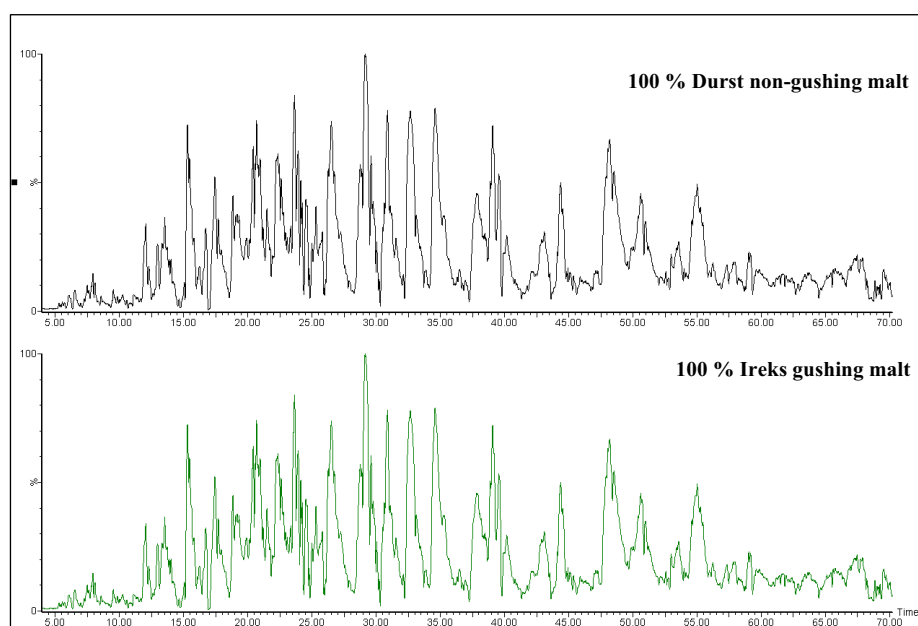


**Figure 55 UPLC-MS BPI chromatograms (5 – 70 mins) of a gushing Ireks malt and a non gushing Durst malt.** Owing to the application of a lockmass the surveys of the peptide peak signals were regularly interrupted and failed to provide the typical flat survey shape. A chromatogram overlay revealed identical signal patterns, with a small deviation in retention time.

The complexity of each peptide fraction could be reduced by this approach in a manner obviating additional chromatography runs by virtue of unlimited averaging capability and unlimited time for nanoESI tests. The additional time could be used for further optimization of analytical parameters as well as the determination of low abundant peptide ions. Figure 56 summarizes the entire analytical method of this new UPLC-MS approach

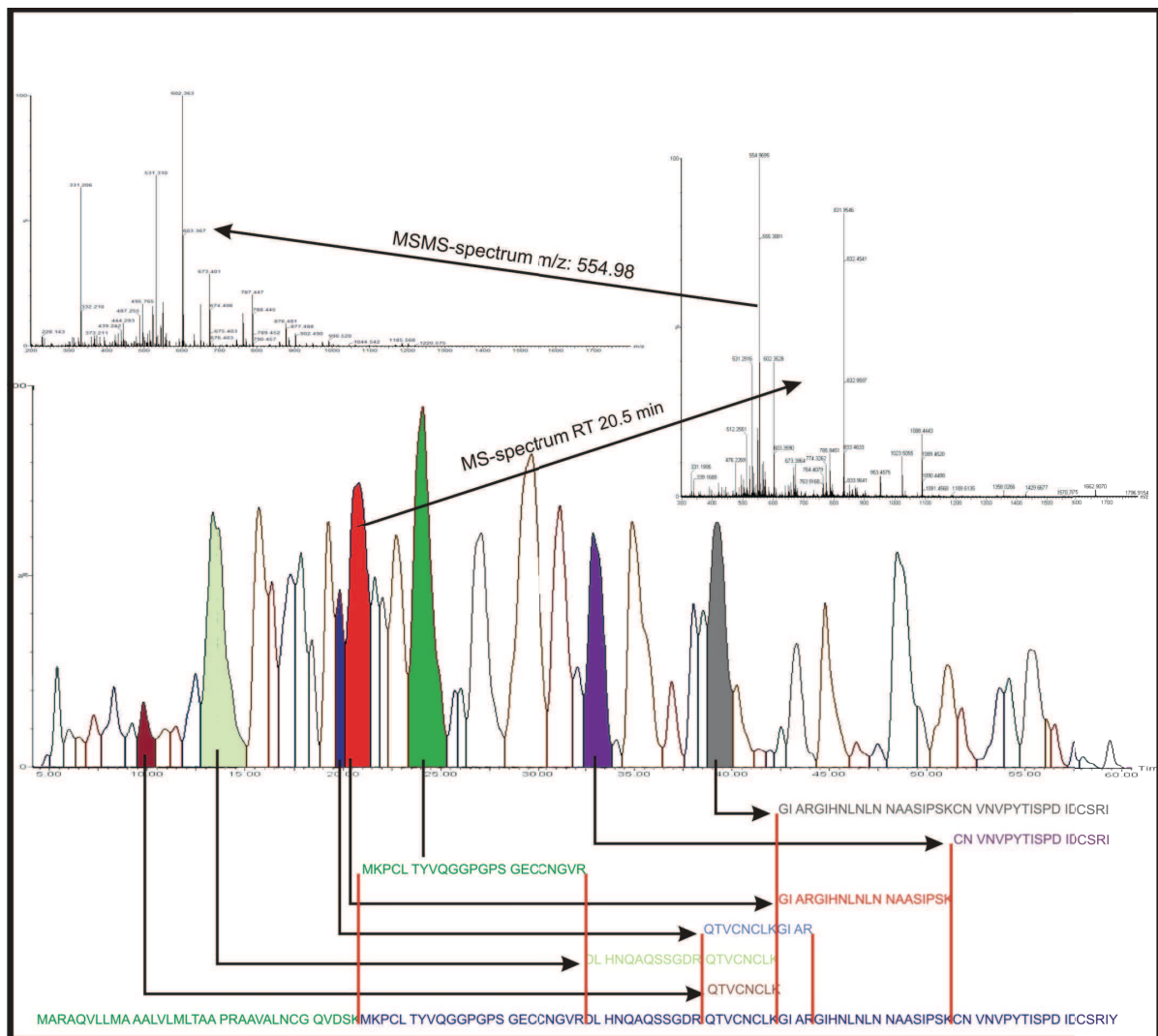


**Figure 56** The analytical path from a TIC chromatogram of a non gushing Cargill malt sample to protein identification using the example of nLTP1 (Swissprot: P07597). The DDA-MS spectrum of a reanalysed fraction (RT = 20.5 mins) is enlarged and the MSMS spectrum of its most abundant nLTP1 precursor ion ( $m/z = 554.98$  Da) shown. All detected peptides associated with nLTP1, as well as their partial amino acid sequences, are highlighted underneath the chromatogram. Once the signal peptide (AA 1 – 26) had been subtracted, the nLTP1 sequence coverage was defined as 73.63 %.

To perform a detailed characterization of the highly complex mixtures of tryptic digested peptides and their attendant protein profiles in malt extracts, method development was aimed at achieving the maximum chromatographic resolution. Prolonged LC run times or the use of longer chromatographic columns failed to further improve the chromatography with the material used here. As only fractions of the most abundant peptide peaks were reinjected and analysed, these fractions failed to cover the whole LC run, or the entire potential number of peptides. In the case of the Cargill malt ca. 44 % of the entire LC run were investigated, while this figure fell to only 25 % for the LC runs of Ireks and Durst malt. Manual analysis of other, less abundant peptide fractions indicated their additional, high analytical potential. Future

gushing research would be well advised to also analyse these fractions in detail, in order to deliver a more exact and complete malt protein pattern.

A second mandatory step of the method development was a database search designed to benefit from the enhanced detection levels of the latest advancements in the presented analytical techniques. The search algorithm and the quality of the database were of critical importance for the accuracy of the protein identifications. As complete genome annotations for plant species are few and far between, databases are usually incomplete, which turned out to be true for barley, as well. Identification was hence not always successful, even where good spectra had been obtained. This fact along with the small overall number of proteins identified in malt indicated database (Swissprot) related problems and sequence limitations. Similar difficulties were known from other barley research groups, too. A new, promising database search approach involves the EST database HarvEST and was introduced by the IPK Gatersleben research group [85]. This approach could not be tested in this study, but could potentially upgrade protein identifications in future malt research.

The research focus of the thesis lay in the aforementioned number of peptide fractions and further development of the method. The proteins identified for malt extracts are summarized in Table 21 for comparison. 27 proteins were commonly found in all malt samples, while 25 were only observable with the Cargill malt, which may be exlicable by the much more detailed analysis of this sample type. IAAC and the grain softness protein were only identified in the two non gushing malts. Eight proteins were found in the Ireks and Durst malts, but not the Cargill malt. 5 other proteins did not exist in the Durst malt. Three species were only found in the gushing malt, while the embryo globulin was only observable in the non gushing Durst malt.

All in all 71 different barley protein hits were detected in the three different malt extracts. This also includes 5 hits of two rowed *Hordeum vulgare*, variance *Distichum*.

The kinship was accepted for a positive annotation of these proteins. As the common Swissprot database, modified wheat- and hop-specific databases as well as a barley specific rodent database were also used for the PLGS research algorithm, a small number of proteins from other origins were identified in the malt extracts (Table 22), as well.

Wheat derived hits were the most commonly found previous results. Owing to the phylogenetic relationship, both *Triticum aestivum* (wheat) and *Oryza sativa* (subspecies *japonica* = rice) identifications were accepted in database annotation.

## RESULTS AND DISCUSSION

**Table 21 Summary of identified barley (HORVU) proteins in bottom up experiments with malt extracts.**

Full protein name HORVU = Hordeum vulgare	Protein ID Swissp./NCBI	MM unprocessed [Da]	MM mature form [Da]	pI after PTM	Cargill non gushing	Ireks gushing	Durst non-gushing
SPZ4: Protein Z4	P06293	43276.38	43276.38	5.72	x	x	x
BSZ7: Serpin-Z7	Q43492	42821	42689.61	5.45	x		x
BSZx: Protein Zx	Q40066	42947.14	42947.14	6.77		x	
IAAB: $\alpha$ -amylase/trypsin inhibitor CMb	P32936	16526	14192.28	5.78	x	x	x
THNA: $\alpha$ -hordothionin [Acidic protein]	P01545	13597	6820.6	3.82	x		
LE19A: Late embryogenesis abun. protein	Q05190	9961.75	9961.75	6.33	x	x	x
LE19B: Late embryogenesis abun. protein	P46532	9972.73	9972.73	5.49		x	x
LE193: Late embryogenesis abun. protein	Q02400	14604.89	14604.89	5.38		x	x
LE194: Late embryogenesis abun. protein	Q05191	16896.41	16896.41	5.58		x	x
IAAA: $\alpha$ -amylase/trypsin inhibitor Cma	P28041	15500	13112.86	5.51	x	x	x
ICIC: Subtilisin-chymotrypsin inhi. CI-1C	P01054	8258.13	8258.13	6.79	x	x	x
ICIA: Subtilisin-chymotrypsin inhi. CI-1A	P16062	8882.24	8882.24	5.24	x	x	x
ICIB: Subtilisin-chymotrypsin inhi. CI-1B	P16063	8963.4	8963.4	5.33	x		
THHR: Antifungal protein R [Fragment]	P33044	4453.12	4453.12	9.5	x		
IAAE: Trypsin inhibitor Cme	P01086	16136	13626.56	6.95	x	x	x
BARW: Barwin	P28814	13737.22	13737.22	7.76	x	x	x
THN5: Leaf-spec. thionin [Acidic protein]	P09617	14662	6838.62	4.14	x		
THN7: Thionin BTH7 [Acidic protein]	Q42838	14676	6866.68	4.14	x		
THNX: Prob. leaf thionin [Acidic protein]	Q8H0Q5	14615	6824.6	4.11	x		
NLTP1: Nonspecific lipidtransfer protein1	P07597	12301	9694.96	8.19	x	x	x
Q5UNP2: Non-specific LTP <sup>2</sup>	Q5UNP2	12362.42	12362.42	9.22	x	x	x
Q9SES6: Non-specific lipid-transfer prot.	Q9SES6	12340.45	12340.45	8.9	x	x	x
IAAC: Trypsin inhibitor Cmc	P34951	15179	12848.94	6.45	x		x
UBIQ: Ubiquitin	P69314	8524.78	8524.78	6.56	x		
IAA1: $\alpha$ -amylase inhibitor BMAI-1	P16968	15816	14442.58	6.16	x	x	x
HOG3: Gamma-hordein-3	P80198	33188.8	33188.8	6.7	x	x	x
REHY: 1-Cys peroxiredoxin PE	P52572	23963.49	23963.49	6.31	x	x	x
PR12: Pathogenesis-related protein PRB1-2	P35792	17679	15225.81	8.95	x	x	x
PR13: Pathogenesis-related protein PRB1-3	P35793	17697	15199.77	8.77	x	x	x
PR1: Pathogenesis-related protein 1	Q05968	17683	15229.79	8.77	x	x	
LEA1: ABA-inducible protein PHV A1	P14928	21819.79	21819.79	9.02	x	x	
NLTP2: Probable non-specific LTP	P20145	10357	6987.99	6.98	x	x	x
HOR3: B3-hordein [fragment]	P06471	30195.42	30195.42	7.74	x		
IAAS: $\alpha$ -amylase/subtilisin inhibitor	P07596	22164	19879.3	6.58	x		
IAAD: $\alpha$ -amylase/trypsin inhibitor Cmd	P11643	18526	16102.59	5.24	x		x
IAA2: $\alpha$ -amylase inhibitor BDAI-1	P13691	16429	13101.11	5.06	x	x	x
Q02056: D-hordein (fragment)	Q02056	45994.05	45994.05	8.32		x	
Q84LE9: D-hordein	Q84LE9	80409.65	80409.65	8.01	x	x	x
Q40054: D-hordein	Q40054	75108	72113.4	7.74	x	x	x
Q40045: D-hordein	Q40045	50785.65	50785.65	7.6	x	x	x
Q1ENF0: Cystatin Hv-CPI8	Q1ENF0	12861.57	12861.57	9.8	x	x	x
Q1ENF3: Hv-CPI5	Q1ENF3	15958.03	15958.03	8.45	x		
Trypsin/amylase inhibitor pUP13	gi: 225102	14746.83	14746.83	5.35	x	x	x
P93180: Pathogenesis related protein 4	P93180	15694	13647.23	8.27	x	x	x
IAA: $\alpha$ -amylase/trypsin inhibitor	P16969	15965	13740.87	7.73		x	x
HINB1: Hordoindoline-B1	Q9FSI9	16110	14115.12	8.55		x	
CYSP1: Cysteine proteinase EPB 1	P25249	40358	25180.96	4.77		x	x
CYSP2: Cysteine proteinase EP-B 2	P25250	40511	25318.16	4.96		x	x
Q2V8X0: Limit dextrinase inhibitor	Q2V8X0	16006.53	16006.53	7.56		x	x
B5TWD1: Late embryogenesis abun prot.	B5TWD1	21748.71	21748.71	9.02	x	x	
B5TWD0: Late embryogenesis abun prot.	B5TWD0	21819.79	21819.79	9.02	x	x	
B5TWC8: Late embryogenesis abun prot.	B5TWC8	20722.55	20722.55	8.55	x		
B5TWC9: Late embryogenesis abun prot.	B5TWC9	21937.88	21937.88	8.83	x	x	
Q40036: Putative protease inhibitor	Q40036	9405	9405	8.37		x	x
Q40035: Type-1 pathogenesis-related prot.	Q40035	18871.26	18871.26	8.58	x		
O23997: pathogenesis related prot. PR5	O23997	25172	22797.69	6.74	x		
Q946Z0: Thaumatin-like protein TLP6	Q946Z0	23725.95	23725.95	7.33	x		
Q946Y9: Thaumatin-like protein TLP7	Q946Y9	23643.79	23643.79	7.36	x		
Q946Y8: Thaumatin-like protein TLP8	Q946Y8	24316.57	24316.57	7.38	x		
THHS: Antifungal protein S	P33045	3873.82	3873.82	8.22	x		
Glucose/ribitol dehydrogenase homolog	T06212	31646.94	31646.94	6.54	x		
CHS2: Chalcone synthase 2	Q96562	43188.91	43188.91	6.24	x		
Barperm1	O22462	21656.41	21656.41	8.15	x		
putative synaptobrevin VAMP	Q5URW2	24312.14	24312.14	8.7	x		
Grain softness protein (23 homology hits)	A9E4H2	14106.05	14106.05	4.59	x		x
THNB: $\beta$ -hordothionin	P21742	14603	4926.88	9.75	x		
Embryo globulin	Q03678	72252.62	72252.62	6.8			x
Seed storage protein Fragment	Q9SAT9	3369.09	3369.09	9.49	x		
Peroxidase fragment PE 2 SV 1	Q42852	19741.31	19741.31	6.7	x		
CMd3 protein	Q24000	18471	15976.52	6.98	x	x	x
G3PC: Glyceraldehyde 3 phos. dehydro.	P08477	33235.79	33235.79	6.2	x		

## RESULTS AND DISCUSSION

**Table 22 Ancient protein species identified in bottom up experiments with malt extracts.**

Full protein name ID's	Protein ID Swissprot/NCBI	MM unprocessed [Da]	MM mature form [Da]	pI after PTM	Cargill non-gushing	Ireks gushing	Durst non-gushing
GLT3_WHEAT Glutenin, high molecular mass subunit 12	P08488	70876	68713.5	6.97	x	x	x
GLT0_WHEAT Glutenin, high molecular mass subunit DY10	P10387	69629	67475.03	6.97	x	x	x
GRXC6_ORYSJ Glutaredoxin-C6	P55142	11774.5	11774.5	5.77	x	x	
GRDH_ORYSJ Glucose and ribitol dehydrogenase homolog	Q75KH3	32267.54	32267.54	5.76	x	x	
Q41540_WHEAT CM 17 protein	Q41540	15989	13431.42	4.87		x	
Q43663_WHEAT Wali3 protein	Q43663	9496.19	9496.16	8.75		x	
IAC16_WHEAT $\alpha$ -amylase/trypsin inhibitor CM16	P16159	15782	13437.43	5.02			x
GLT2_WHEAT Glutenin, high molecular mass subunit PC237	P02862	4060.7	4060.7	8.21	x	x	x
GLT1_WHEAT Glutenin, high molecular mass subunit PC256	P02861	10895.89	10895.89	8.18		x	x
GLT4_WHEAT Glutenin, high molecular mass subunit PW212	P08489	89173	87007.62	5.39		x	x
GLT5_WHEAT Glutenin, high molecular mass subunit DX5	P10388	89316	87149.89	5.73		x	x
Q4W1F9_WHEAT 5a2 protein	Q4W1F9	10439.19	10439.19	8.38	x	x	x

In the databank search a certain number of protein hits based on the correlation of multiple peptides to the protein sequence (Table 23, Table 24 and Appendices B1 – B4). These matches were considered to be valid and the protein sequence coverages were estimated and also stated. The databank annotations also retrieved a number of single peptide matches, which were manually examined according to their score and probability, the quality of the MSMS spectra and a continuous stretch of the protein sequence (either y- or b-ion series). With some peptide sequences this strategy failed to facilitate an exclusion of close protein sequence homologies and multiple protein hits. These ambiguities emerged with the serpins BSZ7 and SPZx, the plant thionin family (proteins THN5, THN7 and THNX), the late embryogenesis abundant protein family with B5TWD1 or B5TWD0, the pathogenesis related protein family with O23997 (PR5) and the grain softness protein, as well as the thaumatin like proteins TLP6 and TLP7.

Despite additional *de novo* sequencing, not all the mass data of the reinjected fractions allowed for protein identification. This is another fact suggesting that complete sequence data for these proteins were unavailable in the database.

Most of the proteins identified in malt extracts were water soluble with the exception of the D-hordein species (Q02056, HOG3, HOR3, Q84LE9, Q40045, Q40054), the embryo globulin, the seed storage fragment (Q9SAT9), and the subunits of wheat glutenin with a high molecular mass (GLT0 – GLT5).

## RESULTS AND DISCUSSION

**Table 23 Barley peptide masses and sequences identified in a non gushing Cargill malt.**

Full protein name	Detected sequence	AA	Ion charge positive	[M+H] <sup>+</sup> average peptide	No. of AA mature	Sequence coverage [%] mature protein
SPZ4_HORVU	L-KVLKLPYAK	229-236	2	932.19	399	23.5
	K-QILPPGSVDNNTK	161-173	2	1369.64		
	K-QYISSDNLK	219-228	2	1155.24		
	K-GAWDQKFDESNTK	184-196	3	1525.83		
	K-R <sup>2</sup> LSTEPEFIENHIPK	262-276	3	1811.04		
	K-R <sup>2</sup> LSTEPEFIENHIPKQTVVEVGR	262-282	4	2580.98		
	K-FKISYQFEASSLLR	289-302	3	1689.95		
	K-ISYQFEASSLLR	291-302	2	1414.6		
	R-LA <sup>2</sup> SAISSNPER	22-36	2	1145.45		
	BSZ7_HORVU	R-LVLGNALYFK	175-184	2		
K-TFVEVDEEGTK		336-346	2	1254.33		
IAAB_HORVU	R-KSRPDQSGLM <sup>1</sup> ELPGCPR	92-107	3	1759.99	125	60.8
	R-DYVEQQACR	46-54	2	1112.20		
	R-EVQM <sup>1</sup> DFVR	106-115	2	1040.17		
	R-IETPGPPYLAK	55-65	2	1186.39		
	K-QQCCGELANIPQQCR	66-80	2	1691.93		
	R-KSRPDQSGLMELPGCPR	91-107	3	1872.16		
	R-IETPGPPYLAKQQCCGELANIPQQCR	55-80	3	2859.30		
	R-EVQMDFVR	108-115	2	1024.17		
	R-C <sup>3</sup> QALRFFMGR	81-90	2	1300.58		
	K-SRPDQSGLMELPGCPR	92-107	3	1743.99		
	R-FFM <sup>1</sup> GRK	86-91	2	785.98		
	THNA_HORVU	K-YCNLGCGR	78-84	2		
LE19A_HORVU	K-SLEAQQNLAEGR	30-41	2	1316.41	93	12.9
IAAA_HORVU	R-CCQELDEAPQHCR	74-86	3	1532.70	120	36.67
	K-DLPGCPKEPQR	107-117	2	1240.41		
	R-RSHPDWSVLK	97-106	3	1225.39		
	R-SHPDWSVLK	98-106	2	1069.20		
	K-DLPGCPKEPQRDFAK	107-121	3/4	1701.93		
	R-SHPDWSVLKDLPGCPKEPQR	98-117	4	2290.60		
	R-YFIGR	92-96	2	655.77		
	R-SHPDWSVLKDLPGCPK	98-113	3	1779.88		
ICIC_HORVU	A-KTSWPEVVGM <sup>1</sup> SAE	16-27	2	1421.60	77	24.7
	K-AKEIILR	29-35	2	843.05		
ICIA_HORVU	A-KTSWPEVVGM <sup>1</sup> SAE	26-38	2	1421.60	83	30.86
	K-AKEIILR	39-45	2	843.05		
	K-YPEPTESIGASSAK	11-25	2	1493.63		
	K-RSWPEVVGM <sup>1</sup> SAEK	26-38	2	1492.68		
ICIB_HORVU	K-AKEIILR	39-45	2	843.05	83	37.35
	R-DKPDQAQIEVIPVDAMVPLDFNPNR	46-69	3	2695.60		
THHR_HORVU	ATITVVNR	1-8	2	874.02	44	18.2
IAAE_HORVU	R-TYVVSQICHQGPR	45-57	2/3	1488.70	124	15.3
	R-LLTSDMK	58-64	2	807.98		
BARW_HORVU	R-VTNPATGAQITAR	69-81	2	1300.45	125	69.6
	R-SK <sup>2</sup> YGWTAFCGPAGPR	44-58	2/3	1598.81		
	K-YGWTAFCGPAGPR	46-58	2	1383.56		
	R-ATYHYRPAQN <sup>1</sup> WDLGAPAVSAYCATWDASKPLSWR	8-43	4	4132.56		
	K-CLRVTNPATGAQITAR	66-81	3	1672.94		
	R-IVDQCANGGLDLDWDVTFK	82-101	3	2211.45		
THN5_HORVU	K-IISGPTCPR	62-70	2	944.13	63	20.6
	K-IISGPTCPRDYPK	62-74	3	1447.69		
THN7_HORVU	K-IISGPTCPR	62-70	2	944.13	63	20.6
	K-IISGPTCPRDYPK	62-74	3	1447.7		
THNX_HORVU	K-IISGPTCPR	62-70	2	944.13	63	20.6
	K-IISGPTCPRDYPK	62-74	3	1447.69		
NLTP1_HORVU	R-DLHNQAQSSGDRQTV <sup>1</sup> CNCLK	59-78	3/4	2218.42	91	73.63
	R-GIHNLN <sup>1</sup> NNAASIPSK	83-98	2/3	1663.87		
	K-M <sup>1</sup> KPCLTYVQGGPGPSGECCNGVR	36-58	3	2370.73		
	D-RQTV <sup>1</sup> CNCLKGIAR <sup>2</sup>	71-82	3	1306.58		
	K-MKPC <sup>1</sup> LTYVQGGPGPSGECCNGVR	36-58	2/3	2354.73		
	R-GIHNLN <sup>1</sup> NNAASIPSKCNVNPY <sup>1</sup> TISPDIDCSR	83-115	4	3541.97		
	K-CNVNVPY <sup>1</sup> TISPDIDCSR	99-115	2	1897.12		
	R-DLHNQAQSSGDRQTV <sup>1</sup> CNCLKGIAR	59-82	4	2615.90		
	K-CNVNVPY <sup>1</sup> TISPDIDCSR <sup>1</sup>	99-116	2	2010.93		
Q5UNP2_HORVD	R-SLNA <sup>1</sup> AATPADR	66-77	2	1158.25	124	19.35
	K-CGVNIPY <sup>1</sup> AISPR	106-117	2	1290.52		
Q9SES6_HORVU	K-ISPSVDCNSIH	111-121	2	1172.29	121	20.7
	K-NVANAAPGGSEITR	82-95	2	1357.46		
IAAC_HORVU	R-ELAGISSNCR	71-80	2	1049.5	119	26.9
	R-TLALPGQC <sup>1</sup> NLPAIHGGAYCVFP	122-143	3	2242.11		
UBIQ_HORVU	R-TLADYNIQK	55-63	2	1066.19	76	11.84
IAA1_HORVU	K-SQCAGGQV <sup>1</sup> VEIQK	40-53	2/3	1434.6	132	33.33
	R-ALVK <sup>2</sup> QCAGGQV <sup>1</sup> VEIQK	36-43	3	1846.15		
	K-ELGVALADDK	82-91	2	1031.15		
	K-ATVAEVFP <sup>1</sup> GCR	92-102	2	1150.33		
	R-GSMYKELGVALADDK	77-91	2/3	1597.82		
	R-GSMYKELGVALADDKATVAEVFP <sup>1</sup> GCR	77-102	3/4	2729.13		
	K-ELGVALADDKATVAEVFP <sup>1</sup> GCR	82-102	3	2162.08		
HOG3_HORVU	R-QQCCQLANINEQSR	181-195	2	1763.94	289	5.2

## RESULTS AND DISCUSSION

Full protein name	Detected sequence	AA	Ion charge positive	[M+H] <sup>+</sup> average peptide	No. of AA mature	Sequence coverage [%] mature protein
REHY_HORVU	R-TLHIVGPKVVK <sup>2</sup> K-VTYPIPADPDR	127-139 94-104	3 2	1306.59 1278.46	218	10.6
PR12_HORVU	K-LQAF AQNYANQR K-VCGHYTQVVWR	53-64 118-128	2 3	1424.55 1348.56	140	16.4
PR13_HORVU	K-LQAF AQNYANQR K-VCGHYTQVVWR K-ASDAVNSWVSEK K-ASDAVNSWVSEKK	53-64 118-128 92-103 92-104	2/3 3 2 3	1424.55 1348.56 1293.37 1420.89	140	25.71
PR1_HORVU	K-LQAF AQNYANQR K-VCGHYTQVVWR K-ASDAVNSWVSEK K-ASDAVNSWVSEKK	53-64 118-128 92-103 92-104	2 3 2 3	1424.55 1348.56 1293.37 1420.89	140	25.71
LEA1_HORVU	K-DAVANTLGM <sup>1</sup> GGDNTSATKDATTGATVK K-DAVANTLGMGGDNTSATK	178-204 178-195	3 2	2584.77 1723.85	312	8.7
NLTP2_HORVU	R-AQQGCLCQYVK R-AQQGCLCQYVKDPNYGHYVSSPHAR R-DTLNLCCGIPVPHC	65-75 65-89 90-102	2 4 2	1241.46 2823.13 1382.63	67	56.7
HOR3_HORVU	R-TLPTMCSVNPLYR	239-252	2	1594.92	264	5.3
IAAS_HORVU	R-ITPYGVAPSDK R-ADANYYVLSANR	84-94 38-49	2 2	1148.30 1357.46	181	12.7
IAAD_HORVU	R-LLVAPGQCNLATIHNVNR K-LYCCQELAEIPQQCR R-YFMALPVPSQPVPDPSTGNVQSGMLDLPGCPR R-YFM <sup>1</sup> ALPVPSQPVPDPSTGNVQSGML <sup>1</sup> DLPGCPR	144-160 84-98 104-135 104-135	2/3 2/3 3 3	1820.16 1798.09 3332.5 3348.83	147	43.6
IAA2_HORVU	K-LECVGNRVPEDVLR R-ALVK <sup>2</sup> LECVGNRVPEDVLR R-CGDLGSMRLR R-SVYAALGVGGGPEEVFPGCQKDV MK R-VPEDVLR R-DCCQEVANISNEWCR R-SVYAALGVGGGPEEVFPGCQK L-LVAGVPALCNVIPNEAAGTR	57-70 53-69 86-94 95-119 64-70 71-85 95-115 120-141	3 3 2 3 2 2/3 2 3	1599.84 2011.39 952.13 2539.92 827.95 1770.94 2065 2176.58	122	46.72
Q84LE9_HORVU	R-DVSPECRPVALSQVVVR R-ELQESSLEACRR R-ELQESSLEACR K-AQQLAAQLPAMCR	81-96 44-55 44-54 734-736	3 3 2 2	1756.02 1421.56 1265.38 1401.68	757	5.42
Q40054_HORVU	R-DVSPECRPVALSQVVVR R-ELQESSLEACRR R-ELQESSLEACR K-AQQLAAQLPAMCR	81-96 44-55 44-54 684-696	3 3 2 2	1756.02 1421.56 1265.38 1401.68	679	6.04
Q40045_HORVU	R-DVSPECRPVALSQVVVR R-ELQESSLEACRR R-ELQESSLEACR	81-96 44-55 44-54	3 3 2	1756.02 1421.56 1265.38	454	6.2
Q1ENF0_HORVU	R-LFVDAADGSGR R-GEQVVSVMNYR	85-95 73-84	2 2	1108.19 1368.50	122	18.9
Q1ENF3_HORVU	K-VGGWTEVR	43-50	2	904.01	151	5.3
trypsin/α-amylase inhibi. pUP13	K-SIPINLPACR R-DYGEYCRV GK R-ELSDLPESCR R-CAVGDQVVPDVLK R-CDALSILVNGVITEDGSR	26-36 16-25 61-70 43-55 71-88	2 3 2 2 3	1181.40 1990.31 1149.21 1372.57 1863.09	136	42.6
B5TWD1_HORVD	K-DAVANTLGM <sup>1</sup> GGDNTSATK K-DAVANTLGM <sup>1</sup> GGDNTSATKDATTGATVK	178-195 178-204	2 3	1723.85 2568.77	212	12.7
B5TWD0_HORVD	K-DAVANTLGM <sup>1</sup> GGDNTSATK K-DAVANTLGM <sup>1</sup> GGDNTSATKDATTGATVK	178-195 178-204	2 3	1723.85 2568.77	213	12.7
B5TWC8_HORVD	K-DAVANTLGM <sup>1</sup> GGDNTSATK	167-184	2	1723.85	202	8.9
B5TWC9_HORVD	K-DAVANTLGM <sup>1</sup> GGDNTSATK	178-195	2	1723.85	214	8.4
Q40035_HORVU	K-VCGHYTQVVWR	118-128	3	1348.56	174	6.3
P93180_HORVU	R-ATYHYRPAQNNWDLGAPAVSAYCATWDASKPLSWR R-SKYGWTAFCGPAGPLGQAACGK	29-64 65-86	4 3	4132.56 2171.2	146	26.0
O23997_HORVU	R-LDPGQSWALNMPAGTAGAR	49-67	2	1914.14	213	8.9
Q946Z0_HORVU	R-LDPGQSWALNMPAGTAGAR	49-67	2	1914.14	226	8.4
Q946Y9_HORVU	R-LDPGQSWALNMPAGTAGAR	49-67	2	1914.14	227	8.4
Q946Y8_HORVU	K-VITPACPNELR	154-164	2	1213.43	233	8.2
THHS_HORVU	ATFTVINK	1-8	2	894.05	37	21.6
glucose/ribose dehydrogenase	K-VALVTGGDSGIGR	42-54	2	1202.35	293	4.4
CHS2_HORVU	R-KSSAK	353-357	1	520.6	399	1.3
O22462_HORVU	R-LDPGQSWALNMPAGTAGAR	27-45	2	1914.14	205	9.3
Q5URW2_HORVD	R-EVPLAFLEK	71-80	2	1315.59	215	4.7
A9E4H2_HORVU	K-LNSCSDYVM <sup>1</sup> DR R-SCEEVQDQCQQLR K-LNSCSDYVMDR	59-69 89-102 59-69	2 2 2	1319.44 1669.83 1303.44	127	19.7
THNB_HORVU	R-NCYNLCR	38-44	2	886.03	45	15.6
Q9SAT9_HORVU	R-TLPTMCSVNPLYR	6-19	2	1593.67	31	45.2
Q42852_HORVU	R-TPNVFDNKYYIDL VNR	77-92	3	1972.18	180	8.9
CMd3_HORVU	R-YFM <sup>1</sup> ALPVPSQPVPDPSTGNVQSGML <sup>1</sup> DLPGCPR	104-135	3	3364.83	146	21.91
G3PC_HORVU	R-AASFNIIPSSGAAK	171-185	2	1434.82	305	4.9

<sup>1</sup> methionine oxidized to methionine sulfoxide, <sup>2</sup> sequence conflict, <sup>3</sup> Cys\_PAM acrylamide adducts, <sup>4</sup> Cys\_CAM carbamidomethyl-cysteine  
HORVD = *Hordeum vulgare* var. *Distichum*

## RESULTS AND DISCUSSION

**Table 24 Peptide masses and sequences of other origin identified in a non-gushing Cargill malt.**

Full protein name	Detected sequence	Position	Ion charge	[M+H] <sup>+</sup> average	No. of AA	Sequence coverage [%]
GLT3_WHEAT Glutenin, high molecular mass subunit 12	R-ELQESSLEACR	34-44	2	1265.38	639	1.7
GLT0_WHEAT Glutenin, high molecular mass subunit DY10	R-ELQESSLEACR	34-44	2	1265.38	627	1.8
GRXC6_ORYSJ Glutaredoxin-C6	R-TVPNVFINGK	66-75	2	1089.27	112	8.9
GRDH_ORYSJ Glucose and ribitol dehydrogenase homolog	K-VAIVTGGDSGIGR	42-54	2	1202.35	300	4.3
GLT2_WHEAT Glutenin, high molecular mass subunit PC237	K-AQQLAAQLPAMCR	16-28	2	1400.71	39	33.3
Q4W1F9_WHEAT 5a2 protein	K-ANIPCLCAGVTK	46-57	2	1189.6	94	12.8

According to the classification of water-soluble proteins postulated by Østergaard, the most prominent group to be found was the defense protein plus inhibitor class. Fifty-three proteins could be clearly attributed to this class, including the protease inhibitor protein family (IAAE, IAAA, IAAB, IAAD, IAA1, IAAC, IAA2, IAA, pUP 13, IAC16\_WHEAT, ICIC, ICIA, ICIB, IAAS, the cystatins Hv-CPI8, Hv-CPI5, CYSP1 and CYSP2, thiol proteases Q1ENF0, Q1ENF3 and the 5a2 wheat protein), the serine type endopeptidase inhibitor family (HINB1, putative protease inhibitor, CMd3, limit dextrinase inhibitor, CM17 and Wali3 protein), the thaumatin, CRISP and pathogenesis related protein families (THHR, THHS, PR12, PR13, PR1, PR5, PR4, BARW, TLP6, TLP7, TLP8, Barperm1 and type1 PR), the serpin family (PRZ4, BSZ7 and BSZx), the plant thionin family (THNA, THN5, THN7, THNX and THNB), the plant LTP family (NLTP1, NLTP2, Q5UNP2, Q9SES6), and CHS2.

REHY and the peroxidase fragment PE2 SV1 were identified as proteins related to oxidative stress. The late embryogenesis abundant protein family (LEA1, B5TWD1, B5TWD0, B5TWC9 and B5TWC8), the small hydrophilic plant seed family (LE19A, LE19B, LE193 and LE194), as well as the glucose/ribitol dehydrogenase homologue and GRXC6 were classified as desiccation stress related proteins. The remaining five proteins (UBIQ, VAMP, grain softness protein, G3PC) were found to serve other function.

The two barley serpins BSZ7 and SPZ4 were commonly found members of the serine protease inhibitor family provided in all malt samples. The same results had also been found by the Perrocheau research group [55]. The presence of both proteins could be explained by their expression from two small, highly related gene families. A third BSZx serpin was only found in the gushing Ireks malt included in this study. As explained above, the protein hit might derive from a false positive identification owed to peptide sequence homologies in the database. The only peptide fragment found for BSZx also matched BSZ7, but one needs to remember that the results for haze had also included a positive hit for BSZx. It was therefore



impossible to entirely exclude the possibility that the hit concerns the serpin Zx subfamily, which is closely related to the protein Z4 subfamily (sequence homology of ca. 70 %).

The second most prominent malt protein class included four different lipid transfer proteins, which were detected in all malt samples. The literature contains a great number of different nLTP data, that normally refer to the PTM of barley protein during malting and brewing, but the information available on the different nLTP species in malt samples is scant. nLTP1 and nLTP2 were also detected by Perrocheau [55]. nLTP1 featured the highest protein sequence coverage (84.6 % in the case of Durst malt) of all the protein species detected in the entire study. Both the other nLTPs (Q5UNP2 and Q9SES6) found in this study had never been mentioned before. Taking into account the additionally available information about nLTP and the serpin protein class, citations often refer to different protein isoforms and glycosylated species (varying molecular masses after PTM) found in 2D gelelectrophoretic separation [55, 56]. In this regard the developed bottom up approach is limited, as different protein isoforms and native protein species with varying pI or molecular masses could not be distinguished after the preliminary digestion of the sample's basic protein content. These limitations provided one of the reasons for continued method development and the combination of bottom up and top down approaches in a single experiment.

A direct comparison of the findings of the LC-MS proteomic malt study discussed here and the 2D gel results of Perrocheau *et al.* revealed that they had sixteen barley derived proteins in common. Again the inhibitor protein class was represented most frequently (IAAE, IAAA, IAAB, IAAD, IAA1, IAA2, pUP13 and CMd3), but the aforementioned nLTP1 and 2, as well as Barwin, BSZ7, the D-hordein fragment, HOG3 and HOR3 also figured prominently. A cold regulated protein 1 fragment and BTI-CMe2.1 protein could not be confirmed by the results of this study. The two 12 S seed storage proteins identified in the *Arabidopsis thaliana* organism by the 2D gel approach could also be successfully identified in the barley organism here (here barley and not arabidopsis origin). A total number of 20 proteins (in both barley and other organism) had been identified via the 2D gel approach by Perrocheau. The study in hand hence helped to boost the number of protein hits by a factor of three. The advantages of the LC-MS method really come into their own with proteins in molecular mass ranges up to 45 kDa, but four larger proteins could also be identified in the present study (embryo globulin = 72 kDa and the D-hordeins with 80, 75 and 50.1 kDa). All these protein species were members of the non watersoluble fraction. Proteins belonging to the larger 90 – 1000 kDa fraction and mentioned in literature could not be identified. The tryptic cleavage might be insufficient for these proteins (remember the prominent signals late in the LC runs).

The number of identified stress proteins potentially induced by fungal or microbial decay nevertheless deserves to be mentioned here, especially the low molecular mass protein fragments of antifungal proteins R and S. An upregulation of single pathogenesis related proteins, antifungal proteins or proteins not yet identified might induce gushing. No metabolites of the predicted gushing inducing organism could be identified, despite the application of specific microbial databases. Their impact could not be excluded, as own tests performed with hydrophobin standards revealed a number of problems in detecting and identifying these proteins.

### **6.4.7 Summary**

As the LC runs had not been analysed in their entirety, a direct comparison of gushing and non-gushing malt was impossible, nor could any conclusions be drawn concerning different protein contents, or as yet only notional conclusions, respectively.

In the following sections of this thesis the results of the proteomic malt study will only be used to provide means of comparison and a clearer view of the proteins recovered in beer. The UPLC-MS method developed is a powerful tool for boosting protein identification in future research. A more definitive differentiation might be possible following the detailed analysis of gushing and non-gushing malts. Future analyses should therefore be aimed at creating a detailed protein data background that would promote the detection of proteinogenic gushing agents or the general differences between malt varieties.

## **6.5 *From malt to beer and beyond***

### **6.5.1 Top down approaches**

The resolution and mass accuracy specifications are largely determined by the instrumental and analysis technology. The TOF analyser with integrated reflectron used in this study normally provides a resolution not exceeding FWHM 5.000. For the top down investigations, the MS tuning and calibration were performed with a mixture of horse heart myoglobin and bovine trypsinogen (Figure 57), in order to achieve good resolutions over a wide mass range. The capabilities of the analyser are usually limited to a mass range of 300 – 3000 Da, but given this special tuning analyses up to 3500 Da were also successful. The tuning was mainly focused on balancing the ion count rates for both protein ion series.

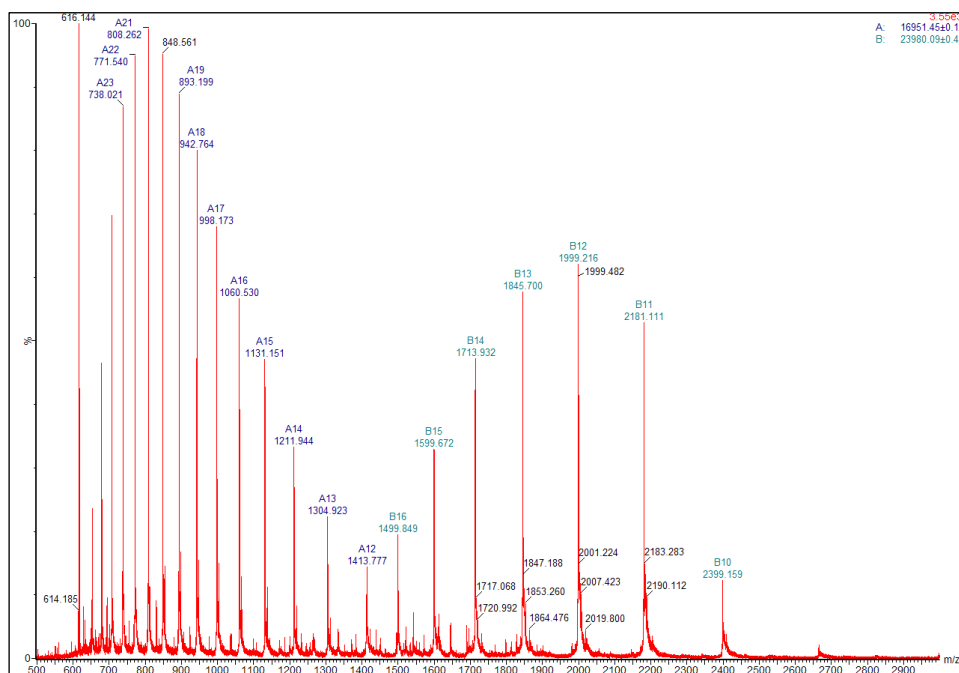


**Figure 57** Spectrum of a mixture of bovine trypsinogen (10 pM/ $\mu$ L, molecular mass = 23980.987 Da) and horse heart myoglobin (5 pM/ $\mu$ L, molecular mass = 16951.499 Da). 616.144 Da is the monoisotopic mass of heme. The positive ion average  $m/z$  values were calculated to be 23980.09 Da (mass deviation = 0.89 Da  $\pm$  0.47 Da mass error) for the trypsinogen and 16951.45 Da (mass deviation = 0.049 Da  $\pm$  0.12 Da mass error) for myoglobin. The tuning was optimized for balanced ion counts with both protein ion series. Both proteins show an ESI characteristic multiple protein charge, with up to 15/10 charge states observable for trypsinogen/myoglobin, respectively.

A number of single protein standards, as well as mixtures of the standards were tested with the LC-MS method, in order to evaluate the accuracy of mass measurements performed in the top down approach. The agents of choice once more included bovine trypsinogen (molecular mass = 23980.987 Da) and horse heart myoglobin (molecular mass = 16951.499 Da), but also bovine serum albumin (molecular mass = 66432.2 Da), lectin (molecular mass  $\approx$  110000 Da) and cytochrom C (molecular mass  $\approx$  12400 Da). The quaternary structure of the lectin was found to be unstable in the LC-MS run and could only be observed in fragments. All other protein standards proved analysable with an adequate resolution and accuracy in terms of mass measurement (Appendix C). The BEH  $C_4$  column used allowed proteins to be determined with standards of an even higher molecular mass such as BSA. Depending on the MS tuning, calibration and the protein standard, mass deviations ranged around 0.08 – 0.49 Da at best and 3 Da at worst, even with the larger proteins. A standard sample set comprising malt extracts, congress wort, unhopped first wort, cold wort, Pilsener beer (with and without KZE treatment), haze sample supernatants and haze dissolved in DMSO was analysed for "whole" proteins. The term "whole" here includes undigested proteins, but certain kinds of denaturation owed to the precipitation and LC conditions need to be kept in mind. LC-MS chromatograms revealed an enormous reduction in total protein content from the MCT extract

or related congress wort extract up to the bottled end product (Figure 58), and beyond that in the haze samples (Figure 59).

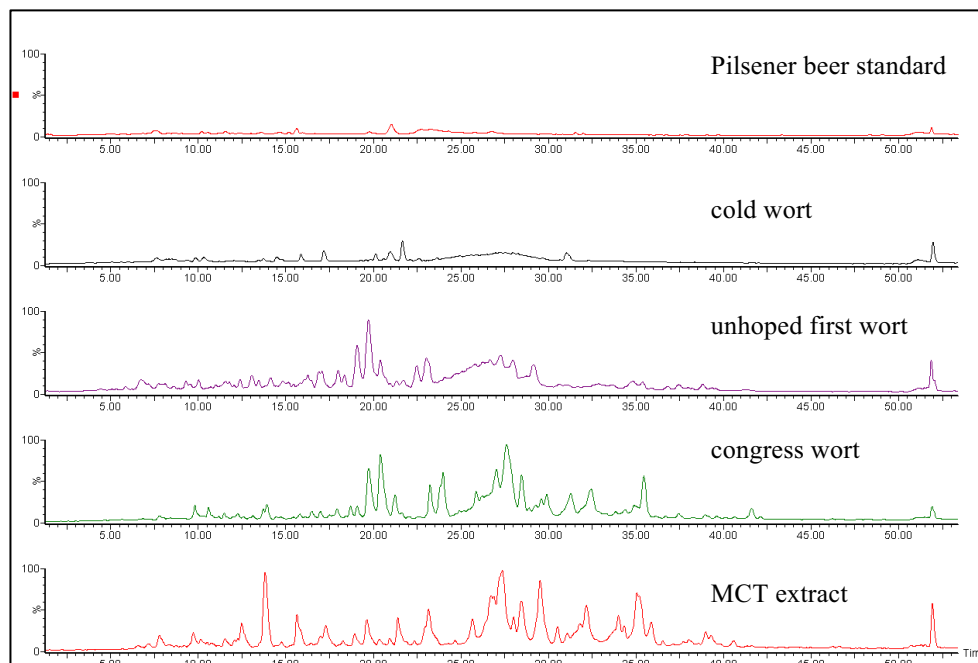


**Figure 58** Top down UPLC nanoESI-QTOF-MS BPI-chromatograms of brewing process samples. The samples show a dramatic reduction in the total protein content from the malt- and congress wort extract via the unhoped first and cold wort through to the finished beer.

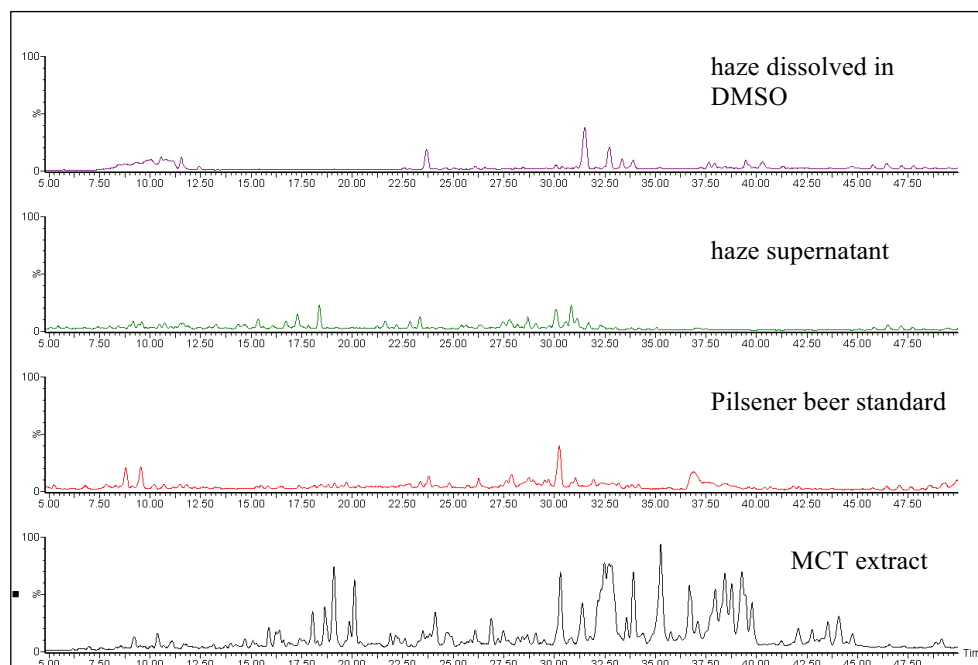


**Figure 59** Comparison of 45 minute details of the BPI-chromatograms for malt extract, beer, haze supernatant and haze dissolved in DMSO. The ion count rates of the 3 upper chromatograms are enlarged to gain a better view of the low peaks. Especially the haze sample shows an additional loss of protein peaks and new non-proteinogenous peaks, as discussed immediately above.

The protein content is dramatically changed by the brewing process. Several process operations such as the boiling of the wort, the addition of hops, the fermentation, the filtration procedure, and in some cases the flash pasteurization basically determine the total protein content. These drastic changes are even more obvious in the three dimensional data maps of the entire UPLC-MS protein runs (Figure 60).

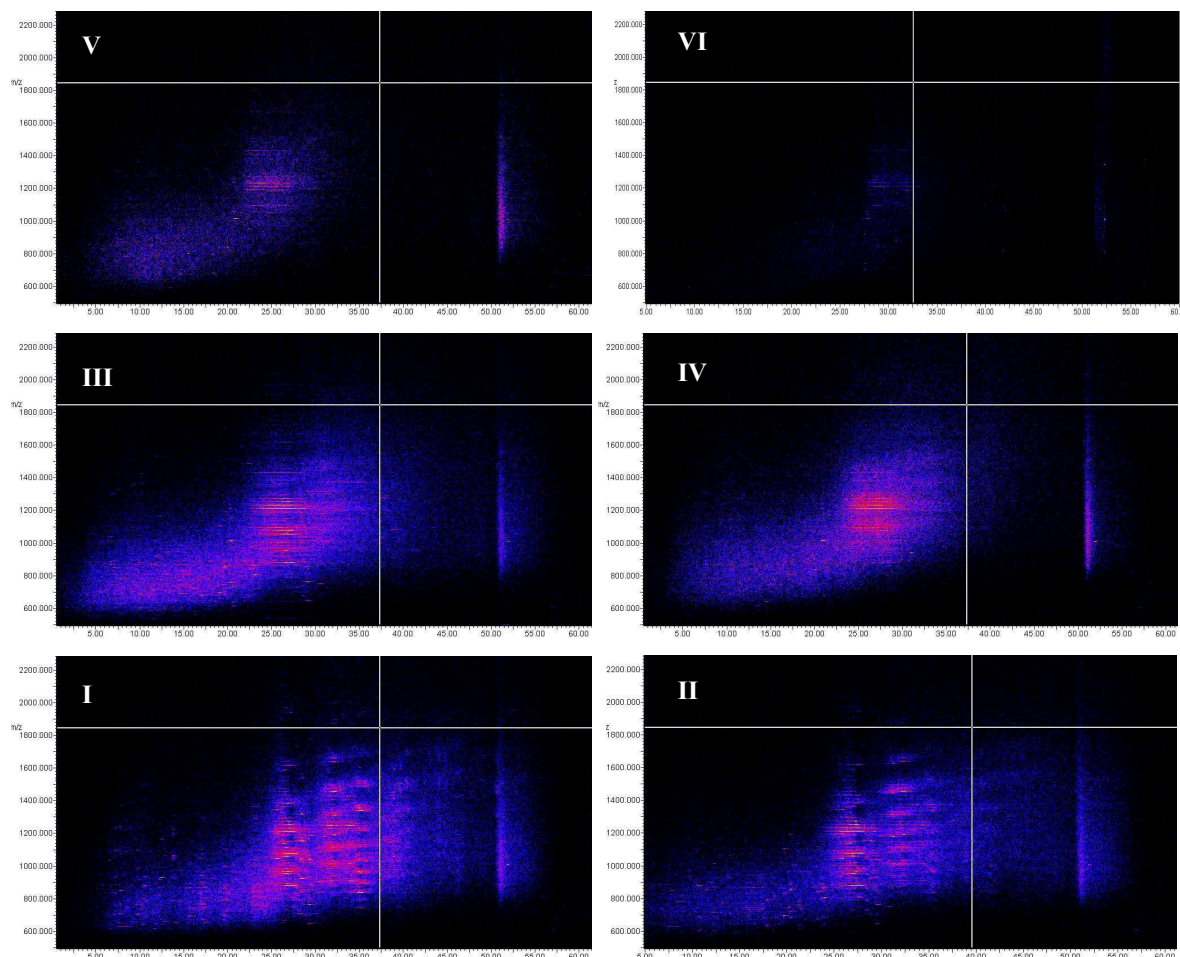


**Figure 60 3D data maps of top down UPLC-MS experiments.** I.) MCT extract of a brewing malt, II.) congress wort of the same brewing malt, III.) unhopped first wort, IV.) cold wort, V.) bright beer standard, VI.) haze sample supernatant. The maps show data against retention time: the vertical axis shows the mass/charge units (Da/e), the horizontal axis the retention time in minutes. The colouration highlights the most intensive signals.

The maps clearly show the enormous reduction in the protein content. The changes in the colour code intensities indicate that only a few protein species remain in the bottled beer after the brewing process. Extracted mass chromatograms and the attendant protein spectra could be shown for single proteins by applying the inverse crosshair marker. The overlay function, which includes the entire BPI chromatogram and the extracted mass chromatogram, supported the allocation of single proteins. Only a few heat stable proteins were identified in

## RESULTS AND DISCUSSION

bright beer, including protein Z, various nLTP1 species, and members of the inhibitor protein class.

### 5.6.2 Bottom up experiments

The same sample set of brewing process and beer samples was also analysed by bottom up approaches. Two different analytical methods were used to reveal the protein content. In the first, direct DDA experiments were performed in UPLC-MS coupling mode following tryptic digestion of the total protein content. In the second the DDA tests of reinjected fractions in infusion mode followed UPLC-MS separation with parallel fractionation. The protein results of the bottom up experiments are summarized in Table 25, with only the common protein hits marked for different sample types. Five proteins originating from wheat and one yeast protein were furthermore observable in the sample set (Table 26). Additional information on the peptide precursor ion masses, charges and sequences is provided in Appendix D.

**Table 25 Summary of protein hits identified in bottom up experiments with brewing process samples.**

Full protein name ID's	MM after PTM [Da]	pI	MCT extracts	Congress wort	Unhopped first wort	Cold wort	UF of beer	Bright beer	Haze
P06293 SPZ4_HORVU	43276.38	5.72	x	x	x	x	x	x	x
Q43492 BSZ7_HORVU	42689.61	5.45	x			x	x		
Q40066 SPZx_HORVU	42947.14	6.77	x						x
P32936 IAAB_HORVU	14192.28	5.78	x	x	x	x	x		x
P28041 IAAA_HORVU	13112.86	5.51	x	x	x		x		x
P01054 ICIC_HORVU	8258.13	6.79	x		x		x		
P16062 ICIA_HORVU	8882.24	5.24	x	x	x		x		
P01086 IAAE_HORVU	13626.56	6.95	x	x			x		x
P28814 BARW_HORVU	13737.22	7.76	x	x	x	x	x		x
P07597 NLTP1_HORVU	9694.96	8.19	x	x	x	x	x	x	x
Q5UNP2_HORVD ns-LTP	12362.42	9.22	x	x	x	x	x	x	
Q9SES6_HORVU ns-LTP	12340.45	8.9	x	x	x	x	x	x	
P52572 REHY_HORVU	23963.49	6.31	x				x		
P14928 LEA1_HORVU	21819.79	9.02	x	x					
P11643 IAAD_HORVU	16102.59	5.24	x	x		x			x
P13691 IAA2_HORVU	13101.11	5.06	x				x		x
Q02056_HORVU D-hordein	45994.05	8.32	x				x		
Q1ENF0_HORVU Cystatin Hv-CPI8	12861.57	9.8	x	x	x				
225102 trypsin/amylase inhibitor pUP13	14746.83	5.35	x			x	x		
P16969 IAA_HORVU	13740.87	7.73	x	x					
Q9FSI9 HINB1_HORVU	14115.12	8.55	x	x	x	x	x		
Q2V8X0_HORVU Limit dextrinase inhibitor	16006.53	7.56	x	x					
Q40036_HORVU Putative protease inhibitor	9405	8.37	x	x	x	x	x	x	
O23997_HORVU Basic pathogenesis-related protein PR5	22797.69	6.74	x	x			x		
Q946Z0_HORVU Thaumatin-like protein TLP6	23725.95	7.33	x	x					
O22462_HORVU Barperm1	21656.41	8.15	x	x					
Q03678_HORVU Embryo globulin	72252.62	6.8	x	x	x	x			
O24000_HORVU CMD3	15976.52	6.98	x				x		

## RESULTS AND DISCUSSION

**Table 26 Ancient protein species identified in bottom up experiments of brewing process samples.**

Full protein name ID's	MM after PTM [Da]	pI	MCT extracts	Congress wort	Unhopped first wort	Cold wort	UF of beer	Bright beer	Haze
P08488 GLT3_WHEAT	68713.5	6.97	x						x
P10387 GLT0_WHEAT	67475.03	6.97	x						x
Q41540_WHEAT CM 17 protein	13431.42	4.87	x	x	x				
Q43663_WHEAT Wali3 protein	9496.16	8.75	x				x		
P16159 IAC16_WHEAT $\alpha$ -amylase/trypsin inhibitor CM16	13437.43	5.02	x	x					
P00358 G3P2_YEAST Glyceraldehyde-3-phosphate dehydrogenase 2	35715.66	6.49	x				x		

The MCT extract samples and the beer ultrafiltrate were analysed in direct infusion mode following fractionation. 22 of the 180 fractions detected in the beer ultrafiltrate led to protein hits. The analysed fractions comprised the most abundant peptide peaks. As the ultrafiltrate was analysed in an 80 minute UPLC-MS run including the collection of 380 fractions (collection time window = 12 sec.), approximately 47.4 % of the entire LC run were covered by the analysed fractions. Due to the lack of peptide peaks in the first 2 and final 12 minutes of the run, these periods could be rejected, increasing the coverage to as much as 58.8 %.

The congress wort, unhopped first wort, cold wort and bright beer were analysed in direct DDA tests. A direct comparison of the number of protein hits for MCT extracts and congress wort, or MCT extracts and the beer/bright beer ultrafiltrations clearly showed that they are reduced by a minimum factor of 3 for congress wort, and even by a factor of 5 for beer in the direct DDA tests. This problem has already been mentioned above concerning analysis of MCT extract and could be explicable by the narrow width of the peptide peak. The DDA channels showed an enormous number of peptide precursor masses in only a single scan. In spite of the good ion count rates of these single scans, the MSMS test was stopped immediately after the first scan owing to the small peptide peak width. As the DDA experiments were determined by the ion count rates, the instrumental limitations of the QTOF (inadequate resolution and scan rates) also had a significant limiting impact. Many peptide precursor masses yielded no or inadequate fragmentation data. Incomplete database information could additionally also diminish the identification rate. Manual observations of the chromatograms, potential number of peptide precursor masses and PLGS fragmentation data revealed a greater number of peptide precursor masses. Just to give an impression: with the congress wort the approximately 1500 peptide precursor masses recognized by the PLGS software only resulted in 22 protein hits. The investigations performed for the study in hand provide a first insight into the protein content of different brewing process samples, but these

need to be confirmed by additional in depth analyses. In the case of stand alone bottom up experiments, the UPLC-MS strategy with parallel fractionation should be used in this respect. 28 barley, five wheat and one yeast protein could be identified in a minimum of two sample types of the sample set (see Appendix D). Only nLTP1 and protein Z4 were observable in all the samples. The number of identified peptide precursor ions varied, depending on the sample type and analytical approach, but usually more than one precursor ion could be found for both proteins. In contrast to the results for haze, these peptides had larger masses and also occurred in triple and quaternary charge states. This phenomenon has also been discussed with respect to a potentially rather peptidic character of haze components. Whereas a typical proteinogenic character was observable for nLTP1 in the top down experiments and thought to be the source of the larger peptide varieties, these charge state distributions were not observable in the dissolved haze samples. In the case of protein Z, the experiments again failed to reveal a characteristic, proteinogenic charge state in the top down investigations, but the bottom up experiment provided proof that peptide fragments also derived from the upper AA sequence of the RCL domain. Therefore the existence of an entire protein Z molecule that might not be recognized in the ionization (neutral loss) can still be assumed.

In view of the problems with direct DDA testing, the different sample types and their respective total number of protein hits can not be compared. In addition, attention was not only focused on the results for bright beer, but instead the combined results for beer ultrafiltrate and bright beer. By doing so, nearly all the proteins described for haze were also identified in beer. In spite of the  $\alpha$ -amylase/trypsin inhibitor Cmd (IAAD), a Cmd3 subunit with 97 % sequence homology could be identified.

The proteins identified in beer for this study could be allocated to three water soluble protein families. The only water insoluble protein was found to be a D-hordein fragment. This result matches the findings of the Japanese research group led by Hao. Additional D hordein species found by Perrocheau *et al.* could not be confirmed by the results of this study.

The majority of protein species (10 proteins), to survive the brewing process belong to the class of protease inhibitors. IAAA, IAAB, IAAE, IAA2 and pUP13 are members of the cereal  $\alpha$ -amylase/trypsin inhibitor L6 family, ICIC and ICIA can be allocated to the potato type serine protease inhibitor family, and HINB1, the putative protease inhibitor, as well as the Cmd3 are serine type endopeptidase inhibitor proteins. The combined identification of IAAA, IAAB and the Cmd3 subunits supports the theory that these proteins could be attached to a heterotetramer. The same results applied to the MCT extracts and other brewing process samples. Reducing conditions in protein precipitation and the LC run might lead to a



reduction and dissociation of the oligomeric structure into the monomeric protease inhibitor units. Regardless of the REHY, ICIC and ICIA hits, the protein identifications match the results of 2D gel tests performed by Hao *et al.* with beer. ICIA had in contrast also been identified in the 2D gel investigations of beer performed by Perrocheau *et al.*

The second pertinent protein group is the pathogenesis related family. Barwin and the basic pathogenesis related protein PR5 were the two members identified from this family. The barwin protein was already known from 2D gels, but the PR5 protein was a new protein hit that had not been mentioned for beer before.

In addition to protein Z4, BSZ7 was also identified. The close relationship of both these proteins has already been described in relation to the MCT results and will not be explained here again. Both protein species were identified in 2D gels, as well. Whereas the gel separations performed by Hao also confirm the existence of BSZx and an additional protein Z homologue, no BSZx could be found in beer in the present study, where only the haze samples and MCT extracts indicated a BSZx protein. The barley protein Z homologue could not be identified in any sample in the study in hand.

The final two protein hits belong to the plant LTP family and concern non specific lipid transfer proteins (Q5UNP2 and Q9SES6). Both proteins have not been mentioned in relevant beer tests before. Whereas other research groups had identified nLTP2, this protein could only be found in the MCT extracts and not be traced through the brewing process. Neither could any other nLPT species be identified. As described above, the protein approaches used for this study show a need for further investigations. The existence of these and additional proteins so far unidentified can hence not be excluded.

All the protein species identified in beer in the present study either feature the common trait of heat stability or are thought to be substrates of the glycation and other modifications in the brewing process, which might explain their survival of the procedure. As the separate top down and bottom up LC-MS approaches applied precluded an analysis of the PTM or brewing process modifications, the research focused on the development of a LC-MS based method that is independent from 2D gel separation.

### **5.6.3 Top down and bottom up investigations in a single experiment**

Bottom up and top down analyses were combined by merging online LC-MS with nanoESI infusion. The approach was developed for protein identification, and in order to characterize post translational modifications in the brewing process. Intact mass measurement and primary

sequence determination were performed by UPLC-MS(MS) with post column splitting and simultaneous fraction collection (Figure 61).

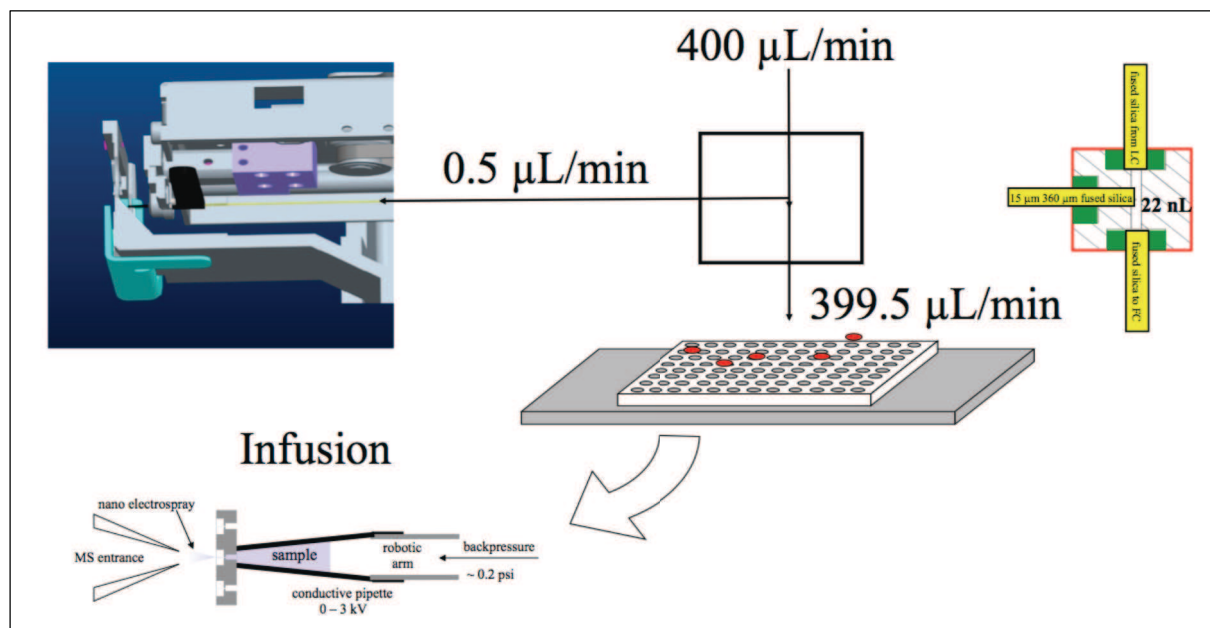


**Figure 61** Schema of post column splitting and Nanomate settings for top down and bottom up tests combined in a single LC-MS run. In the top down experiment the LC flow was split post column and only 500 nL were conducted to the QTOF by the Nanomate coupler. The remaining LC fluid was subjected to parallel fraction collection in protein LoBind well plates. The collected analyte was re-analysed top down in infusion mode (infusion of 5  $\mu\text{L}$  at a flow rate of 200 nL/min). Then the fractions were digested and analysed in infusion mode at 200 nL/min, as well.

The top down run should also allow the observation of post translational modifications following UPLC-MS separation by an automated nanoESI infusion of the previously collected fractions. As the nanoESI spray only consumes very small amounts of the sample analyte, proteolytic digestion could be performed with the remaining sample for the bottom up analysis (Figure 62).

Theoretically the combination of both strategies should allow the characterisation of proteins involved in the brewing process via mass determination, PTM characterization and the corresponding peptide sequence coverage in a single experiment.

The combination of intact protein chromatography and post column splitting system showed the same separation power and signal to noise ratio as standard non splitting set ups. In the online top down analysis, the intact mass could be determined by deconvoluting the charge state envelope (Figure 63).

Online MSMS testing was possible, but identification was precluded owing to the enormous number of proteins eluted from the column. Most proteins were detected, but not very reliably owing to the limited time for the elution.

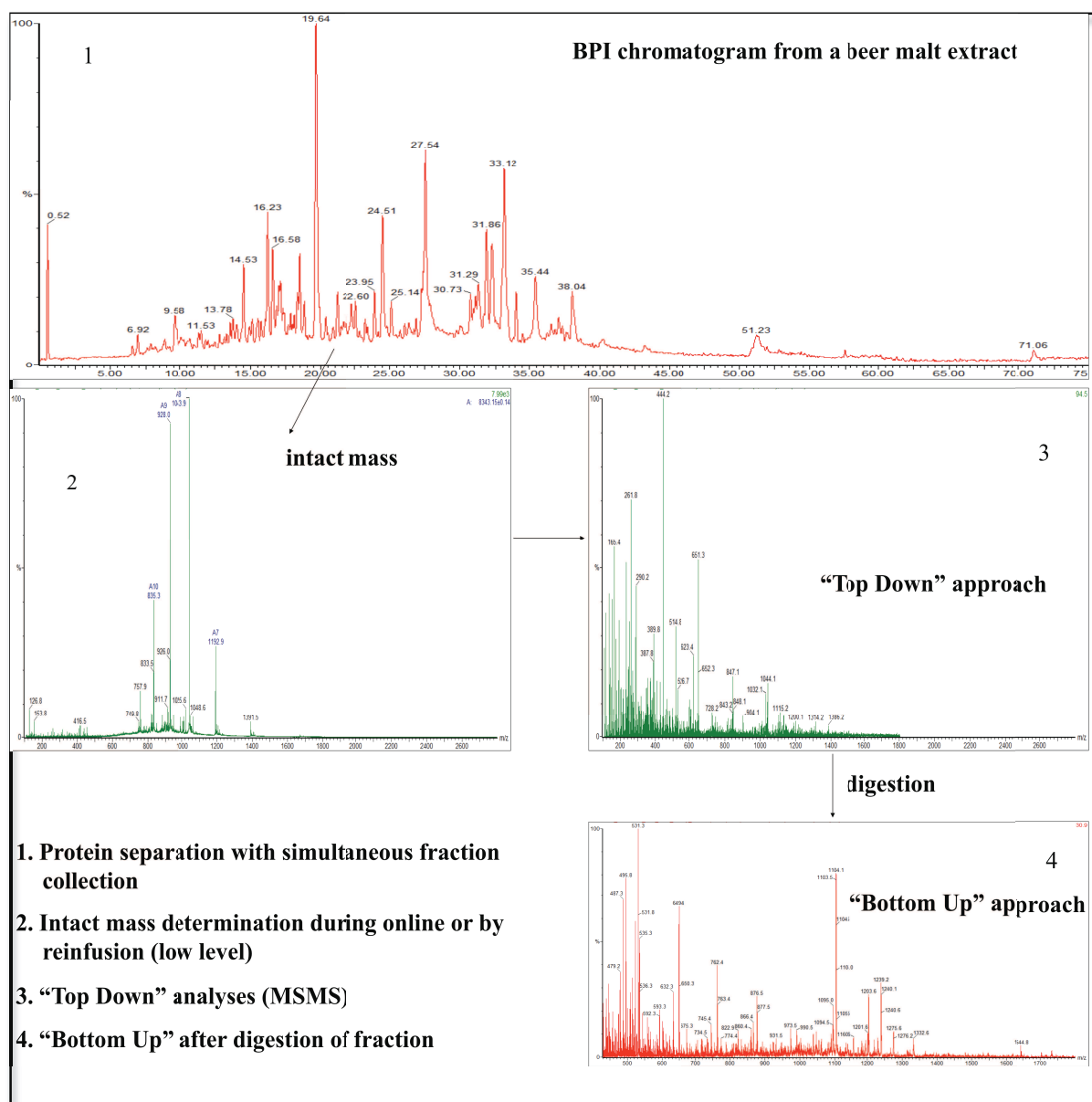
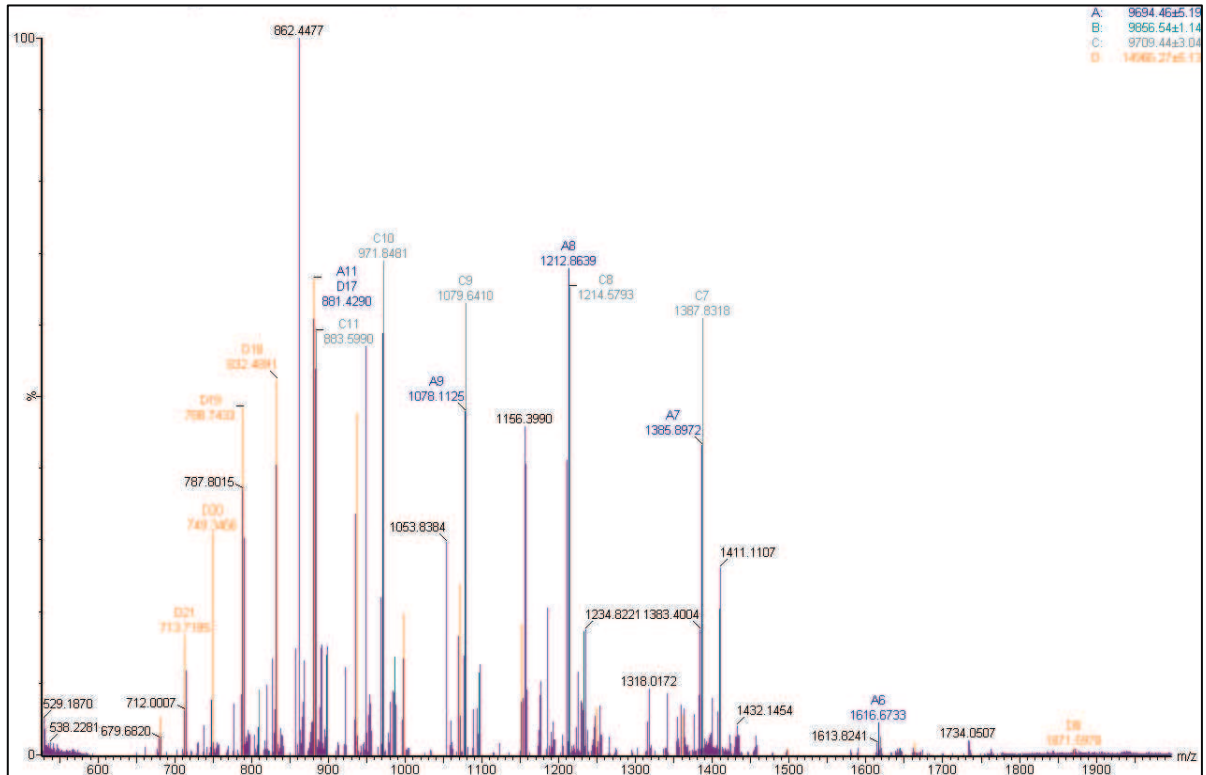


Figure 62 Overview of the analytical strategy in a combined bottom up and top down approach.

Because of these instrumental limitations the proteins were then targeted in offline analyses of the previously collected fractions. Thanks to the low sample consumption of the nanoESI-spray, the offline analyses allowed for an unlimited averaging capability and optimisation of the analytical parameters. Charge state deconvolution and mass measurement proved easily possible (Figure 64).

The MSMS tests were once more successful, but identification was impossible as the ProSight PTM software selected did not include barley specific protein information. For these reasons the protein fractions were digested and reanalysed by offline bottom up experiments. It was possible to individually optimise the analytical conditions.

## RESULTS AND DISCUSSION



**Figure 63 Mass measurement and charge state deconvolution in an online MCT top down test.** The spectrum includes two barley nLTP1 ion series (shown in blue with a calculated molecular mass of 9694.46 Da and turquoise with a sugar related 162 Da mass shift, molecular mass = 9856.54 Da), an additional nLTP ion series (HORVD = Q5UNP2, molecular mass = 9475 Da, AA sequence positions 31 – 124) and possible modified IAAA ion series (molecular mass = 14966.27 Da).

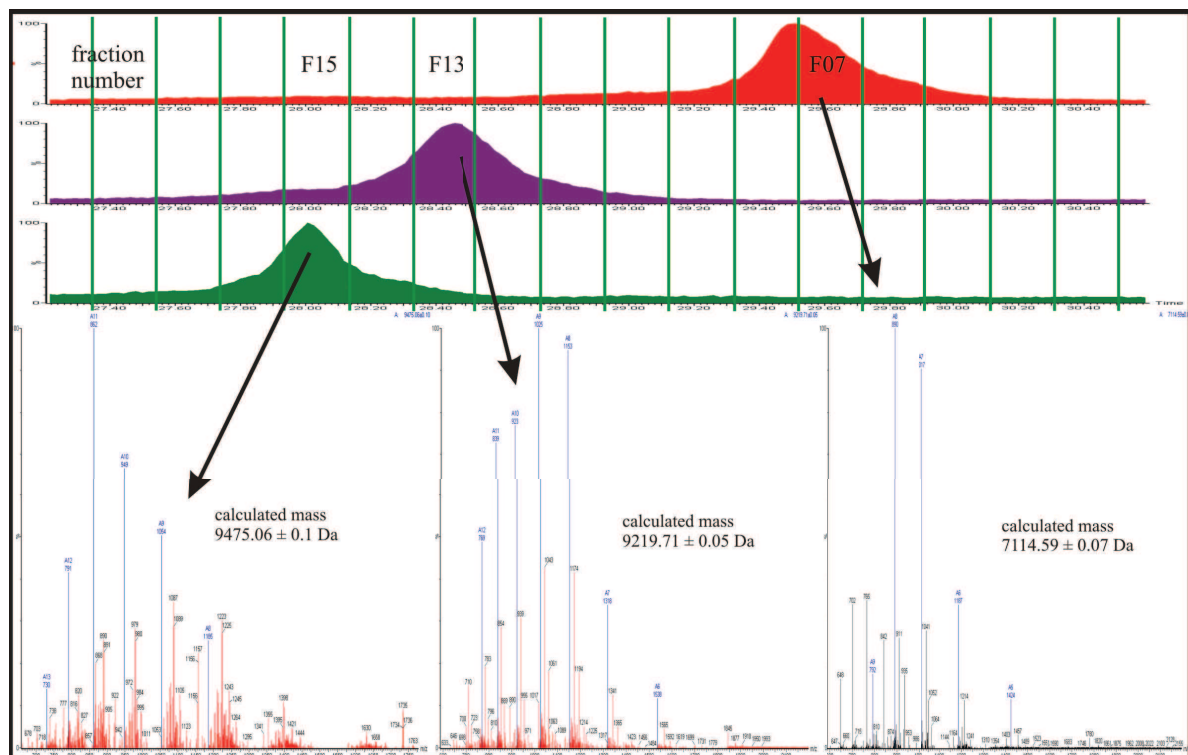


**Figure 64 Extracted protein spectra of undigested protein fractions following offline application.** The calculated mass of fraction F15 matches one of the proteins determined in online application (Figure 63).

The exact UPLC separation of intact proteins indicated that the peptides of the fractions identified could potentially correspond to the proteins found in the top down approach previously. Another confidence level was therefore introduced to the analyses. The complexity of each protein fraction was reduced in a manner ensuring that no preliminary 2D gel run would be required.

In the final phase of this study the analytical approach could not be optimised any further in order to reveal PTMs. The combination of both these analytical methods is therefore only suitable for measuring the intact mass measurement and identify the peptide sequence. In theory, a combination of top down and bottom up approaches should facilitate the interpretation of so far unknown proteins, as well as PTMs, given the application of other, more sensitive instruments and/or software.

## CHAPTER VII

---

CONCLUSIONS

### 7 Conclusions

Proteomic studies carried out during this thesis mainly based on HPLC- and UPLC-ESI-MS(MSMS) analyses. The developed approaches were found to be powerful protein identification tools, even with highly complex protein mixtures. Single usage of "top down" or "bottom up" experiments revealed a number of new findings with beer, haze, brewing process related and malt samples.

HPLC-MS investigations with a nLTP1 standard gave a hint to glycation of nLTP1 during the brewing process. In addition the high sugar content of beer samples exerted a strong interference during LC-MS analysis and was found to be an interfering substance for a lot of protein quantification methods, too. Therefore quantification results remain inexact, even with the 2D-Quant used during this study. Independent on the sugar stability results might be negatively influenced by other beer substances. Quantification results only give a hint to 0.5 g protein per litre beer, but no proof.

Results from protein Z research supported a possible internal fragmentation around the protein's RCL region giving rise to an about 4 kDa terminal fragment. These findings might also explain results of other research groups, who worked with 2D gel separation and found manifold or false positive identifications (protein Z artefacts) over a wide range of the gel molecular mass scale (around 5 – 10 kDa and spreaded above the whole gel up to 45 kDa)

Investigations with haze did not support a classical protein-polyphenol haze model. Results of this study gave a hint to a physical attachment process during haze formation, as a general input of basic beer turbidity with filtration aid origin was found. Whole proteins could not be identified from haze. In contrast peptides of heatstable protein Z and nLTP1, some protease inhibitor species and D-hordeins were found, but were only thought to be minor components.

MCT investigations with gushing revealed a general uncertainty of this method. Only the treatment of gushing positive samples with unspecific cleaving proteases resulted in gushing inhibition, a fact which supported the presumption of proteins being involved in this phenomenon. Despite of improvements with "bottom up" and "top down" methods single proteinogenic gushing inhibitors could not be identified during this study. Nevertheless, the developed methods and their results point out that further investigations will boost protein identifications and create a data background, which might deliver the basis for distinct differentiation between gushing-positive and gushing-negative malts. Protein identifications on molecular level might deliver a chance to narrow down gushing agents.

## CONCLUSIONS

---

”Top down” analyses of malt extract, brewing process and beer samples revealed dramatical changes in the protein content during the brewing process. A huge decrease could be visualised from malt or lab-scale congress wort, over unhoped first wort and cold wort to final beer. Several production steps like wort boiling, the addition of hops, fermentation, the filtration procedure and in some cases flash pasteurization configure the basic, total protein content. Therefore only a small amount of protein species remains in the finished beer.

By the help of ”bottom up” investigations remaining species were found to be members of the nLTP and serpin (protein Z) protein classes, of the protease inhibitor classes (largest number of hits), as well as water-insoluble hordein class. All protein species identified from beer during this study have a heat-stability or possible glycation/modification during the brewing process in common; a fact which was thought to be an explanation of their survival during the brewing process.

Bottom up and top down analysis were combined by merging online LC-MS with nanoESI infusion in a single LC-MS run. As another confidence level could be introduced into the analyses by parallel fractionation the method was found to operate irrespectively from gel separation, especially with high complex protein samples. The approach was developed for protein identification and to characterize post-translational modifications during the brewing process. In praxis the identification of PTM’s was not successful due to instrumental and database limitations but in theory the combination of top down and bottom up approaches should be able to facilitate the interpretation of just unknown proteins as well as PTM’s by the usage of another, more sensitive instrumentation and/or software.



## REFERENCES

---

**X References**

- 1 Urbanavicius, A. "Free radical damages in proteins", *Internet-Source*, [www.cryst.bbk.ac.uk/pps97/assignments/projects/adomas/Free\\_Radical\\_Damages\\_In\\_Proteins.html](http://www.cryst.bbk.ac.uk/pps97/assignments/projects/adomas/Free_Radical_Damages_In_Proteins.html).
- 2 Kunz, T., Methner, F.-J., Huttermann, J., Kappl, R. (2008) "Method for determining the endogenous antioxidative potential of beverages by means of esr spectroscopy", *Internet-Source*, [www.freshpatents.com](http://www.freshpatents.com), UPSTO **Application-No. 20080248580**.
- 3 De Schutter, D.P., Saison, D., Delvaux, F., Derdelinckx, G., Delvaux, F.R. (2008) "The Chemistry of Aging Beer", *Beer in Health and Disease Prevention Volume 1*, Elsevier, **Chapter 36**: pp. 375-388.
- 4 Schildbach, R. (2009) "Krankheiten und Schädlinge", *Brauerei Forum*, **5/09**: pp. 8-11.
- 5 Hippeli, S., Elstner, E.F. (2002) "Are Hydrophobins and/or Non-Specific Lipid Transfer Proteins Responsible for Gushing in Beer? New Hypotheses in the Chemical Nature of Gushing Inducing Factors", *Z. Naturforsch.*, **57c**: pp 1-8.
- 6 Hipelli, S., Hecht, D. (2008) "Die Rolle von ns-LTP1 und Proteasen bei der Entstehung des primären Gushing", *Brauwelt*, **No. 32**: pp. 900-904.
- 7 "Basic structure of an amino acid", *Internet-Source*, [www.protocolsupplements.com/Sports-Performance-Supplements/wp-content/uploads/2009/06/amino-acid-mcat1.png](http://www.protocolsupplements.com/Sports-Performance-Supplements/wp-content/uploads/2009/06/amino-acid-mcat1.png)
- 8 Asano, K., Shinagawa, K., Hashimoto, N. (1982) "Characterization of Haze-Forming Proteins of Beer and Their Role in Chill Haze Formation", *J. Am. Soc. Brew. Chem.* **40/4**: pp. 147-154.
- 9 Bamforth, C.W. (1999) "Beer Haze", *J. Am. Soc. Brew. Chem.*, **57(3)**: pp. 81-90.
- 10 Evans, E., Sheehan, M., Robinson, L., Hill, A., Tolhurst, R., Gale, K., Barr, A. "The influence of protein composition on beer haze and foam stability", *Proceedings of the 10th Australian Barley Technical Symposium*, *Internet-Source*, [www.regional.org.au/au/abts](http://www.regional.org.au/au/abts).
- 11 Evans, E., Robinson, L. H., Sheehan, M. C., Tolhurst, R. L., Hill, A., Skerrit, J. S., Barr, A. R. (2003) "Application of Immunological Methods to Differentiate Between Foam-Positive and Haze-Active Proteins Originating from Malt", *J. Am. Soc. Brew. Chem.*, **61(2)**: pp. 55-62.
- 12 Ishibashi, Y., Terano, Y., Fukui, N., Honbou, N., Takui, T., Kawasaki, S., Nakatani, K. (1996) "Development of a New Method for Determining Beer Foam and Haze Proteins by Using the Immunochemical Method ELISA", *J. Am. Soc. Brew. Chem.*, **54(3)**: pp. 177-182.
- 13 Siebert, K. J., A., Lynn, P. Y. (1997) "Mechanism of Beer Colloidal Stabilization", *J. Am. Soc. Brew. Chem.*, **55(2)**: pp. 73-78.
- 14 Bewley, J.D., Black, M., Halmer, P. (2006) "The encyclopedia of seeds: science, technology and uses", *CABI Publishing*.
- 15 Busch-Stockfisch (2005) "Lebensmittellexikon", *Behr's Verlag*: pp. 462, 721, 1339.
- 16 Siebert, K. J., Lynn, P.Y. (1997) "Effect of Protein-Polyphenol Ratio on the Size of Haze Particles", *J. Am. Soc. Brew. Chem.*, **58(3)**: pp. 117-123.

## REFERENCES

---

- 17 Siebert, K. J., Lynn, P.Y. (2003) "Effects of Alcohol and pH on Protein-Polyphenol Haze Intensity and Particle Size", *J. Am. Soc. Brew. Chem.*, **61(2)**: pp. 88-98.
- 18 Siebert, K.J., Lynn, P.Y. (2005) "Comparison of Methods for Measuring Protein in Beer", *J. Am. Soc. Brew. Chem.*, **63/4**: pp. 163-170.
- 19 Schnick, A. (2001) „Untersuchung zur Klärwirkung modifizierter Kieselsole und Kieselolgemische am Beispiel einer Modelltrübungsreaktion“, *Dissertation, Internet-Source*, Fakultät für Prozesswissenschaften, Technische Universität Berlin; [www.edocs.tu-berlin.de/diss/2001/schnick\\_alexander.pdf](http://www.edocs.tu-berlin.de/diss/2001/schnick_alexander.pdf)
- 20 Rehmanji, M., Gopal, C., Mola, A. (2005) "Beer Stabilization Technology – Clearly a Matter of Choice", *Master Brewers Association of the Americas, Technical Quarterly*, **Vol. 42/4**: pp. 332-338.
- 21 "Chemical structure of L-proline", *Internet-Source Wikimedia*, <http://upload.wikimedia.org/wikipedia/commons/d/d7/L-proline-skeletal.png>.
- 22 Kunz, T., Methner, F.-J. (2009) "The influence of radical reactions on the haze formation in stabilized beer", *EBC-Congress Hamburg*, May 2009.
- 23 "2D-structure of myoglobin", *Internet-Source*, <http://www.pdb.org/pdb/explore/mediatedSequence.do?structureId=1WLA>.
- 24 "Fusarium diseases", *Internet-Source*, [www.hgca.com/images/upload/Fusarium.gif](http://www.hgca.com/images/upload/Fusarium.gif).
- 25 O'Rourke, T. (2002) "Colloidal stabilisation of beer – Technical Summary 1", *The BREWER International*, **Jan. 2002**: pp. 23-25.
- 26 O'Rourke, T. (2002) "Predicting colloidal stability in beer – Technical Summary 4", *The BREWER International*, **Apr. 2002**: pp. 41-42.
- 27 Leiper, K. A., Stewart, G., McKeown, I. P. (2003) "Beer Polypeptides and Silica Gel-Part I. Polypeptides Involved in Haze Formation", *J. Inst. Brew.*, **109(1)**: pp. 57-72.
- 28 Leiper, K. A., Stewart, G., McKeown, I. P. (2003) "Beer Polypeptides and Silica Gel-Part II. Polypeptides Involved in Foam Formation", *J. Inst. Brew.*, **109(1)**: pp. 73-91.
- 29 Hartmann, K., Kreis, S., Zarnkow, M., Back, W. (2005) "Detection of haze particles", *Proceedings of the 30<sup>th</sup> EBC Congress Prag*, **58**: pp. 503-512.
- 30 Kusche, M. (2005) "Kolloidale Trübungen in untergärigen Bieren – Entstehung, Vorhersage und Stabilisierungsmaßnahmen", *Dissertation*.
- 31 Asano, K., Hashimoto, N. (1980) „Isolation and Characterization of Foaming Proteins of Beer“, *J. Am. Soc. Brew. Chem.*, **38(4)**: pp. 129-137.
- 32 Leisegang, R., Stahl, U. (2005) "Degradation of a Foam-Promoting Barley Protein by a Proteinase from Brewing Yeast", *J. Inst. Brew.*, **111(2)**: 112-117.
- 33 Hanke, S., Kern, M., Back, W., Becker, T., Krottenthaler, M. (2009) "Gushing suppressing effects of hop constituents", *Proceedings of the 31<sup>th</sup> EBC Congress Hamburg*, Poster, May 2009.
- 34 Hao, J., Li, Q., Dong, J., Yu, J., Gu, X., Fan, W., Chen, J. (2006) "Identification of the Major Proteins in Beer Foam by Mass Spectrometry Following Sodium Dodecyl Sulfate-Polyacrylamide Gel Electrophoresis", *J. Am. Soc. Brew. Chem.*, **64(3)**: pp. 166-174.

- 35 He, G.-Q., Wang, Z.-Y., Liu, Z.-S., Chen, Q.-H., Ruan, H., Schwarz, P. B. (2006) „Relationship of Proteinase Activity, Foam Proteins, and Head Retention in Unpasteurized Beer“, *J. Am. Soc. Brew. Chem.*, **64(1)**: pp. 33-38.
- 36 Bamforth, C.W. (2004) "The relative Significance of Physics and Chemistry for Beer Foam Excellence: Theory and Practice", *J. Inst. Brew.*, **110(4)**: pp. 259-266.
- 37 Perrocheau, L., Rogniaux, H., Boivin, P., Marion, D. (2005) „Probing heatstable, watersoluble proteins from barley to malt and beer“, *Proteomics*, **5/05**: pp. 2849-2858.
- 38 Heinemann, B., Vilbour Andersen, K., Nielsen, P. R., Bech, L. M., Poulsen, F. M. (1995) “Structure in solution of a four-helix lipid binding protein“, *Protein Science*, **5**: pp. 13-23.
- 39 Federico, M.L., Kaeppler, H.F., Skadsen, R.W. (2005) "The complex developmental expression of a novel stress-responsive barley LTP gene is determined by a shortened promotor sequence", *Plant Mol. Biol.* **57(1)**: pp. 35-51.
- 40 Loch-Ahring, S., Decker, F., Robbert, S., Andersson, J.T. (2008) “Chill-haze - Identification and determination of Haze-active constituents by HPLC and Mass spectrometry. Part I: The role of polyphenols and the astonishing impact of hop components on chill haze formation.“, *Brewing Science*, **Vol. 2/2008**: pp. 32-48.
- 41 Narziß, L. (2005) „Abriss der Bierbrauerei“, 7.te Auflage, *WILEY-VCH*.
- 42 Pfenninger, H. (1993) „Brautechnische Analysemethoden, Band II“; Methodensammlung der Mitteleuropäischen Brautechnischen Analysenkommission (MEBAK).
- 43 Robinson, L.H., Home, S., Kaukovirta-Norja, A., Vilpola, A., Aldred, P., Ford, C.M., Healy, P., Gibson, C.E., Evans, D.E. (2005) “Improving beer haze stability by investigating the interaction between malt protein quality and brewing conditions”, *Proceedings of the 30<sup>th</sup> EBC Congress Prag*, **64**: pp. 580-590.
- 44 Mikyska, A., Hrabak, M., Haskova, D., Srogl, J. (2002) “The Role of Malt and Hop Polyphenols in Beer Quality, Flavour and Haze Stability”, *J. Inst. Brew.*, **108(1)**: pp. 78-85.
- 45 Harborne, J. B. (1994) “The flavanoids – Advances in Research since 1986“, *Chapman&Hall*, **1.te Auflage**.
- 46 Bellmer, H.G., Galensa, R., Gromus, J. (1995) „Bedeutung der Polyphenole für die Bierherstellung – Teil 1“, *Brauwelt*, **28/29**: pp.1372-1379.
- 47 Bellmer, H.G., Galensa, R., Gromus, J. (1995) „Bedeutung der Polyphenole für die Bierherstellung – Teil 2“, *Brauwelt*, **30**: pp. 1477-1483.
- 48 Roeder, A., Lam, T.M.L., Galensa, R. (1995) „Thermospray-LCMS-Untersuchungen über Proanthocyanidine und andere Polyphenole im Malz, Bier und Hopfen“, *Monatsschrift für Brauwissenschaft*, **11/12**: pp. 390-396.
- 49 Whittle, N., Eldridge, H., Bartley, J. (1999) “Identification of the Polyphenols in Barley and Beer by HPLC/MS and HPLC/Electrochemical Detection”, *J. Inst. Brew.*, **105(2)**: pp. 89-99.
- 50 Forster, A. (1998) „Hopfen – mehr als nur ein  $\alpha$ -Säureträger“, *Internet-Source*, [www.nateco2.de](http://www.nateco2.de).

## REFERENCES

---

- 51 Wollersen, H. (2004) „Bestimmung und Identifizierung von Flavonoiden in Gerste mit HPLC-DAD-MS/MS“, *Dissertation*, Naturwissenschaftliche Fakultät der Universität Paderborn.
- 52 Omura, F., *et al.* (2005) “The influence of yeast cell wall mannoproteins on beer haze stability”, *Proceedings of the 30<sup>th</sup> EBC Congress Prag*, **65**: pp. 591-597.
- 53 Jegou, S., Douliez, J.-P., Molle, D., Boivin, P., Marion, D. (2001) “Evidence of the Glycation and Denaturation of LTP1 during the Malting and Brewing Process”, *J. Agric. Food Chem.*, **49**: pp. 4942-4949.
- 54 Jegou, S., Douliez, J.-P., Molle, D., Boivin, P., Marion, D. (2000) “Purification and Structural Characterization of LTP1 Polypeptides from Beer”, *J. Agric. Food Chem.*, **48**: pp. 5023-5029.
- 55 Perrocheau, L., Bakan, B., Boivin, P., Marion, D. (2006) “Stability of Barley and Malt Lipid Transfer Protein 1 (LTP1) toward Heating and Reducing Agents: Relationships with the Brewing Process“, *J. Agric. Food Chem.*, **54(8)**: pp. 3108-3113.
- 56 Iimure, T., Nankaku, N., Watanabe-Sugimoto, M., Hirota, N., Tiansu, Z., Kihara, M., Hayashi, K., Ito, K., Sato, K. (2009) "Identification of novel haze-active beer proteins by proteome analysis", *Journal of Cereal Science*, **49**: pp. 141-147.
- 57 Laitila, A., Sarlin, T., Kotaviita, E., Huttunen, T., Home, S., Wilhelmson, A. (2007) "Yeasts isolated from industrial maltings can suppress Fusarium growth and formation of gushing factors", *J. Ind. Microbiol. Biotechnol.*, **34**: pp. 701-713.
- 58 Finnie, C., *et al.* (2004) “Aspects of the barley seed proteome during germination and development“, *Biochemical Society Transactions*, **Vol. 32, part 3**: pp. 517-519.
- 59 Skriver K., Leah R., Mueller-Uri F., Mundy J., Olsen F. (1992) "Structure and expression of the barley lipid transfer protein gene Ltp1", *Plant Mol. Biol.*, **18**: pp. 585-589.
- 60 Runavot, J.-L., *et al.* (2009) "Impact of the steeping process on the modifications of lipid transfer protein (LTP1) from malt". *Proceedings of the 31<sup>th</sup> EBC-Congress Hamburg*, Poster-Presentation **104**.
- 61 Lerche, M., Flemming, M.P. (1998) “Solution structure of barley lipid transfer protein complexed with palmitate“, *Protein Science*, **7**: pp. 2490-2498.
- 62 Gorjanovic', S., *et al.* (2005) "Malting Barley Grain Non-Specific Lipid-Transfer Protein (ns-LTP): Importance for Grain Protection“, *J. Inst.Brew.*, **111(2)**: pp. 99-104.
- 63 Evans, D.E., Hejgaard, J. (1999) "The impact of Malt Derived Proteins on Beer Foam Quality Part I. The Effect of Germination and Kilning on the Level of Protein Z4, Protein Z7 and LTP1", *J. of the Inst. of Brew.*, **Vol. (105) No.3**: pp. 159-169.
- 64 Bobalova, J., *et al.* (2008) "Investigations of protein Composition of Barley by Gel electrophoresis and MALDI mass spectrometry with regard to the malting and brewing process.“, *J.Inst.Brew.*, **Vol 114, No. 1**: pp.22-26.
- 65 “Concise Encyclopedia Biochemistry“, *de Gruyter*, **Second Edition**.
- 66 Svensson, B., *et al.* (1992) “Primary Structure of Barwin: A Barley Seed Protein Closely Related to the C-Treminal Domain of Proteins Encoded by Wound-Induced Plant Genes“, *Biochemistry*, **(31)**: pp. 8767-8770.

## REFERENCES

---

- 67 Sarlin, T., Nakari-Setälä, T., Linder, M., Penttilä, M., Haikara, A. (2005) "Fungal hydrophobins as predictors of the gushing activity of malt", *J. Inst. Brew.*, **111(2)**: pp. 105-111.
- 68 Zapf, M.W., Theisen, S., Vogel, R. F., Niessen, L. (2006) "Cloning of wheat LTP1500 and two *Fusarium culmorum* hydrophobins in *Saccharomyces cerevisiae* and assessment of their gushing inducing potential in experimental wort fermentation", *J. Inst. Brew.*, **112(3)**: pp. 237-245.
- 69 Sarlin, T., Laitila, A., Pekkarinen, A., Haikara, A. (2005) "Effects of three *Fusarium* species on the quality of Barley and Malt", *J. Am. Soc. Brew. Chem.*, **63(2)**: pp. 43-49.
- 70 Torkkeli, M., Serimaa, R., Ikkala, O., Linder, M. (2002) "Aggregation and Self-Assembly of Hydrophobins from *Trichoderma reesei*: Low-resolution structural models", *Biophysical Journal*, **Vol.83**: pp. 2240-2247.
- 71 Sarlin, T., Vilpola, A., Kotaviita, E., Olkku, J., Haikara, A. (2007) "Fungal Hydrophobins in the Barley-to-Beer Chain", *J. Inst. Brew.*, **113 (2)**: pp. 147-153.
- 72 "3D-structure of myoglobin", *Internet-Source*, **Structure 1AZI** [www.pdb.org/pdb/](http://www.pdb.org/pdb/).
- 73 Westermeier, R., Naven, T., Höpker, H.-R. (2008) "Proteomics in Practice", *Wiley VCH, Second Edition*.
- 74 Bradshaw, T. (2003) "Introduction to Peptide and Protein HPLC", *User's Guide Phenomenex, Volume 1*.
- 75 "Waters Homepage", *Internet-Source*, [www.waters.com](http://www.waters.com).
- 76 "Micromass Q-TOF micro Mass Spectrometer", *Instrument User's Guide Waters, 2002*.
- 77 "Electrospray Tip", *Internet-Source*, [www.chemistry.nmsu.edu/Instrumentation/Image44.gif](http://www.chemistry.nmsu.edu/Instrumentation/Image44.gif).
- 78 "Construction of the ESI-chip of the Nanomate robot system", *Internet-Source* [www.advion.com](http://www.advion.com).
- 79 "Peptide fragmentation", *Internet-Source*, [http://upload.wikimedia.org/wikipedia/commons/f/fb/Peptide\\_fragmentation.gif](http://upload.wikimedia.org/wikipedia/commons/f/fb/Peptide_fragmentation.gif).
- 80 "Top down versus bottom up approach", *Internet-Source*, [http://upload.wikimedia.org/wikipedia/commons/thumb/f/f0/Bottom-up\\_top\\_down.svg](http://upload.wikimedia.org/wikipedia/commons/thumb/f/f0/Bottom-up_top_down.svg)
- 81 Arbeitsgruppe Niehaus, K. (2007) "Phenolextraktionsmethode" based on: Watt S.A., Niehaus, K. (2005) "Comprehensive analysis of the extracellular proteins from *Xanthomonas campestris* pv. *campestris* B100", *Proteomics*, **5(1)**: pp 153 – 167, *Uni Bielefeld, Biologische Fakultät*.
- 82 Almeida, R., Decker, F., Robbert, S. (2009) "Combining Top down and Bottom up analyses in a single LCMS experiment", *Poster Presentation 18<sup>th</sup> IMSC, Bremen, Poster No. PMM 133*.
- 83 Na, Y.-R., Im, H. (2009) "The length of the reactive center loop modulates the latency transition of plasminogen activator inhibitor-1", *Protein Science*, **14(1)**: pp.55 – 63.
- 84 Hackbarth, J. J. (2006) "Multivariate Analysis of Beer Foam stand", *J. Inst. Brew.*, **112(1)**: pp. 17-24.

## REFERENCES

---

- 85 Kaspar. S., Matros, A., Kipping, M., Seiffert, U., Mock, H-P. (2009) “Analysis of kinetic patterns in barley grain development using LC-MS<sup>E</sup> approach coupled to multivariate statistics“, *Poster Presentation 18<sup>th</sup> IMSC, Bremen*, **Poster No. PMM 203**.
- 86 Pancholi, V., Chhatwal. G. S. (2003) “Housekeeping enzymes as virulence factors for pathogens“, *Int. J. Med. Microbiol.*, **293**: pp. 391-401.

## APPENDIX

---



APPENDIX

Appendix A

Appendix A Summary of enzymatic MCT approaches.

enzyme product	Corolase 7089	Corolase TS	Corolase L10	Corolase LAP	Gammaprotease RFG 660L	Corolase PP	Rohalase Barley L	Rohalase SEP
<b>enzyme type</b>	Bacillolysin ( <i>Bac. subtilis</i> )	Thermolysin ( <i>Bac. staerothermophilus</i> )	Papain ( <i>Papain peptidase II</i> )	Leucylaminopeptidase ( <i>Asp. sojae</i> )	Subtilisin Carlsberg	Trypsin ( <i>Bovine Pancreas</i> )	Endo-1,3 (4)- $\beta$ -glucanase	Endo-1,4- $\beta$ -xylanase
<b>description</b>	neutral endopeptidase	solely endopeptidase	endopeptidase	exopeptidase	bacterial, alkaline protease	endo-, amino- and carboxypeptidase	$\beta$ -glucanase activity	xylanase and $\beta$ -glucanase activity
<b>activity</b>	850 UHb/g minimum activity	550 UHb/g minimum activity	850 UHb/g	350 LAP/g	no definition	2500 UHb/g	300000 BU/g	225000 BXU/g 250500 Bu/g
<b>function</b>	hydrolysis of peptide bonds	hydrolysis in high temperature	hydrolysis	hydrolysis (combined with endopeptidase)	hydrolysis of peptides/amides	undefined	xylanase- and cellulase-activity	degradation of soluble pentosans
<b>mechanism I</b>	cleavage of Gly, Ala, Leu and rarely Val	cleavage at neutral/weak alkaline	cleavage at hydrophobic side chains	N-terminal cleavage of single AA	prefers large, uncharged bonds at position P1	Arg-t, Lys-t	degradation of $\beta$ -glucane, pentosane and polysaccharide (but no starch)	degradation of polysaccharides (but no starch)
<b>mechanism II</b>	Gly-tLeu or Phe-tLeu; -/-/Gfa/Gf-tL/A/-/-	X-tLeu, X-tPhe		X-tY (X mostly leucine and Y proline)				
<b>optimal pH</b>	7 – 7.5	7 – 7.5	6 – 7	6 – 9	9 – 10 (range 7 – 10.5)	7 – 9	5 – 6 (range 3 – 7)	5
<b>optimal temperature [°C]</b>	50 – 55 (max.)	70 – 75 (max.)	60	60 – 65 (max.)	55 – 60 (range 30 – 65)	40 – 45	55 – 65 (range 30 – 70)	50
<b>MM [Da]</b>	56522	59580	38922	41179	38908	32499	undefined	undefined
<b>dosage (adapted to protein amounts)</b>	0.01 – 0.5 %	0.01 – 0.5 %	1 – 3 mL per hL beer	0.02 – 0.5 %	0.05 – 0.5 %	0.01 – 0.5 %	0.1 – 0.3 mL per hL beer	no data
<b>dosage (adapted to brew house)</b>	50 – 250 g/t malt	no data	no data	no data	no data	no data	20 – 100 g/t malt	25 – 100 g/t malt
<b>test dosage I (wort)</b>	15 $\mu$ L (10-fold concentration)	7.2 $\mu$ L (10-fold concentration)	15 $\mu$ L	15 $\mu$ L	10 $\mu$ L (0.05 %)	0.01 %	2 $\mu$ L (0.01 %)	2.5 $\mu$ L (0.01 %)
<b>result I</b>	gushing inhibition in MCT-extract	gushing inhibition	maybe positive in malt extract	negative in extract	gushing inhibition in malt extract but no effect in barley	decrease in malt extract	suppression of gushing in malt extract, no effect with barley	decrease in barley and malt extract
<b>test dosage II</b>	2 $\mu$ L (equalling 0.01 % protein)	2 $\mu$ L (equalling 0.01 % protein)	2 $\mu$ L (equalling 0.01 % protein)	4 $\mu$ L (equalling 0.02 % protein)		0.01 %		
<b>result II</b>	inhibition in malt extracts, decrease with barley	inhibition of only gushing malt	decrease of gushing tendencies	inhibition in malt extract, decrease with barley		inhibition in malt extract, decrease with barley		

APPENDIX

enzyme product	Rohament CL	$\alpha$ -chymo- trypsin	Heparinase I	Papain	Thermolysin	Alkozym S 500	Dexlo CL	Lyticase
enzyme type	endo-1,4- $\beta$ -glucanase	$\alpha$ -chymotrypsin (bovine pancreas)	Heparinase I ( <i>Flavobacterium heparinum</i> )	papain ( <i>papaya latex</i> )	<i>Bacillus thermoproteolyticus</i>	<i>Aspergillus niger</i>	bacterial source	lyticase ( <i>Athrobacter luteus</i> )
description	carbohydrase	serine-protease	glycosamine-glycane	cystein-protease	extracellular metallo-endopeptidase	amyl-glucosidase	$\alpha$ -amylase	carboenzyme
activity	15000 ECU/g	102 U/mg	97 U/mL	16 – 40 U/mg	40 U/mg	32400 AGI/mL	24000 RAU/g	$\geq$ 2000 U/g
function	cleaves glucanes, xylane, cellulose	cleavage of peptidic bonds	creates disaccharides	cleavage at alkaline amino acids	cleavage at hydrophobic AA	cleaves starch bonds	digestion of starch	yeast cell wall glucan hydrolysis
mechanism	degradation of polysaccharides (no starch)	bonds with large hydrophobic or aromatic side chains preferred	cleavage between hexoseamines and O-sulfurized iduronacids	cleavage at Leu and Gly hydrolysis of esters and amids	cleaves bonds with hydrophobic amino acids (N-terminus)	hydrolysis of 1,4- and few 1,6- $\alpha$ -starch bonds	cleavage of $\alpha$ -bonds	hydrolyses poly- $\beta$ -(1 $\rightarrow$ 3)-glucose
optimal pH	4 – 5	7.8	pI 8.5	6 – 7	8	4.2 – 5	6 (range 4 – 8)	7.5
optimal temperature [°C]	60	25	25	25	70	55 – 60	up to 80	25
molecular mass [Da]	no definition	25000	43000	23406	37500	undefined	undefined	undefined
dosage (adapted to protein)	0.5 – 1 mL/hL wort	8 U per CBT	8 U per CBT	8 U per CBT	8 U per CBT	0.5 L/t cereal starch	0.2 L/t cereals	no data
dosage (adapted to brew house)	100 – 150 mL/t malt	no data	no data	no data	no data	no data	no data	no data
test dosages (wort)	5 $\mu$ L	70 $\mu$ L (8 U)	82 $\mu$ L (8 U)	15 $\mu$ L	100 $\mu$ L	50 $\mu$ L (8 U)	20 $\mu$ L	3.2 $\mu$ L (8 U)
results	only decrease of gushing, effect better than with Rohalase Barley L and SEP	decrease of gushing with malt, no effect with barley	no effect in barley extract, decrease in malt extract	bisection of gushing potential of barley and malt samples	bisection of barley gushing potential barley, complete suppression in malt	decrease with barley, nearly suppression with malt	decrease with barley, stronger suppression with malt but no total inhibition	decrease of gushing in case of malt extract but no complete inhibition

APPENDIX

Appendix B

Appendix B1: Barley peptide masses and sequences identified in a gushing Ireks (100 %) malt.

Full protein name	Detected sequence	Position	Ion charge	[M+H] <sup>+</sup> average	No. of AA	Sequence coverage [%]
SPZ4_HORVU	K-VLKLPLYAK	229 – 236	2	932.19	399	4.5
BSZ7_HORVU	R-LVLGNALYFK	175 – 184	2	1138.39	396	2.5
BSZx_HORVU	R-LVLGNALYFK	171 – 180	2	1138.39	398	3.01
IAAB_HORVU	R-FFMGRK	86 – 91	2	785.98	125	40.8
	R-DYVEQQACR	46 – 54	2	1112.2		
	R-IETPGPPYLAK	55 – 65	2	1186.39		
	R-KSRPDQSGLMELPGCPR	91 – 107	3	1872.16		
	K-SRPDQSGLMELPGCPR	92 – 107	3	1743.99		
	R-EVQMDFVR	108 – 115	2	1024.18		
LE19A_HORVU	R-EGIDIDESKFK	80 – 90	2	1281.40	93	11.8
LE19B_HORVU	R-EGIDIDESKFK	80 – 90	2	1281.40	93	11.8
LE193_HORVU	R-EGIDIDESKFK	120 – 130	2	1281.40	133	8.3
LE194_HORVU	R-EGIDIDESKFK	140 – 150	2	1281.40	153	7.2
IAAA_HORVU	R-CCQELDEAPQHCR	74 – 86	3 and 2	1532.70	120	18.3
	R-SHPDWSVLK	98 – 106	2	1069.20		
ICIC_HORVU	K-TSWPEVVGMSAE	16 – 28	2	1421.60	77	15.6
ICIA_HORVU	K-TSWPEVVGMSAEK	26 – 38	2	1421.60	83	15.7
IAAE_HORVU	R-LLTSDMKR	58 – 65	2	964.17	124	16.9
	R-TYVVSQICHQGPR	45 – 57	2 and 3	1488.70		
BARW_HORVU	R-VTNPATGAQITAR	69 – 81	2	1300.45	125	26.6
	K-YGWTAFCGPAGPRQAACGK	46 – 65	3	1999.27		
	K-YGWTAFCGPAGPR	46 – 58	2	1383.56		
NLTP1_HORVU	R-QTVCNCLK	71 – 78	2	909.10	91	70.32
	R-GIHNLNLNNAASIPSK	83 – 98	2 and 3	1663.87		
	K-CNVNVPYTISPDIIDCSR	99 – 115	2	1897.12		
	R-GIHNLNLNNAASIPSKCNVN	83 – 115	4	3541.97		
	VPLYTISPDIIDCSR					
	K-CNVNVPYTISPDIIDCSRI	83 – 116	2	2008.93		
K-M <sup>1</sup> KPCLTYVQGGPGSPGECNGVR	36 – 58	3	2370.73			
Q5UNP2_HORVD	K-CGVNIPYAISPRDTCCK	106 – 122	2	1967.26	124	21.77
	K-CGVNIPYAISPR	106 – 117	2	1290.52		
	R-SLNAAAATPADR	66 – 77	2	1158.25		
Q9SES6_HORVU	K-CNVNLPYKISPSVDCNSIH	103 – 121	3	2103.99	121	27.3
	K-NVANAAPGGSEITR	82 – 95	2	1357.46		
IAA1_HORVU	K-S QCAGGQVVES IQK	40 – 53	2	1434.6	132	26.5
	K-ELGVALADD KATVAEVFPG CR	82 – 102	3	2162.46		
HOG3_HORVU	R-QQCCQQLANINEQSR	181 – 195	2	1763.84	289	5.2
REHY_HORVU	K-LSFLYPSCTGR	140 – 150	2	1244.45	218	5.0
PR12_HORVU	K-LQAFANQYANQR	53 – 64	2	1424.55	140	8.6
	R-GVFITCNYEPR	145 – 155	2	1299.48		
PR13_HORVU	K-LQAFANQYANQR	53 – 64	2	1424.55	140	25.7
	R-AAVGVGAVSWSTK	40 – 52	2	1233.40		
	R-GVFITCNYEPR	145 – 155	2	1299.48		
PR1_HORVU	K-LQAFANQYANQR	53 – 64	2	1424.55	140	25.7
	R-GVFITCNYEPR	145 – 155	2	1299.48		
	R-AAVGVGAVSWSTK	40 – 52	2	1233.40		
LEA1_HORVU	K-AAEAKDKTAQTAQAAK	67 – 93	4	2811.07	213	30.5
	DKTYETAQAAK					
	K-ASDTAQYTKESAVAGKDKTG SVLQQAGETVVNAVVGAK					
NLTP2_HORVU	R-DTLNLCCGIPVPHC	90 – 102	2	1382.63	67	19.4
IAAD_HORVU	R-LLVAPGQCENLATIHNVNR	144 – 160	3	1820.16	147	21.8
	K-LYCCQELAEIPQQCR	84 – 98	2	1798.09		
IAA2_HORVU	K-LECVGNRVPEDVLR	57 – 70	3	1599.84	122	53.3
	R-ALVK <sup>2</sup> LECVGNRVPEDVLR	53 – 70	3	2011.39		
	R-SVYAALGVGGGPEEVFPGCQ	95 – 119	3	2539.92		
	KDVMK					

## APPENDIX

	R-DCCQEVANISNEWCR	71 – 85	2	1770.94		
	K-LLVAGVPALCNVPIPNAAAGTR	120 – 141	3	2176.58		
Q02056_HORVU	K-AQQLAAQLPAMCR	418 – 430	2	1401.68	441	5.2
	K-AQQLAAQLPAM <sup>1</sup> CR	418 – 430	2	1417.68		
Q84LE9_HORVU	K-AQQLAAQLPAMCR	734 – 736	2	1401.68	757	1.8
	K-AQQLAAQLPAM <sup>1</sup> CR	734 – 736	2	1417.68		
	R-ELQESSLEACR	44 – 54	2	1265.38		
Q40054_HORVU	R-ELQESSLEACR	44 – 54	2	1265.38	679	3.5
	K-AQQLAAQLPAMCR	684 – 696	2	1401.68		
	K-AQQLAAQLPAM <sup>1</sup> CR	684 – 696	2	1417.68		
Q40045_HORVU	R-ELQESSLEACR	44 – 54	2	1265.38	454	2.4
Q1ENF0_HORVU	R-LFVDAADGSGR	85 – 95	2	1108.19	122	9.0
	R-GEQQVVSVMNYR	73 – 84	2	1368.50		
tryp./amyl. pUP13	K-SIPINPLPACR	26 – 36	2	1181.40	136	22.8
	R-DYGEYCRVVK	16 – 25	3	1990.31		
	R-ELSDLPESCR	61 – 70	2	1149.21		
P93180_HORVU	R-VTNPATGAQITAR	90 – 102	2	1299.75	146	8.9
IAA_HORVU	R-ELAAVPDHCR	73 – 82	2	1111.26	126	7.9
HINB1_HORVU	K-LGGIFGIGGGDVFK	108-121	2	1337.56		
CYSP1_HORVU	R-AVANQPVSVAVEASGK	262 – 277	2	1527.71	238	12.6
	K-NSWGPSWGEQGYIR	318 – 331	2	1637.75		
CYSP2_HORVU	R-AVANQPVSVAVEASGK	262 – 277	2	1527.71	240	12.5
	K-NSWGPSWGEQGYIR	318 – 331	2	1637.75		
Q2V8X0_HORVU	R-ELAAVPDHCR	73 – 82	2	1111.26	147	6.8
B5TWD1_HORVD	K-ESAVAGKDKTGSVLQQAGET VVNAVVGAK	149 – 177	4	2815.15	212	17.9
	K-ASDTAQYTKESAVAGKDKTG SVLQQAGETVVNAVVGAK	140 – 177	4	3781.16		
B5TWD0_HORVD	K-ESAVAGKDKTGSVLQQAGET VVNAVVGAK	149 – 177	4	2815.15	213	17.8
	K-ASDTAQYTKESAVAGKDKTG SVLQQAGETVVNAVVGAK	140 – 177	4	3781.16		
B5TWC9_HORVD	K-ESAVAGKDKTGSVLQQAGET VVNAVVGAK	149 – 177	4	2815.15	214	17.8
	K-ASDTAQYTKESAVAGKDKTG SVLQQAGETVVNAVVGAK	140 – 177	4	3781.16		
Q40036_HORVU	R-VVTTNPQTR	61 – 70	2	1163.31	89	11.2
CMd3_HORVU	R-LLVAPGQCNLATIHNR	144 – 160	3	1820.16	146	11.64

<sup>1</sup>methionine oxidized to methionine sulfoxide, <sup>2</sup>sequence conflict, <sup>3</sup>Cys\_PAM acrylamide adducts, <sup>4</sup>Cys\_CAM carbamidomethyl cysteine

### Appendix B2: Peptide masses and sequences of other origin identified in a gushing Ireks malt.

Full protein name	Detected sequence	Position	Ion charge	[M+H] <sup>+</sup> average	No. of AA	Sequence coverage [%]
GLT3_WHEAT Glutenin, high molecular mass subunit 12	R-ELQESSLEACR	34 – 44	2	1265.38	639	1.7
GLT0_WHEAT Glutenin, high molecular mass subunit DY10	R-ELQESSLEACR	34 – 44	2	1265.38	627	1.8
GRXC6_ORYSJ Glutaredoxin-C6	R-TVPNVFINGK	66 – 75	2	1089.27	112	8.9
GRDH_ORYSJ Glucose and ribitol dehydrogenase homolog	K-VAIVTGGDSGIGR	42 – 54	2	1202.35	300	4.3
Q41540_WHEAT CM 17 protein	R-IEMPGPPYLAK	55 – 65	2	1216.48	119	9.2
Q43663_WHEAT Wali3 protein	R-FFSGAVVCDDAGPK	37 – 50	2	1413.58	88	15.9
P02862 GLT2_WHEAT Glutenin, high molecular mass subunit PC237	K-AQQLAAQLPAMCR	16 – 28	2	1400.71	39	33.3
P02861 GLT1_WHEAT Glutenin, high molecular mass subunit PC256	K-AQQLAAQLPAMCR	78 – 90	2	1400.71	101	12.9
P08489 GLT4_WHEAT Glutenin, high molecular mass subunit PW212	K-AQQLAAQLPAMCR	815 – 827	2	1400.71	817	1.6
P10388 GLT5_WHEAT Glutenin, high molecular mass subunit DX5	K-AQQLAAQLPAMCR	816 – 828	2	1400.71	818	1.6
Q4W1F9_WHEAT 5a2 protein	K-ANIPCLCAGVTK	46 – 57	2	1189.6	94	12.8

APPENDIX

**Appendix B3: Barley peptide masses and sequences identified in a non gushing Durst (100 %) malt.**

Full protein name	Detected sequence	Position	Ion charge	[M+H] <sup>+</sup> average	No. of AA	Sequence coverage [%]
SPZ4_HORVU	K-VLKLPLYAK	229 – 236	2	932.19	399	15.04
	K-ISYQFEASSLLR	291 – 302	2	1414.6		
	R-LA <sup>2</sup> SAISSNPER-A	22 – 36	2	1145.45		
	K-R <sup>1</sup> LSTEPEFIENHIPK	262 – 276	3	1811.04		
BSZ7_HORVU	K-TFVEVDEEGTK	336 – 346	2	1254.33	396	2.78
IAAB_HORVU	R-FFMGRK	86 – 91	2	785.98	125	52.8
	R-DYVEQQACR	46 – 54	2	1112.2		
	R-IETPGPPYLAK	55 – 65	2	1186.39		
	R-KSRPDQSGLMELPGCPR	91 – 107	3	1872.16		
	K-SRPDQSGLMELPGCPR	92 – 107	3	1743.99		
	K-QCCGELANIPQQCR	66 – 80	2	1691.93		
	R-EVQMDFVR	108 – 115	2	1024.18		
LE19A_HORVU	K-SLEAQQNLAEGR	30 – 41	2	1316.41	93	26.8
	R-EGETVVPGGTGGK	17 – 29	2	1188.27		
LE19B_HORVU	R-EGETVVPGGTGGK	17 – 29	2	1188.27	93	14
LE193_HORVU	R-EGETVVPGGTGGK	17 – 29	2	1188.27	133	9.8
LE194_HORVU	R-EGETVVPGGTGGK	17 – 29	2	1188.27	153	8.5
IAAA_HORVU	R-CCQELDEAPQHCR	74 – 86	2	1532.70	120	23.3
	R-RSHPDWSVLK	97 – 106	3	1225.39		
	R-YFIGRRSHPDWSVLK	92 – 106	3	1862.14		
	R-SHPDWSVLK	98 – 106	2	1069.20		
ICIC_HORVU	K-TSWPEVVGMSAE	16 – 28	2	1421.60	77	15.6
ICIA_HORVU	K-TSWPEVVGMSAEK	26 – 38	2	1421.60	83	15.7
IAAE_HORVU	R-LLTSDMKR	58 – 65	2	964.17	124	16.9
	R-TYVVSQICHQGPR	45 – 57	2 and 3	1488.70		
BARW_HORVU	R-VTNPATGAQITAR	69 – 81	2	1300.45	125	28
	R-SK <sup>2</sup> YGWTAFCGPAGPR	44 – 58	2 and 3	1598.81		
	K-YGWTAFCGPAGPRGQAACGK	46 – 65	3	1998.90		
NLTP1_HORVU	R-DLHNQAQSSGDRQTVCNCLK	59 – 78	2 and 3	2218.42	91	84.6
	R-GIHNLNLNNAASIPSK	83 – 98	2 and 3	1663.87		
	K-M <sup>1</sup> KPCLTYVQGGPGPSGECNGVR	36 – 58	2 and 3	2370.73		
	D-RQTVCNCLKGIAR <sup>2</sup>	71 – 82	2 and 3	1306.58		
	R-GIHNLNLNNAASIPSKCNVNPY TISPDIDCSR	83 – 115	4	3541.97		
	R-QTVCNCLK	71 – 78	2	909.10		
	K-MKPCLTYVQGGPGPSGECNGVR	36 – 58	2 and 3	2352.2		
	K-MKPCLTYVQGGPGSGEC-CNGVRDLHNQAQSSGDR	36 – 70	4	3664.6		
	K-CNVNPY TISPDIDCSR I	99 – 116	2	2010.93		
Q5UNP2_HORVD	R-SLNAATAADR	66 – 77	2	1158.25	124	25.8
	K-QQTSGMGGIKPDLVAGIPSK	86 – 105	3	1986.05		
Q9SES6_HORVU	K-ISPSVDCNSIH	111 – 121	2	1172.29	121	19.8
	K-NVANAAPGGSEITR	82 – 95	2	1357.46		
IAAC_HORVU	R-ELAGISSNCR	71 – 80	2	1049.5	119	8.4
IAA1_HORVU	K-S QCAGQVVES IQK	40 – 53	2	1434.6	132	26.5
	K-ELGVALADD KATVAEVFPG CR	82 – 102	3	2162.46		
	K-ATVAEVFPG CR	92 – 102	2	1150.33		
HOG3_HORVU	R-QCCQQLANINEQSR	181 – 195	2	1763.84	289	5.2
REHY_HORVU	K-RGVKLLGISC <sup>4</sup> DDVQSHK	63 – 79	3	1913.2	218	12.8
	K-VTYPIMADPDR	94 – 104	2	1277.6		
PR12_HORVU	R-GVFITCNYEPR	145 – 155	2	1299.48	140	7.9
	K-LQAFAQNYANQR	53 – 64	2	1424.55		
PR13_HORVU	R-GVFITCNYEPR	145 – 155	2	1299.48	140	7.9
NLTP2_HORVU	R-AQQGLCQYVK	65 – 75	2	1241.46	67	35.8
	R-DTLNLCGIPVPHC	90 – 102	2	1382.63		
IAAD_HORVU	R-LLVAPGQC NLATIHNVR	144 – 160	3	1820.16	147	21.8

APPENDIX

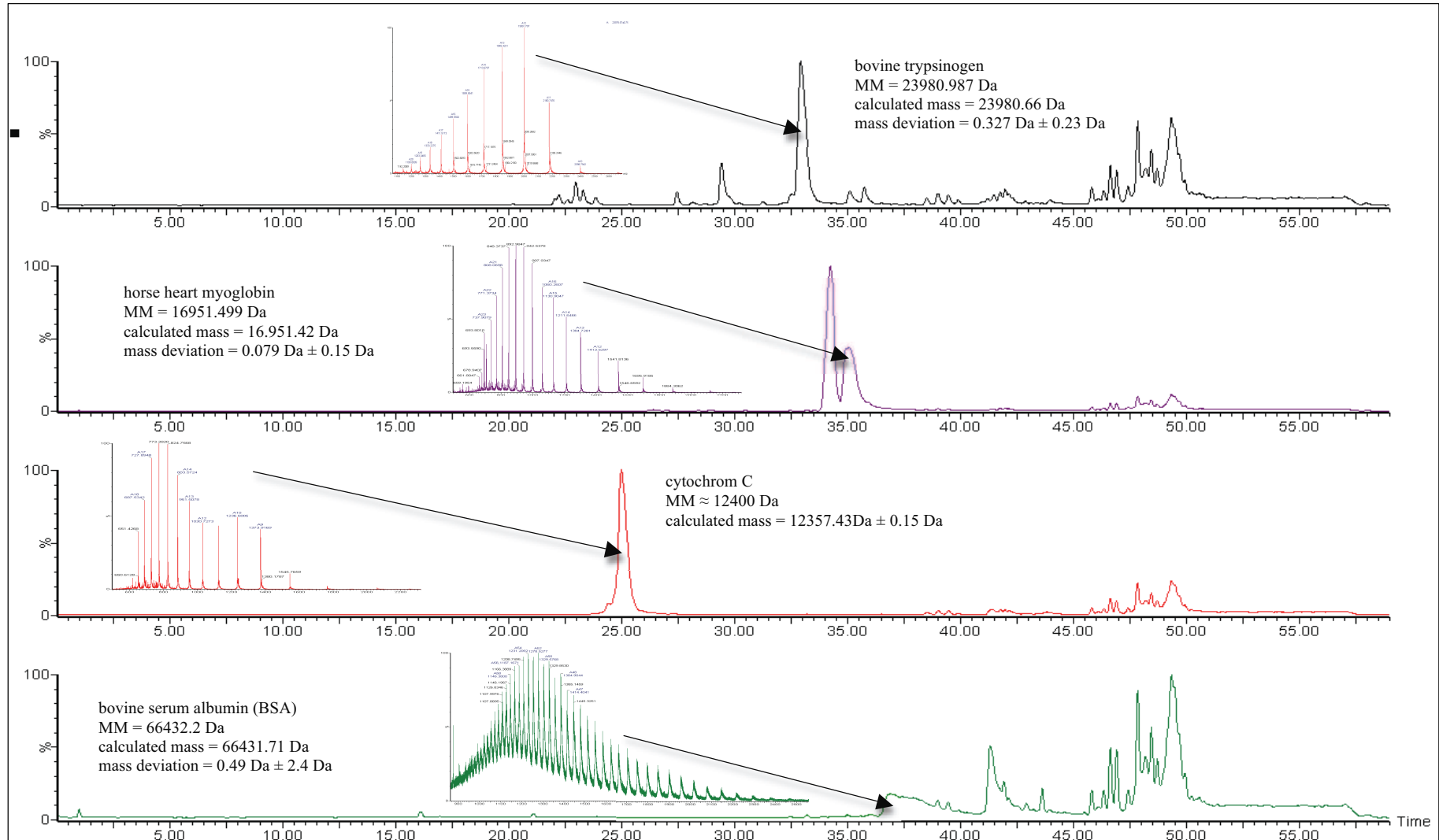
	K-LYCCQELAEIPQQCR	84 – 98	2	1798.09		
IAA2_HORVU	K-LECVGNRPEDVLR	57 – 70	3	1599.84	122	69.7
	R-CGDLGSMRLR	86 – 94	2	952.13		
	R-SVYAAALGVGGGPEEVFPGCQ KDVMK	95 – 119	3	2539.92		
	R-DCCQEVAANISNEWCR	71 – 85	2	1770.94		
	K-LLVAGVPALC NVPIPNEAAGTR	120 – 141	2	2176.58		
	R-SVYAAALGVGGGPEEVFPGCQ K	95 – 115	2	2066.33		
	R-SVYAAALGVGGGPEEVFPGCQ KDVM <sup>1</sup> K	95 – 119	3	2555.92		
	Q84LE9_HORVU	R-ELQESSLEACR	44 – 54	2	1265.38	757
R-LFVDAADGSGR		85 – 95	2	1108.19		
K-AQQLAAQLPAMCR		734 – 746	2	1400.7		
R-DVSPECRPVALSQVVR		81 – 96	3	1755.9		
Q40054_HORVU	R-ELQESSLEACR	44 – 54	2	1265.38	679	5.89
	R-LFVDAADGSGR	85 – 95	2	1108.19		
	K-AQQLAAQLPAMCR	684 – 696	2	1400.7		
	R-DVSPECRPVALSQVVR	81 – 96	3	1755.9		
Q40045_HORVU	R-ELQESSLEACR	44 – 54	2	1265.38	454	5.9
	R-LFVDAADGSGR	85 – 95	2	1108.19		
	R-DVSPECRPVALSQVVR	81 – 96	3	1755.9		
Q1ENF0_HORVU	R-LFVDAADGSGR	85 – 95	2	1108.19	122	18.9
	R-GEQQVVSGMNYR	73 – 84	2	1367.63		
tryp./amyl. pUPI3	R-CAVGDQQVPDVLK	43 – 55	2	1372.57	136	9.6
P93180_HORVU	R-VTNPATGAQITAR	90 – 102	2	1299.75	146	8.9
IAA_HORVU	R-ELAAVPDHCR	73 – 82	2	1111.26	126	7.9
CYSP1_HORVU	R-AVANQPVSVAVEASGK	262 – 277	2	1527.71	238	6.7
CYSP2_HORVU	K-NSWGPSWGEQGYIR	318 – 331	2	1637.75	240	12.5
	R-AVANQPVSVAVEASGK	262 – 277	2	1527.71		
Q2V8X0_HORVU	R-ELAAVPDHCR	73 – 82	2	1111.26	147	6.8
A9E4H2_HORVU*	R-SCEEVQDCCQQLR	89 – 102	2	1669.83	127	11.0
Q03678_HORVU	K-LGSPAQELTFGRPAR	566 – 580	3	1600.81	637	3.9
Q40036_HORVU	R-VVTTNPQTFR	61 – 70	2	1163.31	89	11.2
Cmd3_HORVU	R-LLVAPGQCNLATIHNV	144 – 160	3	1820.16	146	11.64

<sup>1</sup>methionine oxidized to methionine sulfoxide, <sup>2</sup>sequence conflict, <sup>3</sup>Cys\_PAM acrylamide adducts, <sup>4</sup>Cys\_CAM carbamidomethyl-cysteine, \*43 grain softness protein species possible

**Appendix B4: Peptide masses and sequences of other origin identified in a non gushing Durst malt.**

Full protein name	Detected sequence	Position	Ion charge	[M+H] <sup>+</sup> average	No. of AA	Sequence coverage [%]
GLT3_WHEAT Glutenin, high molecular mass subunit 12	R-ELQESSLEACR	34 – 44	2	1265.38	639	1.7
GLT0_WHEAT Glutenin, high molecular mass subunit DY10	R-ELQESSLEACR	34 – 44	2	1265.38	627	1.8
GRXC6_ORYSJ Glutaredoxin-C6	R-TVPNVFINGK	66 – 75	2	1089.27	112	8.9
GRDH_ORYSJ Glucose and ribitol dehydrogenase homolog	K-VAIVTGGDSGIGR	42 – 54	2	1202.35	300	4.3
P16159 IAC16_WHEAT Alpha-amylase/trypsin inhibitor CM16	K-QQCCGELANIPQQCR	66 – 80	2	1690.74	119	10.9
P02862 GLT2_WHEAT Glutenin, high molecular mass subunit PC237	K-AQQLAAQLPAMCR	16 – 28	2	1400.71	39	33.3
P02861 GLT1_WHEAT Glutenin, high molecular mass subunit PC256	K-AQQLAAQLPAMCR	78 – 90	2	1400.71	101	12.9
P08489 GLT4_WHEAT Glutenin, high molecular mass subunit PW212	K-AQQLAAQLPAMCR	815 – 827	2	1400.71	817	1.6
P10388 GLT5_WHEAT Glutenin, high molecular mass subunit DX5	K-AQQLAAQLPAMCR	816 – 828	2	1400.71	818	1.6
Q4W1F9_WHEAT 5a2 protein	K-ANIPCLCAGVTK	46 – 57	2	1189.6	94	12.8

## Appendix C



Appendix C Measurement of the mass accuracy with protein standards for top down investigations. The standards were analysed as single proteins but also in mixture.

APPENDIX

**Appendix D**

**Appendix D1: Precursor ion masses and charges for proteins identified in malt extracts via bottom up approaches with fractionation and DDA experiments in infusion mode.**

Full protein name	Accession	No. of ions	Peptide ion [m/z] and ion charge		
SPZ4_HORVU Protein Z4	P06293	9	577.71 (2+)	509.21 (3+)	685.28 (2+)
			563.7 (3+)	707.44 (2+)	466.29 (2+)
			572.78 (2+)	603.95 (3+)	645.66 (4+)
BSZ7_HORVU Serpin-Z7	Q43492	2	569.33 (2+)	627.24 (2+)	
Q40066 SPZx_HORVU protein Zx	Q40066	1	569.34 (2+)		
IAAB_HORVU Alpha-amylase/trypsin inhibitor CMb	P32936	11	556.29 (2+)	520.23 (2+)	586.92 (3+)
			593.4 (2+)	845.84 (2+)	512.22 (2+)
			650.27 (2+)	952.96 (3+)	393.21 (2+)
			581.36 (3+)	624.27 (3+)	
IAAA_HORVU Alpha-amylase/trypsin inhibitor CMa	P28041	9	620.32 (2+)	328.15 (2+)	408.86 (3+)
			593.63 (3+)	573.06 (4+)	511.15 (3+)
			425.93 (4+)	567.69 (3+)	534.72 (2+)
ICIC_HORVU Subtilisin-chymotrypsin inhibitor CI-1C	P01054	2	421.78 (2+)	710.92 (2+)	
ICIA_HORVU Subtilisin-chymotrypsin inhibitor CI-1A	P16062	4	421.78 (2+)	747.32 (2+)	710.92 (2+)
			747.33 (2+)		
IAAE_HORVU Trypsin inhibitor CMe	P01086	3	404.20 (2+)	744.38 (2+)	496.58 (3+)
BARW_HORVU Barwin	P28814	7	650.31 (2+)	557.98 (3+)	533.21 (3+)
			799.26 (2+)	1033.05 (4+)	737.44 (3+)
			691.81 (2+)		
NLTP1_HORVU Non-specific lipid transfer protein 1	P07597	11	554.94 (3+)	831.97 (2+)	790.36 (3+)
			784.97 (2+)	1004.98 (2+)	654.36 (4+)
			885.52 (4+)	739.63 (3+)	435.92 (3+)
			948.35 (2+)	1177.0 (2+)	
Q5UNP2_HORVD Non-specific lipid transfer protein	Q5UNP2	2	579.34 (2+)	645.35 (2+)	
Q9SES6_HORVU Non-specific lipid transfer protein	Q6SES6	2	678.87 (2+)	586.22 (2+)	
REHY_HORVU 1-Cys peroxiredoxin PE	P52572	2	435.89 (3+)	639.29 (2+)	
LEA1_HORVU ABA-inducible protein PHV A1	P14928	2	861.66 (2+)	861.66 (3+)	
IAAD_HORVU Alpha-amylase/trypsin inhibitor CMd	P11643	6	910.05 (2+)	607.03 (3+)	1116.28 (3+)
			1110.84 (3+)	599.67 (3+)	898.95 (2+)
IAA2_HORVU Alpha-amylase inhibitor BDAI-1	P13691	9	533.72 (3+)	670.00 (3+)	476.2 (2+)
			1033.01 (2+)	846.75 (3+)	725.82 (3+)
			414.19 (2+)	590.55 (3+)	885.34 (2+)
Q02056_HORVU D-hordein (fragment)	Q02056	2	700.86 (2+)	708.85 (2+)	
Q1ENF0_HORVU Cystatin Hv-CPI8 trypsin/amylase inhibitor pUP13	Q1ENF0	2	554.27 (2+)	684.27 (2+)	
			225102 (NCBI)	574.78 (2+)	686.32 (2+)
			663.93 (3+)	509.97 (3+)	621.35 (3+)
IAA_HORVU Alpha-amylase/trypsin inhibitor	P16969	1	555.77 (2+)		
HINB1_HORVU Hordoindoline-B1	Q9FSI9	1	668.87 (2+)		
Q2V8X0_HORVU Limit dextrinase inhibitor	Q2V8X0	1	555.78 (2+)		
Q40036_HORVU Putative protease inhibitor	Q40036	1	581.77 (2+)		
O23997_HORVU PR5	O23997	1	956.95 (2+)		
Q946Z0_HORVU Thaumatin-like prot. TLP6	Q946Z0	1	956.95 (2+)		
O22462_HORVU Barperml	O22462	1	956.95 (2+)		
Q03678_HORVU Embryo globulin	Q03678	1	533.96 (3+)		
O24000_HORVU CMd3	O24000	1	1121.61 (3+)		
GLT3_WHEAT Glutenin, high molecular mass subunit 12	P08488	1	632.71 (2+)		
GLT0_WHEAT Glutenin, high molecular mass subunit DY10	P10387	1	632.71 (2+)		
Q41540_WHEAT CM 17 protein	Q41540	1	608.37 (2+)		
Q43663_WHEAT Wali3 protein	Q43663	1	706.82 (2+)		
IAC16_WHEAT $\alpha$ -amylase/trypsin inh. CM16	P16159	1	845.88 (2+)		
G3P2_YEAST Glyceraldehyde-3-phosphate dehydrogenase 2	P00358	1	687.86 (2+)		



## APPENDIX

### Appendix D2: Precursor ion masses and charges for proteins identified in congress wort in bottom up approaches with direct DDA experiments.

Full protein name	Accession	No. of ions	Peptide ion [m/z] and ion charge		
SPZ4_HORVU Protein Z4	P06293	1	707.32 (2+)		
IAAB_HORVU Alpha-amylase/trypsin inhibitor CMb	P32936	4	593.38 (2+)	512.29 (2+)	556.29 (2+)
IAAA_HORVU Alpha-amylase/trypsin inhibitor CMa	P28041	1	534.76 (2+)		
ICIA_HORVU Subtilisin-chymotrypsin inhibitor CI-1A	P16062	1	747.32 (2+)		
IAAE_HORVU Trypsin inhibitor CMe	P28041	1	764.67 (3+)		
BARW_HORVU Barwin	P28814	1	650.31 (2+)		
NLTP1_HORVU Non-specific lipid transfer protein 1	P07597	1	554.94 (3+)		
Q5UNP2_HORVD Non-specific lipid transfer protein	Q5UNP2	1	579.3 (2+)		
Q9SES6_HORVU Non-specific lipid transfer protein	Q6SES6	1	678.81 (2+)		
LEA1_HORVU ABA-inducible protein PHV A1	P14928	1	861.87 (2+)		
IAAD_HORVU Alpha-amylase/trypsin inhibitor CMd	P11643	1	606.99 (3+)		
Q1ENF0_HORVU Cystatin Hv-CPI8	Q1ENF0	1	554.28 (2+)		
IAA_HORVU Alpha-amylase/trypsin inhibitor	P16969	1	448.55 (3+)		
HINB1_HORVU Hordoindoline-B1	Q9FSI9	1	668.87 (2+)		
Q2V8X0_HORVU Limit dextrinase inhibitor	Q2V8X0	1	448.55 (3+)		
Q40036_HORVU Putative protease inhibitor	Q40036	1	581.77 (2+)		
O23997_HORVU pathogenesis-related protein PR5	O23997	2	965.93 (2+)	638.27 (3+)	
Q946Z0_HORVU Thaumatin-like protein TLP6	Q946Z0	2	965.93 (2+)	638.27 (3+)	
O22462_HORVU Barperml	O22462	2	956.93 (2+)	638.27 (3+)	
Q03678_HORVU Embryo globulin	Q03678	1	533.96 (3+)		
Q41540_WHEAT CM 17 protein	Q41540	1	608.37 (2+)		

### Appendix D3: Precursor ion masses and charges for proteins identified in unhopped first wort in bottom up approaches with direct DDA experiments.

Full protein name	Accession	No. of ions	Peptide ion [m/z] and ion charge		
SPZ4_HORVU Protein Z4	P06293	6	572.76 (2+)	645.55 (4+)	577.75 (2+)
IAAB_HORVU Alpha-amylase/trypsin inhibitor CMb	P32936	2	603.97 (3+)	879.11 (4+)	707.32 (2+)
IAAB_HORVU Alpha-amylase/trypsin inhibitor CMb	P32936	2	593.29 (2+)	512.26 (2+)	
IAAA_HORVU Alpha-amylase/trypsin inhibitor CMa	P28041	2	534.81 (2+)	408.85 (3+)	
ICIC_HORVU Subtilisin-chymotrypsin inhibitor CI-1C	P01054	1	710.84 (2+)		
ICIA_HORVU Subtilisin-chymotrypsin inhibitor CI-1A	P16062	2	710.84 (2+)	747.3 (2+)	
BARW_HORVU Barwin	P28814	1	650.34 (2+)		
NLTP1_HORVU Non-specific lipid transfer protein 1	P07597	2	554.99 (3+)	664.28 (2+)	
Q5UNP2_HORVD Non-specific lipid transfer protein	Q5UNP2	1	579.3 (2+)		
Q9SES6_HORVU Non-specific lipid transfer protein	Q6SES6	1	678.81 (2+)		
Q1ENF0_HORVU Cystatin Hv-CPI8	Q1ENF0	1	554.28 (2+)		
IAAD_HORVU Alpha-amylase/trypsin inhibitor CMd	P11643	1	606.99 (3+)		
HINB1_HORVU Hordoindoline-B1	Q9FSI9	1	668.87 (2+)		
Q40036_HORVU Putative protease inhibitor	Q40036	1	581.77 (2+)		
Q03678_HORVU Embryo globulin	Q03678	1	533.96 (3+)		
Q41540_WHEAT CM 17 protein	Q41540	1	608.32 (2+)		

APPENDIX

**Appendix D4: Precursor ion masses and charges for proteins identified in cold wort in bottom up approaches with direct DDA experiments.**

Full protein name	Accession	No. of ions	Peptide ion [m/z] and ion charge	
SPZ4_HORVU Protein Z4	P06293	2	645.55 (4+)	707.39 (2+)
BSZ7_HORVU Serpin-Z7	Q43492	2	627.3 (2+)	569.34 (2+)
IAAB_HORVU Alpha-amylase/trypsin inhibitor CMb	P32936	2	593.29 (2+)	512.26 (2+)
BARW_HORVU Barwin	P28814	1	650.34 (2+)	
NLTP1_HORVU Non-specific lipid transfer protein 1	P07597	1	554.99 (3+)	
Q5UNP2_HORVD Non-specific lipid transfer protein	Q5UNP2	1	579.3 (2+)	
Q9SES6_HORVU Non-specific lipid transfer protein	Q6SES6	1	678.78 (2+)	
IAAD_HORVU Alpha-amylase/trypsin inhibitor CMd	P11643	1	606.99 (3+)	
trypsin/amylase inhibitor pUP13	225102 (NCBI)	1	590.83 (2+)	
Q40036_HORVU Putative protease inhibitor	Q40036	1	581.76 (2+)	

**Appendix D5: Precursor ion masses and charge for proteins identified in ultrafiltrate of bright beer in bottom up approaches with fractionation and DDA experiments in infusion mode.**

Full protein name	Accession	No. ions	Peptide ion [m/z] and ion charge		
SPZ4_HORVU Protein Z4	P06293	4	641.83 (2+)	466.3 (2+)	604.11 (3+)
BSZ7_HORVU Serpin-Z7	Q43492	2	627.3 (2+)	569.34 (2+)	
IAAB_HORVU Alpha-amylase/trypsin inhibitor CMb	P32936	2	593.29 (2+)	845.86 (2+)	
IAAA_HORVU Alpha-amylase/trypsin inhibitor CMa	P28041	1	534.81 (2+)		
ICIA_HORVU Subtilisin-chymotrypsin inhibitor CI-1A	P16062	1	710.84 (2+)		
ICIC_HORVU Subtilisin-chymotrypsin inhibitor CI-1C	P01054	1	710.84 (2+)		
IAAE_HORVU Trypsin inhibitor CMe	P01086	3	490.26 (2+)	744.35 (2+)	569.34 (2+)
BARW_HORVU Barwin	P28814	1	650.34 (2+)		
NLTP1_HORVU Non-specific lipid transfer protein 1	P07597	5	554.99 (3+)	832.09 (2+)	443.23 (3+)
Q5UNP2_HORVD Non-specific lipid transfer protein	Q5UNP2	2	785.19 (3+)	678.84 (2+)	
Q9SES6_HORVU Non-specific lipid transfer protein	Q6SES6	1	645.33 (2+)	579.3 (2+)	
REHY_HORVU 1-Cys peroxiredoxin PE	P52572	1	678.84 (2+)		
IAAD_HORVU Alpha-amylase/trypsin inhibitor CMd	P11643	1	639.28 (2+)		
IAA2_HORVU Alpha-amylase inhibitor BDAI-1	P13691	4	606.99 (3+)	414.26 (2+)	533.72 (3+)
Q02056_HORVU D-hordein	Q02056	2	1088.1 (2+)	670.7 (3+)	
trypsin/amylase inhibitor pUP13	225102 (NCBI)	3	706.86 (2+)	700.86 (2+)	
HINB1_HORVU Hordoindoline-B1	Q9FSI9	1	574.74 (2+)	686.49 (2+)	590.83 (2+)
Q40036_HORVU Putative protease inhibitor	Q40036	1	668.87 (2+)		
O23997_HORVU Basic pathogenesis-related protein PR5	O23997	1	581.81 (2+)		
O24000_HORVU Cmd3	O24000	1	956.95 (2+)		
Q43663_WHEAT Wali3 protein	Q43663	1	606.99 (3+)		
G3P2_YEAST Glyceraldehyde-3-phosphate dehydrogenase 2	P00358	1	706.82 (2+)		
			687.86 (2+)		

## APPENDIX

### Appendix D6: Precursor ion masses and charge for proteins identified in bright beer in bottom up tests with direct DDA experiments.

Full protein name	Accession	No. of ions	Peptide ion [m/z] and ion charge		
SPZ4_HORVU Protein Z4	P06293	3	381.94 (4+)	645.55 (4+)	707.39 (2+)
NLTP1_HORVU Non-specific lipid transfer protein 1	P07597	1	554.93 (3+)		
Q5UNP2_HORVD Non-specific lipid transfer protein	Q5UNP2	1	579.3 (2+)		
Q9SES6_HORVU Non-specific lipid transfer protein	Q6SES6	1	678.78 (2+)		
Q40036_HORVU Putative protease inhibitor	Q40036	1	581.76 (2+)		

### Appendix D7: Precursor ion masses and charge of proteins identified in haze in bottom up approaches.

Full protein name	Accession	No. of ions	Peptide ion [m/z] and ion charge		
SPZ4_HORVU Protein Z4	P06293	5	707.47 (2+)	750.51 (2+)	685.48 (2+)
Q40066_SPZx_HORVU protein Zx	Q40066	1	423.23 (2+)		
IAAA_HORVU Alpha-amylase/trypsin inhibitor CMa	P28041	1	534.81 (2+)		
IAAB_HORVU Alpha-amylase/trypsin inhibitor CMb	P32936	1	593.29 (2+)		
IAAE_HORVU Trypsin inhibitor CMe	P01086	2	772.84 (2+)	807.81 (2+)	
BARW_HORVU Barwin	P28814	1	650.34 (2+)		
NLTP1_HORVU Non-specific lipid transfer protein 1	P07597	5	664.33 (2+)	832.09 (2+)	1005.51 (2+)
IAA2_HORVU $\alpha$ -amylase inhibitor BDAI-1	P13691	5	443.23 (3+)	554.99 (3+)	
			414.16 (2+)	552.65 (3+)	970.94 (2+)
			1116.67 (2+)	828.47 (2+)	
GLT3_WHEAT Glutenin, high molecular mass subunit 12	P08488	1	661.33 (2+)		
GLT0_WHEAT Glutenin, high molecular mass subunit DY10	P10387	1	661.33 (2+)		

APPENDIX

Appendix D8: Summary of peptide masses and sequences identified in the standard sample set.

Full protein name	Detected sequence	Position	MCT extracts	congress wort	Unhoped first wort	Cold wort	Beer + UF	Haze
SPZ4_HORVU	L-KVLKLPYAK	229 – 236	x				x	
	K-QILPPGSVDNTTK	161 – 173	x					x
	K-QYISSDNLK	219 – 228	x		x			x
	K-GAWDQKFDESNTK	184 – 196	x				x	
	K-R <sup>2</sup> LSTPEFIENHIPK	262 – 276	x		x		x	
	K-R <sup>2</sup> LSTPEFIENHIPKQTV	262 – 282	x		x	x	x	
	K-FKISYQFEASSLLR	289 – 302	x					
	K-ISYQFEASSLLR	291 – 302	x	x	x	x	x	x
	R-LA <sup>2</sup> SAISSNPERA	22 – 36	x		x			
	R-DQLVAILGDGGAGDAK	61 – 76						x
	K-QTVEVGR	277 – 283						x
	K-KQYISSDNLK	218 – 228					x	
	R-ALGLQLPFSEEADLSEMVDVDSQGLEISHVFHK	303 – 344			x			
BSZ7_HORVU	R-LVLGNALYFK	175 – 184	x					
	K-TFVEVDEEGTK	336 – 346	x			x	x	
SPZx_HORVU	R-LVLGNALYFK	171 – 180	x			x	x	
	R-SLPVEPVK	357 – 364						x
IAAB_HORVU	R-KSRPDQSGLM <sup>1</sup> ELPGCPR	92 – 107	x					
	R-DYVEQQACR	46 – 54	x	x				
	R-EVQM <sup>1</sup> DFVR	106 – 115	x	x				
	R-IETPGPPYLAK	55 – 65	x	x	x	x	x	
	K-QQCCGELANIPQQCR	66 – 80	x				x	
	R-KSRPDQSGLMELPGCPR	91 – 107	x					
	R-IETPGPPYLAKQQCCGELANIPQQCR	55 – 80	x					
	R-EVQMDFVR	108 – 115	x	x	x	x		
	R-C <sup>3</sup> QALRFFMGR	81 – 90	x					
	K-SRPDQSGLMELPGCPR	92 – 107	x					
R-FFM <sup>1</sup> GRK	86 – 91	x						
IAAA_HORVU	R-CCQELDEAPQHCR	74 – 86	x					
	K-DLPGCPKEPQR	107 – 117	x					
	R-RSHPDWSVLK	97 – 106	x		x			
	R-SHPDWSVLK	98 – 106	x	x	x		x	x
	K-DLPGCPKEPQRDFA K	107 – 121	x					
	R-SHPDWSVLKDLPGCPKEPQR	98 – 117	x					
	R-YFIGR	92 – 96	x					
	R-SHPDWSVLKDLPGCPK	98 – 113	x					
ICIC_HORVU	A-KTSWPEVVGMSAE	16 – 27	x		x		x	
	K-AKEIILR	29 – 35	x					
ICIA_HORVU	A-KTSWPEVVGMSAE	26 – 38	x		x		x	
	K-AKEIILR	39 – 45	x					
	K-YPEPTEGSIGASSAK	11 – 25	x	x	x			
	K-RSWPEVVGMSAEK	26 – 38	x					
IAAE_HORVU	R-TYVVSQICHQGPR	45 – 57	x				x	
	R-LLTSDMK	58 – 64	x					
	R-TYVVSQIC*HQGPR	45 – 57		x				x
	R-C <sup>*</sup> C*DELSAIPAYC*R	67 – 79						x
	R-LLTSDM <sup>1</sup> KR	58 – 65					x	
	R-LLTSDM <sup>1</sup> KRR	58 – 66					x	
BARW_HORVU	R-VTNPATGAQITAR	69 – 81	x	x	x	x	x	x
	R-SK <sup>2</sup> YGWTAFCGPAGPR	44 – 58	x					
	K-YGWTAFCGPAGPR	46 – 58	x					
	R-ATYHYRPAQNNWDLGAPAVSAYCATWDASKPLSWR	8 – 43	x					
	K-CLRVNTPATGAQITAR	66 – 81	x					
	R-IVDQCANGGLDLD	82 – 101	x					
	WDTVFTK							

APPENDIX

NLTP1_HORVU	R-DLHNQAQSSGDR	59 – 78	x					
	QTVCNCLK							
	R-GIHNLNLNNAASIPSK	83 – 98	x	x	x	x	x	x
	K-M <sup>1</sup> KPCLTYV							
	QGGPGPSGECNGVR	36 – 58	x					
	D-RQTVCNCLKGIAR <sup>2</sup>	71 – 82	x					
	K-MKPCCLTYVQ							
	GGPGPSGECNGVR	36 – 58	x					x
	R-GIHNLNLNNAASIPSKCNVN							
	VPTYISPDIDCSR	83 – 115	x					
	K-CNVNVPYITISPDIDCSR	99 – 115	x					
	R-DLHNQAQSSGDRQ							
TVCNCLK GIAR	59 – 82	x						
K-CNVNVPYITISPDIDCSRI	99 – 116	x					x	
R-DLHNQAQSSGDR	59 – 70			x			x	
							x	
Q5UNP2_HORVD	R-SLNAATAADR	66 – 77	x	x	x	x	x	
	K-CGVNIPYAIAPR	106 – 117	x					x
Q9SES6_HORVU	K-ISPSVDCNSIH	111 – 121	x					
	K-NVANAAPGGSEITR	82 – 95	x	x	x	x	x	
REHY_HORVU	R-TLHIVGPKVVK <sup>2</sup>	127 – 139	x					
	K-VTYPIMADPDR	94 – 104	x					x
LEA1_HORVU	K-DAVANTLGM <sup>1</sup> GGDNTSAT							
	KDATTGATVK	178 – 204	x					
	K-DAVANTLGMGGDNTSATK	178 – 195	x	x				
IAAD_HORVU	R-LLVAPGQCNLATIHNR	144 – 160	x	x	x	x	x	
	K-LYCCQELAEIPQQCR	84 – 98	x					
	R-YFMALPVPSQPVPDSTGNVG							
	QSGLMDLPGCPR	104 – 135	x					
	R-YFM <sup>(1)</sup> ALPVP SQPVPDST							
GNVQSGLM <sup>1</sup> DL PGCP	104 – 135	x						
IAA2_HORVU	K-LECVGNRVPEDVLR	57 – 70	x					x
	R-ALVK <sup>2</sup> LECVGNRVPEDVLR	53 – 69	x					x
	R-CGDLGSMR	86 – 94	x					
	R-SVYAAALGVGG							
	GPEEVFGCQ KDVMK	95 – 119	x					
	R-VPEDVLR	64 – 70	x					x
	R-DCCQEVANISNEWCR	71 – 85	x					x
	R-SVYAAALGVGGG							
	PEEVFGCQ K	95 – 115	x					
	L-LVAGVPALCNVPI							
	PNEAAGTR	120 – 141	x					x
	K-LEC*VGNRVPEDVLR	57 – 70						x
	R-DC*C*QEVANISNEWCR	71 – 85						x
K-LLVAGVPALC*NVP								
NEAAG TR	120 – 141						x	
Q02056_D-hordein	K-AQQLAAQLPAMCR	684 – 696	x					
	K-AQQLAAQLPAM <sup>1</sup> CR	684 – 696						x
Q1ENF0_HORVU Hv-CPI8	R-LFVDAADGSGR	85 – 95	x	x	x			
	R-GEQQVVSGMNYR	73 – 84	x					
Q1ENF3_HORVU Hv-CPI5	K-VGGWTEVR	43 – 50	x					
trypsin/amylase inhibitor pUP13	K-SIPINLPACR	26 – 36	x				x	x
	R-DYGEYCRVGK	16 – 25	x					
	R-ELSDLPESCR	61 – 70	x					x
	R-CAVGDQQVPDVLK	43 – 55	x					x
	R-CDALSILVNGVITEDGSR	71 – 88	x					
IAA_HORVU	R-ELAAVPDHCR	73 – 82	x	x				
HINB1_HORVU	K-LGGIFGIGGGDVF	108 – 121	x		x		x	
Q2V8X0_HORVU Limit dextrinase inhibitor	R-ELAAVPDHCR	73 – 82	x					
Q40036_HORVU Putative protease inhibitor	R-VVTTNPQTFR	61 – 70	x	x	x	x	x	
Q23997_HORVU PR5	R-LDPGQSWALNMPAGTAGAR	49 – 67	x	x				
Q946Z0_HORVU TLP6	R-LDPGQSWALNMPAGTAGAR	49 – 67	x	x			x	
Q22462_HORVU Barperml	R-LDPGQSWALNMPAGTAGAR	27 – 45	x					

## APPENDIX

Q03678_HORVU Embryo globulin	K-LGSPAQELTFGRPAR	566 – 580	x	x	x	
Cmd3_HORVU	R-LLVAPGQC�LATIHNVR	144 – 160				x
HINA_HORVU	R-CNIIQGSIQR	97 – 106				x
GLT3_WHEAT	R-ELQESSLEACR	34 – 44	x			
	R-ELQESSLEAC*R	34 – 44				x
GLT0_WHEAT	R-ELQESSLEACR	34 – 44	x			
	R-ELQESSLEAC*R	34 – 44				x
Q41540_WHEAT CM 17 protein	R-IEMPGPPYLAK	55 – 65			x	
Q43663_WHEAT Wali3 protein	R-FFSGAVVCDDAGPK	37 – 50	x			x
G3P2_YEAST	R-TASGNIIPSSTGAAK	199 – 213	x			x

<sup>1</sup>methionine oxidized to methionine sulfoxide, <sup>2</sup>sequence conflict, <sup>3</sup>Cys\_PAM acrylamide adducts, \*Cys\_CAM carbamidomethyl-cysteine

## POSTER PUBLICATIONS

---

Poster presentation: "First international symposium for young scientists and technologists in malting, brewing and distilling", Poster No. 27, Cork (Ireland), November 6 – 7, 2008.

**The influence of enzymes on the gushing tendency of malt and barley samples analysed via "Modified Carlsberg Test" and UPLC nano ESI-QTOF-MS and -MSMS.**

Fabienne Decker,  
Stefan Loch-Ahring,  
Sascha Robbert

Brewery  
C.&A. Veltns  
Germany



**Introduction**

Brewing malts from the barley crop 2007 caused a huge and wide spread increase of gushing in middle European countries. As the result of an unusual annual climate the raw material showed noticeable quality changes. Anyway the prediction of gushing tendencies remains difficult because gushing provoking parameters are not known definitely. Fungi decay is the most discussed presumption with primary gushing. In this case fungal metabolites (proteins and peptides) are predicted to be the gushing activators whereas the exact mechanism remains unclear.

In some cases commercialised, undefined hydrolysing enzymes (proteases), applicable during the brewhouse procedure, result in gushing inhibition.

In order to investigate the impact of proteases on the protein content of barley and malt samples and their gushing behaviour, several proteases were analysed as additives in "Modified Carlsberg Test" (MCT).

In this paper we present recent results obtained with "MCT" and additional UPLC nanoESI-QTOF-MS/MSMS analysis for elucidating the role of proteins in gushing and to demonstrate the positive effect of enzymatical digestion resulting in gushing inhibition.

**Methods**

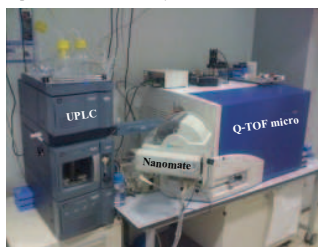
**"Modified Carlsberg Test" with Bonaqua®**  
Homogenised barley or malt sample  
Standard procedure with 0.33 L Bonaqua® bottles (6.5 g CO<sub>2</sub>)  
  
Addition of enzymes after boiling at temperature optimum  
Enzyme volume adapted to protein content (2D-Quant®)  
a) minimum concentration as per manufacturer's data  
b) enzymes without known parameters: 8 U/approach  
3 h period of cleavage with/without temperature stabilisation  
  
Remaining steps similar to standardised "MCT"-procedure

**Sample preparation protein identification**  
Lyophilisation of the "MCT"-extracts, 1-2 d  
0.5 g lyophilisat: phenol protein extraction  
Pellet reextracted in 3 M Gua-HCl, 15mM DTT  
Digestion with "Sequencing Grade Modified Trypsin"  
Protein/enzym ratio 100:1

**UPLC separation**  
Waters Acuity™ UPLC  
LC separation on an Acuity UPLC™ BEH-C<sub>18</sub> column  
1.7 µm, 2.1 x 50 mm  
Mobile phase: eluent A 0.1 % FA/H<sub>2</sub>O,  
eluent B 0.1 % FA/ACN  
80 minutes gradient from 5% to 80 % eluent A  
Flow: 0.2 mL/min  
3-fold sample loading

**UPLC/MS and UPLC/MSMS detection**  
Micromass QTOF-micro (ESI-Z-Spray)  
ESI(+)-mode, lockmass (Glu)-Fibrinopeptide  
Chip-based Triversa Nanomate® robot system  
  
Scan mode or Data Directed Analysis (DDA)  
In parallel: fraction collection (12 sec.) into 384 well plates  
380 fractions per samples

The MS and MSMS experiments were carried out on an orthogonal hybrid quadrupole time-of-flight mass spectrometer (QTOF Micro Micromass, Manchester, U.K.). The Triversa Nanomate® (Advion, Ithaka, USA) includes a fully automated chip-based nano-electrospray ionisation and allows for LC, fraction collection and chip-based infusion in one system.



**Results**

**"Modified Carlsberg Test" with Bonaqua®**

Enzyme	Amount added to protein content	Effect on gushing	Inhibition in MCT
Carlsberg® TSP	0.05%	decreased	total inhibition
Carlsberg® T2	0.05%	decreased	total inhibition
Carlsberg® T10	0.05%	no effect	decreased
Carlsberg® TAP	0.02%	decreased	total inhibition
Carlsberg® TSP + LAP	0.05% + 0.02%	decreased	total inhibition
Genesinger® BFG	0.05%	no effect	inhibition
Carlsberg® pp	0.05%	decreased	decreased
Carlsberg® T2 + LAP	0.05% + 0.02%	decreased	decreased
Robusta® Bacter L	0.05%	no effect	inhibition
Robusta® TSP	0.05%	decreased	decreased
Robusta® CL	5 ul	decreased	decreased
Chromastar® CL	5 ul	no effect	decreased
Protease P	5 U	decreased	decreased
Protease P	5 U	decreased	no effect
Thermolysin®	5 U	decreased	total inhibition
Alcalase® 240	5 U	decreased	total inhibition
Alcalase®	20 ul	decreased	decreased
Alcalase®	5 U	not listed in this list	decreased
Trypan®	20 U	of extract	inhibition

Figure 1. Overview of barley and malt "MCT" with enzyme additives. Notation: "total inhibition" only allow for 0 g gushing volume; "inhibition" means  $\leq 5$  g; "decreased" is used in case of reduction and "no effect" in case of amplification to the gushing.

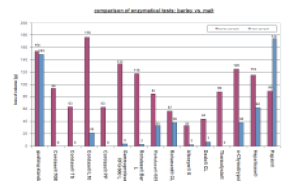


Figure 2. Comparison of the gushing behaviour of enzymatically treated barley and malt samples.

Four enzymes and one mixture showed a total inhibition of gushing behaviour in comparison to their standard gushing sample. This effect could only be obtained with malt extracts. Lacking or diminished hydrolysis of origin barley proteins give a hint to chemical or enzymatical changes in barley grains during the malting process. These modifications seem to benefit further hydrolysis with enzymes.  
One mutuality of the enzymes (successful in operating) is a favoured digestion of hydrophobic amino acids or side chains. Corolase® 7089 was chosen as the enzyme for UPLC-MS proteomic studies. This approach showed the best inhibitory effect and a reproducibility with minimum variance.

**UPLC nanoESI-QTOF-MS analysis of "MCT" malt extracts without phenol extraction**

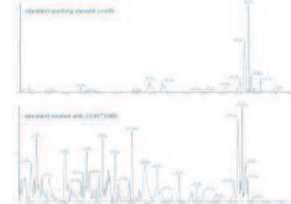


Figure 3. Comparison of UPLC nanoESI-QTOF-MS chromatogram of a standard malt sample operated in ESI(+)-mode. Treatment with Corolase® 7089 shows a typical increase of peptide specific peaks whereas the huge protein peaks of the origin sample are still



Figure 4. UPLC nanoESI-QTOF-MS analysis of an untreated standard gushing and non-gushing malt sample. The chromatograms show a strong correlation on protein level and did not allow for further differentiation of the protein content.

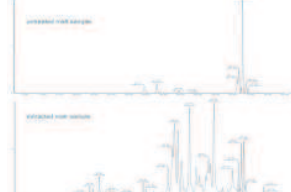


Figure 5. Chromatograms of a non-gushing malt samples. The upper picture shows an untreated sample and the lower one reveals the native protein pattern of a phenol extracted sample.

With the help of an adjusted phenol extraction the sensitivity of the recent method could be up-graded. The number of native protein peaks multi-piled in UPLC-MS scan mode.

**UPLC nanoESI-QTOF-MS and -MSMS analysis after phenol extraction/**

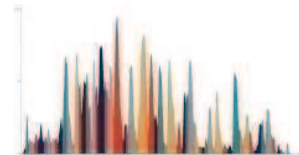


Figure 6. 55 minutes scan from a chromatogram (UPLC-MS scan mode) of a tryptic digested malt sample. Main peaks are displayed in coloured shape and equate to the most abundant peptide precursor-ion masses. These 55 minutes were splitted into equal well plate volumes resulting in 380 fractions per sample. The first 5 and last 20 minutes of the LC run did not show arising peptide peaks.

The nanoESI-QTOF-MS scan mode showed an efficient ionization/detection of precipitated and digested proteins with a stable and constant ESI spray. Parallel fraction collection allowed for re-infusion of fractions with abundant peptide ions to MS/MS investigations. DDA analysis of both gushing and non-gushing samples under defined parameters obtained a complete set of fragment ions (up to 20) of high signal-to-noise ratio could within 20/30 minutes of acquisition. Up to now 29 proteins could be identified through data base (Swiss-Prot/TrEMBL and a self created barley specific one) alignment.

accession number	entry name	no. of identified peptides	peptide coverage at total protein
P07597	NLTP1_HORVU	9	67.5%
P28814	BAW_HORVU	4	53.6%
P52936	IAAB_HORVU	7	40.3%
P11643	IAAD_HORVU	3	38.0%
P13691	IAA2_HORVU	4	31.6%
P06471	ROB3_HORVU	1	30.0%
P16968	IAA1_HORVU	6	29.8%
P16962	ICIA_HORVU	2	26.5%
P20145	NLTP2_HORVU	2	24.5%
P35792	PR12_HORVU	2	21.3%
Q09966	PR1_HORVU	3	21.3%
P06295	PRTE_HORVU	6	21.1%
P33044	THFR_HORVU	1	18.2%
P14928	LEA1_HORVU	1	12.7%
P01086	IAAE_HORVU	2	12.2%
P05241	ICBQ_HORVU	1	11.8%
P07596	IAAC_HORVU	2	11.5%
Q05190	LE19A_HORVU	1	10.8%
P52572	REHY_HORVU	2	10.1%
P06165	THNS_HORVU	2	9.5%
Q23838	THNX_HORVU	2	9.5%
Q88005	THNX_HORVU	2	9.5%
P01054	ICIC_HORVU	1	9.1%
P16965	ICBI_HORVU	1	8.4%
P49451	IAAC_HORVU	1	7.0%
P01545	THNA_HORVU	1	7.0%
P80196	HOG3_HORVU	1	5.2%
P28141	IAAA_HORVU	5	2.2%

Figure 7. Summary of identified proteins out of a non-gushing sample. Donations analogue to Swiss-Prot/TrEMBL data base.

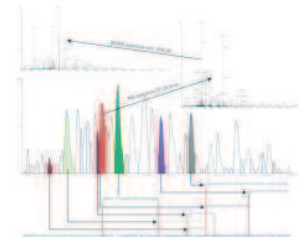


Figure 8. The analytical way from a TIC chromatogram of a non-gushing malt sample to a protein identification using the example of NLTP1 (P07597). The following DDA/MS spectrum of one identified fraction (RT: 28.5 min) is enlarged. Out of this the MS/MS spectrum of the most abundant precursor ion (m/z = 554.98) is shown. All detected peptides associated with this protein as well as their partial amino acid sequences are highlighted beneath the chromatogram.

Non-gushing as well as gushing malt samples were analysed with the help of the presented technique. Recent results did not show peculiar differences between both sample types.  
The enzymatical treatment of gushing positive malt samples resulted in gushing inhibition. This reaction provides an indication of proteins involved in the gushing phenomenon.  
The developed LC-MS method represents a powerful tool for proteomic studies and points out that further protein identifications will be possible. Future analysis aim to boost the number of identified proteins to create a data background which helps to work out differences between gushing and non-gushing malt samples.



Poster presentation: "32nd EBC Congress", Poster No. 033 Hamburg (Germany), May 10 – 14, 2009.

## Novel proteomic studies performed with UPLC and nano ESI-QTOF-MS/MSMS identification: comparison of the protein content in unhoped wort, cold wort and bright beer.

Fabienne Decker,<sup>1</sup>  
 Sascha Robbert,<sup>1</sup>  
 St. Loch-Ahring,<sup>1</sup>  
 Fabian Schulte<sup>2</sup>

<sup>1</sup>University of Bielefeld  
<sup>2</sup>Brewery C.&A. Veltnis, D  
<sup>3</sup>University of Bielefeld, D

### Introduction

Proteomic studies are usually performed with (2D-) gel-electrophoresis and additional MALDI-analysis. A distinct protein identification out of complex sample matrices could be difficult because of false- or manifold-positiv identifications (overloading and -lapping-effects, awkward concentration ratio, fragmentation, artefacts).

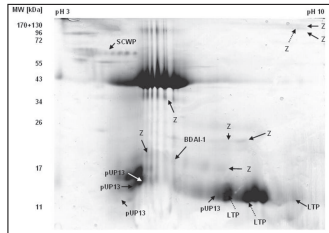


Figure 1. (Fabian Schulte) 15% Tris-Tricin 2D-gel of beer. Phenol extraction with 2M Tris-HCl, pH 7.4. The first dimension isoelectric focusing was made with 500µg protein in pH-range from 3 to 10. MALDI protein identification after colloidal Coomassie staining revealed following protein species: Z: protein Zepes serpin (thordum vulgare P196293); pUP13: tryptophanase inhibitor (thordum vulgare); BDAI-1: alpha-amylase inhibitor precursor (thordum vulgare P13691); LTP: lipid transfer protein (hordeum vulgare P07597); SCWP: soluble cell wall protein (Sac. cerevisiae A6ZU3).

In this poster we present a new way for proteomic studies irrespectively operating from gel separation. A six-step sample pretreatment consisting of lyophilisation, phenolic extraction, UPLC-separation and fractionation, tryptic digestion and peptide mass fingerprinting was performed. An Acquity UPLC<sup>TM</sup> chromatography has been introduced for native and denaturated proteomic studies using an Acquity UPLC<sup>TM</sup> BEH300-C<sub>18</sub> column (1.7µm, 2.1x50mm) and a micromass Q-ToF micro<sup>TM</sup>. The chip-based Triversa Nanomate<sup>®</sup> robot system was used for MS infusion in combination with protein fraction collection in 384-well plates. Subsequently this method was upgraded for protein identification with nano ESI-MS and -MSMS (Data Directed Analysis) as the protein fraction were digested and reinfused.

According to our former proteom UPLC-separation method<sup>1</sup> the chromatography was upgraded with a new Acquity UPLC<sup>TM</sup> column (BEH Shield RP<sub>18</sub> 1.7µm, 2.1x100mm). This analytical combination should lead to a better separating capacity and higher protein identification ratio.

### Sample preparation

Preparation of "Modified Carlsberg-Test" extracts  
 Lyophilisation of 100mL sample volume (wort, beer, MCT-extract), 1-2d

0.5g MCT-extract or beer lyophilisat,  
 2g unhoped wort or  
 1.5g cold wort lyophilisat  
 for phenol protein extraction

Pellet dissolved in 3M Gua-HCl, 15mM DTT

Digestion with "Sequencing Grade Modified Trypsin"<sup>®</sup>  
 Protein/enzym ratio 100:1

### UPLC separation

Waters Acquity UPLC<sup>TM</sup>  
 LC separation on an Acquity<sup>TM</sup> UPLC BEH-C18 column  
 1.7µm, 2.1 x 50mm  
 Mobile phase: eluent A 0.1% FA/H<sub>2</sub>O,  
 eluent B 0.1% FA/ACN  
 80 minutes gradient from 5% to 80% eluent A  
 Flow: 0.4ml/min  
 3-fold sample loading

Scan mode or Data Directed Analysis (DDA)  
 In parallel: fraction collection (12sec.) into 384 well plates  
 360 fractions per samples

### Direct infusion of digested fractions with DDA

QTOF micro (ESI-Z-Spray)  
 ESI(+)-mode,  
 Triversa Nanomate<sup>®</sup> robot system

### UPLC-separation of digested fractions with DDA

QTOF micro (ESI-Z-Spray)  
 ESI(+)-mode, lockmass:  
 [Glu]-Fibrinopeptide  
 Triversa Nanomate<sup>®</sup> LC-  
 chip coupling

The MS and MSMS experiments were carried out on an orthogonal hybrid quadrupole time-of-flight mass spectrometer (QTOF micro, Micromass, Manchester, U.K.). The Triversa Nanomate<sup>®</sup> (Advion, Ithaka, USA) includes a fully automated chip-based nano-electrospray ionisation and allows for LC, fraction collection and chip-based infusion in one system.

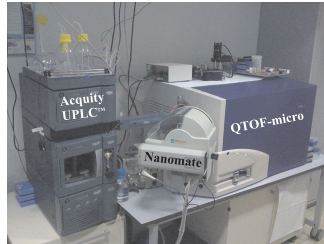


Figure 2. Acquity UPLC<sup>TM</sup> system with Triversa Nanomate<sup>®</sup> and QTOF micro

### Results

#### UPLC nanoESI-QTOF-MS-analysis of proteins

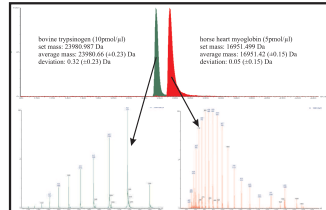


Figure 3. Mass accuracy and separation capacity in positive ion mode. Average m/z values from a standard protein calibration mixture of horse heart tryptosinogen and bovine tryptosinogen in 50% ACN plus 0.1% FA.

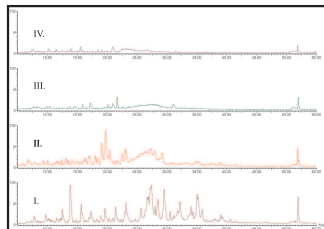


Figure 4. Comparison of UPLC nanoESI-QTOF-MS chromatograms. I) MCT-extract of a brewing malt; II) unhoped wort; III) cold wort and IV) bright beer. The chromatograms show a huge decrease of the protein level during wort boiling up to the bottled end product. Still detectable peaks could be allocated to heat-stable proteins.

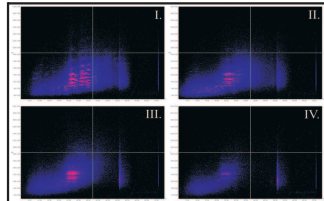


Figure 5. Three dimensional data maps of entire UPLC nanoESI-QTOF-MS protein analysis: I) MCT-extract of a brewing malt; II) unhoped wort; III) cold wort and IV) bright beer. The maps display the data against retention time. The vertical axis shows mass charge units (Da/e) whereas the horizontal axis display retention times in minutes. The colour code highlights most intensive signals.

During the brewing process the protein content dramatically changes: wort boiling, the addition of hop, fermentation, filtration procedure and in some cases flash pasteurization exert influences, which configure the protein pattern in the bottled beer. The total protein content strongly decreases till the end product.

#### Direct infusion of digested fractions with DDA

Extracted and separated proteins were lyophilised. After tryptic digestion the samples were reinfused with the Triversa Nanomate<sup>®</sup> in direct infusion mode and analysed by DDA. An optimal mass accuracy was achieved by [Glu]-Fibrinopeptide spiking. In case of adequate background information the software annotation led to protein hits on one hand and peptide ladder sequences on the other one.

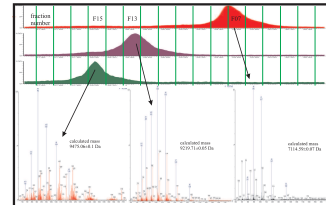


Figure 6. Extracted protein spectra of unhoped wort fractions. The masses were calculated for the extracted ion series and can be allocated to single native and denaturated proteins.

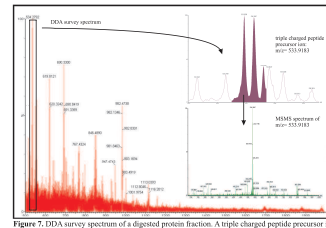


Figure 7. DDA survey spectrum of a digested protein fraction. A triple charged peptide precursor ion (m/z= 533.9183 Da) is enlarged and the belonging MSMS-spectrum is given below.

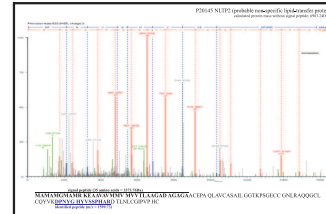


Figure 8. MSMS-spectrum of a m/z= 533.9183Da peptide. The amino acid sequence was calculated from the b-ion series by the help of a Biogen tool (Market-Lynn software). A database-search allowed for eLTP2 identification. The entire protein amino acid sequence is given below, whereas the signal peptide is marked by bold letters and the peptide sequence by blue, bold ones.

DDA experiments in infusion mode even allow for MSMS fragmentation of low concentrated ions with a good signal to noise ratio. A deep insight into the protein composition of malt, wort and finally beer is possible by this analytical tool.

#### UPLC-separation of digested fractions with DDA

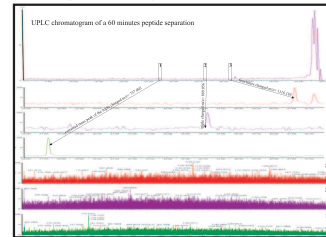


Figure 9. For direct DDA experiments the UPLC was connected to the MS by the Triversa Nanomate in LC-chip-coupling mode. The upper chromatogram gives an overview of the peptide chromatography (digested MCT-protein fraction). Single extracted mass peaks are enlarged in the chromatograms below, as the count ratios are very low. In addition the belonging spectra are shown.

DDA experiments following peptide chromatography are successful but up to now difficult as the ion count rates are very low. Manifold sample loading and chromatography extension are helpful method alterations. Tests with a BSA standard protein were performed and are adapted to the fractionated sample material now.

#### Conclusions and perspectives

The developed method is a powerful protein identification tool independently working of gel separation. Accurate protein separation into fractions and protein identification by amino acid ladder sequencing could prevent false positive indications. A highly efficient first peak separation even allows for the account of single protein modifications during the brewing process. Further analysis aim to observe changes and modifications of the raw material protein content during the brewing process till the bottled end product.

[1] F. Decker et al. "The influence of enzymes on the glyking tendency of malt and barley samples analyzed via "Modified Carlsberg Test" and UPLC nano ESI-QTOF-MS and MSMS". First International Symposium for Young Scientists and Technologists in Malting, Brewing and Distilling, Cork, Ireland, November 2008.

Poster presentation: IMSC, Poster No. PMM133, Bremen (Germany), September 2009.



## Combining Top down and Bottom up analyses in a single LCMS experiment

Reinaldo Almeida<sup>1</sup>, Fabienne Decker<sup>2</sup>, Sascha Robbert<sup>2</sup>

<sup>1</sup> Advion Biosciences Limited, Rowan House, 26 Queens Road, Hethersett NR9 3DB, UK

<sup>2</sup> Brewery C&A Veltins, An der Streue, Meschede- Grevenstein, 59872, Germany

### Overview

- UPLC Protein Separation by C18 RP chromatography using elevated temperature
- Online LCMS with Fraction collection
- Intact mass determination by online LCMS
- PTM Characterization by Infusion
- Bottom up analyses by Infusion of previous collected fractions after digestion

### Introduction

In this work we combine “bottom up” and “top down” analyses by merging online LCMS with nanoESI infusion for the identification of proteins and characterizing their post-translational modifications. The intact mass measurement and primary sequence determination is performed by online UPLC-MS(MS) with simultaneous fraction collection.

Post-translational modification are observed by automated nano ESI Infusion of the previously collected fractions. Since nanoESI consumes just a small amount of the analyte, proteolytic digestion was performed on the remaining sample for “bottom up” analyses..

### Methods

#### Protein Separation

- Waters Acquity UPLC, BEH C18, 1.7µm 2.1 mm x 50 mm ; 65 C Column temperature
- Mobile Phase
- A: 0.1 % FA
- B: 70% IPA,20%ACN, 9.5% H<sub>2</sub>O,0.5 % FA
- Run time:75 min , Flow rate: 400 uL/min

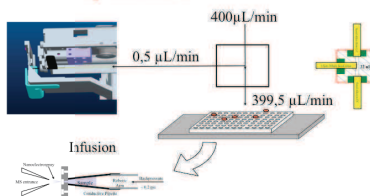
#### MS Settings

- Waters QTOF micro
- Scan time: Online 0.48 s ; Infusions 3s
- Scan range: MS 400-2800 : MS<sup>2</sup> 100-1900

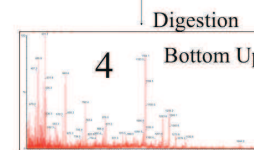
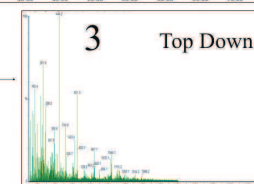
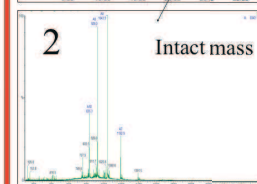
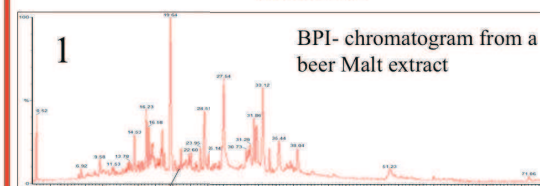
#### TriVersa Nanomate Settings

- Spray Volt. : Online 1,7 kV; Infusion 1.4 kV
- Fraction collection : 10 s/fraction

#### LC/MS with simultaneous fraction collection followed by Infusion



### Results



1. Protein Separation with simultaneous fraction collection
2. Intact mass determination during online or by Reinfusion (low level)
3. Top Down analyses (MSM<sup>3</sup>)
4. Bottom up after digestion of Fraction

### Conclusion

- Protein Separation fraction collection, and nanospray reinfusion enables the intact mass measurement, top down analyses and bottom up sequence information in a single LCMS experiment
- Post LCMS Infusion provides better quality MS<sup>n</sup> spectra because of longer analyses time
- Optimization of parameters ( e.g.. collision energy) without the need for reinjection

## CURRICULUM VITAE

---

## Curriculum vitae

### PERSONAL DATA

Date of birth 13. May 1979  
Place of birth Brilon, Germany

### SCIENTIFIC CAREER

01/2007 – 12/2009 QC/QA researcher, Research group: Instrumental Analytics  
Brewery C.&A. Veltins, Meschede, Germany

### EDUCATION

01/2007 – 12/2009 **Doctoral thesis**, Research group: Instrumental analytics,  
Brewery C.&A. Veltins, Meschede, Germany in cooperation  
with University of Bielefeld, Faculty of Technology  
Title: From malt to bright beer and beyond -Proteomic  
studies performed with HPLC and UPLC chromatography  
followed by (nano)ESI-QTOF-MS/MSMS identification-

10/2006 – 12/2006 Internship: QC/QA, instrumental and microbiological  
analytics, Brewery C.&A. Veltins, Meschede, Germany

10/2003 – 09/2006 **Diploma thesis in Biotechnology**, University of Bielefeld,  
Faculty of Technology, Studies: Molecular Biotechnology  
Title: Sequential identification of protein components in beer  
haze by the use of nano ESI-QTOF-MS. - Tracing of nLTP in  
the brewing process –  
Grade: outstanding  
Place of performance: Research group: Instrumental  
Analytics, Brewery C.&A. Veltins, Meschede, Germany  
Diploma project title:  
„Verification of *Escherichia coli* – clone plasmid stabilities –  
optimization of recombinant Streptavidin recovery“.

10/2002 – 09/2003 Studies: Molecular Biotechnology (Bachelor of Science)  
University Lübeck, Faculty of Technical and Natural Science

09/2000 – 07/2002 **Certified Biological Technician (BTA)**, Berufskolleg  
Olsberg des Hochsauerlandkreises, Olsberg, Germany  
Grade: outstanding, ranked first among the graduates

## CURRICULUM VITAE

---

- 10/1998 – 09/2000                      Studies: Agrar Biotechnology (Diploma), Universtiy of Hohenheim, Stuttgart, Germany  
3 terms and 1 leave of absence because of illness
- 08/1989 – 05/1998                      Allgemeine Hochschulreife (equivalent to A – levels), Gymnasium Petrinum, Brilon, Germany  
Grade: 1.5

### ADDITIONAL SCIENTIFIC WORK

- Scientific Assistant,                      University of Bielefeld, Faculty of Biotechnology  
Scientific Assistant                      University of Hohenheim, Institut of Plant breeding

### PUBLICATIONS

Article published in Brewing Science, Vol. 2 (March/April) 2008, pp. 32-48:

„Chill-haze - Identification and determination of Haze-active constituents by HPLC and Mass spectrometry. Part I: The role of polyphenols and the astonishing impact of hop components on chill haze formation.“

Authors: S. Loch-Ahring, F. Decker, S. Robbert and J.T. Andersson

Poster presentation at the „First International Symposium for Young Scientists and Technologists in Malting, Brewing and Distilling“, UCC Cork, Ireland, November 5 – 7, 2008:

„The influence of enzymes on the gushing tendency of malt and barley samples analysed via “Modified Carlsberg Test“ and UPLC nano ESI-QTOF-MS and MS/ MS.“

Authors: F. Decker, S. Loch-Ahring and S. Robbert

Poster presentation at the 32<sup>nd</sup> EBC Congress, Hamburg, May 10 – 14, 2009:

„Novel proteomic studies performed with UPLC chromatography and nano ESI-QTOF-MS/MSMS identification: comparison of the protein content in unhoped wort, cold wort and bright beer.“

Authors: F. Decker, S. Robbert, S. Loch-Ahring and F. Schulte

Poster presentation at the 18<sup>th</sup> IMSC, Bremen, March 8 – 11, 2009:

„Combining Top down and Bottom up analyses in a single LCMS experiment.“

Authors: R. Almeida, F. Decker and S. Robbert